A Delineation of Mesenchymal Stromal Cell Therapeutic Action in New Models of Acute and Chronic Graft versus Host Disease

By

Marc E. Healy

B.Sc. M.Sc.

A thesis submitted to

The National University of Ireland, Maynooth for the degree of

Doctor of Philosophy

Department of Biology

Institute of Immunology

National University of Ireland, Maynooth

February 2015

Research Supervisors: Dr. Karen English & Prof. Bernard P. Mahon

TABLE OF CONTENTS:

LIST OF FIGURES:

PAGE NO.

LIST OF TABLES:

DECLARATION OF AUTHORSHIP

I certify that the work presented herein is, to the best of my knowledge, original, resulting from research performed by me, except where acknowledged otherwise. This work has not been submitted in whole, or in part, for a degree at this or any other university.

Marc E. Healy B.Sc. M.Sc. Date

ABSTRACT

The potent immune regulatory capacity of mesenchymal stromal cells (MSC) has been extensively characterised in terms of T cells, natural killer cells and dendritic cells suppression; however the ability of MSC to modulate B cell biology is not fully understood. This immune suppressive ability has led to the development of MSC therapy for the treatment of inflammatory and auto-immune disease, and has already demonstrated beneficial effects during GvHD and Crohn's disease. However, the mechanisms employed by MSC therapy to modulate disease progression have not been identified. The key goals for this thesis were (1) to determine how MSC effect B cell function and to identify the mechanisms by which this effect is mediated, and (2) the development of novel mouse models of chronic and acute GvHD to elucidate the mechanism of action by which MSC attenuate disease progression.

This study demonstrated than MSC support the activation, proliferation and survival of human $CD19^+$ peripheral B cells *in vitro*. MSC support of B cell survival was mediated through the cell contact dependent up-regulation of VEGF production by the MSC. Soluble VEGF bound by B cells induced AKT phosphorylation, inhibited caspase 3 cleavage and reduced apoptosis.

The second part of this thesis focused on developing murine models of chronic and acute GvHD and to investigate the efficacy of xenogeneic MSC therapy in these models. In addition, a robust humanised model of aGvHD was developed to investigate mechanism of MSC protection. MSC therapy significantly increased survival of aGvHD mice and this protection correlated with significantly reduced TNF-α production and significantly increased numbers of regulatory T cells in aGvHD target organs.

These findings further the understanding of the immune regulation capacity of MSC *in vitro* and provide a robust and clinically relevant model of aGvHD from which the mechanisms behind MSC modulation can be investigated.

PEER REVIEWED PUBLICATIONS

- Tobin, L. M., **Healy, M. E.,** English, K., Mahon, B. P. Human mesenchymal stem cells suppress donor CD4+ T cell proliferation and reduce pathology in a humanized mouse model of acute graft-versus-host disease. Clinical & Experimental Immunology, 172: 333–348 (2013). IF: 3.278

- Yang, S., Wang, B., Humphries, F., Jackson, R., **Healy, M. E.,** Bergin, R., Aviello, G., Hall, B., McNamara, D., Darby, T., Shanahan, F., Melgar, S., Fallon, P. G., Moynagh, P. N. Pellino3 ubiquitinates RIP2 and mediates Nod2-induced signaling and protective effects in colitis. Nature Immunol. 14, 927–936 (2013). IF:24.973

SUBMITTED MANUSCRIPTS

- **Healy, M. E.,** Bergin R., Mahon, B.P., English, K. Human mesenchymal stem cells promote B cell survival through contact dependent up-regulation of Vascular Endothelial Growth Factor (VEGF). Stem Cells and Development.
- McClean, S., **Healy, M. E.,** Carberry, S., Shaughnessy, L., Dennehy, R., Callaghan, M., Mahon, B. P., Doyle, S., Shinoy, M. A platform for identification of bacterial adhesins for vaccine antigen discovery – protection against a Cystic fibrosis associated lung pathogen. Infection and Immunity.

MANUSCRIPTS IN PREPARATION

- **Healy, M. E.**[1], Aldridge, A[1]., English, K., O'Neil, S. Fasciola hepatica tegulmental antigen as a novel modulator of human immune cell mediated inflammation *in vitro* and *in vivo*.

ABBREVIATIONS

APC	Antigen presenting cell
ATG	anti-Thymocyte globulin
BAFF	B cell activating factor
BAL	Bronchoalveolar lavage
BCR	B cell receptor
Bcl-2	B cell lymphoma 2
BMT	Bone marrow transplant
BRG	BALB/c-Rag2^{null}IL-2Rγ^{null}
BSA	Bovine serum albumin
cAMP	Cyclic adenosine monophosphate
CD	Cluster of differentiation
cDNA	Complementary Deoxyribonucleic acid
CFSE	Carboxyfluorescein succinimidyl ester
CMV	Cytomegalovirus
CpG	Caffeoyl phenylethanoid glycoside
DC	Dendritic cell
dH_2O	Distilled Water
DMEM	Dulbecco's modified eagle's medium
DMSO	Dimethyl sulfoxide
DNA	Deoxyribonucleic acid
EAE	Experimental autoimmune encephalomyelitis
EB/AO	Ethidium bromide/ Acridine orange
EBV	Ebstein-Barr virus
ECP	Extracorporeal photophoresis
EDTA	Ethylenediaminetetraacetic acid
EGFR	Epidermal growth factor receptor
ELISA	Enzyme linked immunosorbent assay
FACS	Fluorescence-activated cell sorting
FBS	Fetal bovine serum
Fh-Teg	*Fasciola hepatica* tegumental antigen
Fix/Perm	Fixation/ Permeabilisation

FSC	Forward scatter
GAPDH	Glyceraldehyde 3-phosphate dehydrogenase
GI	Gastrointestinal
GMCSF	Granulocyte macrophage colony stimulating factor
GMP	Good manufacturing practice
GSI XII	γ-secretase inhibitor XII
GvHD	Graft versus host disease
GvL	Graft versus lymphoma
GvT	Graft versus tumour
Gy	Gray
H&E	Hematoxylin and Eosin
HEL	Hen egg lysozyme
HGF	Hepatocyte growth factor
HLA	Human leukocyte antigen
HRP	Horseradish peroxidase
HSC	Hematopoietic stem cell
HSCT	Hematopoietic stem cell transplantation
i.v.	Intravenous
ICAM-1	Intracellular adhesion molecule-1
IDO	Indoleamine 2,3-dioxygenase
IFN	Interferon
IgG	Immunoglobulin G
IgM	Immunoglobulin M
IL	Interleukin
IMDM	Iscove's modified dulbecco's medium
iNKT	Invariant natural killer T cells
ISCT	International Society for Cellular Therapy
kDa	Kilodalton
kg	Kilogram
KGF	Keratinocyte growth factor
LPS	Lipopolysaccharide
MACS	Magnetic-activated cell sorting
MCP-1	Monocyte chemoattractant protein-1

MHC	Major histocompatibility molecule
miHA	Minor histocompatibility antigen
MLC	Mixed lymphocyte culture
MS	Multiple Sclerosis
MSC	Mesenchymal stromal cell
γMSC	IFN-γ stimulated mesenchymal stromal cell
NK	Natural killer cell
NO	Nitric oxide
NOD	Non-obese diabetic
NSG	NOD-Scid IL-2rγ^{null}
NUI	National University of Ireland
OD	Optical density
PBMC	Peripheral blood mononuclear cells
PBS	Phosphate buffered saline
PCR	Polymerase chain reaction
Pen/Strep	Penicillin/ Streptomycin
PGE_2	Prostaglandin E_2
PI	Propidium Iodide
RA	Rheumatoid arthritis
RBC	Red blood cell lysis
RNA	Ribonucleic acid
mRNA	Messenger Ribonucleic acid
RPM	Revolutions per minute
RPMI	Roswell Park Memorial Institute
SCID	Severe combined immunodeficiency
SDS-PAGE	Sodium dodecyl sulphate polyacrylamide gel electrophoresis
SLE	Systemic Lupus Erythematosus
SSC	Side scatter
Tcm	Central memory T cell
Tem	Effector memory T cell
TGF-β	Transforming growth factor-β
TI	T cell independent
TLR	Toll like receptor

TNF	Tumour necrosis factor
TNFSFR	Tumour necrosis factor superfamily receptor
TSG-6	Tumour necrosis factor-α stimulated gene/protein 6
Treg	Regulatory T cell
VCAM-1	Vascular cell adhesion molecule-1
VEGF	Vascular endothelial growth factor
VZV	Varicella zoster virus

Acknowledgements

First of all I would like to thank Bernie for the opportunity to pursue my PhD. From the first time I came here you have offered me unwavering support, excellent advice and a depth of knowledge. I am also extremely grateful for your confidence in me to represent you and the lab in Cleveland. I hope you continue to enjoy your new position as V.P. and that it opens the door to even more prosperous positions in the future. Thank you.

Karen, I wish to offer you my sincerest gratitude for all the help, guidance and friendship you have provided me with over the last few years. I truly believe you will become a world leading researcher and it has been a privilege to be your PhD student. I know that I am a much better scientist now than I would have become without you and I hope we can continue our work as collaborators in the near future. Thank you.

To everyone who has been part of the Cellular Immunology Lab over my 4 years here, Cariosa, Heather, Aine, Laura Tobin, Emer, Helen, Laura Cahill, Jen, and Fiona, I want to thank you for all the help which you have given me over the years but also for your friendship. I hope you all succeed in not only your work in the lab but for everything in life. Thank you.

Ruaidhri, over the last 8 years we have become great friends and I would not have enjoyed my undergraduate or PhD half as much without your friendship. Your advice and support during my time here really meant a lot to me. As with Karen, I am sure you

will become one of the world's leading researchers in the next few years. I hope you enjoy the experience of working in Yale but also that you receive the rewards from your work that you definitely deserve. Ronan, thank you for your friendship and support over the last few years. I hope your final few months here go well and you get the recognition your hard work and dedication deserve. I also hope that your continued research into your condition will prove rewarding. Enda, you have been one of my best friends here over the last few years and I am really grateful for this. I hope you are happy in New York and that everything goes well in your new lab. Eoin, in addition to your friendship over the years I am sure that without your detailed knowledge surrounding the mitochondria this thesis would still have been entirely possible. Alan, thank you for everything over the years and I hope your new life in America brings you all the happiness you desire. Thank you.

To my mother and father, your encouragement and support (emotional and financial) have made it possible for me to finish my PhD. You have thought me the value of hard work since I was a child and for this I will be eternally grateful. I am very proud to call you my parents. Cian and Aoife, thank you for supporting me throughout not only this project but everything I do. Thank you.

Finally to Rossella, since the first time that we met you have been there to support me through all the good times and the bad in my life. Your love and friendship is more important to me than anything else in this world and has been essential in getting through PhD. You are always there for me and although I cannot express how much I love you here but the importance you have played in my life is huge. Ti amo. Thank you.

CHAPTER 1

INTRODUCTION

1.1 MESENCHYMAL STROMAL CELLS

The field of mesenchymal stromal cell (MSC) research traces its origin to 1966 when Alexander Friedenstein first described a rare, non-haematopoietic, osteogenic precursor cell population (0.01-0.001%) from the bone marrow which formed plastic adherent colonies *in vitro* (Friedenstein *et al.* 1966; Friedenstein *et al.* 1968; Friedenstein *et al.* 1974). The multi-lineage differentiation capacity of these cells was first suggested by Owen and colleagues after observing bone and cartilage formation following implantation of cells into rats (Ashton *et al.* 1980). In 1991, Arnold Caplan identified their potential in regenerative medicine and coined the phrase "mesenchymal stem cells" (Caplan 1991). However, it was not until 1999 that Pittenger *et al.* demonstrated the ability of MSC to differentiate into osteocytes, chondrocytes and adipocytes (Pittenger *et al.* 1999).

In the last decade, *in vitro* and *in vivo* data has highlighted the potential of MSC therapy in regenerative medicine. Initial studies focused on the differentiation ability of MSC and examined the capacity of MSC therapy to repair bone damage or regenerate cartilage in arthritis patients. However, the conceptual focus of using MSC in regenerative medicine has shifted with an appreciation of the wide range of MSC secreted trophic factors capable of promoting tissue repair and potent immune-modulation (Barry *et al.* 2005). In 2005, the International Society for Cellular Therapy (ISCT) suggested that the nomenclature of these cells be changed to "mesenchymal stromal cell" to provide a more accurate reflection of their functional capacity (Horwitz *et al.* 2005). However, the *in vivo* identification and subsequent isolation of human MSC remained a controversial issue, complicated by the lack of a specific set of surface markers capable of identifying human MSC populations. Therefore, the ISCT proposed the minimal criteria for defining human MSC *in vitro* (Dominici *et al.* 2006), suggesting that human MSC must be plastic adherent, should express CD73, CD90 and CD105 but not CD10, CD11b, CD14, CD34,

CD45, CD79α or HLA-DR and furthermore, MSC must be capable of differentiating to osteocytes, chondrocytes and adipocytes *in vitro* (Dominici *et al.* 2006).

1.2 MSC AND IMMUNE REGULATION

The capacity of allogeneic MSC to influence immune responses was first described by Bartholomew *et al.* (2002). The authors demonstrated that baboon derived MSC potently suppressed allogeneic lymphocyte proliferation *in vitro* and furthermore showed that allogeneic baboon MSC were capable of prolonging skin graft survival *in vivo* (Bartholomew *et al.* 2002). The following year, an *in vitro* allogeneic immune suppressive capacity was reported for human MSC (Tse *et al.* 2003) and in 2004, allogeneic MSC therapy was successfully used to treat a paediatric patient suffering from grade IV steroid resistant GvHD (Le Blanc *et al.* 2004). The last decade has seen advances in understanding the mechanism by which MSC modulate specific immune cell populations. The ability of allogeneic MSC to suppress T cell proliferation (English *et al.* 2007; Tobin *et al.* 2013), dendritic cell (DC) maturation, antigen presentation (Wang *et al.* 2008; English *et al.* 2008; Spaggiari *et al.* 2009) and natural killer (NK) cell function (Spaggiari *et al.* 2008; Noone *et al.* 2013) has now been extensively characterised. It has also become apparent that the activation of MSC following exposure to pro-inflammatory cytokines promotes the immune suppressive ability of these cells (Ryan *et al.* 2007; Polchert *et al.* 2008). However, the extent to which allogeneic MSC therapy enjoy immune privilege remains a matter of debate. The original hypothesis suggesting that MSC are invisible to allogeneic immune cells has been challenged by studies which suggest that MSC evade allogeneic immune responses (Ankrum *et al.* 2014). Studies investigating the engraftment of MSC in murine systems have shown that transplanted MSC were undetectable after 48 hours of infusion (Lee *et al.* 2009; Toma *et al.* 2009). In

a direct comparison with autologous MSC, the infusion of allogeneic murine MSC to healthy mice resulted in significantly lower engraftment (Zangi *et al.* 2009); however allogeneic MSC were rejected at a significantly slower rate than allogenic fibroblasts (Zangi *et al.* 2009). This study also demonstrated that mice which had received allogeneic MSC, rapidly rejected a subsequent infusion of fibroblasts from the same donor suggesting an acquired immunological memory following allogeneic MSC recognition (Zangi *et al.* 2009). These results suggest that allogeneic MSC are not immune privileged but should be more accurately referred to as immune evasive and that local immune suppression by the allogeneic MSC may be key to their prolonged survival. Therefore an understanding of the *in vivo* action of MSC in cell therapy requires an appreciation and exploration of MSC-immune system interaction.

1.3 MSC AND THE INNATE IMMUNE SYSTEM

1.3.1. MSC AND NATURAL KILLER CELLS

The innate immune system is the primary barrier and defence against infection and is also the first set of confounding processes encountered by an allogeneic cell therapy. Therefore developing an understanding of exactly how MSC interact with cells of the innate immune system is essential for progressing MSC therapy. MSC have been shown to interact with cells of both the innate and adaptive immune system through a repertoire of soluble factors and cell contact signals. Natural killer (NK) cells are major lymphoid effector cells of the innate immune system which play a key role in the recognition and destruction of virally infected, allogeneic or abnormal host cells (Biron 1997; Moretta *et al.* 2002). NK cell activation also helps to trigger the adaptive immune response through the production of pro-inflammatory cytokines including IFN-γ (Fauriat *et al.* 2010). The innate immune system represents one of the primary obstacles

encountered by an allogeneic stem cell therapy and understanding how MSC interact with NK cell *in vivo* is essential to generate a successful cell therapy (Gill 2010). Over the last 8 years there have been a number of breakthroughs in identifying how allogeneic MSC therapies evade clearance by NK cells. Some of the initial studies showed that MSC reduced NK cell proliferation *in vitro* (Sotiropoulou *et al.* 2006; Boissel *et al.* 2008; Spaggiari *et al.* 2008). However, subsequent studies reported the capacity for IL-2 or IL-15 activated NK cells to kill autologous or allogeneic MSC (Spaggiari *et al.* 2008; Götherström *et al.* 2011). Interestingly, MSC derived from adipose tissue were shown to be less susceptible to NK cell mediated killing than bone marrow derived MSC (DelaRosa *et al.* 2012). Noone *et al.* demonstrated that resting NK cells do not kill MSC, however, following NK activation, cytotoxicity is restored. NK cytotoxicity of MSC is mediated through the NKG2D-perforin granzyme pathway (Noone *et al.* 2013). The mechanism by which MSC evade NK cell killing was also investigated by Noone *et al.* They showed that MSC suppress NK cell activation through the secretion of prostaglandin and IDO without a requirement for cell contact. The pre-stimulation of MSC with IFN-γ protected MSC from NK mediated apoptosis through the elevated expression of the inhibitory MHC Class I molecules (HLA-ABC) and IDO production. More recently, TLR stimulation has also been shown to protect MSC from NK cell mediated apoptosis (Giuliani *et al.* 2014). Many studies have demonstrated that IDO is significantly increased upon IFN-γ stimulation (English *et al.* 2007; Ryan *et al.* 2007). Importantly, Noone *et al.* further identified that increased HLA-ABC expression (following IFN- γ stimulation) inversely correlated with NK cell cytotoxicity (Noone *et al.* 2013).

1.3.2. MSC AND DENDRITIC CELLS

Dendritic cells (DC) are specialised antigen presenting cells capable of inducing a T cell mediated response against a specific antigen. In recent years there has been a range of studies that have strived to identify how MSC interfere with DC function, resulting in the identification of 3 key processes by which MSC modulate DC. Firstly, MSC limit the normal up-regulation of co-stimulatory molecules CD40, CD80, CD86 and MHC Class II by DC in response to LPS stimulation (Jung *et al.* 2007; English *et al.* 2008). Secondly, MSC impair the antigen presentation ability of DC (English *et al.* 2008) and thirdly, MSC abrogate the capacity of DC to migrate to the lymph node derived chemokines by down-regulating CCR7 and maintaining the expression of e-cadherin on DC (English *et al.* 2008). The ability of MSC to impair DC maturation is mediated through a combination of soluble factors and cell contact signals. The two main soluble factors are IL-6 and PGE_2 (Djouad *et al.* 2007; Chen *et al.* 2007). IL-6 secretion by the MSC induces a semi-mature phenotype in DC and subsequently reduces the differentiation of progenitor cells to DC (Djouad *et al.* 2007). Chen *et al.*, also demonstrated that the chemical inhibition of PGE_2 synthesis within MSC restored DC differentiation and function (Chen *et al.* 2007). The cell contact signal contributing to the MSC ability to modulate DC maturation remains unclear but recent studies have indicated that there may be a role for the notch signalling pathway (Tobin *et al*, In re-submission). Aldinucci *et al.* demonstrated that cell contact was required for complete inhibition of DC function (Aldinucci *et al.* 2010). In the presence of MSC, DC remained in an immature state and were unable to form functional immune synapses, retained endocytic activity and podosome-like structures. MSC suppression of DC function *in vitro* is also maintained *in vivo*. Chiesa *et al* demonstrated that MSC therapy significantly impaired the migration of LPS activated DC to draining lymph nodes and subsequently inhibited T cell priming (Chiesa *et al.* 2011).

1.4. MSC AND THE ADAPTIVE IMMUNE SYSTEM

1.4.1 MSC AND T CELLS

MSC inhibition of T cell activation and proliferation has been extensively characterised over the last decade and has been the foundation behind the progression of MSC therapy to clinical application. *In vitro*, MSC suppress T cell function through a combination of chemokines (Ren *et al.* 2008), direct cell contact and release of soluble factors (Di Nicola 2002). MSC first attract T cells through the production of CXCR3 (Ren *et al.* 2008) and MCP-1 (Akiyama *et al.* 2012) before binding the T cell via the ICAM-1 and VCAM-1 (Ren *et al.* 2010). MSC secrete a wide range of soluble factors, including HGF, TGF-β (Di Nicola 2002), IDO (Meisel *et al.* 2004), PGE_2 (Németh *et al.* 2009), IL-10 (Yang *et al.* 2009), IL-6 (Najar *et al.* 2009), semaphorin-3A, Galectin-1 (Lepelletier *et al.* 2010), Galectin-9 (Gieseke *et al.* 2013), adenosine (Sattler *et al.* 2011) and TSG-6 (Lee *et al.* 2009) which suppress the proliferation and cytotoxic function of activated T cells. The immune suppression ability of MSC is not restricted to naïve T cell activation and proliferation; MSC are also capable of inhibiting the response of antigen specific memory T cells to their cognate peptide (Krampera *et al.* 2003).

An alternative concept of how MSC modulate T cell function is the induction of T cell apoptosis, first described *in vitro* by Plumas *et al.* (Plumas *et al.* 2005). A few years later, Akiyama *et al.* demonstrated that, following MCP-1 mediated chemo-attraction, MSC induced T cell apoptosis through Fas/FasL signalling *in vivo* (Akiyama *et al.* 2012). The authors further suggested that the subsequent increase in TGF-β, produced by macrophages in response to T cell apoptosis, significantly up-regulates the generation of regulatory T cells and supports immune tolerance (Akiyama *et al.* 2012).

MSC can modulate T cell function and potentially play a role in generating tolerance through the generation of Treg cells *in vitro* and *in vivo* (Casiraghi *et al.* 2008;

English *et al.* 2009; Kavanagh & Mahon 2011). MSC support of Treg cells *in vitro* is dependent on cell contact, PGE_2 and TGF-β1 and results in fully functional regulatory T cells capable of suppressing alloreactivity (English *et al.* 2009). Selmani *et al.* proposed a mechanism by which cell contact between $CD4^+$ T cells and MSC results in HLA-G production by the MSC which results in Treg generation (Selmani *et al.* 2008). The generation of Treg cells following MSC administration has also been observed *in vivo* in a wide range of disease models. MSC therapy generates significantly increased Treg cell numbers in animal models of asthma (Kavanagh & Mahon 2011), acute renal injury (Hu *et al.* 2013; Kilpinen *et al.* 2013), kidney transplantation (Ge *et al.* 2010), skin transplantation (Lee *et al.* 2013) and colitis (Zuo *et al.* 2013). A recent small scale phase I clinical trial examining the ability of MSC therapy to support renal transplantation (Mudrabettu *et al.* 2014), has also reported significantly increased Treg cell expansion and reduced allo-responsive T cell proliferation following MSC therapy.

1.4.2 MSC AND B CELLS

In contrast to the detailed understanding of how MSC modulate T cell function, the effect of MSC on B cell biology *in vitro* is poorly characterised and studies into MSC modulation of B cell biology have presented conflicting results (Corcione *et al.* 2006; Tabera *et al.* 2008; Rasmusson *et al.* 2007; Traggiai *et al.* 2008; Comoli *et al.* 2008; Franquesa *et al.* 2012). While the majority of the published data suggest that MSC inhibit B cell function (Franquesa *et al.* 2012; Corcione *et al.* 2006; Tabera *et al.* 2008), other publications have demonstrated a supportive role for MSC in B cell expansion and differentiation (Rasmusson *et al.* 2007; Traggiai *et al.* 2008). The mechanism by which MSC either support or inhibit B cell function has yet to be identified; however a requirement for cell contact has been suggested (Rasmusson *et al.* 2007; Traggiai *et al.*

2008). Possible explanations for the variability observed between these studies are the different experimental conditions utilised in each study, in particular the ratio of MSC to B cells, the purity of B cell populations, the activation status and indeed the maturational stage of the B cell population.

1.5 B CELL DEVELOPMENT

1.5.1 PRO-B CELL DEVELOPMENT

Mature B cells and the antibodies they produce represent an essential element of the adaptive immune response. B cells develop from pluripotent hematopoietic progenitor cells in the fetal liver and postnatal bone marrow (Kiel & Morrison 2008). In adults, early B cell development occurs within the bone marrow and consists of tightly controlled stepwise processes culminating in the functional rearrangement of immunoglobulin gene segments (Tonegawa *et al.* 1974; Matthyssens *et al.* 1976.; Hardy & Hayakawa 2001). Progenitor cells programmed to differentiate through the B cell lineage begin this transition as pro-B cells. The sole function of the pro-B cell is the immunoglobulin gene rearrangement which leads to the generation of a functional B cell receptor (BCR) complex. The BCR complex is responsible for antigen recognition and is composed of 2 identical heavy and light chains which can be further divided in to variable and constant regions (Schatz & Ji 2011). The variable domain of the heavy chain is encoded by Variable, Diversity and Joining (VDJ) gene segments and the functional rearrangement of the VDJ gene segments for the immunoglobulin heavy chain signals the progression of the pro-B cell to the pre-B cell phase of development (Pieper *et al.* 2013).

1.5.2 PRE-B CELL DEVELOPMENT

In humans, the pre-B cell undergoes 1 or 2 phases of cell division with the purpose of rearranging the immunoglobulin light chain. In the case of the immunoglobulin light chain, the focus is on rearranging the κ gene segment. If the rearrangement of the κ gene segment fails to make a viable chain, the rearrangement of the λ chain occurs (van Zelm *et al.* 2007). Successful rearrangement of the immunoglobulin light chain results in the cell surface expression of the BCR. At this stage, the B cell is classified as an immature B cell and expresses cell specific surface IgM. The immature B cell then completes its maturation process by leaving the bone marrow and migrating to the secondary lymphoid organs as a transitional B cell (Sims *et al.* 2005).

1.6 B CELL ACTIVATION

The ability of B cells to recognise and produce specific antibodies against invading pathogens is one of the fundamental mechanisms by which the humoral immune response functions. Upon recognition of specific pathogens, B cell activation is generally dependent on the presence of activated helper T cells (Kubota *et al.* 1991; Parker 1993); however under particular circumstances B cell activation can occur in the absence of T cell help (Mond *et al.* 1995; Vos *et al.* 2000).

1.6.1 T CELL DEPENDENT B CELL ACTIVATION

Signalling through the BCR is essential for B cell development and antigen recognition; however, aberrant B cell activation and recognition of self-antigens result in the development of auto-immune disease (Tuscano *et al.* 2003). To reduce the risk of this from occurring the immune system has evolved a series of complex checkpoints which

must be passed during development and activation of B cells (Tussiwand *et al.* 2009). In general, antigen recognition is not enough to induce B cell activation and proliferation and B cells require the help of T cells which have also been activated against the same antigen (Parker 1993). Antigen bound to B cells is internalised and processed into peptides which can be presented to T cells via major histocompatibility complex (MHC) class II molecules (Lanzavecchia & Bove 1985; Stern *et al.* 1994; Forquet *et al.* 1999). Helper T cells which recognise this peptide then provide cell contact signals and cytokines to B cells which induce proliferation and differentiation of B cells into antibody secreting plasma cells or long lived memory B cells (Parker 1993).

1.6.2 T CELL INDEPENDENT B CELL ACTIVATION

While the majority of B cell activation is dependent on T cell help, there are certain circumstances where B cell activation can occur in the absence of MHC class II restricted T cell signalling. T cell independent B cell activation occurs in response to T cell independent (TI) antigens, which are classified as either TI-1 or TI-2 antigens (Zhang *et al.* 1988; Mond *et al.* 1995). TI-1 antigens are generally mitogenic and include LPS expressed on the outer membrane of gram negative bacteria. These antigens are recognised by Toll like receptors (TLRs) and induce polyclonal B cell expansion. TI-2 antigens are generally simple polysaccharide structures with repeating subunits. B cells activation in response to TI-2 antigens is caused by the crosslinking of these repeating subunits to a number of B cell receptors (Mond *et al.* 1995). The activation of B cells following exposure to TI antigens is restricted to IgM production and requires IL-3, GMCSF or IFN-γ to induce isotype class switching and IgG production (Snapper *et al.* 1992; Mond *et al.* 1995; Vos *et al.* 2000).

1.6.3 ISOTYPE CLASS SWITCHING

Somatic hypermutation is essential in the development of high affinity antibodies during T cell dependent B cell activation. B cells which have bound antigen undergo point mutations in the variable regions of the heavy and light chains at a very high rate. These mutations result in an altered immunoglobulin molecule which binds the antigen with a much higher affinity than the original surface molecule. In parallel with somatic hypermutation, B cells also undergo isotype class switching. Human B cells produce 5 major classes of antibody (IgM, IgD, IgG, IgA and IgE) but also produce 4 sub-classes of IgG and 2 sub-classes of IgA (Janeway 2001). During isotype class switching the variable region of the BCR does not change, therefore retaining the specificity against the particular antigen. Instead, changes in the constant region allow the antibodies to interact with different effector cells. The induction of isotype switching in activated B cells requires both CD40 ligation and cytokine signalling; with the sub-class of secondary isotype produced dependent on the cytokines present. In this study B cell activation is driven by a cocktail containing CD40L and CpG, and is supplemented with B cell supportive cytokines IL-10, IL-2 and IL-21. Binding of CD40L to CD40 on B cells results in the activation of several transcription factors including NFκB and CREB (Francis *et al.* 1995; Zhu *et al*. 2002). CpG Oligodeoxynucleotide (CpG) are single stranded synthetic DNA molecules which are recognised by TLR9 (Bauer *et al*. 2001). Stimulation of peripheral B cells with CD40L in conjunction with CpG is known to enhance B cell activation (Carpenter *et al.* 2009). The production of IL-10, IL-2 and IL-21 by T cells enhances B cell activation, proliferation and influences immunoglobulin class switching (Malisan *et al.* 1996; Ettinger *et al.* 2005; Cerutti 2008; Tangye *et al*. 2013) (Table 1.1). The addition of these cytokines to the B cell media was designed to mimic the *in vivo* environment.

Table 1.1. Effect of Th1, Th2 and Tfh cytokines on Immunoglobulin class expression

		Immunoglobulin Isotypes					
T Helper Cell	**Cytokines**	**IgG1**	**IgG2a**	**IgG2b**	**IgG3**	**IgA**	**IgE**
Th1	**IFN-γ**	↓	↑	↓	↓	↓	↓
	IL-2	↑	—	—	—	—	↑
Th2	**IL-4**	↑	↓	↓	↓	↓	↑
	IL-5	—	—	—	—	↑	—
	IL-10	↑	↑	↑	↑	↑	↑
Tfh	**IL-21**	↑	↑	↑	↑	↑	—

1.6.4 CLONAL SELECTION

Immune recognition and the subsequent expansion of B cells specific for the recognised pathogen are fundamental to the development of immune memory and acquired immunity. The exponential expansion and long lasting memory against specific pathogens is a result of B cell clonal selection (Burnet 1959). The B cell clonal selection principle states that only B cells which are specific for the detected antigen will proliferate in response (Hodgkin *et al.* 2007). Activated B cells capable of binding the antigen subsequently undergo affinity maturation, a process designed to improve the BCR affinity to the antigen. B cells which express the highest antibody affinity to the detected antigen are selected to undergo rapid proliferation and differentiate into antibody secreting plasma cells or long lived memory cells. Long lived plasma cells circulate the body indefinitely after antigen exposure and upon reinfection these cells can rapidly differentiate to plasma cells capable of producing high affinity antibodies (Yu *et al.* 2008).

1.7 CENTRAL B CELL TOLERANCE

The randomised nature of BCR heavy and light chain variable domain recombination is fundamental to the development of a vast naïve B cell repertoire. However, randomised recombination will also result in the generation of BCRs which are capable of reacting with self-antigens (Wardemann *et al.* 2003). Therefore, the immune system has evolved stringent selection processes which are designed to remove auto-reactive B cells (MacLennan 1995). The first checkpoint for B cell auto-reactivity occurs at the immature B cell stage and determines whether or not immature B cells migrate to the periphery. B cells which are not detected as auto-reactive continue development and migrate to the periphery as transitional B cells (Loder *et al.* 1999; Allman *et al.* 2001; Tarlinton *et al.* 2003). Studies on the early B cell repertoire have reported that between 50 and 75% of immature B cells in the bone marrow are capable of recognising self-antigens (Grandien *et al.* 1994; Wardemann *et al.* 2003). These studies also examined the auto-reactivity of transitional and mature B cells recovered from the periphery and found a lower frequency of auto-reactive B cells (20-40%). While considerably lower than the proportion of auto-reactive B cells in the bone marrow, the presence of auto-reactive B cells in the periphery highlights the limitations associated with this system. Patients suffering from auto-immune disorders such as Systemic Lupus Erythematosus or Rheumatoid Arthritis also display a higher proportion of auto-reactive transitional and mature B cells than healthy patients (Samuels *et al.* 2005; Yurasov *et al.* 2005), indicating a potentially defective central B cell selection. Central B cell tolerance is mediated through a number of steps including clonal deletion, receptor editing and the positive selection of immature B cells (Pelanda & Torres 2012), which are explained in more detail below.

1.7.1 CLONAL DELETION

The clonal selection theory was first proposed over 50 years ago and suggested that immune cells capable of auto-reactivity were eliminated to prevent auto-immune responses (Burnet 1959). In order to discover the fate of newly generated auto-reactive B cells, several research groups delivered IgM and IgD responsive antibodies to new-born mice and rabbits (Lawton *et al.* 1972; Manning & Jutila 1972; Finkelman *et al.* 1983; Pelanda & Torres 2012). The injected antibodies mimicked 'self-antigens' and the administration of IgM and IgD responsive antibodies resulted in the elimination of IgM and IgD expressing B cells (Lawton *et al.* 1972; Manning & Jutila 1972; Finkelman *et al.* 1983; Pelanda & Torres 2012). The development of transgenic mice allowed more complex studies on clonal deletion to be performed. Some of the first immunoglobulin transgenic mice to be developed were the anti-hen's egg lysosome (HEL) and anti-H-$2K^{k,b}$ mice which furthered the understanding of the fate of auto-reactive B cells in the bone marrow (Pelanda & Torres 2012). These studies were the first to show that upon the detection of strongly auto-reactive B cells, the differentiation process is halted and B cell apoptosis is induced (Nemazee & Buerki 1989; Hartley *et al.* 1991; Hartley *et al.* 1993). Around the same time, it was also discovered that the differentiation of weakly auto-reactive B cells was not blocked and these were allowed to migrate from the bone marrow; however these cells had a shorter life-span due to auto-reactive cell deletion in the periphery (Goodnow *et al.* 1988). Clonal deletion plays a major role in central B cell tolerance but subsequent studies have proved that it is not the primary mechanism of preventing auto-reactive B cell development but only operates after receptor editing has failed (Halverson *et al.* 2004).

1.7.2 RECEPTOR EDITING

The concept of receptor editing was derived by two separate research groups who hypothesised that the immune system could selectively dispose of auto-reactive BCRs while preserving the cell originally producing this specificity (Gay *et al.* 1993; Radic *et al.* 1993; Tiegs *et al.* 1993). Using transgenic mice, it was possible to show that auto-reactive immature B cells were given the opportunity to edit their antigen specificity towards a non-self-antigen (Gay *et al.* 1993; Radic *et al.* 1993; Tiegs *et al.* 1993). Auto-reactive immature B cells were capable of essentially discarding their self-specific BCRs and re-activating the immunoglobulin light chain gene rearrangement program. The rearranged light chain would re-associate with the heavy chain to form a new BCR; this time however, specific for a different antigen (Gay *et al.* 1993; Radic *et al.* 1993; Tiegs *et al.* 1993). Re-edited immature B cells which were no longer auto-reactive could then progress into the periphery to continue development. At the time of conception, the phenomenon of receptor editing was very controversial and sceptically regarded as an artefact of transgenic animal models (Pelanda & Torres 2012). However, receptor editing has since been conclusively demonstrated through the use of immunoglobulin 'knock-in' mice (Pelanda *et al.* 1997; Hippen *et al.* 2005). Although this process mainly involves rearrangement of the immunoglobulin light chain, editing of the immunoglobulin heavy chain alleles can also occur (Chen *et al.* 1995). There are some potential hazards associated with receptor editing, mainly the production of intermediate B cells which express both the original auto-reactive BCR and the new rearranged BCR (Li *et al.* 2002). Through mechanisms which remain undetermined, some of these dual receptor B cells are selected into the periphery and continue their development to mature B cells (Rezanka *et al.* 2005). These dual receptor B cells can constitute up to 10% of mature B cells in mice and Casellas *et al.* suggest that dual receptor auto-reactive B cells are more potent than regular auto-reactive B cells (Casellas *et al.* 2007).

1.8 PERIPHERAL B CELL TOLERANCE

Although the mechanisms controlling central B cell tolerance are tightly regulated, they are not completely effective and some auto-reactive B cells manage to escape detection and enter the periphery. Therefore, the immune system has adapted an alternative mechanism for controlling auto-reactive B cells in the periphery. In the majority of cases, B cell activation is dependent on T cell help (Parker 1993). This is also the case for auto-reactive B cells. Auto-reactive B cells activate upon recognition of self-antigens; however, the absence of specific T cell help results in apoptosis or functional inactivation of the auto-reactive B cells (Gavin *et al.* 2004). Therefore, functional central tolerance in the T cell compartment will reduce the auto-reactivity of B cells.

1.9 MSC IN B CELL MEDIATED DISEASE

As described above, the immune system has developed a number of stringent selection processes designed to remove potentially auto-reactive B cells from development before they leave the bone marrow (MacLennan 1995). However these selection processes are not perfect and as much as 20% of auto-reactive B cells reach circulation (Grandien *et al.* 1994; Wardemann *et al.* 2003). The activation of auto-reactive B cells and subsequent production of auto-reactive antibodies can result in the development of auto-immune disorders such as rheumatoid arthritis (RA) Multiple Sclerosis (MS) or Systemic Lupus Erythematosus (SLE). The current gold standard of treatment for auto-immune disorders depends on the specific disease and symptoms but generally consist of anti-inflammatory and immuno-suppressive drugs designed to control rather than cure the disease. The potent immune modulatory ability of MSC has made them an attractive candidate for novel cell therapy for treatment for auto-immune disorders such as RA, MS and SLE.

Pre-clinical models of collagen induced arthritis have been used to investigate the potential of MSC therapy as a treatment for RA; however these studies have provided conflicting results (Augello *et al.* 2007; González *et al.* 2009b; Zheng *et al.* 2008; Djouad *et al.* 2005; Papadopoulou *et al.* 2012). The majority of these studies suggest that MSC reduced the severity of disease and resulted in lower levels of pro-inflammatory cytokines, increased anti-inflammatory cytokines and the development of regulatory T cells (Augello *et al.* 2007; Liu *et al.* 2010; González *et al.* 2009b; Zheng *et al.* 2008). However, other research groups have reported no beneficial effects of MSC therapy in murine models of RA (Djouad *et al.* 2007; Papadopoulou *et al.* 2012). Despite conflicting results, MSC therapy has undergone clinical trials for the treatment of rheumatoid arthritis and have demonstrated positive results (Liu *et al.* 2010; Wang *et al.* 2013). These studies demonstrated that MSC therapy did not result in adverse effects up to 6 months after administration. MSC therapy in conjunction with anti-rheumatic drugs significantly decreased the presence of pro-inflammatory cytokines TNF-α and IL-6 and increased regulatory T cell production (Wang *et al.* 2013).

Experimental autoimmune encephalomyelitis (EAE) is currently the most applicable mouse model in which to study MS. The administration of MSC therapy to murine models of EAE has demonstrated beneficial effects (Rafei *et al.* 2009; Zappia *et al.* 2005; Bai *et al.* 2012; Fisher-Shoval *et al.* 2012; Guo *et al.* 2013); however there have also been reports where MSC therapy exacerbated disease (Grigoriadis *et al.* 2011; Glenn *et al.* 2014). Despite the concerns raised by these studies, MSC therapy has progressed to small scale clinical trials as a treatment for MS. In early trials, the administration of autologous MSC to MS patients was well tolerated but did not result in significant improvements (Yamout *et al.* 2010; Karussis *et al.* 2010). However recent phase II trials have demonstrated efficacy of MSC therapy using autologous (Llufriu *et al.* 2014) or allogeneic MSC (Li *et al.* 2014).

The ability for MSC therapy to treat SLE has also been examined using murine models and has again produced conflicting results (Zhou *et al.* 2008; Sun *et al.* 2009; Gu *et al.* 2010; Youd *et al.* 2010). The majority of published studies suggest that MSC therapy results in significant improvement in SLE pathology, joint pain and antibody production (Zhou *et al.* 2008; Sun *et al.* 2009; Gu *et al.* 2010); however the administration of MSC therapy to SLE mice has also been reported to exacerbate disease (Youd *et al.* 2010). As a result of the inconsistencies observed in animal models, the administration of human MSC as a cell therapy to Lupus patients has been limited. However, the clinical studies which have been conducted to date provide promising results (Sun *et al.* 2010; Liang *et al.* 2010; Wang *et al.* 2014). The administration of MSC therapy to SLE patients did not result in adverse effects for the 18 month duration of follow up studies. Significant improvements in disease score, levels of auto-antibody, proteinuria, renal function and increased presence of regulatory T cell were observed in SLE patients following MSC therapy (Sun *et al.* 2010; Liang *et al.* 2010; Wang *et al.* 2014). Interestingly MSC isolated from Lupus patients demonstrate slower proliferation and limited cytokine production compared to MSC isolated from healthy donors (Sun *et al.* 2007). These results suggest that allogeneic MSC isolated from healthy donors may be more useful in treating auto-immune disorders.

While acute GvHD (aGvHD) is considered to be a T cell mediated disease, the progression of chronic GvHD (cGvHD) shares a number of key features with the pathology of autoimmune disorders such as scleroderma or SLE (Ratanatharathorn *et al.* 2001; Zhang *et al.* 2006). In contrast to acute aGvHD, cGvHD pathology is mediated by Th2 cytokines and results in B cell dysregulation and elevated serum antibody levels (Ratanatharathorn *et al.* 2001). Clinical approaches to controlling cGvHD have focused on the administration of the monoclonal antibody rituximab during disease development, designed to deplete $CD20^{+}$ B cells (Ratanatharathorn *et al.* 2000; Cutler *et al.* 2006;

Clavert *et al.* 2013). Eliminating $CD20^+$ B cells significantly reduced disease pathology with some patients reporting the alleviation of clinical cGvHD symptoms (Clavert *et al.* 2013). As a result of the beneficial effects observed following MSC therapy in models of autoimmune disorders, pre-clinical models of cGvHD were established to determine possibility of MSC as a cell therapy. The results were promising and MSC promoted Th1 and Th2 balance in cGvHD mice in addition to alleviating cGvHD symptoms.

MSC therapy for cGvHD has rapidly progressed to clinical trials (Weng *et al.* 2010). This study demonstrated MSC therapy was safe and also effective in treating cGvHD patients, with 78% of patients demonstrating partial or full resolution of symptoms in the skin, gut and liver (Weng *et al.* 2010). More recently, another clinical trial successfully administered MSC therapy to 23 refractory cGvHD patients. 20/23 patients reported partial or complete responses (Peng *et al.* 2014). The authors suggested that the decrease in pathology was mediated by MSC induction of IL-10 producing $CD5^+$ regulatory B cells. MSC therapy significantly increased the survival and enhanced the proliferation capacity of these cells through a mechanism involving IDO production (Peng *et al.* 2014).

1.10 MAJOR HISTOCOMPATIBILITY COMPLEX IN TRANSPLANTATION

The major histocompatibility complex (MHC), human leukocyte antigen (HLA) in humans, is an integral part of the immune system and contains important polymorphic genes which encode proteins that present antigen to self-restricted T cells (Snell 1948). MHC are essential in the discrimination of self from non-self (Doherty & Zinkernagel 1975b; Doherty & Zinkernagel 1975a) and the induction of immune tolerance, first proposed by Peter Medawar in 1953. The exact pattern of MHC gene expression, known as the haplotype, is almost unique to each individual; therefore transplanted allogeneic T

cells which do not recognise the recipient's MHC molecules become activated (Snell 1948). As a result of this, immune cells recognise non-self MHC as foreign and attempt to clear these cells from the body.

MHC recognition is one of the major limiting factors affecting the success of both solid organ and bone marrow transplantation. Donor derived cells which express different MHC molecules are subject to recognition and clearance by the recipient's immune system in a similar manner to an invading pathogen. The identification and characterisation of MHC molecules by Gorer, Snall and Daussett and others in the first half of the 20th century has been essential to the progression made in understanding the immune system and its manipulation during transplantation. Gorer first identified natural antibodies in human sera which were capable of distinguishing between red blood cells isolated from 3 different strains of mice (Gorer 1936). Around the same time, Snell had identified tumor transplantation resistant genes that he termed histocompatibility or H genes. Together with Gorer, Snell discovered the major histocompatibility (MHC) antigen, which resulted in rapid transplant rejection compared to minor histocompatibility molecules (miHA) (Gorer 1936; Snell 1948; Snell & Higgins 1951).

The above studies propelled MHC genes to the forefront of transplant research and their role in human transplantation. In 1958, the first human HLA was identified following the screening of patients who had undergone multiple blood transfusions (Degos 2009). This study discovered that administering sera from some donors resulted in clumping of leukocytes and they subsequently discovered an anti-sera capable of detecting allogeneic antigen expressed by human leukocytes, which he termed MAC but is now known as HLA-A2 (Degos 2009). From these studies, Daussett hypothesised that MAC, along with then uncharacterised antigens, would be essential in the success of human bone marrow transplantation between MHC mismatched donors.

The discovery of HLA genes and subsequent understanding of their importance in transplant rejection supported the concept of immunological tolerance and tissue transplantation derived by Billingham, Medawar and Brent (Billingham *et al.* 1953) and contributed hugely to the fields of solid organ and bone marrow transplantation. These fields were further advanced following the discovery of powerful immunosuppressants (cyclosporine A and tacrolimus) which have permitted solid organ transplantation between MHC mismatched patients (Messina *et al.* 2008).

1.11 HAEMATOPOIETIC STEM CELL TRANSPLANTATION

Haematopoietic stem cell transplantation (HSCT) is the current gold standard of treatment for patients suffering with haematological malignancies and inherited blood disorders (Reddy & Ferrara 2003). HSCT has become common practice with over 25,000 procedures carried out globally (Ferrara *et al.* 2009). Patients of HSCT first undergo a conditioning regimen which can consist of chemotherapy, radiotherapy and/or T cell depletion (Shlomchik 2007). Pre-conditioning regimens are designed to eliminate the patient's T and B cells leaving them highly immunocompromised and more permissive to the engraftment of donor bone marrow. The engraftment of activated donor T cells has an effect on the remaining leukaemia (Graft versus Leukaemia (GvL)) or tumor cells (Graft versus Tumor (GvT)) (Horowitz & Bortin 1990; Trenado *et al.* 2003). This represents a double edged sword however, as active donor T cells may also cause pathology (GvHD) as a result of donor/host MHC mismatch at both MHC and miHA level (Korngold & Sprent 1978). GvHD can be considered a mirror image of solid organ transplant rejection in that donor cells reject the recipient's cells by recognising recipient's MHC as foreign.

1.12 PATHOPHYSIOLOGY OF GVHD

Graft versus host disease is a major complication associated with HSCT which results in target tissue apoptosis. In order for the development of GvHD to occur, the recipient must be immunodeficient (unable to mount a successful immune response against the graft), the donor graft must contain immunocompetent cells and the tissue antigens (HLA) expressed by the patient must be recognised by the donor's HSC (the graft) (Billingham 1966.). Over the last number of years, improvement in donor selection, conditioning regimens, GvHD prophylaxis and treatment, and attention to infectious complications means that the majority of transplant related mortality is caused by a relapse of primary malignancies (Markey *et al.* 2014). Despite the recent advances, GvHD still remains a major cause of treatment failure, and mortality in approximately 20% of transplant patients; and a study of HSCT transplant patients from 2003 – 2007 showed that 70% of patients developed some level of GvHD (Gooley *et al.* 2010).

Originally characterised as a cytokine storm (in particular TNF-α) (Ferrara & Deeg 1991), the development of GvHD occurs in 3 phases: (1) pre-transplant conditioning regimen and associated inflammation, (2) donor T cell priming and differentiation and (3) the effector phase of tissue apoptosis mediated by inflammatory cytokines and effector cells (Figure 1.1).

As mentioned above HSCT patients undergo a pre-conditioning regimen of myeloablative chemotherapy, with or without total body irradiation. Although necessary to facilitate the engraftment of donor immune cells, the intensity of the pre-conditioning regimen can influence the timing and nature of GvHD development. Pre-conditioning regimens are known to affect the permeability of the gut which results in the leakage of LPS into the system and a subsequent inflammatory response (Ferrara *et al.* 2009). There have been attempts to improve the integrity of the GI tract by the administration of IL-11

and keratinocyte growth factor (KGF) (Hill & Ferrara 2000). Despite promising results in animal models, toxicity and incomplete efficacy in patients has hampered progression (Antin *et al.* 2002).

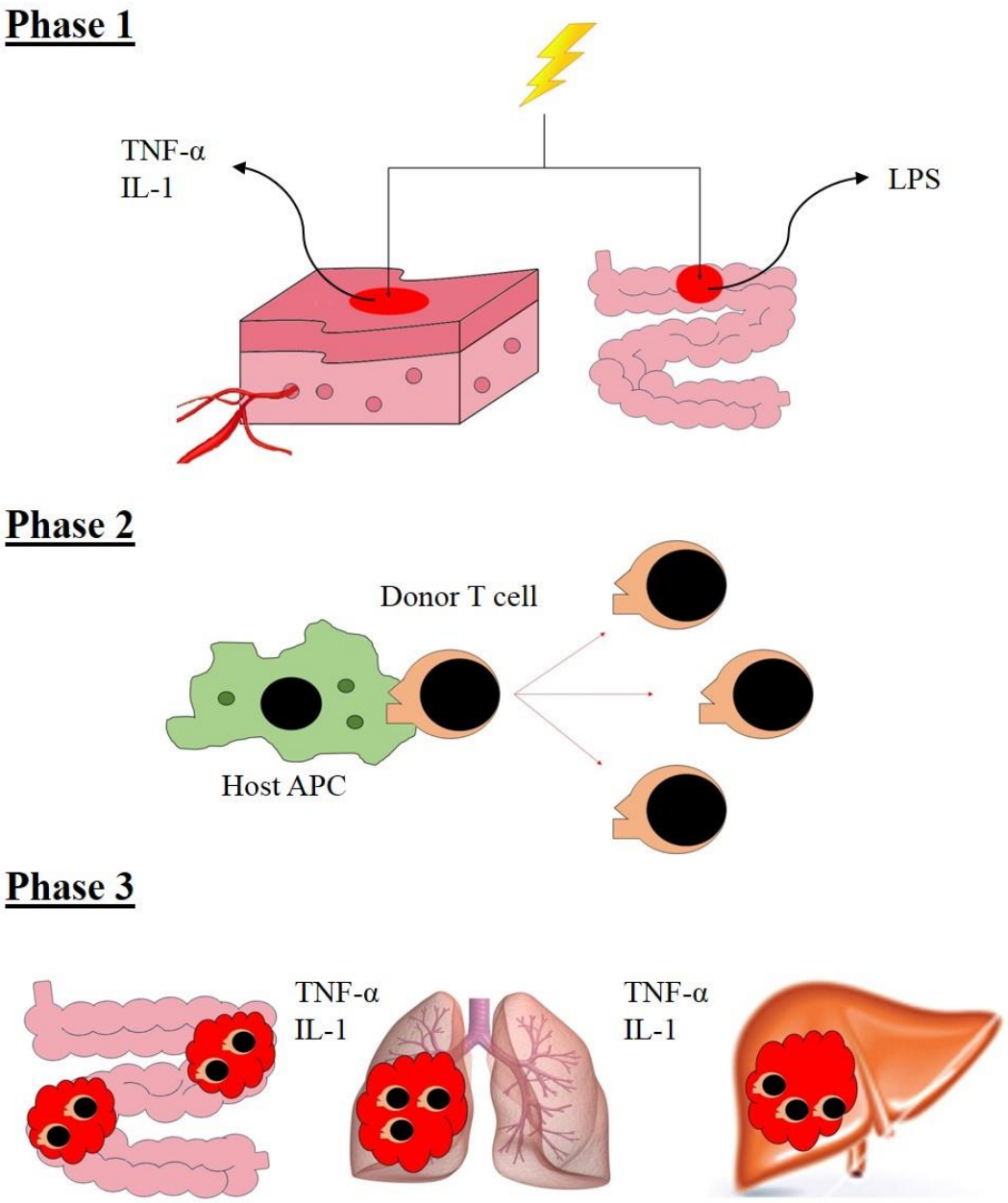

Figure 1.1. Pathophysiology of GvHD during murine model occurs in 3 phases. In phase 1, the pre-conditioning regimen damages host tissue resulting in the secretion of pro-inflammatory cytokines TNF-α and IL-1. Increased expression of these cytokines leads to host antigen presenting cell (APC) activation. The pre-conditioning regimen can also damage intestinal mucosa leading to leakage of lipopolysaccharide (LPS) into the periphery. During phase 2, activated host APC activate mature donor T cells. The donor T cells then proliferate and differentiate to effector T cells. Donor derived effector T cells then migrate to target tissues. In phase 3, effector T cells infiltrate small intestine, lungs and liver and can directly induce apoptosis. Subsequent increases in TNF-α result in necrosis and apoptosis.

The priming and differentiation of donor T cells is the hallmark of the second phase of GvHD pathogenesis. Donor T cells contained within the graft become activated by the inflammatory environment created by the conditioning regimen. The priming and differentiation of donor T cells is dependent on direct interaction with both host and donor derived antigen presenting cells (APC) (Ferrara *et al.* 2009). The current understanding is that $CD8^+$ T cells become activated after encountering the host's haematopoietic APC while $CD4^+$ T cells are activated by non-haematopoietic APC in the gut. Donor APC can further contribute to T cell priming. To date, a number of steps have been taken to try to inhibit the activation and expansion of donor T cells. Ablative cell therapies have been explored but studies have shown that no single recipient APC subset is essential for the development of GvHD; however donor DC appear to be the critical APC in the presentation of allogeneic antigen and maintenance of GvHD (Markey *et al.* 2014). Studies investigating blocking of co-stimulatory molecules (CD40-CD154 or CD80/86-CD28/CTLA4) in renal transplant patients have demonstrated some efficacy (Kinnear *et al.* 2013); however this strategy is only now being explored for bone marrow transplantation. Upon activation, donor T cells proliferate and differentiate to pro-inflammatory cytokine producing cells with cytolytic function. Novel methods to control the activation and differentiation of donor T cells after HSCT have focused on controlling the naïve T cell population. Mouse models have suggested a role for naïve T cells in aGvHD development and there has been some human data to support this (Dutt *et al.* 2007). Therapies focusing on ablating naïve T cells in the graft before administration are currently under clinical investigation in the US. However, the current standard of treatment against GvHD is to use immunosuppressants to prevent T cell expansion and differentiation but GvHD still occurs, suggesting novel methods of treatment need to be identified.

The combined effect of the inflammatory environment created by pre-conditioning regimens along with donor T cell activation and differentiation results in an uncontrolled immune response in which inflammatory cytokines and cytotoxic T cells mediate antigen dependent and independent destruction of target tissues (Ferrara *et al.* 2009). TNF-α, IL-1 and IFN-γ are some of the main cytokines involved in driving GvHD and can induce apoptosis of target tissues without direct interaction. Pro-inflammatory cytokine production is mediated by differentiated T cells which amplifies the production from monocytes or macrophages (Hill & Ferrara 2000). In contrast GvHD driven by $CD8^+$ T cells is dependent on cognate interaction between $CD8^+$ T cells and target tissues. $CD8^+$ T cells induce tissue apoptosis through perforin & granzyme molecules, TNF signalling and the Fas/FasL pathway (Graubert *et al.* 1997; Hattori *et al.* 1998; Maeda *et al.* 2005).

While efforts to control GvHD have examined the possibility of interfering with the progression of disease at this phase, these activated T cells are required to attack remaining leukaemia (GvL) through perforin granzyme, TNF-related apoptosis inducing ligand and Fas/FasL mediated apoptosis pathways (Pan *et al.* 1999; Schmaltz *et al.* 2003; Hill *et al.* 1999). Therefore inhibiting the apoptotic abilities of these cells may be deleterious to the GvL function of the graft; however this may offer a viable option for patients who have already cleared the leukemic cells but are presenting severe GvHD symptoms.

1.13 Clinical features of GvHD

GvHD is a systemic condition characterised by the targeted apoptosis of the skin, liver and GI tract. Although idiopathic pneumonia syndrome is commonly associated with the progression of GvHD, it is regarded as a manifestation of the lung rather than

apoptosis (Markey *et al.* 2014). The most common clinical symptom occurs in the skin (81%) followed by the GI tract (54%) (Martin *et al.* 1990). The painful maculopapular rash which develops on the skin of aGvHD patients is caused by necrosis of the epithelial cells and presents on the palms of the hands or soles of the feet in most patients (Ferrara *et al.* 2009). In severe cases, the rash can lead to blistering and ulcer formation causing excruciating pain and discomfort to patients. Targeted apoptosis of the epithelial cells which line the GI tract results in severe abdominal pain and diarrhoea (Martin *et al.* 1990). As the damage to the GI tract progresses it can lead to bloody diarrhoea, vomiting, and extreme weight loss in patients. Damage to the liver is more difficult to diagnose and quantify during GvHD and is difficult to distinguish from other causes of damage during HSCT (secondary effects from pre-conditioning regimen or drug toxicity) (Ferrara *et al.* 2009). Damage of hepatic tissue is generally detected as hyperbilirubinaemia and jaundice (Ferrara *et al.* 2009; Tolar *et al.* 2011).

aGvHD progression is classified as grade I to grade IV (mild, moderate, severe and very severe) depending on the number of target organs involved and the extent of damage in each. Each grade of disease correlates directly with the chance of survival (Ferrara *et al.* 2009). The average long term survival rate for patients diagnosed with grade III aGvHD is ~25%; however this survival rate drops to 5% for patients diagnosed with grade IV aGvHD (Cahn *et al.* 2005). The therapeutic prevention of aGvHD has focused on the reduction of pathology in an attempt to prolong survival.

1.14 THERAPEUTIC PREVENTION OF GVHD

1.14.1 THERAPEUTIC PREVENTION OF AGVHD

Despite the recent advances and the level of research currently being dedicated to controlling the development of aGvHD, the progress made in terms of eliminating the

disease has been modest. In Europe, the current standard of treatment remains the administration of glucocorticosteroids (methylprednisolone) in combination with immunosuppressive drugs (cyclosporine A or Tacrolimus) (Dhir *et al.* 2014). The combination of steroid therapy and immunosuppressant drugs is designed to trigger lymphocyte lysis and promote an anti-inflammatory environment (steroid therapy) while dampening down the activation of immune cells by keeping the patient in an immunocompromised state. The type and dose of steroid therapy and immunosuppressant drugs are personalised for each patient and patient responsiveness is generally dependant on the severity of disease (MacMillan *et al.* 2002; Van Lint *et al.* 2006). However a typical course of treatment for patients diagnosed with aGvHD is the administration of methylprednisolone (2 mg/kg) for 7-14 days with a gradual reduction depending on patient responsiveness (Van Lint *et al.* 1998; Messina *et al.* 2008). The administration of these drugs have resulted in significant increases in survival and provided huge improvements to the standard of living for GvHD patients (Van Lint *et al.* 1998; MacMillan *et al.* 2002; Van Lint *et al.* 2006) and depending on the patient's response and severity, the dose and period of treatment can be reduced. However, there are major limitations to these treatments including the risk of infection, hyperglycaemia, osteoporosis, potentially life threatening growth defects and the financial burden of life long treatment (Reddy *et al.* 2009). The biggest problem with this therapy is the development of steroid resistant GvHD in certain patients who no longer respond to treatment. In these patients a second line of treatment is required.

The decision to progress from the primary course of treatment to a secondary line of treatment is dependent on the progression of the disease. A secondary line of treatment is deemed necessary for patients where there is a worsening in disease pathology in any organ over 3 days, if there has been no improvement in condition over 7 days or if there is incomplete response to treatment over 14 days (Deeg 2007). The most commonly

prescribed secondary line of treatments consist of monoclonal or polyclonal antibodies (Doney *et al.* 1985; Carpenter *et al.* 2002). To date, there have been a number of approaches taken in an attempt to prevent the development of aGvHD including the partial depletion or elimination of specific T cells from the graft before administration to patients; however the depletion of T cell subsets from the graft resulted in inconsistent results and increased the possibility of graft failure or leukemic relapse (Horowitz & Bortin 1990). Over the last few decades, the potent immunosuppressant anti-thymocyte globulin (ATG) has been administered to patients of aGvHD. ATG has been successful in reducing the frequency of aGvHD development in related-donor HSCT patients without increasing the risk of tumor relapse (Doney *et al.* 1985; Kröger *et al.* 2002). However, the administration of ATG has proven clinically problematic with patients presenting high levels of variability as well as the development of adverse effects (hypotension, anaphylactic reactions) in up to 80% of patients. The median long term survival for patients receiving ATG remained ~5-32% (MacMillan *et al.* 2002; Graziani *et al.* 2002).

Another technique developed to prevent the development of GvHD was to induce apoptosis of activated T cells using the anti-CD3 monoclonal antibody Visilizumab. Initial results from clinical trials were very promising and it was determined that outcome of treatment was dependent on the initial dose administered (Carpenter *et al.* 2002). However, as with ATG, there were complications associated with the use of Visilizumab clinically. Patients who received Visilizumab were prone to reactivation of Ebstein Barr Virus (EBV) which led to post transplant lymphoproliferative disease (Carpenter *et al.* 2002). The monoclonal antibody Alemtuzumab binds to CD52 and induces apoptosis of lymphocytes, monocytes and DC. Initial results from phase II clinical trials found that administration of Alemtuzumab lowered the frequency of both acute and chronic GvHD development (Pérez-Simón *et al.* 2005). However, subsequent studies reported

complications with infection and increased relapse rates leading to graft failure (Delgado *et al.* 2006).

One of the most successful second line treatments developed to date has been in targeting the production of TNF-α during aGvHD. Elevated levels of TNF-α have long been associated with severe GvHD development (Holler *et al.* 1990; Kitko *et al.* 2008). 2 different drugs targeting TNF-α have been investigated in clinical trials, etanercept which binds trimeric and membrane bound TNF-α, and infliximab, a monoclonal antibody designed to bind monomeric, trimeric soluble and membrane bound TNF-α (Ehlers 2005). The phase II clinical trial of etanercept (in combination with steroid therapy) resulted in complete resolution of symptoms in 70-80% of patients of GI tract or skin aGvHD (Levine *et al.* 2008). Despite this result, the adverse effects associated with etanercept make it difficult to use as a treatment (MacMillan *et al.* 2002; Graziani *et al.* 2002; Carpenter *et al.* 2002; Levine *et al.* 2008). The efficacy of infliximab was investigated in a small scale clinical trial of 11 steroid refractory aGvHD patients (Jacobsohn *et al.,* 2003). The results from the study were not promising as only 2 out of 11 patients treated completely responded to infliximab treatment. Another 5 patients partially responded to the treatment however 4 patients were unresponsive to infliximab (Jacobsohn *et al.* 2003). One result which was of note was that the 2 patients which responded to infliximab had acute GI GvHD, suggesting that infliximab treatment may be appropriate under certain circumstances (Jacobsohn *et al.* 2003). Infliximab administration also increased patient susceptibility to infection with 6 of the 11 patients presenting fungal infections at the time of death (Jacobsohn *et al.* 2003). More recently, a large scale trial investigated the efficacy of infliximab therapy in conjunction with corticosteroid treatment in 52 refractory aGvHD patients (Pidala *et al.* 2009). The complete response rate of aGvHD patients was not significantly higher than the initial trial and infliximab administration again resulted in extensive bacterial and fungal

infection (Pidala *et al.* 2009). The incomplete efficacy and adverse effects of monoclonal antibodies as second line treatments for aGvHD patients indicate that a more effective therapy needs to be designed. Recent approaches to treating aGvHD have focussed on designing cellular therapies for inflammatory mediated disease.

1.14.2 THERAPEUTIC PREVENTION OF CGVHD

The pathophysiology of cGvHD can affect almost every organ and generally requires lengthy and intensive immune suppression. As with aGvHD, the current approach to treating cGvHD patients is to administer strongly immune suppressive corticosteroids in combination with calcineurin inhibitors (Dhir *et al.* 2014). The dosing concentration and frequency is generally tailored for each individual patient and is dependent on the severity of disease (Dignan *et al.* 2012); however a standard course of treatment is the daily administration of Prednisolone (1mg/kg) in combination with cyclosporine reduced to alternative day dosing after 1-2 months (Dhir *et al.* 2014). However, the side effects associated with long term administration of cyclosporine, long term toxicity and renal failure, emphasise the need to identify alternative treatment (Hingorani *et al.* 2005). In addition, the nature of this therapy can result in the development of steroid refractory GvHD.

A number of different approaches have been examined as potential second line treatments for cGvHD including mTOR inhibitors, pentostatin and extracorporeal photophoresis (ECP). The ability to modulate cGvHD through the administration of the mTOR inhibitor Sirolimus has demonstrated promising results in a phase II clinical trial. Refractory cGvHD patients which received Sirolimus in combination with Tacrolimus and corticosteroids demonstrated a 60% complete response rate (Couriel *et al.* 2005); however there are significant side effects associated with the use of mTOR inhibitors

including toxicity and renal failure (Schwarz *et al.* 2010) making them unsuitable for routine clinical use. Pentostatin is a chemotherapeutic agent used in the treatment of hairy cell leukemia (Maloisel *et al.* 2003). A phase II clinical trial investigating the administration of Pentostatin to refractory cGvHD patients demonstrated promising results with over 50% of patients demonstrating complete response (Jacobsohn *et al.* 2009). However, infusion of Pentostatin led to high incidence of serious infection and may not be suitable for long term clinical use (Jacobsohn *et al.* 2009). A more promising method of treating refractory cGvHD patients may well be extracorporeal photophoresis (ECP). ECP is an apheresis based therapy originally designed to treat cutaneous T cell lymphoma (Edelson *et al.* 1987) but has since been tested in patients with solid organ allograft rejection (Barr *et al.* 1998), Crohn's disease (Abreu *et al.* 2009) and GvHD (F L Dignan *et al.* 2012; Tsirigotis *et al.* 2012). The concept of ECP therapy is that patient's blood is passed through UV light which induces apoptosis of mononuclear cells. Upon subsequent re-infusion, these apoptotic cells are processed by DC which induce anti-imflammatory cytokine production and the generation of Treg cells. Clinical trials which have investigated ECP therapy for cGvHD patients have demonstrated promising results with very few side effects (Flowers *et al.* 2008; Greinix *et al.* 2011).

1.15 CELL THERAPIES FOR GVHD

1.15.1 REGULATORY T CELLS

Regulatory T cells (Treg) are a subset of $CD4^+$ T cells which possess potent immunomodulatory ability and are defined as $CD4^+CD25^{high}FoxP3^+$. The expression of CD127 has been used to separate immune suppressive Treg cells ($CD127^{low}$) from activated effector T cell populations ($CD127^{high}$) (Seddiki *et al.* 2006; Hartigan-O'Connor *et al.* 2007). Treg cells can be thymus derived (natural Treg) or generated in the periphery

and whose activation is dependent on T cell receptor engagement and cytokines (induced Treg). It is believed that natural Treg cells hold a more stable and potent role in promoting self-tolerance and preventing auto-immunity (Safinia *et al.* 2013). Treg cells also express CD27, CD45RA, CD39, CD122 and glucocorticoid-induced tumor necrosis factor receptor (GITR) (Fletcher *et al.* 2009; Dieckmann *et al.* 2001; Jonuleit *et al.* 2001).

Treg cells are potent regulators of the inflammatory response and modulate immune cells through the production of the anti-inflammatory cytokines IL-10, TGF-β and IL-35 and by signalling directly through cell contact (Chen *et al.* 2003; Roncarolo *et al.* 2006; Collison *et al.* 2007). The ability of Treg cells to directly induce T cell apoptosis through a perforin-granzyme dependant mechanism has also been demonstrated (Grossman *et al.* 2004; Gondek *et al.* 2005). Co-culture of Treg cells in the presence of DC reduced the antigen presentation ability and co-stimulatory function of DC through cyclic adenosine monophosphate (cAMP) production by the Treg cell and subsequently reduced the expression of the co-stimulatory molecules CD80 and CD86 on DC (Safinia *et al.* 2013; Fassbender *et al.* 2010).

Adaptive immunity is a term first coined by Billingham and colleagues in 1953 to describe the successful generation of a tolerant immune system following the transfer of active immune cells but it wasn't until 1990 that $CD4^+CD25^+$ T cells were identified as the cells responsible (Wood & Sakaguchi 2003; Hall *et al.* 1990). The study of Hall *et al.* determined that the adoptive transfer of $CD4^+CD25^+$ T cells generated tolerance in rats which received cardiac allograft (Hall *et al.* 1990). Since this there has been a number of studies which have investigated a role for Treg cells as a cell therapy against the rejection of solid organ transplants. Sakaguchi *et al.* used Treg cells from naïve mice to prevent the rejection of allogeneic skin grafts in T cell deficient nude mice (Sakaguchi *et al.* 1995). Subsequent studies have highlighted that the presence of Treg cells at the time

of transplantation is critical for the inducing and maintaining tolerance to the graft (Wood & Sakaguchi 2003).

Despite the difficulties associated with the isolation and expansion of Treg cells, a number of clinical trials have been undertaken to determine the therapeutic values of Treg cells. The first clinical trial to report beneficial effects of Treg cell therapy on allograft survival was conducted by Trzonkowski *et al.* This small scale study demonstrated the ability of Treg cells to reduce pathology in GvHD patients. This small scale study followed 2 patients (Trzonkowski *et al.* 2009). The first patient developed cGvHD within 2 years of receiving the transplant. The patient received 1 x 10^5/kg autologous Treg cells which had been FACS purified and expanded *ex vivo*. GvHD symptoms were reduced and the patient was removed from immunosuppressive treatment without recurrence (Trzonkowski *et al.* 2009). The second patient was diagnosed with acute GvHD within the first month following transplantation and received several infusions of autologous Treg cells. Despite initial improvements, the patient succumbed to the disease (Trzonkowski *et al.* 2009). Although these results were sub-optimal, this study demonstrated that *ex vivo* expanded Treg cells were tolerated by the patient and gave rise to further large scale clinical trials.

A larger phase I/II clinical trial involving 23 patients undergoing umbilical cord blood stem cell transplantation who received escalating doses of Treg cells (1 x 10^5 to 30 x 10^5 Treg cells) was subsequently completed (Brunstein *et al.* 2011) $CD4^+CD25^{high}$ Treg cells were isolated from third party umbilical cord blood and expanded *ex vivo* using anti-CD3/CD28 coated beads and recombinant IL-2 for 18 days. The administration of Treg cells reduced the instances of grade II – IV acute GvHD in comparison to historic controls; however, overall GvHD occurrence was not significantly reduced (Brunstein *et al.* 2011).

A third clinical trial (phase I/II) investigated the effect of Treg cell therapy on GvHD development after HSCT to treat haematological malignancies (Di Ianni *et al.* 2011). This study also focused on the administration of donor Treg cells as well as donor conventional T cells to HSCT patients without the use of adjuvants or patient immunosuppression. Different dosing conditions were implemented at the beginning with patients receiving doses of between 5 x 10^5/kg conventional T cells with 2 x 10^6/kg Treg cells to 2 x 10^6/kg conventional T cells with 4 x 10^6/kg Treg cells. However 2 patients receiving the highest dose of treatment developed GvHD; therefore the authors recommended a dose of 1 x 10^6/kg conventional T cells with 2 x 10^6/kg Treg cells (Di Ianni *et al.* 2011). Patients which received Treg cell therapy had accelerated immune engraftment, reduced reactivation of latent cytomegalovirus (CMV) with a lower instance of GvHD compared to historic controls. However, the survival rate of GvHD patients who had received Treg cell therapy remained at 50% (Di Ianni *et al.* 2011).

1.15.2 MESENCHYMAL STROMAL CELLS

Over the last number of years, the array of potential applications for MSC therapy has grown significantly. Allogeneic MSC therapies have been tested in clinical trials for the prevention or treatment of GvHD, Crohn's disease, Multiple Sclerosis and critical limb ischemia. The first indication that MSC could be developed into a cell therapy came from a study by Lazarus *et al.* where they reported that the administration of autologous MSC to cancer patients resulted in accelerated haematopoietic recovery (Lazarus *et al.* 1995). In 2002, Bartholomew *et al.* demonstrated that MSC derived from baboons were capable of prolonging survival of autologous, donor or allogeneic skin graft transplantations in a primate model (Bartholomew *et al.* 2002). Since this study, both

autologous and allogeneic MSC have been administered to patients receiving HSCT for haematological malignancies in clinical trials.

By far the most successful results for MSC therapy have been observed in the treatment of aGvHD after allogeneic stem cell transplantation. In 2004, the first transplantation of MSC as an allogeneic cell therapy for patients with steroid resistant grade IV GvHD was performed by Le Blanc *et al.* and demonstrated remarkable immunosuppressive effects (Le Blanc *et al.* 2004). A 9 year old patient who had received a MHC-matched HSC transplant from a non-related donor to treat leukaemia was diagnosed with severe steroid-resistant acute GvHD of the gut and the liver. A cell therapy of haplo-identical MSC was generated and administered over 2 doses. However the exact mechanisms by which the MSC therapy mediated this effect was not determined (Le Blanc *et al.* 2004). Importantly this study demonstrated that MSC therapy was safe, MSC did not inhibit the engraftment of the transplanted graft and complete chimerism was observed in the patient (Le Blanc *et al.* 2004). In a later study, the same research group demonstrated that the source of MSC (autologous or allogeneic) had no effect on their ability to treat GvHD (Le Blanc *et al.* 2008).

Despite this very promising progress into the development of MSC therapy to treat aGvHD, the results of a large scale phase III clinical trial by Osiris Therapeutics provided a setback for the field. Osiris Therapeutics developed an MSC-like cell therapy called Prochymal™ which demonstrated safety for human administration and benefit to patients with aGvHD during phase II clinical trials (Kebriaei *et al.* 2009). In a large scale phase III clinical trial, Prochymal™ significantly increased response rates in patients with steroid refractory liver GvHD and steroid refractory gastrointestinal disease over patients treated with placebo. However overall the study did not reach its primary endpoint to significantly increase the complete response rates in steroid refractory GvHD patients for at least 28 days in comparison to placebo controls (Martin *et al.* 2010). Notably,

Prochymal cell therapy showed good progression in reducing aGvHD in the liver and gastro-intestinal tract of patients but did not demonstrate any improvement against skin aGvHD symptoms (Martin *et al.* 2010). The potential for MSC to preferentially work in one organ over another is very interesting and raises a lot of questions behind the mechanism of action. The development of novel models of aGvHD are essential to the discovery of why this may happen. Overall, these results highlighted the potential of allogeneic MSC as a candidate therapy to treat acute steroid refractory GvHD when administered after donor T cell recognition but also further emphasized the large gap in our understanding of how MSC mediate their beneficial effect in a clinical setting.

1.16 Animal models of GvHD

Despite the recent advances in understanding and developing therapies against GvHD, only modest improvements have been achieved. This underlines the necessity for more accurate and reproducible animal models to further advance the understanding of the disease and to develop novel therapies. Although non-human primates are currently being used as disease models, these animals are subject to much more vigorous ethical restraints and are far more expensive. Therefore murine models of human disease have become a more feasible and informative option for human observation, in particular when investigating hypotheses. The majority of murine models available to study GvHD are designed for the transplantation of donor lymphocytes to irradiated hosts. In these scenarios the severity of GvHD development is dependent on the dose of pre-conditioning, and the amount and type of transplanted lymphocytes. The most commonly used and straightforward murine models of GvHD involve the transplantation of MHC mismatched lymphocytes into a murine host; however in recent years the development of

humanised mouse models has provided a more clinically relevant system in which to analyse potential cell therapies.

The current knowledge available regarding the stages leading up to GvHD development have largely been identified through the use of murine models (Schroeder & DiPersio 2011). Importantly, the pathogenesis of GvHD in murine models is very similar to that observed in humans. As with human GvHD patients, murine models of GvHD present apoptosis and destruction of the lungs, liver, skin and GI tract. Similar to humans, pre-conditioning regimens and GvHD development results in extensive damage to the integrity of the GI tract in mice, resulting in diarrhoea and significant weight loss. The tissue specific apoptosis observed in human patients can also be observed in murine models through histological analysis. The reproducibility of murine GvHD models allows the development of a standardised and well defined scoring system to determine the severity of GvHD development within each mouse (Tobin *et al.* 2013). As with all models of disease, there are a number of caveats associated with murine models of GvHD. Fundamental differences in murine immunology, including subpopulations of immune cells, MHC molecule expression, costimulatory molecule expression and function, cytokine expression, lymphocyte differentiation as well as immune signalling components, must be considered when interpreting and translating results (Mestas & Hughes 2004). More specifically to GvHD, the pre-conditioning regimen varies between the fractionated administration utilised in humans and the single dose generally used for mouse models. The pre-conditioning regimen results in tissue damage and subsequent pro-inflammatory environment which influences the development of disease (Ferrara *et al.* 2009). Disparities between pre-conditioning regimens may impact experimental outcomes. The source of donor immune cells is also an important difference. In humans HSCT are generally conducted using mobilized stem cells in circulation while BMT conducted in murine models can contain material from the bone marrow and spleen or

peripheral blood in humanised mouse models. The differences in transplanted cell populations is likely to influence GvHD pathology (Schroeder & DiPersio 2011). Despite these differences, murine GvHD models remain the most suitable *in vivo* system currently available in which to study GvHD.

1.16.1 MHC MISMATCH MODELS

The identification of the MHC and miHA have facilitated the development of murine models of aGvHD and cGvHD. While the rejection of foreign cells and tissues is generally mediated through allogeneic MHC recognition, differences in miHA can also result in graft rejection (Schroeder & DiPersio 2011). In contrast to the variability observed between humans, the MHC of inbred mouse strains are very similar; however the recognition of allogeneic miHA can lead to GvHD development in murine models.

The most commonly used MHC mismatch model of aGvHD is the transplantation of whole lymphocyte/purified T cells from a C57BL/6 mouse ($H2^b$) to a sub-lethally irradiated BALB/c mouse ($H2^d$). All MHC mismatch models use pre-conditioning regimens to mimic the process in humans and the most common conditioning regimen is irradiation. Mice can be irradiated in a single dose or in fractionated doses (3-8 hours apart) if the required dose exceeds 1100 Gy. Most of these models are dependent on the administration of $CD4^+$ and $CD8^+$ T cells to develop GvHD.

The C3H/HEJ (H2k) into C57Bl/6 (H2b) model of aGvHD is similar to the model described above in that it is a complete mismatch of MHC I and II as well as miHA. In general, it requires significantly more splenocytes to trigger lethal aGvHD (25-30 x 10^6) and aGvHD generally occurs between days 21-30 (Blazar *et al.* 1991).

Another MHC mismatch model of aGvHD is the 'parent-to-F1 model'. In contrast to the previous model this model of aGvHD can be performed with or without the sub-lethal irradiation conditioning regimen. Utilising the model without irradiation is designed to mimic situations where a patient receives no or reduced intensity conditioning regimens. The development of aGvHD is dependent on class I and class II antigen dependent activation of $CD4^+$ and $CD8^+$ T cells (Hakim *et al.* 1991). Transplanted mice which did not receive myeloablative conditioning display less severe symptoms than mice which received irradiation. Transplanted mice which did not receive irradiation display reduced skin pathology and limited weight loss. In these mice, aGvHD pathology correlated with immune deficiency and did not result in full chimerism. There is also a lower rate of morbidity associated with no irradiation.

1.16.2 MURINE MODELS OF CGVHD

The clinical features and kinetics of cGvHD vary significantly from aGvHD as cGvHD patients develop chronic inflammation and fibrotic regions in a similar manner to patients suffering from auto-immune disorders; however cGvHD and aGvHD mostly target the same organs. The most commonly used cGvHD models currently available are generally classified as sclerodermatous (pro-fibrotic), or auto-antibody mediated (lupus/like) cGvHD models (Jaffee and Claman, 1983; Rolink and Gleichmann, 1983). The sclerodermatous models of cGvHD mimic scleroderma in human cGvHD patients (~15% of cGvHD patients) and are characterised by fibrotic damage to the dermis and also targeted apoptosis in the lungs and liver (Jaffee & Claman 1983; Claman *et al.* 1985; Howell *et al.* 1989; McCormick *et al.* 1999; Skert *et al.* 2006). Sclerodermatous models of cGvHD are MHC matched but disparities in miHA result in cGvHD. Pathology is dependent on donor $CD4^+$ T cell activation and secretion of Th2 cytokines and subsequent

stimulation of pro-fibrotic cytokines IL-13 and TGF-β (Hamilton 1987; Korngold & Sprent 1987). There are 2 commonly used sclerodermatous models of cGvHD. The first is the transplantation of whole splenocytes with bone marrow from B10.D2 mice into sub-lethally irradiated BALB/c mice (Jaffee & Claman 1983) and the second is the transplantation of LP/J cells into irradiated C57Bl/6 mice (DeClerck *et al.* 1986). Sclerodermatous cGvHD models have provided valuable information regarding the progression of cGvHD; however there are some limitations associated with the model. Fibrotic damage in human cGvHD patients is systemic but in this mouse model fibrosis is localised to the skin; this may indicate a different mechanism of action. Finally, sclerodermatous cGvHD models do not give the full spectrum of clinical symptoms observed in humans (Schroeder & DiPersio 2011).

The auto-antibody mediated mouse model of cGvHD results in a similar pathology to lupus. Symptoms associated with this model of cGvHD include nephritis, salivary gland fibrosis, lymphadenopathy, splenomegaly, auto-antibody production and skin pathology, although at a much lower extent than sclerodermatous model (Schroeder & DiPersio 2011). The auto-antibody mediated mouse model of cGvHD is a MHC mismatched mode of parent-F1 transplantation which results in mixed chimerism (Rolink & Gleichmann 1983). Similar to the sclerodermatous model of cGvHD, pathology is dependent on donor $CD4^+$ T cells and Th2 associated cytokines; however in this particular model of cGvHD the recipient B cells play a major role in pathology. Recipient B cells are activated following interaction with donor T cells, through cell surface MHC molecules and recognition of IL-4 and IL-10 (Morris *et al.* 1990; Durie *et al.* 1994; Via *et al.* 1996; Kim *et al.* 2008). The activation of recipient B cells results in lymphadenopathy, splenomegaly and auto-antibody production (Rolink & Gleichmann 1983; Hakim *et al.* 1991). Auto-antibody mediated mouse models of cGvHD are similar to human cGvHD pathology in relation to the production of antibodies; however there are

also differences between them. Nephritis is commonly associated with this cGvHD mouse model but is very rare in humans, the repertoire of antibodies produced during human cGvHD is much more diverse than in murine cGvHD models, and lymphadenopathy and splenomegaly do not occur in human patients.

1.17 HUMANISED MOUSE MODELS FOR AGVHD

The major limiting factors associated with murine models of aGvHD is that disease progression and pathology are not identical between mice and humans. In murine models of aGvHD, pathology is driven by a different effector cell (murine vs human) and these models were not established to investigate the efficacy of human cell therapies. The development of humanised mouse models which are based on severely immunodeficient mice, have addressed some of these issues. The development of humanised mice is a step forward in linking animal models with clinical relevance and is testament to how research tools have progressed over the past decades.

1.17.1 CB17SCID HUMANISED MOUSE

The development of humanised mouse models of disease was facilitated by the identification of the *Prkdc*^{scid} (protein kinase, DNA activated, catalytic peptide; severe combined immunodeficiency) mutation in CB17 mice (Bosma *et al.* 1983). Mice lacking *Prkdc* expression were unable to support VDJ rearrangement and as a result lacked fully mature T or B cells (Lieber *et al.* 1988). While this represented a dramatic step forward in the development of humanised mice, the engraftment of human lymphocytes and stability of the mouse were problematic. The engraftment of human lymphocytes was very low (0.01-0.1%) (Mosier *et al.* 1988) and the CB17scid mouse was 'leaky', i.e. the

mouse can develop clones of functional T and B cells. The development of functional T and B cells can lead to enhanced immune activity which may explain the low levels of human lymphocyte engraftment. Therefore, the scid mutation was introduced to other mouse strains and subsequently the development of the Non-obese Diabetic (NOD)-scid mouse (Hesselton *et al.* 1995). The NOD-scid mouse facilitated significantly higher engraftment of human lymphocytes compared to other murine strains (up to 10 fold) and quickly became the gold standard of humanised mouse model.

1.17.2 NOD-SCID HUMANISED MOUSE

The NOD mice have inherited immune defects, such as impaired macrophage development and function, reduced complement activity and decreased NK activity, which made them attractive candidates for the development of humanised mouse models (Kataoka *et al.* 1983; Baxter & Cooke 1993; Serreze *et al.* 1993) (Kataoka *et al.*, 1983; Baxter *et al.*, 1993; Serreze *et al.*, 1993). As seen with the CB17scid mouse, introducing the *scid* mutation resulted in the absence of fully mature T or B cells. However, the NOD-scid mouse was much more stable than its predecessor, only ~10% of 6 month old mice developing mature T or B cells. The NOD-scid humanised mouse model also demonstrated significantly higher levels of human lymphocyte engraftment than the CB17 mouse; however the engraftment of human lymphocytes remained very low (~10%) (Hesselton *et al.* 1995). Schultz *et al.* hypothesised that the low levels of lymphocyte engraftment may be caused by residual NK cell activity (Shultz *et al.* 1995). Another major limitation of the NOD-scid mouse was the short lifespan (~ 8 months) associated with these mice; the impaired life span of NOD-scid mice was a result of the frequent development of lethal thymic lymphomas (Shultz *et al.* 1995). Therefore,

studies into further developing the NOD-scid humanised mouse model focussed on increasing life span as well as incorporating novel methods of blocking NK cell function.

1.17.3 NOD-SCID B2M^{NULL} AND RAG1^{NULL} PRF1^{NULL} HUMANISED MOUSE

In an attempt to control residual NK activity, the NOD-scid β2microglobulin^{null} (β2m^{null}) mouse was developed. The NOD-scid β2m^{null} mouse lacked NK cell activity and demonstrated reduced innate immunity when compared to NOD-scid mice (Christianson *et al.* 1997). The absence of NK cell activity in NOD-scid β2m^{null} mice resulted in a significant increase in the engraftment of human lymphocytes compared to NOD-scid mice (~7 fold) (Christianson *et al.* 1997). However, NOD-scid β2m^{null} mice were also very susceptible to lethal thymic lymphomas, resulting in a much shorter lifespan (~5 months) than NOD-scid humanised mice. Another humanised mouse model developed with defective NK cells was the NOD-Rag1^{null} Prf1^{null} mouse. Within these mice, NK cells were present but non-functional due to the absence of the *prf1* gene (Shultz *et al.* 2000). The prf2 gene encodes perforin, a cytolitic protein found in the granules of NK cells, which mediates killing ability of NK cells (Shultz *et al.* 2000). The lifespan of the NOD-Rag1^{null} Prf1^{null} mouse was significantly greater than the NOD-scid β2m^{null} and NOD-scid mice and the lack of functional NK cells resulted in significantly higher engraftment of human lymphocytes (Shultz *et al.* 2000). However, the level of lymphocyte engraftment was highly variable between human donors and subsequently the reproducibility of the model was inconsistent. Therefore the focus switched again to developing more robust and reproducible humanised mouse models.

1.17.4 RAG-2$^{-/-}$IL-2Rγ$^{-/-}$ HUMANISED MOUSE

The next wave of humanised mouse models focused on targeting mutations in the cytokine receptor common γ-chain. In humans, X linked SCID occurs due to mutations in the gene which encodes the IL-2rγ chain. This gene contributes to IL-2, IL-4, IL-7, IL-9, IL-15 and IL-21 signalling (Kovanen & Leonard 2004). Patients suffering from this disease are characterised by absent or markedly reduced mature T cells as well as reduced NK cell activity (Sugamura *et al.* 1996). The previously developed RAG-2$^{-/-}$ strain of mice lacked functional T, B and NK cells (Shinkai *et al.* 1992) and it was hypothesised that introducing the IL-2rγ mutation to the RAG-2$^{-/-}$ strain of mice would facilitate significantly higher human lymphocyte development. The RAG-2$^{-/-}$IL2rγ$^{-/-}$ mice were infused with human CD34^{+} progenitor cells. Indeed, human lymphocyte engraftment was significantly increased in the RAG-2$^{-/-}$IL2rγ$^{-/-}$ mice and this mouse model also demonstrated greater multilineage development compared to previous models.

1.17.5 NOD-SCID IL-2Rγ^{NULL} HUMANISED MOUSE

In terms of human lymphocyte engraftment, longevity and reduced NK function, the NOD-scid humanised mouse model was the most complete model developed up to this point. Therefore it was hypothesised that introducing a similar IL-2rγ mutation to the NOD-scid strain would result in a humanised mouse model deficient in mature T or B cells, with reduced NK activity, and more amenable to the engraftment of human lymphocytes (Pearson *et al.* 2008). The subsequent NOD-scid IL-2rγ^{null} humanised mouse model was indeed deficient for mature T and B cells, demonstrated reduced NK cell activity and the engraftment of human lymphocytes was 6 fold higher than observed in the NOD-scid mouse model. In addition to this, the lifespan of the NOD-scid IL-2rγ^{null}

humanised mouse model was considerably longer than the NOD-scid mouse model, making it ideal for long-term studies.

In 2005, the development of a complete human immune system in a NOD-scid IL-2rγ^{null} humanised mouse following the administration of peripheral blood CD34^{+} cells was first describe by Schultz *et al.*, demonstrating the validity of the NOD-scid IL-2rγ^{null} humanised mouse model for studying functional immune disease. Since this study, the NOD-scid IL-2rγ^{null} humanised mouse models has been deemed the most suitable humanised mouse model for studying GvHD (Ali *et al.* 2012) and there has already been a number of GvHD studies using this model (Hippen *et al.*, 2012; Tobin *et al.*, 2013; Miller *et al.*, 2014). For the purpose of this thesis the NOD-scid IL-2rγ^{null} humanised mouse model was used to investigate stem cell therapies for the treatment of aGvHD.

1.18 AIMS & OBJECTIVES

This chapter has highlighted the current understanding of how MSC interact with and regulate cells of the innate and adaptive immune response and the potential of delivering MSC therapy to GvHD patients. This thesis aims to investigate two distinct areas in MSC research which remain to be addressed:

(1) How MSC affect B cell biology and to elucidate the mechanisms by which effects are mediated.

(2) Can novel more clinically relevant animal models be developed to investigate possible mechanisms by which MSC protect from GvHD.

Despite the advances made in our understanding of how MSC modulate the immune system, the effect of MSC on B cell biology remains controversial. The goal of Chapter 3 is to determine how MSC regulate the activation, proliferation and function of CD19^{+} peripheral B cells and to elucidate the mechanism by which the effect is mediated.

Chapters 4 and 5 of this thesis focus on the development of novel animal models of GvHD which more closely resemble clinical pathology and to use these optimised models of GvHD to investigate the efficacy of MSC therapy. These models of GvHD will subsequently be used to examine a number of hypotheses focused on elucidating how MSC therapy exerts a protective effect during GvHD. These hypotheses include:

(1) MSC impair the engraftment of transplanted cells.

(2) MSC prevent the polarisation of transplanted T cells to effector or central memory phenotype.

(3) MSC reduce the production of pro-inflammatory cytokines during GvHD.

(4) MSC therapy results in increased numbers of regulatory T cells.

(5) Pre-licencing MSC with IFN-γ enhances protection in GvHD mice.

(6) The administration of two consequitive MSC doses increases efficacy of cell therapy.

Overall this study is designed to further the current knowledge of immune regulation by MSC and provide important information regarding the selection of MSC therapy for B cell mediated or idiopathic disease. This study will also contribute to the clinical application of MSC therapy for the treatment of GvHD by providing a more refined and clinically relevant model of disease. Taken together this thesis will advance our basic understanding of how MSC mediate their effects *in vivo* and will benefit the development of future clinical trials utilising allogeneic human MSC therapy in GvHD.

CHAPTER 2

MATERIALS AND METHODS

2.1 ETHICAL APPROVAL AND ANIMAL LICENSING

All procedures involving animals or human material were performed by licenced personnel. Ethical approval for all work was granted from the Department of Health and Health Products Regulatory Agency, formerly Irish Medicines Board, and controlled by the ethics committee of NUI Maynooth.

2.2 ANIMAL STRAINS

The following mouse strains were used for the experiments presented throughout this thesis: BALB/c (Harlan), C57Bl/6 (Harlan) and NOD.Cg-Prkdc^{scid}IL2^{tmlWjl}/Szj (Jackson Labs). All mice were housed in accordance to regulations presented by the Department of Health and the Irish Medical Board and experiments were performed under ethically approved licences. Sample size for animal experiments were determined by statistical power calculation.

2.3 ISOLATION AND CULTURE OF CELLS

2.3.1 HUMAN MESENCHYMAL STROMAL CELLS

Bone marrow MSC were isolated and kindly provided by collaborators in NUI Galway. In brief, bone marrow aspirates were taken from the iliac crest of donor patients in accordance to approved clinical protocol (Murphy *et al.* 2002). Isolated human MSC were re-suspended in complete Dulbecco's Modified Eagle's Media (cDMEM, Sigma-Aldrich, St. Louis, USA) supplemented with 10% (v/v) foetal bovine serum (BioSera) and 1% (v/v) Penicillin/Streptomycin (Sigma-Aldrich). Human MSC were seeded at

$1x10^6$ cells per T175 flask and cultured in a 37°C incubator set to 20% O_2 and 5% CO_2. Complete media was replaced every 48-72 hours until cells had reached 70-90% confluence. When 90% confluent, cells were detached using 4ml of 0.25% trypsin/1mM EDTA (Invitrogn-Gibco), counted and either re-seeded or cryo-preserved.

2.3.2 HUMAN PERIPHERAL BLOOD MONONUCLEAR CELL (PBMC) SEPARATION

Buffy packs were obtained from the Irish blood transfusion service. Each buffy pack was transferred to a sterile T75 flask and mixed with 60 ml of sterile PBS. 15 ml of Lymphoprep (StemCell Technologies, Vancouver, Canada) was added to 4 sterile 50 ml tubes and 25 ml of diluted blood was carefully layered on to the Lymphoprep. Samples were centrifuged at 2400 RPM for 25 minutes at room temperature (acceleration = 0, brake = 1). The PBMC layer was then removed using sterile 3 ml transfer pipette and placed in a fresh 50 ml tube. Samples were then centrifuged at 1800 RPM for 10 minutes at 4°C. The supernatant was carefully discarded and the samples were re-suspended in sterile PBS. Samples were washed twice more in PBS by centrifuging at 1500 RPM for 5 minutes at 4°C. Red blood cells were then removed from each sample by re-suspending the pellet in 5 ml of 1X RBC lysis buffer (BioLegend, San Diego, USA) for 5 minutes. Complete Roswell Park Memorial Institute (cRPMI, Table 2.1) media was added to neutralise the lysis and samples were spun down at 1000 RPM for 10 minutes at 4°C. Isolated PBMC were then re-suspended in 25 ml of cRPMI and counted.

2.3.3 $CD19^+$ PERIPHERAL B CELL ISOLATION

$CD19^+$ B cells were purified from PBMC populations using positive selection $CD19^+$ MACS beads (Miltenyi Biotech, Cologne, Germany). 3 x 10^8 PBMC were

washed twice in sterile PBS and once in MACS buffer (PBS with 0.5 % BSA (Sigma) and 2 mM EDTA (Sigma)) by centrifuging at 300 g for 5 minutes. PBMC were then re-suspended in 900 µl of MACS buffer and 100µl of $CD19^+$ MACS beads were added to each sample. Samples were placed at 4°C for 20 minutes before 10 ml MACS buffer was added and cells were spun down at 300 g for 5 minutes at 4°C. PBMC populations were re-suspended in 2 ml of MACS buffer and passed through a 40µM cell strainer and collected in a fresh 15 ml tube. Samples were then passed through LS columns (Miltenyi Biotech) in accordance with manufacturer's specifications before purified $CD19^+$ B cell populations were collected in a fresh 15 ml tube. The purity of peripheral $CD19^+$ B cell isolations was verified using flow cytometry for human CD20. Only isolations yielding greater than 95% were used for experiments.

2.3.4 CRYO-PRESERVATION AND RECOVERY OF CELLS FROM LIQUID NITROGEN

MSC were cryo-preserved in liquid nitrogen for long term storage. Trypsinised MSC were counted and pelleted by centrifugation. Pellets were re-suspended in freezing media (Table 2.1) at 2 x 10^6 per ml and 500 µl of cell suspension was added to labelled 1.5 ml cryo-tube (Thermo Fisher Scientific, Massachusetts, USA). Cells were gradually cooled at 1°C per minute to -80°C and then transferred to liquid nitrogen for long term storage. To retrieve cells, cryo-vials were quickly thawed using a heated water bath set to 37°C. Before completely thawed, cells were transferred to 10 ml of warmed cDMEM and centrifuged at 400 g for 5 minutes. Supernatant was discarded and cells were re-suspended in 1 ml cDMEM. Cells were counted and analysed for viability.

Table 2.1. Description of media for cell culture

Media	Components	Supplier	Cell Type
cDMEM	Dulbecco's Modified Eagle's Media (DMEM) containing 1000 mg/ml glucose	Sigma-Aldrich BioSera	MSC
	FBS (10% v/v)	Sigma-Aldrich	
	Pen/Strep (1% v/v)		
cRPMI	RPMI 1640	Sigma-Aldrich	PBMC
	Heat inactivated FBS (10% v/v)	BioSera	
	Pen/Strep (1% v/v)	Sigma-Aldrich	
	L-Glutamine (1% v/v)	Sigma-Aldrich	
	β-mercapthoethanol (0.1% v/v)	Invitrogen-Gibco	
cIMDM	Iscove's Modified Dulbecco's Media (IMDM)	Sigma-Aldrich	B cells
	Heat inactivated FBS (10% v/v)	BioSera	
	Pen/Strep (1% v/v)	Sigma-Aldrich	
	L-Glutamine (1% v/v)	Sigma-Aldrich	
	β-mercapthoethanol (0.01% v/v)	Invitrogen-Gibco	
Freezing media	cDMEM (70% v/v)	Sigma-Aldrich	
	FBS (20% v/v)	BioSera	
	DMSO (10% v/v)	Sigma-Aldrich	

2.4 CELL VIABILITY AND APOPTOSIS ASSAYS

2.4.1 MEASUREMENT OF CELL VIABILITY

Cells were re-suspended in complete media and 10 µl of sample was removed and diluted with 40 µl of complete media. 10 µl of diluted sample was then mixed with 10 µl of 2% (w/v) ethidium bromide/acridine orange (EB/AO) (Sigma-Aldrich). 10 µl of cells were then pipetted onto a glass haemocytometer chamber and visualised under a fluorescent microscope. Live cells (fluoresced green) were counted while dead cells (fluoresced orange) were excluded.

2.4.2 *IN VITRO* APOPTOSIS ASSAY

B cell apoptosis was detected by the positive expression of Annexin V and Propidium Iodide (PI) as measured by flow cytometry. B cells were harvested and centrifuged at 300 g for 5 minutes. Supernatant was discarded and cells were washed in sterile PBS. Samples were re-suspended in FACS buffer (PBS with 2% (w/v) BSA). Cells were transferred to a V bottom 96 well plate and spun down at 300 g for 5 minutes. Supernatant was discarded and cells were stained with 0.3 µl of CD20 for 15 minutes in the dark at 4°C. Cells were washed once in FACS buffer and once in 1 X Annexin V binding buffer. 2 µl of Annexin V was added to each well and cells were incubated for 15 minutes in the dark at room temperature. Cells were washed twice in 1 X binding buffer and re-suspended in 50µl of counting beads (Becton Dickinson, New Jersey, USA). 1 µl of PI was added to each well and cells were incubated at room temperature for 5 minutes. $CD20^+$ B cells were then analysed for expression of apoptotic markers Annexin V and PI using Acurri C6 flow cytometer.

2.5 FLOW CYTOMETRIC ANALYSIS OF PROTEIN EXPRESSION

2.5.1 CELL SURFACE FLOW CYTOMETRY

To analyse the expression of surface bound proteins by flow cytometry, cells were harvested, washed twice in PBS and re-suspended in FACS buffer to a concentration of 1 x 10^6 cells /ml. 100 µl of cell suspension was transferred to V-bottom 96 well plate (Lennox, Dublin, Ireland) and cells were centrifuged at 950 RPM for 5 minutes at 4°C. Supernatant was discarded and fluorochrome labelled antibodies or isotype controls were added directly to the cells. Samples were incubated in the dark at 4°C for 15 minutes. 150 µl of FACS buffer was then added to each well and samples were centrifuged at 950 RPM for 5 minutes at 4°C. Supernatant was discarded and samples were washed again with 150 µl of FACS buffer. The supernatant was discarded and cells were re-suspended in 50 µl of counting beads (BD) and analysed on a BD Accuri C6 flow cytometer.

2.5.2 INTRA-CELLULAR FLOW CYTOMETRY

In order to determine the expression of intra-cellular transcription factors or pro-inflammatory cytokines, intra-cellular flow cytometry was performed. To analyse the expression of constitutively expressed transcription factors, cells were harvested from co-culture assays, washed twice in PBS and re-suspended in FACS buffer to a concentration of 1 x 10^6 cells /ml. 100 µl of cell suspension was transferred to V-bottom 96 well plate (Lennox) and surface proteins were labelled exactly as described in section 2.5.1. After cell surface protein staining, 100 µl of Fix/Perm buffer (eBioscience, San Diego, USA) was added to each well and samples were incubated in the dark at 4°C overnight. 200 µl of Permeabilisation buffer was added to each well and samples were centrifuged at 950 RPM for 5 minutes at 4°C. Supernatant was discarded and samples were blocked in 3 µl

of 2% rat serum (Sigma Aldrich) for 20 minutes at 4°C. 1 µl of fluorochrome labelled antibodies or isotype controls were added directly to the cells and samples were incubated in the dark at 4°C for 1 hour. 150 µl of FACS buffer was then added to each well and samples were centrifuged at 950 RPM for 5 minutes at 4°C. Supernatant was discarded and samples were washed again with 150 µl of FACS buffer. The supernatant was discarded and cells were re-suspended in 50 µl of counting beads (BD) and analysed on a BD Accuri C6 flow cytometer.

In order to detect the expression of pro-inflammatory cytokines in lymphocytes *ex vivo*, lymphocytes were isolated from lung, liver and spleen of mice as described in section 2.10.4. Lymphocytes were seeded at 1 x 10^5 cells/well in cRPMI. PBMC were stimulated with 100 ng/ml Phorbol Myristate Acetate (PMA, Sigma) and 1 µg/ml Ionomycin (Sigma) for 5 hours in the presence of 1 X Golgi Stop (eBioscience). After stimulation samples were transferred to a V-bottom 96 well plate (Lennox) and cells were centrifuged at 950 RPM for 5 minutes at 4°C. Samples were washed twice in FACS buffer before cell surface proteins were stained as previously described in section 2.5.1. After cell surface protein staining, 100 µl of Fix/Perm buffer (eBioscience) was added to each well and samples were incubated in the dark at 4°C overnight. 200 µl of Permeabilisation buffer was added to each well and samples were centrifuged at 950 RPM for 5 minutes at 4°C. Supernatant was discarded and samples were blocked in 3 µl of 2% rat serum for 20 minutes at 4°C. 1 µl of fluorochrome labelled antibodies or isotype controls were added directly to the cells and samples were incubated in the dark at 4°C for 1 hour. 150 µl of FACS buffer was then added to each well and samples were centrifuged at 950 RPM for 5 minutes at 4°C. Supernatant was discarded and samples were washed again with 150 µl of FACS buffer. The supernatant was discarded and cells were re-suspended in 50 µl of counting beads (BD) and analysed on a BD Accuri C6 flow cytometer.

2.6 CHARACTERISATION OF DIFFERENTIATION

2.6.1 OSTEOGENIC DIFFERENTIATION

MSC were seeded at a density of 1.8 x 10^5 cells/well in a 6 well tissue culture plate (Sarstedt, Numbrecht, Germany) in 3 ml of cDMEM and incubated at 37°C. Once MSC had reached 70% confluence, cDMEM was removed and MSC were incubated in either cDMEM (negative control) or osteogenic differentiation media (Table 2.2). Media was changed every 72 hours for 21 days. On day 21, media was removed and MSC washed gently 3 times with sterile PBS. Cells were then fixed in 10% (v/v) neutral buffered formalin for 20 minutes at room temperature. Formalin was removed and cells were gently washed twice in PBS. 1 ml of 1% Alizarin Red (Table 2.3) was added to each well and cells were stained for 20 minutes at room temperature. Excess stain was removed and cells were gently washed twice with dH_2O. 1 ml of dH_2O was added to each well and cells were examined under light microscope for the presence of positively stained osteocyte like cells.

2.6.2 ADIPOGENIC DIFFERENTIATION

MSC were seeded at a density of 1.8 x 10^5 cells/well in a 6 well tissue culture plate (Sarstedt) in 3 ml of cDMEM and incubated at 37°C. Once MSC had reached 70% confluence, cDMEM was removed and MSC were incubated in either cDMEM (negative control) or adipogenic differentiation media (Table 2.2). Media was changed every 72 hours for 21 days. On day 21, media was removed and MSC washed gently 3 times with sterile PBS. Cells were then fixed in 10% (v/v) neutral buffered formalin for 20 minutes at room temperature. Formalin was removed and cells were gently washed twice in PBS. 1 ml of filtered 0.5% Oil Red O (Table 2.3) was added to each well and cells were

incubated for 20 minutes at room temperature. Excess stain was removed and cells were gently washed twice with PBS. 1 ml of PBS was added to each well and cells were examined under light microscope for positively stained fat globules which indicate the presence of adipogenic differentiation.

2.6.3 CHONDROGENIC DIFFERENTIATION

MSC were seeded at 2.5 x 10^5 cells/pellet culture in 15 ml tube. MSC were centrifuged at 200 g for 8 minutes and pellets were re-suspended in either cDMEM (negative control) or in chondrocyte differentiation media (Table 2.2). Samples were incubated for 21 days at 37°C with caps loosened to allow for gaseous exchange. Media was changed every 72 hours for 21 days. On day 21, all media was removed and pellets were washed twice with PBS. Cell pellets were harvested in 1 ml TriReagent and stored at -20°C overnight. Chondrocyte differentiation was determined by the expression of collagen II and aggrecan by Reverse Transcription PCR (Section 2.8.4)

Table 2.2. Description of media for cell differentiation

Media Name	Components	Supplier
Osteogenic Differentiation media	Dulbecco's Modified Eagle's Media (DMEM) containing 1000 mg/ml glucose	Sigma-Aldrich
	1 mM dexamethasone	Sigma-Aldrich
	20 mM β-glycerolphosphate	Sigma-Aldrich
	50 µM L-ascorbic acid-2-phosphate	Sigma-Aldrich
	50 ng/ml L-thyroxine sodium pentahydrate	Sigma-Aldrich
Adipogenic Differentiation media	Dulbecco's Modified Eagle's Media (DMEM) containing 4500 mg/ml glucose	Sigma-Aldrich
	5 µg/ml insulin (dissolved in 0.1N acetic acid)	Sigma-Aldrich
	50 µM indomethacin	Sigma-Aldrich
	1 µM dexamethasone	Sigma-Aldrich
	0.5 µM 3-Isobutyl-1-methylxanthine (IBMX)	Sigma-Aldrich
Chondrocyte Differentiation media	Dulbecco's Modified Eagle's Media (DMEM) containing 1000 mg/ml glucose	Sigma Aldrich
	100 nM dexamethasone	Sigma-Aldrich
	50 µg/ml ascorbic-acid-2-phosphate	Sigma-Aldrich
	40 µg/ml proline	Sigma-Aldrich
	1 mM sodium pyruvate	Sigma-Aldrich
	1% (v/v) Insulin Transferrin Selenium X	BD Biosciences
	10 ng/ml TGF-β3	BD Biosciences

Table 2.3. Description of reagents used to detect osteocyte and adipocyte differentiation

Reagent	Components	Concentration	Supplier
MSC Osteoblast	Alizarin Red S stain	1% (w/v)	Sigma-Aldrich
Differentiation	dH_2O	100 ml	
	pH 4.1 – 4.3		
MSC Adipocyte	Oil Red O	0.5% (w/v)	Sigma-Aldrich
Differentiation	Isopropanol	30 ml	Sigma-Aldrich

2.7 ENZYME LINKED IMMUNOSORBENT ASSAY

Samples were stored at -80°C until cytokine expression was analysed by ELISA. 96 well NUNC Maxisorb plates (Thermo Fisher Scientific) were used for all ELISA experiments. Plates were coated with 100 µl of capture antibody and stored at 4°C overnight under gentle agitation. Plates were washed 3 times with wash buffer (PBS with 0.05% (v/v) Tween-20) and dried by forcefully inverting the plates onto absorbent tissue paper. Plates were blocked for 1 hour at room temperature using reagent diluent. Plates were then washed 3 times again using wash buffer and samples or standards were added to each well. Samples were incubated overnight at 4°C under gentle agitation. Samples were aspirated off and plates washed 3 times with wash buffer. 100 µl of detection antibody was added to each well and samples were incubated for 1 hour at room temperature. Plates were washed 3 times as before and 100 µl Avidin-HRP was added to each well and left for 30 minutes at room temperature. Samples were washed 5 times with wash buffer and dried as before. 100 µl of substrate solution was added to each well for 15 minutes or until strong colour change was detected. 50 µl of stop solution (2N H_2SO_4) was then added to each well and the OD for each sample was determined using an ELx800TM microplate reader with Gen5 analysis software. Cytokine concentrations for each sample were extrapolated from a standard curve which related the observed OD to a known protein concentration. Data analysis was performed using Graphpad PRISM5 software.

2.8 MOLECULAR IMMUNOLOGICAL TECHNIQUES

2.8.1 RNA ISOLATION

For mRNA analysis on MSC, cells were seeded at 1.8 x 10^5 cells/well in a 6 well plate and stimulated as desired before harvesting. Total RNA was isolated using 1 ml of

Trizol Reagent according to manufacturer's specifications. Briefly, media was removed from wells and samples washed twice with sterile PBS. 1 ml of TriReagent was added to each well and cells were degraded by pipetting up and down. Trizol samples were transferred to RNAse free 1.5 ml tubes and left for 2 minutes at room temperature. 300 µl of chloroform was added and samples were vortexed until in uniform solution. Samples were incubated at room temperature for 5 minutes before being centrifuged at 12,000 g for 15 minutes at 4°C. The RNA containing upper aqueous phase was transferred to fresh RNAse free 1.5 ml tubes. Equal amounts of Isopropanol was added to each tube and samples were again mixed by vigorous shaking. Samples were incubated at room temperature for 10 minutes before being spun down at 12,000 g for 10 minutes at 4°C. Supernatant was discarded and pellet was re-suspended in 1 ml of ice cold 75% (v/v) ethanol and vortexed for 10 seconds. Samples were centrifuged at 7,500 g for 5 minutes at 4°C and supernatant discarded. Samples were left to air dry for approximately 5 minutes. RNA samples were re-suspended in 20-50 µl of nuclease free H_2O depending on the size of the pellet. The concentration of RNA was determined using Nanodrop Spectrophotometer (Nanodrop, Delaware, USA) measuring wavelengths at 260 and 280 nm where the absorbance of 1 unit at 260 nm is 40µg/ml. Only RNA precipitations which yielded an $OD_{260/280}$ ratio of 1.8 – 2.0 were used for cDNA synthesis. RNA was stored at -80°C until required.

2.8.2 Synthesis of cDNA from RNA

Before beginning to generate full length first strand cDNA, genomic DNA was removed from RNA samples by treating 2 µg of RNA with amplification grade DNase I (Invitrogen). 1 µl of DNase I was added to each sample and samples were incubated at room temperature for 15 minutes. DNase I reaction was neutralised using 1 µl of 25 mM

EDTA (Promega) to each mixture and samples were heated to 65°C for 10 minutes. The generation of cDNA was carried out using Tetro cDNA synthesis kit (Bioline). 1 µl of Oligo (dT) and 1 µl of 10mM dNTP were added to each sample and samples were then heated to 60°C for 5 minutes. Samples were cooled on ice before a 10µl of reverse transcriptase master mix was added to each sample. cDNA synthesis was then performed at 45°C for 50 minutes and then 70°C for 15 minutes. Samples were then stored at 4°C until required.

2.8.3 Real time polymerase chain reaction (Real-Time PCR) analysis

cDNA generated as described above, was diluted 1/5 with nuclease free H_2O, was used for quantitative Real-Time PCR analysis using primers specific from gene sequences of interest as outlined in table 2.17. For real-time PCR analysis, a reaction mix was prepared and 9 µl of reaction mix was placed into specialised optical 48 well plates (Illumina, MSC, Dublin, Ireland) followed by 1 µl of template DNA. Each sample was heated to 95°C for 10 minutes, followed by between 40-50 cycles of 95°C for 30 seconds, 58°C for 30 seconds and 72°C for 45 seconds. Amplification of one specific product was determined through melt curve analysis where the presence of one single melting peak indicated the absence of primer-dimer association. Melt curve analysis was performed by heating the products to 95°C after all cycles were completed. Real-time PCR was performed in an illumina Eco Real-Time PCR system (MSC). The relative quantification of target gene expression was determined in relation to GAPDH expression using the ΔCT method. The ΔCT method was determined by subtracting the GAPDH value from the target CT value for each sample. The fold change in relative gene expression was determined by calculating the $2^{-\Delta_{CT}}$ values.

2.8.4 REVERSE TRANSCRIPTION POLYMERASE CHAIN REACTION

PCR was used to determine the presence of specific DNA sequences by targeting specific primers against cDNA templates. Expression of the housekeeping gene, Glyceraldehyde 3-phosphate dehydrogenase (GAPDH) was used as a positive control. PCR reactions contained 2.5 mM MgCl2 (Promega, Wisconsin, USA), 25 mM dNTP (Promega), 1 x GoTaq reaction buffer (Promega), 40 U/ml Taq polymerase (Promega) and 1 pM of specific forward and reverse primers. The reaction mastermix was adjusted to a final volume of 24 µl per sample with nuclease free H_2O. Each sample was subjectd to an initial incubation of 95°C for 10 minutes followed by 29 cycles of 95°C for 30 seconds, 55-60°C (depending on primers) for 30 seconds and 72°C for 1 minute. Samples were then incubated at 72°C for 10 minutes and stored at 4°C.

2.8.5 AGAROSE GEL ELECTROPHORESIS

Agarose gels were prepared by adding 1.3 g (w/v) agarose (Sigma-Aldrich) to 1 X TAE buffer (Table 2.16) and heating in a microwave until completely dissolved. The solution was left to cool to below 50°C and 6 µl of Gel Red (Biotium, California, USA) was added and the solution was poured into a gel tray. When solidified, agarose gels were submerged in TAE buffer and subjected to electrophoresis at 90V for 70 minutes. Samples were run simultaneously to a 100 base pair molecular weight (Promega). Nucleic acid products were visualised under UV light and images acquired using a Gel Logic 212 Pro gel documentation system.

2.8.6 WESTERN BLOT ANALYSIS

2.8.6.1 PROTEIN HARVEST

In order to isolate intra-cellular proteins from adherent cells, 6 well plates were placed on ice and supernatant removed. Cells were washed with 1ml of ice cold PBS. Cells were then scraped in 1ml fresh ice cold PBS and transferred to 1.5ml tube. For non-adherent cells, media containing the suspension cells was transferred to a 15 ml tube. Samples were centrifuged at 6500g for 10 minutes at 4°C. PBS was discarded and cell pellet was re-suspended in 90µl of cell lysis buffer (Table 2.5) and mixed well by pipetting. Samples were placed on ice under constant agitation for 10 minutes. Samples were mixed well again by pipetting and returned to ice for another 10 minutes under constant agitation. Protein lysates were then centrifuged at 12,000g for 10 minutes at 4°C. 80µl of supernatant, which contains the solubilised intra-cellular proteins, was transferred to a new pre-cooled and labelled 1.5ml tube and stored at -20°C. Prior to loading protein lysates, samples were mixed with 4X sample buffer (Table 2.10) (to 1X sample buffer) and heated to 100°C for 5 minutes.

2.8.6.2 BRADFORD ASSAY

In order to determine the concentration of protein harvested and to equalise the amount of protein to load for each sample, a Bradford assay was performed as previously described (Bradford 1976). BSA standards of known protein concentration and samples were diluted in 10µl lysis buffer and mixed with 190µl of Bradford assay reagent (Bio-Rad, California, USA) and the protein concentration was determined by the level of colorimetric change. The OD was measured for each sample at 590nm using an ELx800TM microplate reader with Gen5 Data Analysis software (Bio-Tek, New

England, USA. The protein concentrations of each sample were extrapolated from standard curve generated from known BSA concentrations. Standard samples were analysed in duplicate to create the standard curve. Data analysis was performed using GraphPad Prism 5 software.

2.8.6.3 SDS-POLYACRYLAMIDE GEL ELECTROPHORESIS (SDS-PAGE)

SDS-PAGE was carried out based on methods designed by Laemmli and modified by Studier (Laemmli 1970; Studier 1973). Samples were loaded into individual 0.75 mm wells. A pre-stained molecular ladder (10-180 kDA) was also loaded to each gel. Electrophoresis was performed at 70V through a 5% polyacrylamide stacking gel and then at 90V through an 8-15% polyacrylamide resolving gel for 1.5-2 hours. The percentage of acrylamide gel used was based on the size of the target proteins being analysed. Proteins under 30 kDa in size were electrophoresed on a 15% acrylamide gel, proteins between 30 kDa-80 kDa were analysed on a 10% gel while an 8% gel was used to examine proteins greater than 80kDa in size.

Table 2.4. Lysis Buffer (Stock)

Final Volume	1 Litre
HEPES (pH 7.5)	50 mM
EDTA	1 mM
Glycerol	10% (v/v)
CHAPS	0.05% (w/v)
Triton X	0.5% (v/v)
Sodium Chloride (NaCl)	250 mM
H_2O	Up to 1 Litre

Table 2.5. Cell Lysis Buffer (Working solution)

Final Volume	5 ml
Lysis Buffer	4.75 ml
100 mM Sodium orthovanadate ($NaVO_3$)	50 µl
100 mM Phenylmethanesulfonylfluoride (PMSF)	100 µl
Protease Inhibitor	100 µl

2.8.6.4 IMMUNOBLOTTING

Following protein separation by SDS-PAGE, proteins were transferred electrophoretically from the polyacrylamide gels to nitrocellulose membranes using a Hoefer TE 70 Semiphore semi dry transfer unit (GE Healthcare, Buckinghamshire, England) at 100mA for between 40 and 80 minutes depending on protein size. 3 layers of Whatmann blotting paper (Sigma-Aldrich) were submerged in transfer buffer before being placed on the bottom surface of the transfer unit. One layer of nitrocellulose paper (GE Healthcare) was carefully placed on top followed by the polyacrylamide resolving gel. Finally 3 more layers of Whatmann blotting paper were submerged in transfer buffer and carefully placed on top of the gel and the transfer unit was closed. When protein transfer was complete, non-specific antibody binding was blocked by incubating the nitrocellulose membrane in 1 X TBST containing 5% (w/v) skimmed milk powder for 1 hour under gental agitation. Milk was subsequently removed and membranes were washed with 1 X TBST for 5 minutes under constant agitation (repeated 3 times). The membranes were then incubated at 4°C overnight under gentle agitation with primary antibodies diluted in 1 X TBST containing 5% (w/v) BSA or skimmed milk powder depending on manufacturer's recommendations. The membranes were again washed 3 times in 1 X TBST. Secondary antibodies specific for target antibody (anti-rabbit, anti-goat or anti-mouse) were diluted in 1 X TBST containing 5% (w/v) skimmed milk powder and membranes incubated with secondary antibodies for 1 hour in the dark at room temperature, again under gentle agitation. The membranes were then washed 3 times for 5 minutes each with 1 X TBST in the dark. The immune-fluorescent bands were detected using the Odyssey infrared imaging system (Licor Bioscences, Nebraska, USA) or by using enhanced chemilluminescence development.

2.9 *IN VITRO* MSC FUNCTIONAL ASSAYS

2.9.1 STIMULATION OF MSC WITH INFLAMMATORY CYTOKINES

MSC were stimulated with pro-inflammatory cytokines IFN-γ or TNF-α in order to stimulate immune suppressive abilities of MSC. For IFN-γ stimulation MSC were cultured with 50 ng/ml of recombinant human IFN-γ (Peprotech, New Jersey, USA) for 24 or 48 hours. TNF-α stimulation was performed by stimulating cells at 30 ng/ml recombinant human TNF-α (Peprotech) for 48 hours.

2.9.2 *IN VITRO* CO-CULTURE OF $CD19^+$ B CELLS WITH MSC

MSC were trypsinised from T175 flasks, washed 3 times in sterile PBS. MSC were re-suspended in cIMDM and counted. MSC were seeded into either 96 well (1 x 10^4 cells) or 6 well (1.8 x 10^5 cells) plates. Isolated $CD19^+$ cells were counted and re-suspended in cIMDM and seeded into 96 well (5 x 10^4 cells) or 6 well (9 x 10^5 cells) plates with or without MSC. B cell activating cocktail (Table 2.13) was added to appropriate wells. For cell contact dependence assays, trans-well membrane inserts (Greiner bio-one, Kremsmunster, Austria) were used in 6 well plates.

Table 2.6. 10X TBST

Final Concentration
100 mM Tris
1.5 M NaCl
dH_20
pH 7.5

Table 2.7. 4X Lower Tris Buffer

Final Concentration
1.5 M Tris
0.4% SDS
dH_2O
pH 8.8

Table 2.8. 4X Upper Tris Buffer

Final Concentration
0.5 M Tris
0.4% SDS
dH_2O
pH 6.8

Table 2.9. Resolving (Lower) gel

% Acrylamide Gel	**8%**	**10%**	**15%**
dH_2O	12.1 ml	10.5 ml	6.25 ml
4X Lower Tris Buffer	6.25 ml	6.25 ml	6.25 ml
Protogel	6.67 ml	8.35 ml	12.5 ml
10% APS	130 µl	130 µl	130 µl
TEMED	14 µl	40 µl	40 µl
Total Volume	25 ml	25 ml	25 ml

Table 2.10. Stacking (Upper) gel

% Acrylamide Gel	**5%**
dH_2O	5.8
4X Upper Tris Buffer	2.5
Protogel	1.7
10% APS	40
TEMED	20
Total Volume	10 ml

Table 2.11. 4X Sample Buffer

Final Concentration
0.25 M Tris
6% SDS
40% Sucrose
0.04% Bromophenol Blue
dH_2O
2-mercaptoethanol (add just prior to use)

Table 2.12. 10X Running buffer

Final Volume	1 Litre
Tris Base	30.2 g
Glycine	144 g
SDS	10g
dH_2O	Up to 1 Litre
pH	8.3

Table 2.13. Transfer Buffer

Final Concentration
25 mM Tris Base
20 mM Glycine
20% (v/v) Methanol
dH_2O

Table 2.14. B cell activating cocktail

Final Concentration
100 Units/ml Recombinant IL-2
100 ng/ml Recombinant IL-21
25 ng/ml Recombinant IL-10
ITS (1:1000)
250 ng/ml Recombinant CD40 ligand
2.5 µg/mlCpG

2.10 ANIMAL MODELS OF DISEASE

2.10.1 SYNGENEIC BONE MARROW TRANSPLANT MODEL

Syngeneic bone marrow transplantations were established as negative controls to chronic and acute GvHD. BALB/c mice were exposed to a conditioning dose of 7 gray (Gy) whole body gamma irradiation. Mice were injected with $5x10^6$ bone marrow cells and whole splenocytes limited to $1x10^6$ $CD4^+$ cells isolated from age matched BALB/c mice. Human MSC were administered i.v. to mice at days 1 and 3 post transplantation. Animals were returned to their cages and were closely monitored for the first hour and at regular intervals for signs of distress or ill health. Mice were weighed every 7 days and changes in weight were recorded. Development of GvHD was determined by examining features including weight loss, ruffled fur and hunched posture (Section 2.10.5). Animals which displayed greater than 25% weight loss were sacrificed humanely.

2.10.2 MINOR MHC MISMATCH TRANSPLANT MODEL

A murine model of chronic GvHD was established in this study using a minor MHC mismatched transplant, originally developed by Korngold and Sprent (Korngold & Sprent 1978). BALB/c mice were exposed to a conditioning dose of 7 Gy whole body gamma irradiation. Mice were injected i.v. with $5x10^6$ bone marrow cells and whole splenocytes limited to $1x10^6$ $CD4^+$ cells isolated from age matched B10/D2 mice. Human MSC were administered i.v. to mice at days 1 and 3 post transplantation. Animals were returned to their cages and were closely monitored for the first hour and at regular intervals for signs of distress or ill health. Mice were weighed every 7 days and changes in weight were recorded. Development of GvHD was determined by examining features

including weight loss, ruffled fur and hunched posture (Section 2.10.5). Animals which displayed greater than 25% weight loss were sacrificed humanely.

2.10.3 MAJOR MHC MISMATCH TRANSPLANT MODEL

A murine model of acute GvHD was established in this study using a major MHC mismatched transplant. BALB/c mice were exposed to a conditioning dose of 7 Gy whole body gamma irradiation. Mice were injected with $5x10^6$ bone marrow cells and whole splenocytes limited to $1x10^6$ $CD4^+$ cells isolated from age matched C57BL/6 mice. Human MSC were administered to mice at days 1 and 3 post transplantation. Animals were returned to their cages and were closely monitored for the first hour and at regular intervals for signs of distress or ill health. Mice were weighed every 7 days and changes in weight were recorded. Development of GvHD was determined by examining features including weight loss, ruffled fur and hunched posture (Section 2.10.5). Animals which displayed greater than 25% weight loss were sacrificed humanely.

2.10.4 HUMANISED MOUSE MODEL OF AGVHD

A humanised mouse model previously developed (Tobin *et al.* 2013) in the lab was optimised for the administration of PBMC isolated from buffy packs. NOD.Cg-$Prkdc^{scid}IL2^{tmlWjl}$/Szj (NOD-Scid IL-2rγ^{null}) (NSG) mice were exposed to a conditioning dose of 2.4 Gy whole body gamma irradiation. PBMC, isolated as described in section 2.3.2, were administered via tail vein injection using a 27 gauge needle and 1 ml syringe 6 – 8 hours after irradiation (Section 2.10.6). 8×10^5 $gram^{-1}$ PBMC were administered via tail vein injection using a 27 gauge needle and 1 ml syringe 6 – 8 hours after

irradiation. Animals were returned to their cages and were closely monitored for the first hour and at regular intervals for signs of distress or ill health. Mice were weighed every 2 days until day 7 and every day thereafter and changes in weight were recorded. Development of acute GvHD was determined by examining features including weight loss, ruffled fur and hunched posture (Section 2.10.5). During initial optimisation experiments animals which displayed greater than 20% weight loss were sacrificed humanely; however, in accordance with alterations agreed between the lab and the NUI Maynooth ethics committee, the weight loss threshold was lowered to 15%.

2.10.5 PATHOLOGICAL SCORING SYSTEM FOR GVHD

Development of GvHD was assessed using a series of pathological features. Weight loss in excess of 15% total body weight on successive days were deemed to have acute GvHD and humanely sacrificed. Other pathological features which were taken into consideration were posture (hunching), activity, grooming and diarrhoea. Any animal which scored a cumulative score of 7 or higher were considered to have acute GvHD and sacrificed humanely. The scoring system used to assess experimental mice was as follows:

Posture: 0; normal posture while walking, 0.5; slight hunching that straightens out while walking, 1; animal stays hunched while walking, 1.5; animal does not straighten out, 2; mouse tends to walk on rear toes.

Activity: 0; normal, very mobile and difficult to catch, 0.5; slower than normal and a little easier to catch, 1; no spontaneous activity but will move freely when touched, 1.5; no spontaneous movements and very little when touched, 2; no movements even when touched.

Fur: 0; normal, well groomed, 0.5; ridging of fur on side of belly and neck, 1; ridging throughout belly and neck, 1.5; fur is matted and ruffled, 2; badly matted and unkempt fur on belly and back.

Diarrhoea: 0; normal bowel movements, 1; change in bowel movement frequency and consistency, 2; extensive diarrhoea.

2.10.6 Fh-Teg stimulation of PBMC

PBMC were isolated from buffy packs as described above. PBMC were seeded at 2 x 10^6/ml in T175 flasks and stimulated with Fh-Teg at 10 µg/ml or left untreated. PBMC were incubated at 37°C overnight. The next day, PBMC were harvested and counted. Cells were washed 3 times in sterile PBS and before infusion.

2.10.7 Intra-venous administration of PBMC or MSC

Prior to administration, PBMC or MSC were washed 3 times with sterile PBS. PBMC were administered at 8 x 10^5 $gram^{-1}$ and MSC were administered at 6 x 10^4 $gram^{-1}$. PBMC or MSC were administered through a tail vein injection using a 27G needle and a 1 ml syringe with each mouse receiving a maximum of 300 µl. PBMC were infused on day 0 while MSC were delivered on day 7 or 9. Following injection, animals were returned to their cages and were monitored as described above.

2.10.8 PREPARATION OF BUSULFAN

Prior to administration, Busulfan (Sigma-Aldrich) was weighed out in a fume hood and diluted to a 2mg/ml using sterile PBS. Diluted Busulfan was filter sterilised in a fume hood and was administered at a final concentration of 25mg/kg via tail vein injection using a 27G needle and a 1 ml syringe with each mouse receiving a maximum of 300 µl. Busulfan was administered at 48 and 24 hours before PBMC infusion. Mice which received Busulfan were closely monitored after administration.

2.11 CFSE LABELLING OF CELLS

Purified $CD19^+$ B cells were washed twice in sterile PBS and re-suspended in 1 ml of PBS. Cells were stained with 10 µM Carboxyfluorescein succinimidyl ester (CFSE) for 10 minutes at room temperature in the dark. 2 ml of ice cold PBS was added and cells were centrifuged at 300 g for 5 minutes and washed twice with cold PBS. Labelled $CD19^+$ B cells were re-suspended cIMDM and counted.

2.12 HISTOLOGICAL ANALYSIS

2.12.1 TISSUE PREPARATION

The lungs, liver, spleen and small intestine were harvested from experimental mice at day 12 and fixed in 10% (v/v) neutral buffered formalin for 24 hours. Samples were transferred to 70% ethanol for a further 24 hours. Samples were processed for histology using an automated processor (Shannon Pathcentre) which immersed the tissues in fixatives and sequential dehydration solutions including ethanol (70%, 80%, 95% x 2,

100% x 3) and xylene (x 2) (Sigma-Aldrich). After processing, tissues were embedded in paraffin wax using a Shandon Histocentre 2 (Thermo Fisher Scientific) and left to set at 4°C overnight. A Shandon Finesse 325 microtome (Thermo Fisher Scientific) was used to cut 5 µm sections of each tissue. Sections were placed in cold water before being transferred to a hot water bat (60°C) to remove any folding of the sections. Tissue sections were placed onto microscope slides (Thermo Fisher Scientific) and left to air dry overnight. Samples were then stained with H&E (Section 2.12.2) and blindly scored using the system outlined in section 2.12.3.

2.12.2 HAEMOTOXYLIN/EOSIN STAINING

Before commencing with H&E staining, slides were heated to 60°C for a minimum of 1 hour to aid wax clearance. Slides were then transferred to Xylene (Sigma) for 10 minutes and again to fresh xylene for a further 10 minutes. Samples were then re-hydrated following immersion in 3 decreasing concentrations of ethanol for 5 minutes each (100% x 2, 90% and 80%) for 5 minutes each. Samples were then transferred to dH_2O for 5 minutes before being immersed in Haemotoxylin (Sigma) for 3 minutes. Samples were then washed under H_2O for 2 minutes before being placed in 1% acid alcohol for no longer than 20 seconds. Samples were washed again under H_2O before being immersed in Eosin Y (Sigma-Aldrich) for 3 minutes and back to washing under H_2O again. Slides were dehydrated through immersion in a series of increasing ethanol concentrations (80%, 90%, 100%) for 5 minutes each. Samples were air dried and mounted with DPX mounting media (BDH) and examined under a light microscope.

Table 2.15. Histological staining solutions

Reagent	Components	Concentration	Supplier
Harris Hemotoxylin	Hemotoxylin	Neat	Sigma-Aldrich
Eosin	Eosin Y	1% (w/v)	Sigma-Aldrich
	Potassium dichromate	1.6% (w/v) 100 ml	Sigma-Aldrich
	dH_2O		
Acid alcohol	Hydrochloric acid	1% (v/v)	VWR
	2-propanol	69.3% (v/v)	Sigma-Aldrich
	dH_2O	29.7% (v/v)	

Table 2.16. TAE Buffer (50X Stock)

Final Volume	1 Litre
TRIS Base	242 g
Acetic acid	57.1 ml
EDTA (0.5 M, pH 8.8)	100 ml
dH_2O	Up to 1 Litre

2.12.3 HISTOLOGICAL SCORING

Following H&E staining, slides were coded without reference to treatment groups and examined blindly. A semi-quantitative scoring chart was used to assess disease progression in the lungs, liver, spleen and small intestine (Tobin *et al.* 2013). Pathological scoring was carried out as follows:

Lung: 0; normal, 1; scattered areas of mononuclear cells, 2; mild focussed areas of mononuclear cell infiltration, 3; moderate levels of cellular infiltration and damage to lung architecture, 4; extensive mononuclear cell infiltration and extensive damage to lung architecture.

Liver: 0; normal, 1; sporadic collections of mononuclear cells in the parenchyma, 2; endothelialitis present around at least one periportal vein and marked increase in mononuclear cell infiltration, 3; endothelialitis present in more than one vessel and further increase in mononuclear cell infiltration, 4; endothelialitis present in virtually all vessels with extensive levels of mononuclear cell infiltration.

Small intestine: 0; normal, 1; mild necrotic cells with minor mononuclear cell infiltration, 2; widespread but mild villous blunting, necrosis and increased cell infiltration, 3; widespread and moderate villous blunting, necrosis and further increased cell infiltration, 4; widespread and severe villous blunting, necrotic cells and extensive mononuclear cell infiltration.

Table 2.17. Antibodies used for flow cytometry

Antibody	Conjugate	Clone	Supplier
CD3	APC	UCHT1	eBioscience
CD4	FITC	SK3	eBioscience
CD4	PE	SK3	eBioscience
CD4	PercP	SK3	eBioscience
CD4	APC	SK3	eBioscience
CD8	FITC	RPA-T8	eBioscience
CD8	PE	RPA-T8	eBioscience
CD8	PercP	RPA-T8	eBioscience
CD8	APC	RPA-T8	eBioscience
CD19	FITC	HIB19	eBioscience
CD19	APC	HIB19	eBioscience
CD20	FITC	2H7	eBioscience
CD20	APC	2H7	eBioscience
CD25	PE	BC96	eBioscience
CD27	FITC	0323	eBioscience
CD29	FITC	TS2/16	eBioscience
CD34	PE	4H11	eBioscience
CD44	FITC	IM7	eBioscience
CD44	PE	IM7	eBioscience
CD45	Percp	2D1	eBioscience
CD45	APC	HI30	eBioscience
CD45ro	APC	UCHL1	eBioscience

Table 2.17. (continued): Antibodies used for flow cytometry

Antibody	Conjugate	Clone	Supplier
CD54	FITC	RR1/1	eBioscience
CD62L	PE	DREG-56	eBioscience
CD69	FITC	FN50	eBioscience
CD80	PE	2D10.4	eBioscience
CD86	PE	IT2.2	eBioscience
CD90	FITC	eBio5E10	eBioscience
CD105	APC	SN6	eBioscience
CD106	PE	STA	eBioscience
CD117	PE	YB5.B8	eBioscience
CD154	FITC	24-31	eBioscience
HLA-DR	PE	L243	eBioscience
HLA-ABC	FITC	W6/32	eBioscience
TNF-α	FITC	MAb11	eBioscience
TNF-α	PE	MAb11	eBioscience
IL-2	PE	MQ1-17H12	eBioscience
FoxP3	FITC	236A/E7	eBioscience
FoxP3	APC	236A/E7	eBioscience
B220	APC	RA3-6B2	eBioscience
CXCR4	APC	12G5	eBioscience
Bcl-2	PE	BCL/10C4	BioLegend
IFN-γ	FITC	4S.B3	BioLegend

Table 2.18. Summary of primer sequences for Reverse transcriptase PCR

Primer	Forward 5' – 3'	Reverse 3' – 5'	Product size (bp)	Annealing Temp. (°C)
GAPDH	ACAGTTGCCATG TAGACC	TTTTTGGTTGAGCA CAGG	90	58
Collagen II	GCCCAAGAGGTG CCCCTGGAATA	CCTGAGAAAGAGG AGTGGACATA	703	57
Aggrecan	TGAGGAGGGCTG GAACAAGTACC	GGAGGTGGTAATT GCAGGGAAC	350	55

Table 2.19. Summary of primers for Real Time PCR

Primer	Forward 5' – 3'	Reverse 3' – 5'	Annealing Temp. (°C)
GAPDH	ACAGTTGCCATGTA GACC	TTTTTGGTTGAGCA CAGG	58
BAFF	AATTTAACAGACAG CCACAG	TGTCCTTCCTCCAA GATAAG	58
IL-18	CCTTTAAGGAAATG AATCCTCC	CATCTTATTATCAT GTCCTGGG	58
IL-21	AGAAACACAGACT AACATGC	GTAGATACCTTTTG GAGAAGTG	58
NFKB1	GCTTAGGAGGGAG AGCCCA	TATGGGCCATCTGT TGGCAG	60

Table 2.20. Primary antibodies used for western blot

Antibody	Dilution Factor	Diluent	Supplier
BAFF	1:500	5% BSA in TBST	R&D (Minneapolis, USA)
AKT	1:1000	5% BSA in TBST	Cell Signalling
Phoshorylated AKT	1:1000	5% BSA in TBST	Cell Signalling
Cleaved Caspase 3	1:500	5% BSA in TBST	Cell Signalling
β-actin	1:5000	5% milk in TBST	Sigma-Aldrich

Table 2.21. Secondary antibodies for western blot

Antibody	Dilution Factor	Diluent	Supplier
IRDye 800CW Donkey Anti-Goat	1:5000	5% Milk in TBST	Licor
IRDye 800CW Goat Anti-Rabbit	1:5000	5% Milk in TBST	Licor
IRDye 800CW Goat Anti-Mouse	1:5000	5% Milk in TBST	Licor
Anti-Rabbit HRP	1:1500	5% Milk in TBST	Cell Signalling

CHAPTER 3

MSC PROTECT AGAINST CASPASE 3 MEDIATED APOPTOSIS OF $CD19^+$ PERIPHERAL B CELLS THROUGH CONTACT DEPENDENT UP-REGULATION OF VEGF

3.1 INTRODUCTION

B cell development is a complex and tightly controlled process which occurs in the bone marrow and culminates in the migration of naïve B cells to secondary lymphoid organs via the blood and lymphatic system (Nuñez *et al.* 1996; Cyster 1999). In secondary lymphoid organs, the controlled activation, proliferation and differentiation of B cells upon recognition of foreign antigen represent the cornerstone of the adaptive immune system and are essential in the development of life long memory within the immune system (Yu *et al.* 2008). Consequently, the success of novel cell therapies can depend greatly on how they interact with B cells after administration. For MSC to progress further towards clinical application, it will be essential to clarify exactly how MSC interact with B cells. While the ability of MSC to suppress T cell proliferation (English *et al.* 2007; Tobin *et al.* 2013), DC maturation, antigen presentation (Wang *et al.* 2008; English *et al.* 2008; Spaggiari *et al.* 2009) and NK cell function (Spaggiari *et al.* 2008; Noone *et al.* 2013) have been extensively characterised, the immune-modulatory capabilities of MSC with regard to B cells is poorly understood.

The effect of human MSC on the B cell component of the adaptive immune response has received some attention in recent years; however these studies have reported contrasting and sometimes conflicting results (Franquesa *et al.* 2012; Corcione *et al.* 2006; Tabera *et al.* 2008; Rasmusson *et al.* 2007; Traggiai *et al.* 2008; Rosado *et al.* 2014; Comoli *et al.* 2008). While most of the published data indicated that MSC inhibit B cell proliferation, differentiation and antibody secretion (Franquesa *et al.* 2012; Corcione *et al.* 2006; Tabera *et al.* 2008), other publications have demonstrated a supportive role for MSC in B cell expansion and differentiation (Rasmusson *et al.* 2007; Traggiai *et al.* 2008). The variability observed between studies is probably derived from the different experimental conditions used in each study, in particular the ratio of MSC to B cell and purity of B cell populations. However, the source of B cells and stage of maturity may

also be factors. Recently Rosado *et al.* (2014) have demonstrated that MSC can either inhibit or support B cell proliferation and antibody production depending on the presence of T cells in co-culture (Rosado *et al.* 2014). When peripheral blood lymphocyte populations were used, MSC suppressed the proliferation of stimulated B cells, however when cultured with purified B cell populations, MSC enhanced the proliferation and antibody production of stimulated B cells (Rosado *et al.* 2014).

The capacity of MSC to potently modulate the immune system offers considerable possibilities for regenerative medicine and a potential treatment for a variety of immune disorders including allograft rejection (Breitbart *et al.* 2010). However, in order to further the development of MSC towards clinical application it is essential to clarify exactly how MSC interact with all cells of the immune response. In this study, we sought to determine how MSC alter B cell biology in terms of activation, proliferation and survival and to elucidate the mechanisms involved.

The objectives for this chapter were:

1. To determine the effect of MSC on B cell function; activation, proliferation and antibody production.
2. To elucidate the mechanism of action behind MSC modulation of B cell function.

Table 3.1. Summary of major published works on the effect of MSC on peripheral B cells *in vitro*.

Cell source	B cell isolation	Ratio B cell:MSC	B cell stimuli	Effect of MSC	Reference
Healthy human PBMC	T cell depletion and $CD19^+$ positive selection (MACS)	1:1 2:1	rhCD40L + CpG + anti-Ig + IL-2 + IL-4 +/- IL-10	Inhibition of proliferation (not apoptosis) of cell cycle G0/G1. Mediated by soluble factors. Inhibition of IgG, IgA, IgM secretion. Inhibition of migratory chemokines	Corcione *et al.* (2006)
Healthy human splenocytes or PBMC	Enriched B cell population (MACS)	10:1	LPS CMV VZV	Cell contact dependent increased IgG production.	Rasmusson *et al.* (2007)
Healthy human PBMC	Partial CD4 and full CD8 T cell depletion (MACS)	4:1 20:1	MLC CD40 agonist IL-10	MSC inhibit IgG, IgA, IgM production in MLC. No effect with transwell inserts	Comoli *et al.* (2008)
PBMC from Buffy coat	$CD19^+$ and $CD3^+$ selection (MACS)	5:1 10:1	CpG Anti-Ig CD40L IL-4	Promotes B cell viability, cause B cell cycle arrest in G0/G1. Inhibit plasma cell induction mediated by Erk1/2 phosphorylation.	Tabera *et al.* (2008)
Healthy and PBMC from lupus patients	$CD19^+$ selection (MACS)	1:1	CpG IL-2 CD40L Anti-Ig	Induced survival and proliferation of B cell subsets. No increase in IgA or IgG. Increased IgM and IgG in B cells from SLE patients.	Traggiai *et al.* (2008)
Healthy human PBMC	Whole PBMC or $CD19^+$ separated B cells	10:1	CpG-ODN	MSC suppressed B cell proliferation when cultured with whole PBL but supported proliferation of purified $CD19^+$ B cells	Rosado *et al.*, 2014

3.2 MSC ENHANCED CD19$^+$ PERIPHERAL B CELL ACTIVATION

B cell activation following antigen recognition and appropriate CD4$^+$ T cell signalling, triggers B cell clonal expansion, isotype switching and the development of antibody producing plasma cells and memory B cells (Pieper *et al.* 2013). Previous studies investigating the ability of MSC to modulate B cell activation, proliferation and antibody production have provided contradictory results (Table 3.1) (Franquesa *et al.* 2012; Corcione *et al.* 2006; Tabera *et al.* 2008; Comoli *et al.* 2008; Rasmusson *et al.* 2007; Traggiai *et al.* 2008; Rosado *et al.* 2014). This study was designed to determine how MSC directly affect purified CD19$^+$ B cells. To determine the direct effect of MSC on B cell activation, PBMC were isolated from buffy-coat packs obtained from healthy donors. CD19$^+$ B cells were purified from PBMC using immunomagnetic beads (Miltenyi Biotec) (Figure 3.1) and co-cultured with MSC (5:1 ratio B cell: MSC) for 48 hours in cIMDM containing the B cell activating cocktail described in Table 2.14 (human IL-10, IL-2, IL-21 and activating molecules CD40L and CpG). B cell activation was characterised by increased expression of the early lymphocyte activation marker CD69, co-stimulatory molecules CD86 and CD80, and also CD25 by flow cytometry.

As expected, B cells cultured in cIMDM without the activation cocktail expressed very low levels of CD69, CD80, CD25 and CD86 after 48 hours (Figure 3.2 A – D respectively). Notably, when cultured in the presence of MSC, resting B cells did not up-regulate these activation markers, indicating that MSC do not directly activate peripheral B cells (Figure 3.2). Stimulation of CD19$^+$ B cells significantly increased CD69 expression and also enhanced the expression of CD80, CD25 and CD86 on B cells after 48 hours (Figure 3.2). When activated in the presence of MSC, significantly more peripheral B cells expressed CD69 (Figure 3.2). The expression of CD80, CD86 and CD25 was also higher when B cells were activated in the presence of MSC (Figure 3.2), suggesting that MSC support but do not induce B cell activation.

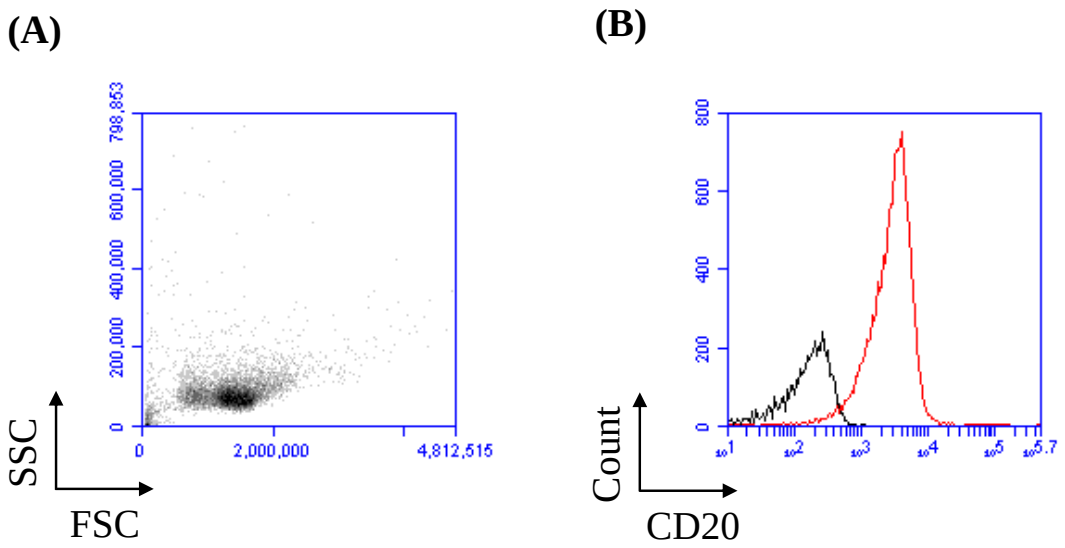

Figure 3.1. CD19$^+$ MACS isolation of B cells from buffy packs results in a single pure B cell population. B cells were purified from PBMC populations using CD19$^+$ MACS beads. The purity of isolated B cells was determined using B cell specific marker CD20 following CD19$^+$ B cell isolation using flow cytometry. CD19$^+$ MACS separation resulted in a single lymphocyte population (A) which were positive for CD20 (B). Only B cell isolations which yielded at least 95% purity, as determined by CD20 expression, were used in experiments.

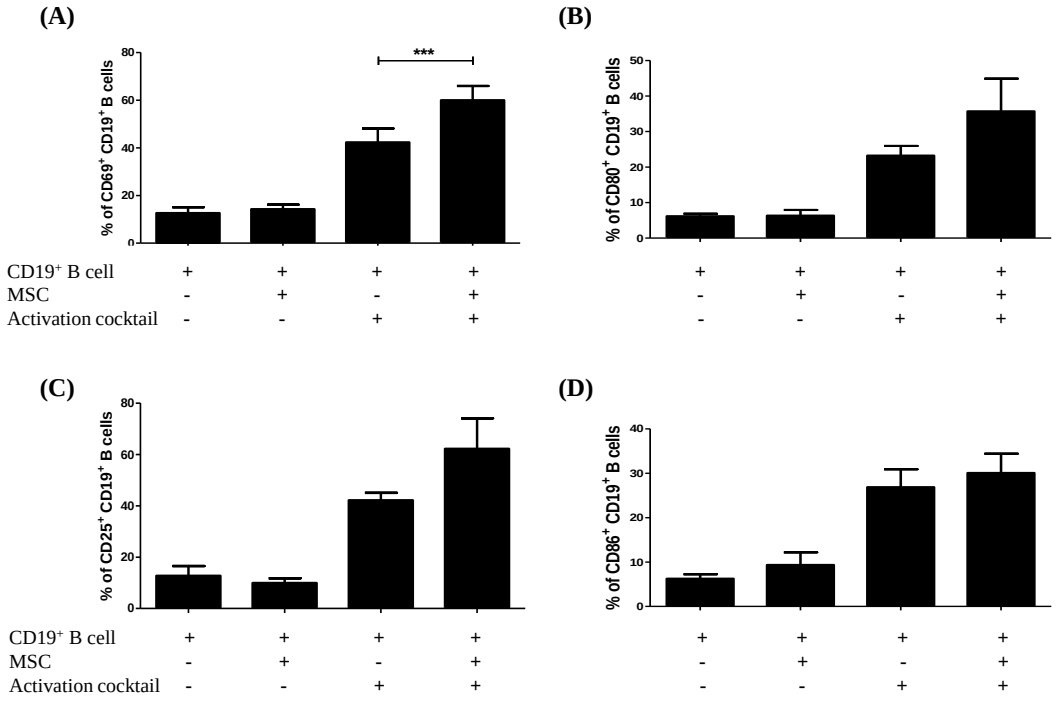

Figure 3.2: MSC support the activation of CD19$^+$ peripheral B cells. CD19$^+$ B cells were purified from PBMC populations using CD19$^+$ MACS beads. 9 x 10^5 B cells were cultured in cIMDM in the presence or absence of 1.8 x 10^5 MSC (5:1) and were activated with a cytokine cocktail of 25 ng/ml recombinant IL-10, 100 U/ml recombinant IL-2, 100 ng/ml recombinant IL-21, ITS (1:1000), 250 ng/ml recombinant CD40L and 2.5 µg/ml CpG for 48 hours. The expression of activation markers CD69 (A), CD80 (B), CD25 (C) and CD86 (D) were analysed after 48 hours by flow cytometry. n=5 for (A) and n=3 for (B – D). Statistical analysis was carried out using a paired student *t* test. *** indicates p-value < 0.001.

3.3 MSC PROMOTE THE EXPANSION OF ACTIVATED $CD19^+$ PERIPHERAL B CELLS IN A CELL CONTACT DEPENDENT MANNER

The rapid proliferation of activated B cells following the recognition of foreign antigen or danger signals is critical to the development of an effective immune response. As described in Table 3.1, previous studies examining how MSC regulate the proliferation of peripheral B cells has provided conflicting results. To determine whether MSC suppressed or supported the proliferation of activated B cells, $CD19^+$ B cells were labelled with proliferation dye (CFSE) and cultured in the presence or absence of MSC for 5 days. B cell proliferation was induced using the same activating cocktail as in section 3.2. After 5 days, B cells proliferation was analysed by flow cytometry.

Activation of $CD19^+$ B cells with the activation cocktail alone potently induced B cell proliferation with approximately 80% of activated B cells undergoing at least one phase of proliferation (Figure 3.3 A & C). However, in the presence of MSC, there were significantly less non-proliferating (0 divisions) B cells and significantly more B cells had gone through at least 5 divisions compared to B cells activated without MSC (Figure 3.3 A & C). Thus B cells activated in the presence of MSC undergo significantly more divisions. The dependence of cell contact in MSC support of B cell proliferation was examined using a transwell co-culture system, separating B cells from the MSC. Inhibition of cell contact completely abrogated the MSC support of B cell proliferation suggesting that the increase in B cell proliferation after co-culture with MSC is mediated through a cell contact dependant mechanism (Figure 3.3 D & E).

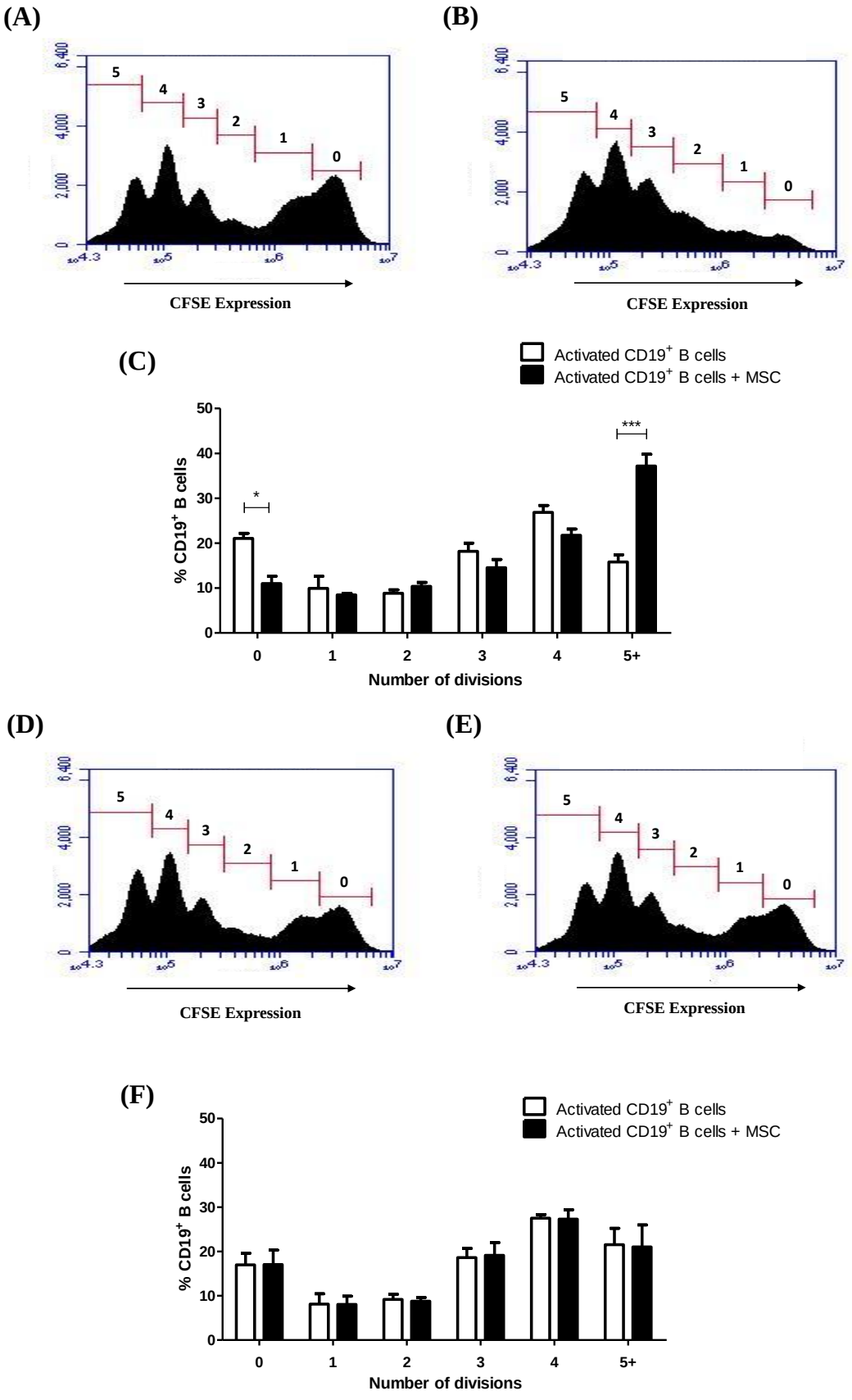
(A)
(B)
5
4
3
2
1
0
CFSE Expression
(C)
Activated CD19+ B cells
Activated CD19+ B cells + MSC
% CD19+ B cells
Number of divisions
*
***
(D)
(E)
(F)

Figure 3.3: MSC enhance the expansion of activated CD19$^+$ peripheral B cells in a cell contact dependent manner. CD19$^+$ B cells were purified from PBMC populations using CD19$^+$ MACS beads and labelled with 10µM CFSE. 9 x 10^5 B cells were cultured in cIMDM in the presence or absence of 1.8 x 10^5 MSC (5:1) and were activated with a cocktail of 25 ng/ml recombinant IL-10, 100 U/ml recombinant IL-2, 100 ng/ml recombinant IL-21, ITS (1:1000), 250 ng/ml recombinant CD40L and 2.5 µg/ml CpG. (A) Representative image of CFSE fluorescence by activated B cells after 5 days. (B) Representative image of CFSE fluorescence by activated B cells cultured in the presence of MSC. (C) Percentage of activated B cells which have undergone cell division in the presence or absence of MSC for 5 days. n=8 PBMC donors with 2 MSC donors. Transwell membrane inserts (0.4 µm pore size) were used to prevent cell contact between MSC and CFSE labelled B cells during co-culture. (D) Representative image of CFSE fluorescence by activated B cells cultured using transwell inserts after 5 days. (E) Representative image of CFSE fluorescence by activated B cells separated from MSC using transwell inserts for 5 days. (F) Percentage of activated B cells which have undergone cell division in the presence or absence of MSC for 120 hours using transwell membranes. n=8 PBMC donors with 2 MSC donors. Statistical analysis was carried out using a paired student *t* test. * < 0.05, *** < 0.001.

3.4 IgG AND IgM PRODUCTION BY $CD19^+$ B CELLS WAS NOT AFFECTED BY MSC

The production of antibodies and isotype switching by B cells is fundamental to maintaining memory against pathogens. However, the production of antibodies is highly regulated and dysregulation of antibody production can result in severe autoimmune disease (Vinuesa *et al.* 2009). Corcione *et al.* and Comoli *et al.* reported that MSC inhibit B cell secretion of IgG and IgM (Corcione *et al.* 2006; Comoli *et al.* 2008) while Rasmusson *et al.* demonstrated that co-culture with MSC resulted in enhanced IgG secretion (Rasmusson *et al.* 2007). The effect of MSC on IgG and IgM production by $CD19^+$ peripheral B cells was examined after 72 hours by ELISA. Purified $CD19^+$ B cells were co-cultured in the presence or absence of MSC (5:1) and activated using B cell activation cocktail described above. A transwell co-culture system was designed to investigate whether MSC modulation of antibody production was dependent on cell contact or mediated by soluble factors.

Supernatant recovered from B cells cultured alone contained approximately 30 ng/ml of IgG (Figure 3.4 A). The levels of IgG produced by B cells was not affected by the presence of MSC (Figure 3.4 A). Separation of B cells from MSC using transwell membranes also had no effect on IgG production (Figure 3.4 A). Similarly the production of IgM by activated B cell populations was unaffected by the presence of MSC in the co-culture (Figure 3.4 B). These results suggest that MSC neither supported nor inhibited antibody production by peripheral B cells.

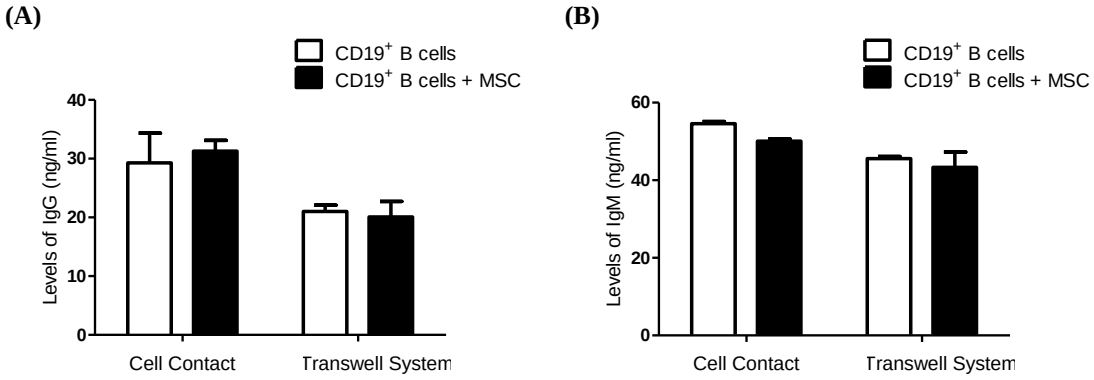

Figure 3.4: MSC had no effect on the production of IgG or IgM by CD19$^+$ B cells. CD19$^+$ B cells were purified from PBMC populations using CD19$^+$ MACS beads. 9 x 10^5 B cells were cultured in cIMDM in the presence or absence of 1.8 x 10^5 MSC (5:1) and were activated with 25 ng/ml recombinant IL-10, 100 U/ml recombinant IL-2, 100 ng/ml recombinant IL-21, ITS (1:1000), 250 ng/ml recombinant CD40L and 2.5 µg/ml CpG for 72 hours. Transwell membrane inserts (0.4 µm pore size) were used to prevent cell contact between MSC and B cells during co-culture. Supernatant was collected and analysed for the expression of IgG (A) or IgM (B) by ELISA. White bars represent B cells cultured alone while black bars represent B cells co-cultured with MSC. n= 2 PBMC donors and 2 MSC donors. Statistical analysis was carried out using a paired student *t*-test.

3.5 MSC SUPPORT OF B CELL PROLIFERATION IS NOT DEPENDENT ON B CELL ACTIVATING FACTOR (BAFF)

As demonstrated above, MSC supported the activation and proliferation of $CD19^+$ peripheral B cells (Figure 3.2 & 3.3). MSC support of B cell proliferation was mediated through a cell contact signal (Figure 3.3). One of the most potent inducers of B cell proliferation is B cell activating factor (BAFF). BAFF is a member of the TNF superfamily of receptors, which functions both as a surface bound protein and soluble factor, and is known to bind TNSFR13 on B cells and support proliferation, activation and survival (Schneider *et al.* 1999). The expression of BAFF by human adipose derived MSC has also previously been shown (Wang *et al.* 2011). Therefore to determine the importance of BAFF in mediating the support of B cell survival and proliferation by MSC, the ability of MSC to produce BAFF was probed by real time PCR and verified by immunoblotting. MSC were seeded into 6 well plate at $1.8x10^5$ cells per well overnight before being stimulated with IFN-γ or TNF-α for 6, 8, 12 or 24 hours and harvested as described in chapter 2.

MSC significantly up-regulated BAFF mRNA expression after 6 hours when stimulated with IFN-γ or TNF-α as measured by real time PCR (Figure 3.5 A). Interestingly, BAFF mRNA expression is differentially regulated by IFN-γ or TNF-α after 24 hours. IFN-γ stimulated MSC continue to up-regulate BAFF expression after 24 hours while TNF-α induced BAFF expression is lower after 24 hours than observed after 6 hours (Figure 3.5 A) suggesting BAFF expression on MSC may be differentially regulated depending on the environment of the cell.

The expression of BAFF by MSC was then verified at the protein level by western blotting. MSC constitutively expressed low levels of membrane bound BAFF but not soluble BAFF (Figure 3.5 B). Similar to the results observed with real time PCR,

expression levels of both membrane bound and soluble BAFF were markedly increased by MSC after IFN-γ or TNF-α stimulation for 8, 12 and 24 hours (Figure 3.5 B). In correlation with results observed at the mRNA level, TNF-α stimulated MSC did not continue to up-regulate membrane bound BAFF at 24 hours while IFN-γ stimulated MSC showed increased BAFF expression at this time-point (Figure 3.5 B). These results illustrate that MSC constitutively express membrane bound BAFF protein which can be significantly up-regulated following the correct signal, which suggests that BAFF may be the contact signal required for MSC support of B cell proliferation.

Constitutive expression of membrane bound BAFF highlighted the potential that BAFF represented the contact signal required by B cells to enhance proliferation. To investigate whether BAFF-BAFFR was the signal used by MSC to promote B cell proliferation, BAFF signalling was neutralised during B cell:MSC co-culture. The efficacy of the BAFF neutralising antibody was determined by examining the expression of NFKB1 on purified $CD19^+$ B cells following stimulation with recombinant human BAFF (rhBAFF) after 6 hours. B cells which were stimulated with rhBAFF in the presence of BAFF inhibitor showed a significant decrease in NFKB1 expression (Figure 3.5 C). Purified and CFSE stained B cells were activated and cultured with or without MSC (5:1), as described in section 3.3, in the presence or absence of BAFF inhibitor (50 µg/ml). After 5 days, B cells proliferation was analysed by flow cytometry. As observed in section 3.3, activation of $CD19^+$ B cells with the activation cocktail potently induced B cell proliferation with approximately 75% of B cells entering at least one phase of proliferation (Figure 3.6) and as expected, the proliferation of B cells activated in the presence of MSC was significantly increased (Figure 3.6). However, the addition of BAFF inhibitor did not reverse MSC support of B cell proliferation, demonstrating that MSC support of B cell proliferation was independent of BAFF signalling.

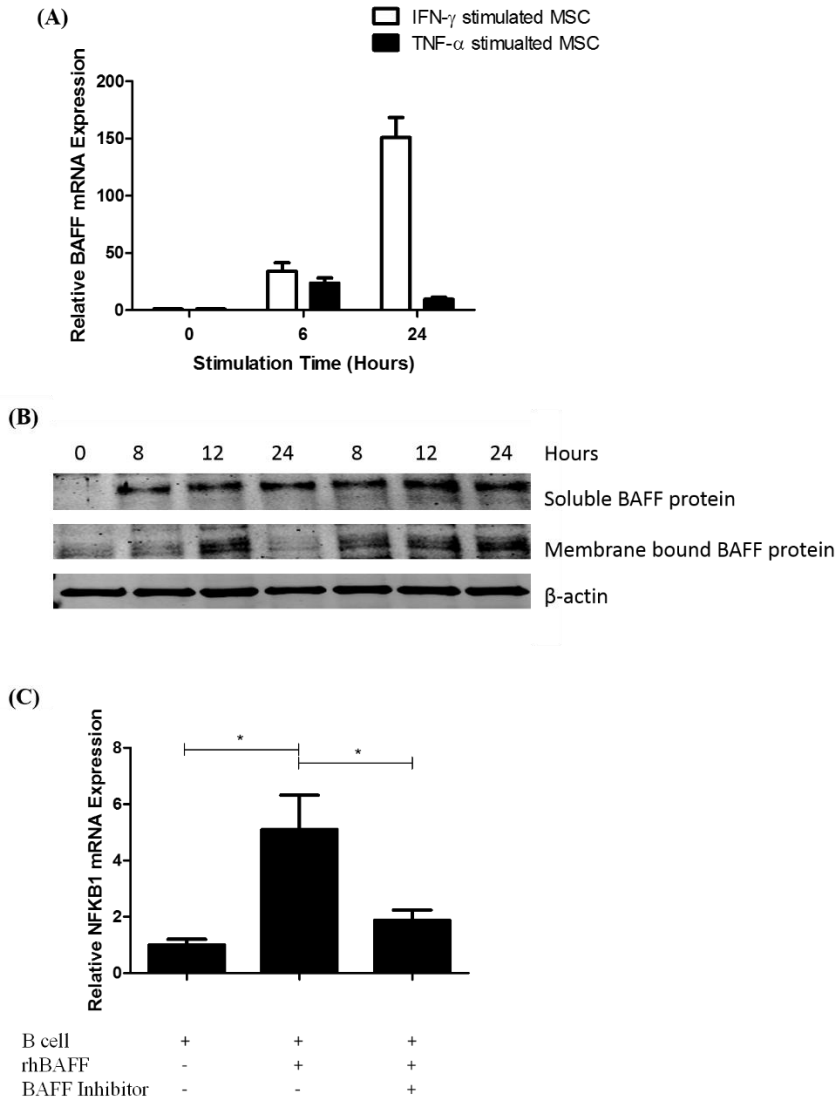

Figure 3.5: Constitutive expression of BAFF by MSC is enhanced by IFN-γ or TNF-α. (A) MSC were seeded at $1.8x10^5$ cells/well and incubated overnight in a 6 well plate and stimulated with 50 ng/ml IFN-γ or 20 ng/ml TNF-α for 6 or 24 hours. The expression of BAFF mRNA was examined by real time PCR. White bars represent IFN-γ stimulated MSC while black bars represent TNF-α stimulated MSC. n= 3 MSC donors. GAPDH expression was used as a house-keeping control. (B) MSC were seeded at $1.8x10^5$ cells/well and incubated overnight in a 6 well plate and stimulated with 50 ng/ml IFN-γ or 20 ng/ml TNF-α for 8, 12 or 24 hours. The expression of soluble BAFF protein (top segment) and membrane bound BAFF (middle segment) was analysed by western blot. β-actin (bottom segment) was used as a loading control. Image representative of 2 MSC donors. (C) The neutralising ability of BAFF antibody was analysed by examining the expression of NFKB1 by real time PCR. Isolated CD19+ B cells were stimulated with recombinant human BAFF (10 ng/ml) in the presence or absence of BAFF inhibitor (50 µg/ml) for 6 hours. n=4 donors.

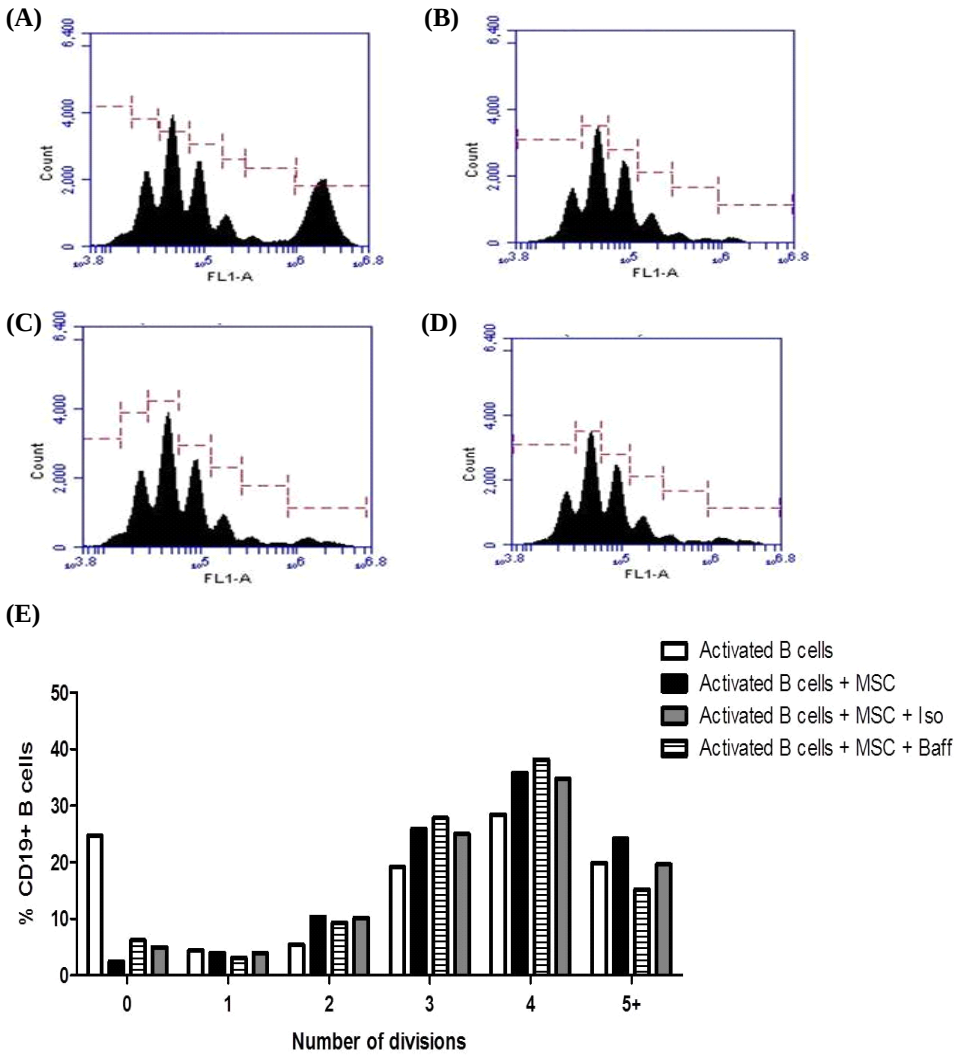

Figure 3.6: Inhibition of BAFF signalling does not prevent MSC from enhancing B cell proliferation. Purified B cell populations were isolated from PBMC using $CD19^+$ MACS beads and labelled with 10µM CFSE. 9 x 10^5 B cells were cultured in cIMDM in the presence or absence of 1.8 x 10^5 MSC (5:1) and were activated with 25 ng/ml recombinant IL-10, 100 U/ml recombinant IL-2, 100 ng/ml recombinant IL-21, ITS (1:1000), 250 ng/ml recombinant CD40L and 2.5 µg/ml CpG for 5 days. (A-D) Representative image of the CFSE expression profile of (A) B cells activated alone, (B) B cells activated in the presence of MSC, (C) B cells activated in the presence of MSC and BAFF inhibitor and (D) B cells activated in the presence of MSC and isotype control. (E) Graphical representation of the percentage of activated B cells which have undergone cell division after 5 days. White bars represent B cells activated alone, black bars represent B cells activated in the presence of MSC, striped bars represent B cells activated in the presence of MSC and BAFF inhibitor and grey bars indicate B cells activated in the presence of MSC and isotype control. n=2 PBMC donors with 1 MSC donors.

3.6 MSC SIGNIFICANTLY INCREASED B CELL SURVIVAL *IN VITRO* THROUGH A CONTACT DEPENDENT MECHANISM

A role for MSC in maintaining the haematopoietic stem cell niche has previously been identified (Méndez-Ferrer *et al.* 2010). MSC are capable of supporting the survival of immune cells through contact dependent and soluble mechanisms (English & Wood 2013). The ability of MSC to support B cell viability *in vitro* may explain the enhanced activation and proliferation of B cells after co-culture with MSC (Figure 3.2 & 3.3). To investigate the effect of MSC on the survival of $CD19^+$ B cells, purified B cells were cultured in the presence or absence of MSC (5:1) for 72 hours. In the absence of MSC, the viability of B cells was very low with approximately 20% of cells negative for apoptosis markers Annexin V/PI, as analysed by flow cytometry (Figure 3.7). However, B cells cultured in the presence of MSC demonstrated significantly increased viability illustrated by the percentage and number of Annexin V^-PI^- B cells (Figure 3.7). Preventing cell contact using transwell membranes (0.4 μm pore) abrogated the protection of $CD19^+$ B cell survival by MSC and the percentage and cell number of Annexin V and PI negative cells was restored to a similar level of B cells cultured alone (Figure 3.7), suggesting that MSC support of B cell survival requires cell contact.

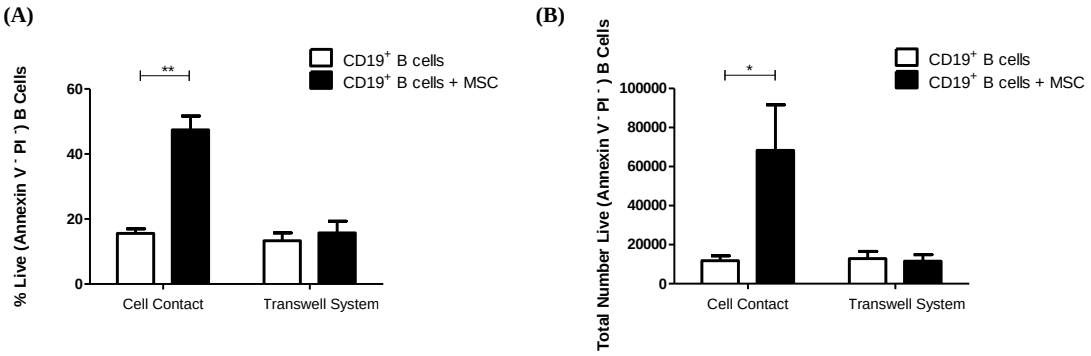

Figure 3.7: MSC support B cell survival through a contact dependent mechanism. Purified B cell populations were obtained from PBMC using $CD19^+$ MACS beads. 9 x 10^5 B cells were cultured in cIMDM in the presence or absence of 1.8 x 10^5 MSC (5:1) for 72 hours and B cell survival was determined by analysing the expression of Annexin V and propidium iodide (PI) on CD45 APC gated B cells. Transwell membrane inserts (0.4 µm pore size) were used to prevent cell contact between MSC and B cells during co-culture. (A) Represents the percentage of live (Annexin V^- PI^-) B cells and (B) represents the total number of live B cells. White bars indicate B cells cultured alone while black bars represent B cells co-cultured with MSC. n=3 PBMC donors with 3 MSC donors. Statistical analysis was carried out using a paired student *t* test. * < 0.05, ** < 0. 01.

3.7 LICENCING OF MSC WITH IFN-γ HAS NO EFFECT ON THEIR SUPPORT OF B CELL SURVIVAL

Pre-stimulation or "licencing" of MSC with IFN-γ has been demonstrated to significantly increase MSC inhibition of T cell function both *in vitro* (Ryan *et al.* 2007) and *in vivo* (Tobin *et al.* 2013). The increased suppression of T cell proliferation by IFN-γ stimulated MSC is mediated in part by an altered proteomic profile of IFN-γ stimulated MSC (Krampera *et al.* 2006; Ryan *et al.* 2007; Polchert *et al.* 2008). MSC do not constitutively express indoleamine 2,3-dioxygenase (IDO), however significant up-regulation in IDO production is induced following IFN-γ stimulation (Ryan *et al.* 2007). Therefore, it was hypothesised that IFN-γ licenced MSC may differentially regulate B cell survival compared to resting MSC. $CD19^+$ B cells were cultured with or without MSC or IFN-γ licensed MSC (γMSC) for 72 hours and B cell viability was determined using Annexin V and PI staining. Viable B cells were distinguished from MSC by gating on $CD45^+$ cells before Annexin V and PI analysis. IFN-γ licencing of MSC was performed as described in section 2.9.1.

There was no difference in B cell viability when B cells were cultured with γMSC compared to cells cultured with resting MSC. $CD19^+$ B cells cultured alone for 72 hours had a survival rate of 22% (Figure 3.8). As expected, the viability of B cells which were cultured in the presence of MSC was significantly enhanced (60%); however, there was no significant difference in viability when B cells were co-cultured with γMSC (62%) (Figure 3.8). There was also no difference in the total number of viable B cells recovered from co-cultures with γMSC compared to resting MSC. These results suggested that the survival signal between MSC and B cells was not altered by IFN-γ stimulation.

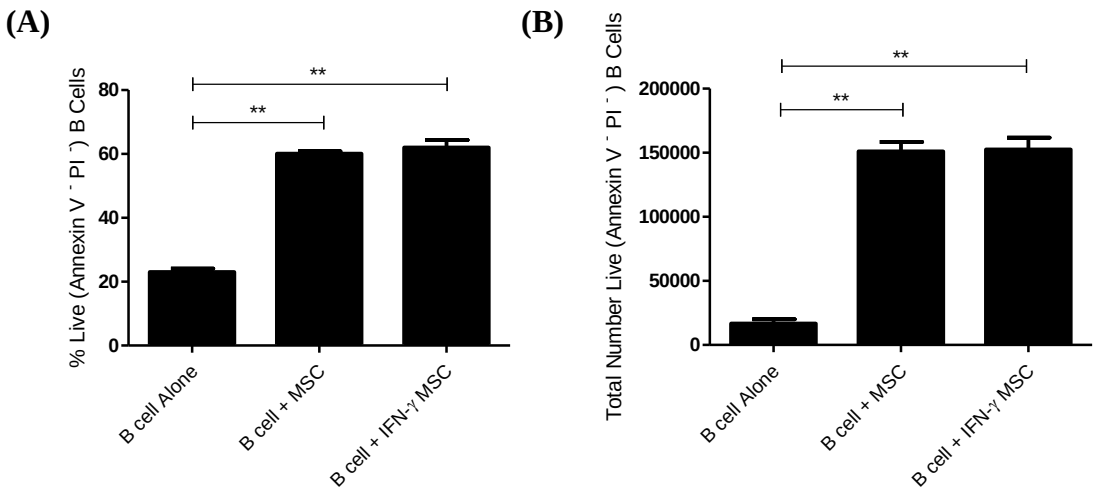

Figure 3.8: Pre-stimulation of MSC with IFN-γ has no effect on their support of B cell survival. Purified B cell populations were obtained from PBMC using $CD19^+$ MACS beads. 9 x 10^5 B cells were cultured in cIMDM in the presence or absence of 1.8 x 10^5 MSC or MSC pre-stimulated with 50 ng/ml IFN-γ for 48 hours. B cell survival was determined by analysing the expression of Annexin V and propidium iodide (PI) on CD45 APC gated B cells after 72 hours co-culture. (A) Represents the percentage of live (Annexin V^- PI^-) B cells and (B) represents the total number of live B cells. n=3 PBMC donors with 2 MSC donors. Statistical analysis was carried out using a paired student *t* test. ** < 0. 01.

3.8 MSC SUPPORT OF B CELL SURVIVAL IS NOT DEPENDENT ON NOTCH SIGNALLING

Notch signalling is a highly conserved immune regulatory pathway which is known to influence cell development, proliferation, differentiation and survival (Fiúza & Arias 2007). Notch signalling is essential for interactions between immune cells and their environment (Radtke *et al.* 2004) and is critical for the development of peripheral B cells (Thomas *et al.* 2007). Notch signalling is known to up-regulate the anti-apoptotic Bcl-2 pathway and support B cell survival (Nwabo Kamdje *et al.* 2011). Over the last number of years, the importance of the notch signalling pathway in immune modulation by MSC has been clearly identified. The roles for notch signalling in MSC modulation of DC maturation and antigen presentation (Chen *et al.* 2007) and in the induction of regulatory T cells (Del Papa *et al.* 2013) have now been established. Therefore it was hypothesised that notch signalling between MSC and $CD19^+$ B cells up-regulated Bcl-2 expression and increased B cell viability. Purified $CD19^+$ B cells were cultured in the presence or absence of MSC for 72 hours. Bcl-2 expression by B cells was analysed by intra-cellular flow cytometry and B cell viability was determined using Annexin V and PI staining. Notch signalling was inhibited during co-culture experiments using a notch γ-secretase inhibitor, GSI XII (Tocris Bioscience, Bristol, England).

Bcl-2 expression was up-regulated in $CD19^+$ B cells cultured in the presence of MSC (Figure 3.9) suggesting that MSC were capable of up-regulating the anti-apoptotic factor Bcl-2 in B cells. As expected, B cell viability was significantly increased when cultured in the presence of MSC (Figure 3.9). However, the addition of increasing concentrations of GSI XII, had no effect on MSC support of B cell survival (Figure 3.9). The percentages (Figure 3.9 A) or total numbers (Figure 3.9 B) of viable B cells were not reduced when notch signalling was inhibited, suggesting that the ability of MSC to support the survival of $CD19^+$ B cells was independent of the notch signalling pathway.

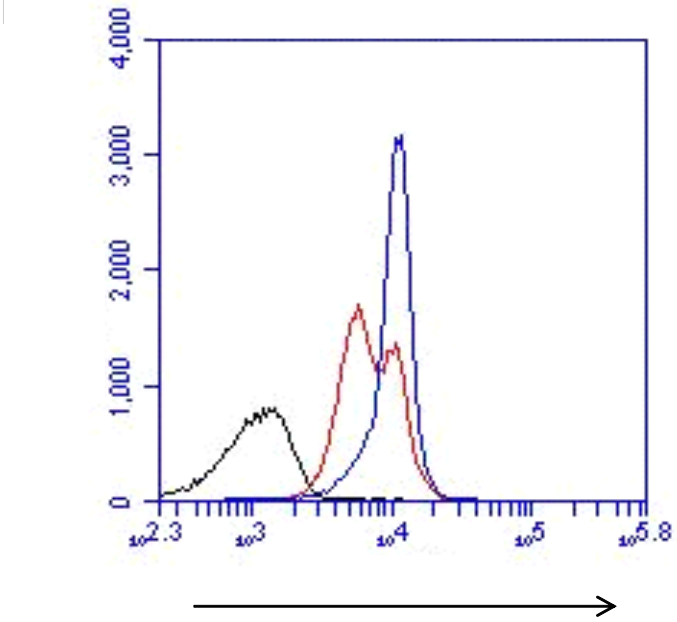

Figure 3.9. MSC induce Bcl-2 up-regulation in B cells. Purified B cell populations were obtained from PBMC using $CD19^+$ MACS beads. 9×10^5 B cells were cultured in cIMDM in the presence or absence of 1.8×10^5 MSC for 72 hours. Bcl-2 expression was determined by intra-cellular flow cytometry of CD45 APC gated B cells after 72 hours co-culture. Black peak represents isotype control, red peak represents B cells cultured alone and blue peak represents B cells cultured in the presence of MSC. Image representative of 2 separate experiments using 4 PBMC donors and 2 MSC donors.

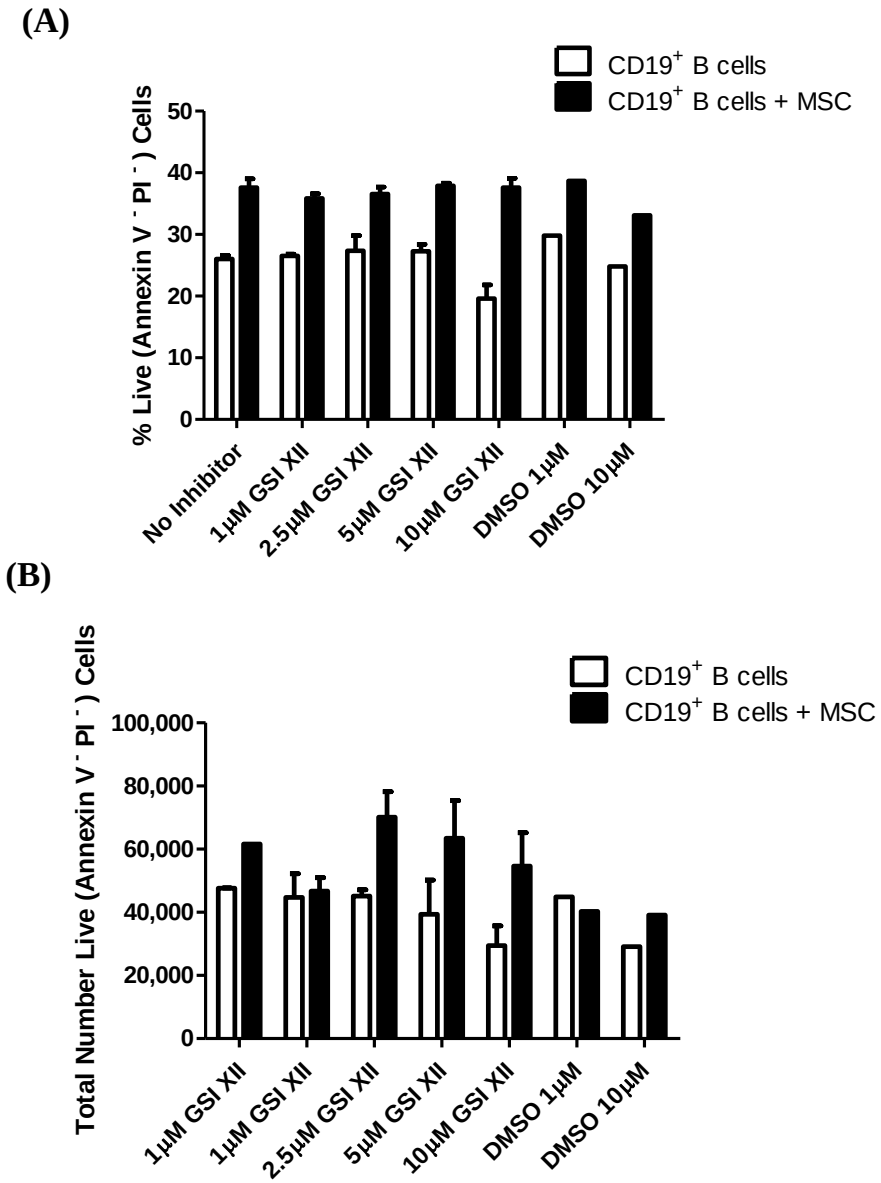

Figure 3.10. MSC support of B cell survival is not dependent on notch signalling. Purified B cell populations were obtained from PBMC using $CD19^+$ MACS beads. 9 x 10^5 B cells were cultured in cIMDM in the presence or absence of 1.8 x 10^5 MSC. Notch signalling was inhibited using specific γ-secretase inhibitor XII at 1μM, 2.5 μM, 5 μM or 10 μM. B cell survival was determined by analysing the expression of Annexin V and propidium iodide (PI) on CD45 APC gated B cells after 72 hours co-culture. (A) Represents the percentage of live (Annexin $V^- PI^-$) B cells and (B) represents the total number of live B cells. n=3 PBMC donors with 2 MSC donors. Statistical analysis was carried out using a paired student *t* test. * < 0.05, ** < 0. 01.

3.9 CELL CONTACT DEPENDENT PRODUCTION OF VEGF BY MSC PROMOTES B CELL SURVIVAL

Vascular Endothelial Growth Factor (VEGF) was identified originally as a pro-angiogenic factor (Gospodarowicz & Lau 1989) and its production has since been identified on a number of stromal cells including MSC (Beckermann *et al.* 2008). Understanding of VEGF function has also expanded and one of the most potent functions of VEGF is in anti-apoptotic signalling (Gupta *et al.* 1999). The anti-apoptotic effect of VEGF has previously been demonstrated by Spyridopoulos *et al.*; they demonstrated that the addition of recombinant VEGF (10 ng/ml) was capable of protecting up to 90% of epithelial cells from TNF-α induced apoptosis (Spyridopoulos *et al.* 1997). Therefore the potential role for MSC produced VEGF in protecting B cells from apoptosis was examined.

VEGF production by B cells cultured alone was very low at 24, 48 and 72 hours while MSC cultured alone produced 1ng/ml VEGF at these time-points (Figure 3.11 A, B & C). However when MSC were cultured in the presence of B cells VEGF production was significantly increased after 48 and 72 hours (Figure 3.11 A, B & C). Interestingly increased VEGF production was not detected in samples where B cells were separated from MSC by transwell membranes (Figure 3.11). To determine the significance of increased VEGF production on B cell survival, a VEGF inhibitor (SU5416; R&D) was added to B cell:MSC co-cultures for 72 hours before B cell viability was determined by Annexin V/PI staining. Inhibiting VEGF signalling during direct B cell:MSC co-culture completely abrogated the promotion of B cell survival by MSC (Figure 3.12). Inhibiting VEGF signalling resulted in a significant reduction in the percentage and number of Annexin V and PI negative B cells after MSC co-culture, restoring them to similar levels as observed when B cells were cultured alone (Figure 3.12). These results demonstrate that cell contact dependent up-regulation of VEGF by MSC induced B cell survival.

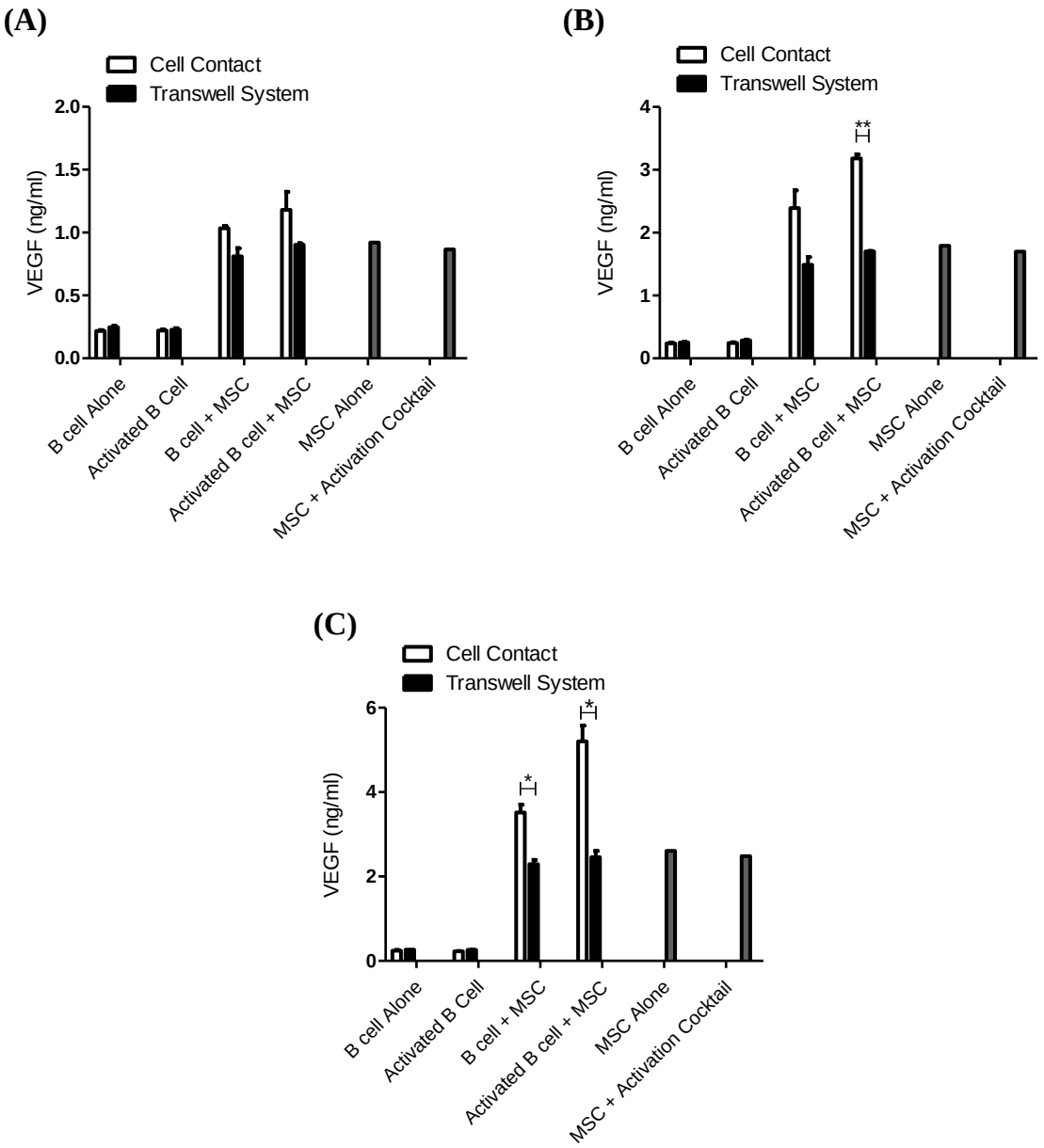

Figure 3.11. Cell contact between MSC and B cells induces up-regulation of VEGF by MSC. Purified B cell populations were obtained from PBMC using $CD19^+$ MACS beads. 9 x 10^5 B cells were cultured in cIMDM in the presence or absence of 1.8 x 10^5 MSC with or without B cell cytokine cocktail for 72 hours. Transwell membrane inserts (0.4 µm pore size) were used to prevent cell contact between MSC and B cells during co-culture. Supernatant was recovered from co-cultures after 24 (A), 48 (B) and 72 (C) hours and VEGF production was determined by ELISA. n=2 PBMC donors with 2 MSC donors. Statistical analysis was carried out using ANOVA analysis. ** < 0. 01.

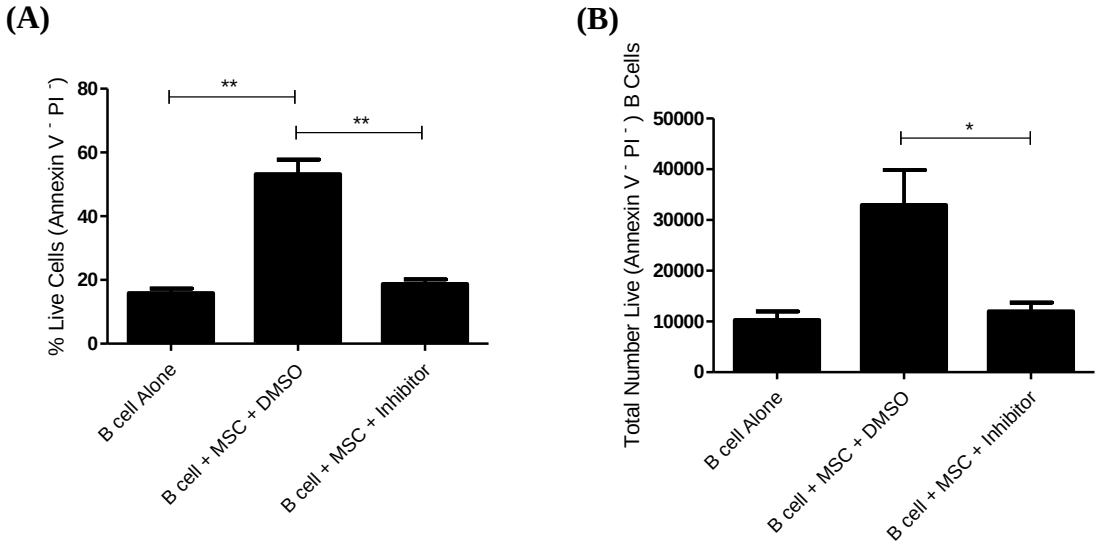

Figure 3.12. Inhibition of VEGF signalling prevents MSC support of B cell survival. Purified B cell populations were obtained from PBMC using $CD19^+$ MACS beads. 9 x 10^5 B cells were cultured in cIMDM in the presence or absence of 1.8 x 10^5 MSC with or without VEGF inhibitor for 72 hours. B cell survival was determined by analysing the expression of Annexin V and propidium iodide (PI) on CD45 APC gated B cells. (A) Represents the percentage of live (Annexin V^- PI^-) B cells and (B) represents the total number of live B cells. n=4 PBMC donors with 2 MSC donors. Statistical analysis was carried out using a paired student *t* test. * < 0.05, ** < 0. 01.

3.10 VEGF PRODUCTION BY MSC INCREASES AKT PHOSPHORYLATION AND PREVENTS CASPASE 3 ACTIVATION

Following the demonstration of the importance of MSC derived VEGF, this study sought to investigate the signalling cascade involved in promoting B cell survival. VEGF signalling has previously been shown to induce cell survival through the phosphorylation of AKT (Abid *et al.* 2004). Phosphorylation of AKT (Phospho-AKT) is known to inhibit the activation of the caspase cascade preventing the cleavage (activation) of caspase 3 (Zhou *et al.* 2000). Therefore, the levels of Phospho-AKT and cleaved caspase 3 were analysed in B cells after 72 hours co-culture with or without MSC by western blot. The role of VEGF signalling in inducing phosphorylation of AKT and the cleavage of caspase 3 was also determined using VEGF inhibitor.

$CD19^+$ B cells cultured in the presence of MSC had a marked increase in levels of Phospho-AKT and displayed very little cleaved caspase 3 (Figure 3.13). B cells which were cultured alone displayed low levels of Phospho-AKT but high levels of cleaved caspase 3 (Figure 3.13). The inhibition of VEGF signalling during co-cultures with MSC clearly reduced the level of AKT phosphorylation and restored levels of cleaved caspase 3 to that of B cells cultured alone (Figure 3.13). These data suggest that the increased VEGF production by MSC during co-culture with B cells induces the phosphorylation of AKT and inhibits the caspase cascade and subsequent cleavage of caspase 3 resulting in reduced apoptosis.

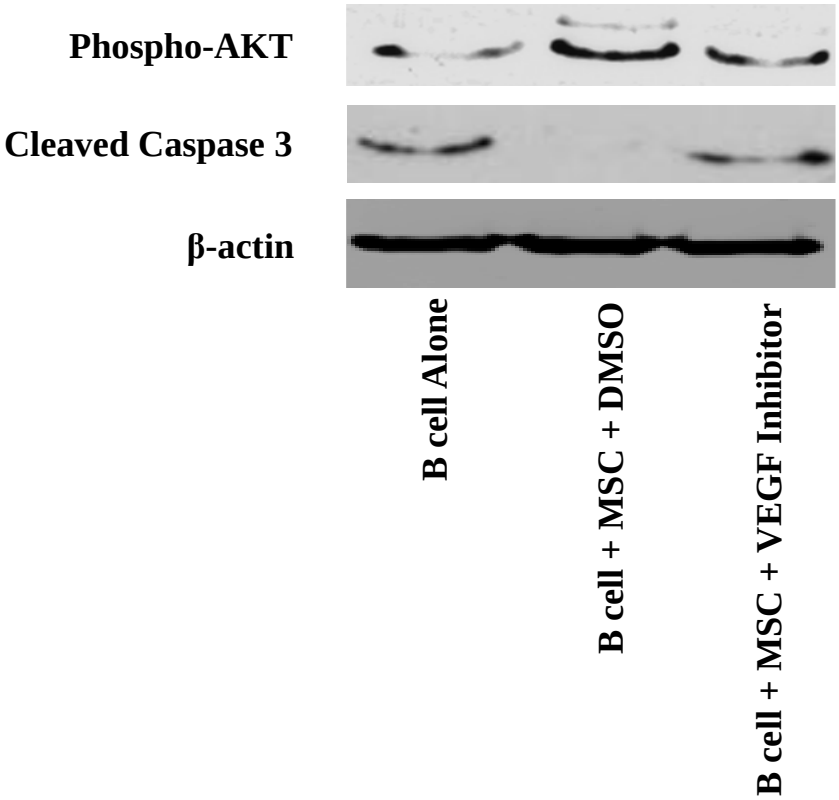

Figure 3.13. VEGF produced by MSC up-regulates Phospho-AKT and subsequently inhibits caspase 3 cleavage. Purified B cell populations were obtained from PBMC using $CD19^+$ MACS beads. 9×10^5 B cells were cultured in cIMDM in the presence or absence of 1.8×10^5 MSC with or without VEGF inhibitor for 72 hours. B cells were recovered from co-culture and the phosphorylation of AKT (lower band) and cleaved caspase 3 were analysed by western blot analysis. β-actin was used as a loading control. Image representative of 3 separate experiments using 4 PBMC donors and 3 MSC donors.

3.11 MSC SUPPORT OF B CELL SURVIVAL IS NOT DEPENDENT ON CXCR4 SIGNALLING

In order to elucidate the cell contact signal responsible for the increased VEGF production and subsequent support of B cell survival by MSC, CXCR4-CXCL12 signalling was identified as a possible candidate. CXCR4 is constitutively expressed on peripheral B cells (Nie *et al.* 2004) and binding of CXCR4 to its ligand CXCL12 has previously been shown induce VEGF production (Liang *et al.* 2007). The expression of CXCL12 on MSC has previously been established and therefore, a competitive inhibitor to CXCR4 (AMD3100) was used to inhibit CXCR4-CXCL12 signalling during B cell:MSC co-cultures. $CD19^+$ B cells were isolated from PBMC and cultured in the presence or absence of MSC (5:1) in the presence or absence of AMD3100 for 72 hours. B cell viability was determined using Annexin V and propidium iodide (PI) viability staining and analysed by flow cytometry.

The capacity for AMD3100 to block CXCR4 on B cells was demonstrated on $CD19^+$ B cells (Figure 3.15). Total CXCR4 binding was achieved by adding 20 µg/ml AMD3100 to B cell culture (Figure 3.15). However, blocking CXCR4-CXCL12 signalling during B cell:MSC co-cultures had no effect on the ability of MSC to support B cell survival (Figure 3.16). As expected, the percentage of viable cells was significantly higher when B cells were cultured in the presence of MSC compared to B cells alone; however the addition of 20 µg/ml or 50 µg/ml of AMD3100 did not significantly reduce the ability of MSC to support B cell survival (Figure 3.16), suggesting that the B cell-MSC interaction is not mediated via CXCR4-CXCL12 signalling.

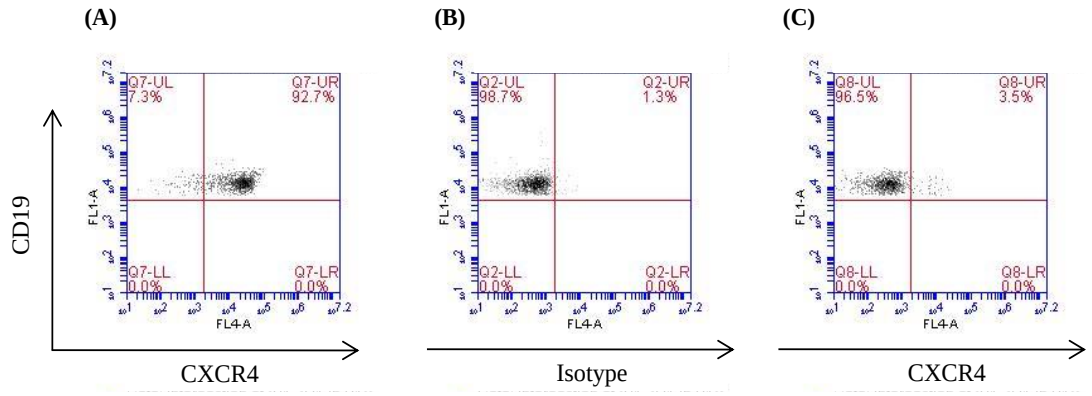

Figure 3.14. AMD3100 binds to CXCR4 on CD19$^+$ B cells. CD19$^+$ peripheral B cells were isolated from PBMC using positive selection MACS beads and cultured with or without 20 µg/ml of CXCR4 inhibitor AMD3100 for 72 hours. Binding of AMD3100 was determined by analysing the expression of CXCR4 or matched isotype control on CD19$^+$ B cells by flow cytometry. (A) Representative image of CXCR4 expression on CD19$^+$ B cells cultured without inhibitor for 72 hours, (B) Isotype control and (C) CXCR4 expression on CD19$^+$ B cells cultured in the presence of 20 µg/ml AMD3100 for 72 hours.

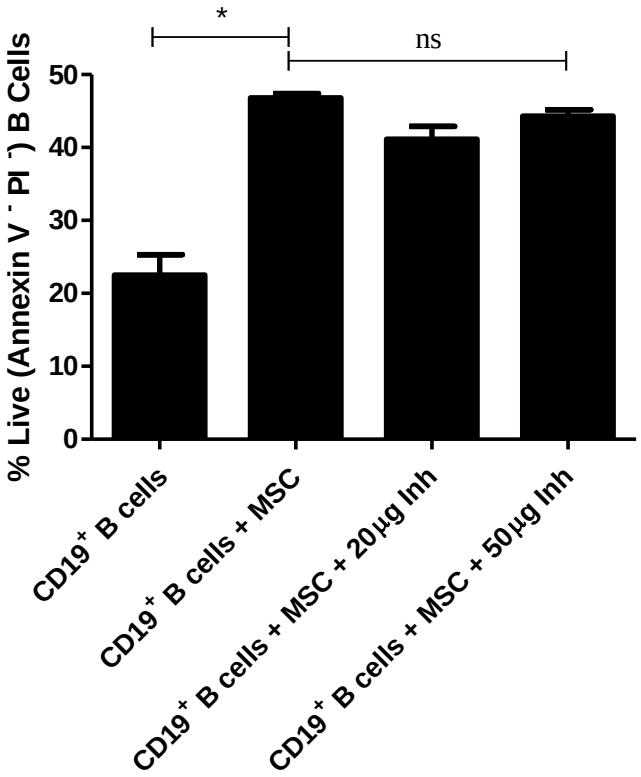

Figure 3.15. Inhibition of CXCR4-CXCL12 signalling had no effect on MSC ability to support B cell survival. Purified B cell populations were obtained from PBMC using $CD19^+$ MACS beads. 9 x 10^5 B cells were cultured in cIMDM in the presence or absence of 1.8 x 10^5 MSC. CXCR4 was neutralised using 20 µg or 50 µg AMD3100 during B cell:MSC co-cultures. B cell survival was determined by analysing the expression of Annexin V and propidium iodide (PI) on CD45 APC gated B cells after 72 hours co-culture. n=2 PBMC donors with 2 MSC donors. Statistical analysis was carried out using a paired student *t* test. * < 0. 05.

3.12 MSC SUPPORT OF B CELL SURVIVAL IS NOT DEPENDENT ON EGFR STIMULATION

Another cell surface receptor involved in VEGF up-regulation upon stimulation is the epidermal growth factor receptor (EGFR). Stimulation of EGFR significantly increases the production of pro-angiogenic factors, including VEGF, by bone marrow derived human MSC (De Luca *et al.* 2011). The stimulation of the EGFR is not limited to a specific ligand; in fact a number of ligands present on the surface of peripheral B cells might be capable of inducing EGFR signalling. Hence, binding of the EGFR was identified as a candidate for the cell contact signal required by MSC to support B cell survival. Therefore EGFR signalling was inhibited by adding a neutralising antibody specific to EGFR to the B cell:MSC (5:1) co-cultures for 72 hours. B cell viability was determined by staining with Annexin V and PI and analysed by flow cytometry.

Co-culture of $CD19^+$ B cells with MSC resulted in significant increase in B cell survival after 72 hours, as expected (Figure 3.17). The addition of the EGFR neutralising antibody to B cell:MSC co-cultures did not significantly reduce the ability of MSC to support B cell survival (Figure 3.17), suggesting that B cell stimulation of the EGFR is not responsible for the enhancement of B cell survival by MSC.

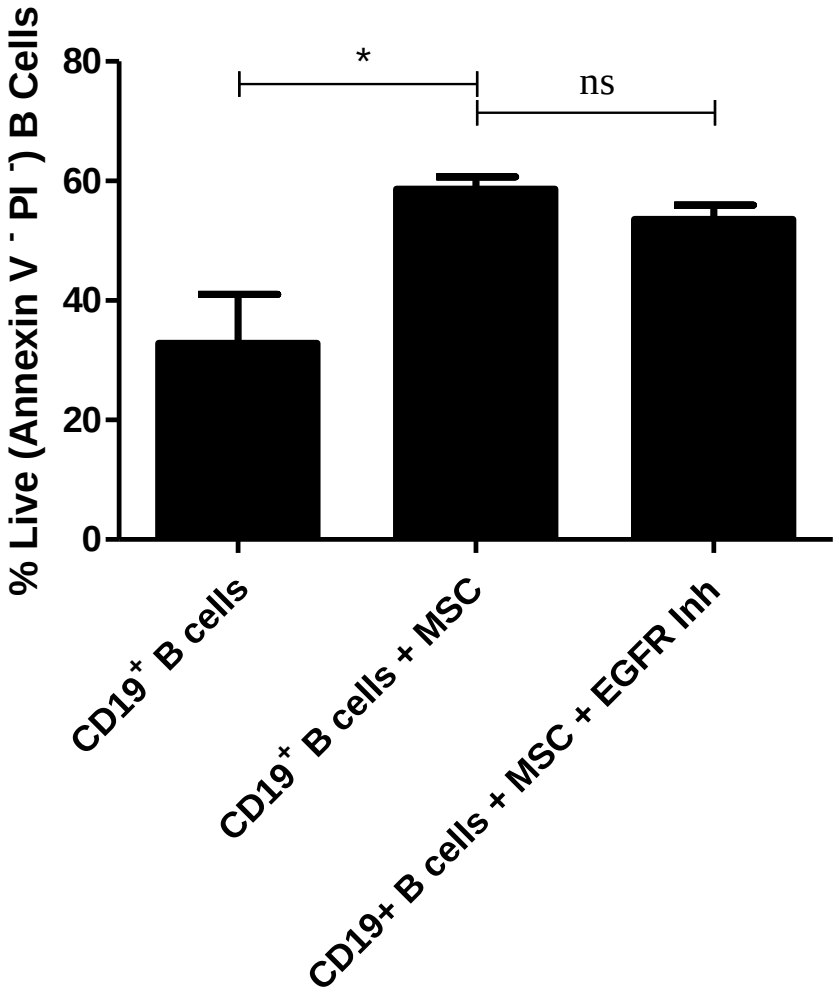

Figure 3.16. Inhibition of EGFR does not prevent MSC from supporting B cell survival. Purified B cell populations were obtained from PBMC using $CD19^+$ MACS beads. 9 x 10^5 B cells were cultured in cIMDM in the presence or absence of 1.8 x 10^5 MSC. EGFR was neutralised using 10 nM EGFR neutralising antibody during B cell:MSC co-cultures. B cell survival was determined by analysing the expression of Annexin V and propidium iodide (PI) on CD45 APC gated B cells after 72 hours co-culture. n=2 PBMC donors with 2 MSC donors. Statistical analysis was carried out using a paired student *t* test. * < 0. 05.

3.13 SUMMARY

The main aims of this chapter were to (1) determine the effect of MSC on B cell function; activation, proliferation and antibody production and (2) to elucidate the mechanism by which MSC modulate B cell function. The activation and proliferation of $CD19^+$ B cells were significantly increased after co-culture with MSC (Figures 3.2 & 3.3); however the production of IgG and IgM were unaffected by the presence of MSC (Figure 3.4). The increase in B cell proliferation was completely dependent on cell contact between the B cell and MSC (Figure 3.3). The viability of $CD19^+$ peripheral B cells was significantly increased when B cells were cultured in the presence of MSC. MSC support of B cell survival was also mediated through a cell contact dependent mechanism (Figure 3.7). These results demonstrate that MSC were supportive rather than suppressive of B cell function.

The second part of this study was to elucidate the mechanism by which MSC supported B cell activation, proliferation and survival. BAFF-TNSFR13 and notch signalling were identified as potential candidates for the cell contact signal between B cells and MSC; however neutralisation of BAFF or notch signalling during B cell:MSC co-cultures had no effect on MSC support of B cell proliferation or survival (Figures 3.6 & 3.10). Therefore the ability of MSC to produce VEGF was investigated. MSC constitutively produced VEGF, however the production of VEGF by MSC was significantly up-regulated after cell contact with $CD19^+$ peripheral B cells (Figure 3.11). Neutralisation of VEGF signalling during B cell:MSC co-cultures completely abrogated the support of MSC on B cell survival suggesting that the increased VEGF production was essential for the survival of B cells (Figure 3.12). Co-culture of $CD19^+$ B cells with MSC resulted in a marked increase in the phosphorylation of AKT (pAKT) and subsequent reduction in the expression of cleaved caspase 3 (Figure 3.13). Inhibition of VEGF signalling during B cell: MSC co-cultures resulted in reduced pAKT within the B cells and increase in

caspase 3 cleavage, to similar levels observed when B cells were cultured alone (Figure 3.13).

Investigations into the cell contact signal driving VEGF production and B cell survival have been unsuccessful. CXCR4-CXCL12 signalling and stimulation of the EGFR were considered likely key targets due to their ability to induce VEGF production and support survival; however neutralisation of CXCR4 or EGFR during B cell: MSC co-culture had no effect on the ability of MSC to promote B cell survival (Figures 3.16 & 3.17).

Therefore we propose a model for MSC support of B cell survival where (1) MSC contact with B cells (contact signal yet to be identified) results in significant up-regulation of VEGF production by MSC. (2) Soluble VEGF is recognised by B cells and induces phosphorylation of AKT. (3) pAKT inhibits the pro-apoptotic caspase cascade resulting in significantly less cleaved caspase 3 and subsequently reduced B cell apoptosis.

CHAPTER 4

DEVELOPMENT OF XENOGENEIC MSC THERAPY IN MURINE MODELS OF GVHD

4.1 INTRODUCTION

Allogeneic hematopoietic stem cell transplantation (HSCT) was first developed by E. Donnall Thomas in 1957 and is now the current treatment of choice for patients with both malignant and non-malignant haematological disorders as well as the most commonly practiced form of stem cell therapy (Peccatori & Ciceri 2010). However, the development of graft-versus-host disease (GvHD) still represents a life threatening complication of HSCT. Corticosteroids are the primary choice of treatment for patients who develop GvHD, however there is no consensus on optimal treatments for patients with steroid refractory GvHD (Ho & Cutler 2008). This has led to huge efforts within the field of GvHD research to identify novel methods of modulating GvHD; from which the use of MSC has emerged as a potential cell therapy.

MSC have become an attractive target for use as a cell therapy against steroid resistant GvHD because of their potent immune suppressive properties and their ability to avoid allogeneic rejection (Ryan *et al.* 2005; Polchert *et al.* 2008). In 2004, the first successful transplantation of MSC as an allogeneic cell therapy for patients with steroid resistant grade IV GvHD was performed by Le Blanc *et al.* and demonstrated remarkable immunosuppressive effects; however the exact mechanisms by which the MSC therapy mediated their effect was not determined (Le Blanc *et al.* 2004). More recently, Osiris Therapeutics published the results of a phase 3 clinical trial where they administered Prochymal™ (a patented MSC like product) to patients with steroid refractory GvHD. Prochymal™ significantly increased response rates in patients with steroid refractory liver GvHD and steroid refractory gastrointestinal disease over patients treated with placebo; however overall the study did not reach its primary endpoint to significantly increase complete response rates in steroid refractory GvHD patients for at least 28 days in comparison to placebo controls (Martin *et al.* 2010). These results highlighted the

potential of allogeneic MSC as a candidate therapy to treat acute steroid refractory GvHD when administered after donor T cell recognition but also demonstrated the little understanding which exists about how MSC mediate their beneficial effect in a clinical setting.

The development of animal models of GvHD which are tailored around the administration of MSC would greatly expand our understanding of how MSC work *in vivo* and provide us with a platform to enhance our knowledge of the immunological interaction between MSC and the immune system. The ability to use human MSC in murine models of GvHD would expand the resources currently available to researchers and allow the further examination of the mechanisms behind how MSC modulate GvHD.

The objectives of this chapter were:

1) To determine if human (xenogeneic) MSC therapies could be assessed in murine models of acute or chronic GvHD.
2) To investigate the capacity for human MSC to promote survival in GvHD mice.
3) To examine the effect of human MSC on GvHD pathology and associated weight loss and to determine the effect of human MSC on the engraftment of donor T lymphocytes.

4.2 XENOGENEIC MSC TRANSPLANTATION HAD NO EFFECT ON THE SURVIVAL OF SYNGENEIC CONTROL MICE

Due to the difficulty in acquisition and precious nature of GvHD patient samples, murine models of GvHD have become essential in furthering our understanding and the development of novel treatments for GvHD. Xenogeneic MSC have been used in a number of animal models, however the success of these experiments has been varied (Lin *et al.* 2012). Human bone marrow derived MSC have been shown to successfully engraft and migrate to the site of damage in a rat model of spinal cord injury (Pal *et al.* 2010) as well as enhance bone formation and increase bone mass in mouse models (Guan *et al.* 2012). However, two studies by Grinnemo *et al*, 2004 and 2006, reported that human MSC showed very poor engraftment in immune-competent mice (Grinnemo *et al.* 2004; Grinnemo *et al.* 2006).

In this study, syngeneic transplant mice were established as a negative control and human MSC were also administered to syngeneic transplant mice to identify any potential adverse effects associated with administering xenogeneic MSC as a cell therapy. BALB/c mice were sub-lethally irradiated (7 Gy) and transplanted with $5x10^6$ bone marrow cells and whole splenocytes limited to $1x10^6$ $CD4^+$ cells isolated from BALB/c mice. Human MSC were administered to mice at days 1 and 3 post transplantation (Figure 4.1). Transplanted mice were monitored on a regular basis and the development of GvHD was defined as total body weight loss of >25% of original starting weight with a series of clinical manifestations including posture, reduction in activity, fur texture and diarrhoea (according to local ethics committee recommendations in Case Western Reserve University, Cleveland Ohio). These parameters were combined into a clinical score and mice which amassed a total score of 6 from 8 or had suffered weight loss in excess of 25% were considered to have severe GvHD and sacrificed humanely (Table 4.1).

Human MSC therapy had no adverse effect on the survival of syngeneic control mice (Figure 4.2 A). Despite an original delay in weight gain, the administration of human MSC did not significantly impair weight gain of syngeneic control mice (Figure 4.2 B). Human MSC therapy had no effect on the pathological score of syngeneic mice throughout this study (Figure 4.2 C).

The main target organs involved in GvHD pathology are the gut, liver, spleen and lung. The use of MSC therapy to treat GvHD has been shown to reduce pathology in target organs with the most significant effect being observed in the gut (Tobin *et al.* 2013). Therefore, histopathology was used to determine if xenogeneic MSC had any adverse effects on the pathology of these organs 28 days after transplantation. Tissue sections were stained by H&E and the histological GvHD score was evaluated for each treatment group according to criteria previously established in the lab (Tobin *et al.* 2013).

Pathology of the gut was determined by the extent of lymphocyte infiltration (L) and villous destruction (V) observed in the small intestine of each mouse. As expected, syngeneic control mice displayed no distinguishable pathological symptoms within the small intestine (Figure 4.3 A). Administration of human MSC had no adverse effect on villi structure but did however lead to increased levels of lymphocyte infiltration resulting in a slightly higher pathological score than non-treated mice (Figure 4.3 B).

Syngeneic bone marrow transplantation did not adversely affect the lung architecture of the mice or induce pathology as measured by peribronchial inflammation (L) and airway epithelium thickening (T) (Figure 4.3 A&B). Human MSC did not significantly affect lung architecture of syngeneic mice (Figure 4.3 A). However, human MSC therapy significantly increased lymphocyte infiltration and thickening of the airway epithelial wall and resulted in a significant increase in pathological score (Figure 4.3 A&B).

Administration of human MSC to syngeneic control mice had no effect on liver pathology, as measured by lymphocyte infiltration around hepatic veins (L) (Figure 4.3 A). Syngeneic control mice which received human MSC displayed no increase in lymphocyte infiltration suggesting that administration of human MSC was not detrimental to the livers of transplant mice (Figure 4.3 A&B).

The spleens of syngeneic mice were unaffected by human MSC therapy with no evidence of pathology, as measured by splenic structure and germinal centre (GC) formation (Figure 4.3 A & B). This suggests that human MSC do not adversely affect splenic tissue in syngeneic control mice after 28 days. Overall, this histological analysis suggest that while xenogeneic transplantation of human MSC had no effect on the survival, weight loss or pathological score of syngeneic mice, the immunogenicity shown by human MSC in a xenogeneic setting may be a problem in xenogeneic transplantation.

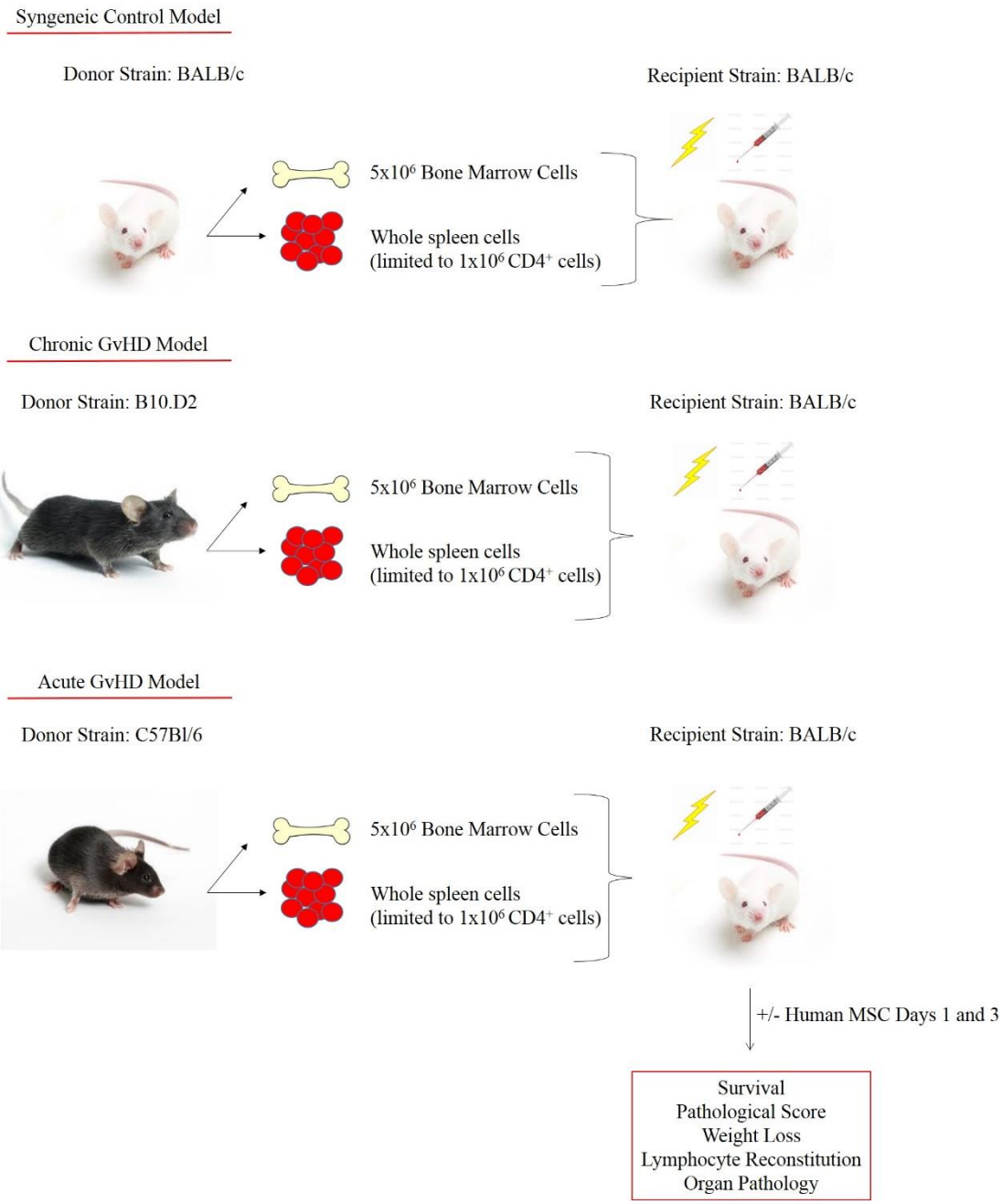

Figure 4.1. Graphical illustration of syngeneic control transplants, chronic GvHD and acute GvHD mouse models. BALB/c mice were irradiated using 7 Gy and 5 x 10^6 bone marrow cells and whole spleen cells (limited to 1 x 10^6 $CD4^+$ cells) from BALB/c (syngeneic), B10.D2 (chronic GvHD) or C57BL/6 (acute GvHD) mice were administered intravenously (i.v.) in 300µl via the tail vein. 1 x 10^6 Human MSC were administered i.v. on days 1 and 3 post transplantation. Development of GvHD was monitored weekly by recording the weight and clinical score of each mouse. Pathological score was determined as described in Table 4.1. Lymphocyte reconstitution was determined using flow cytometry and organ pathology was analysed using H&E staining.

Table 4.1: Pathological scoring system for GvHD

Score	**0**	**0.5**	**1**	**1.5**	**2**
Posture	Normal – No hunching	Slight hunching but straightens while walking	Animal stays hunched while walking	Animal does not straighten out	Animal tends to stand on rear feet
Activity	Normal – Very mobile	Less movement than normal – slower and easier to catch	Animal stays still but will move when touched	Very little activity and very little movement when touched	No activity and animal does not move when touched
Fur	Normal – no fur pathology	Ridging on side of belly and neck	Ridging along belly, hind legs and back	Fur is matted and unkempt	Badly matted all over body
Diarrhoea	Normal – no diarrhoea	Mild change in bowel movements	Moderate changes in bowel movement	Severe changes in bowel movement	Extensive diarrhoea and redness around anus

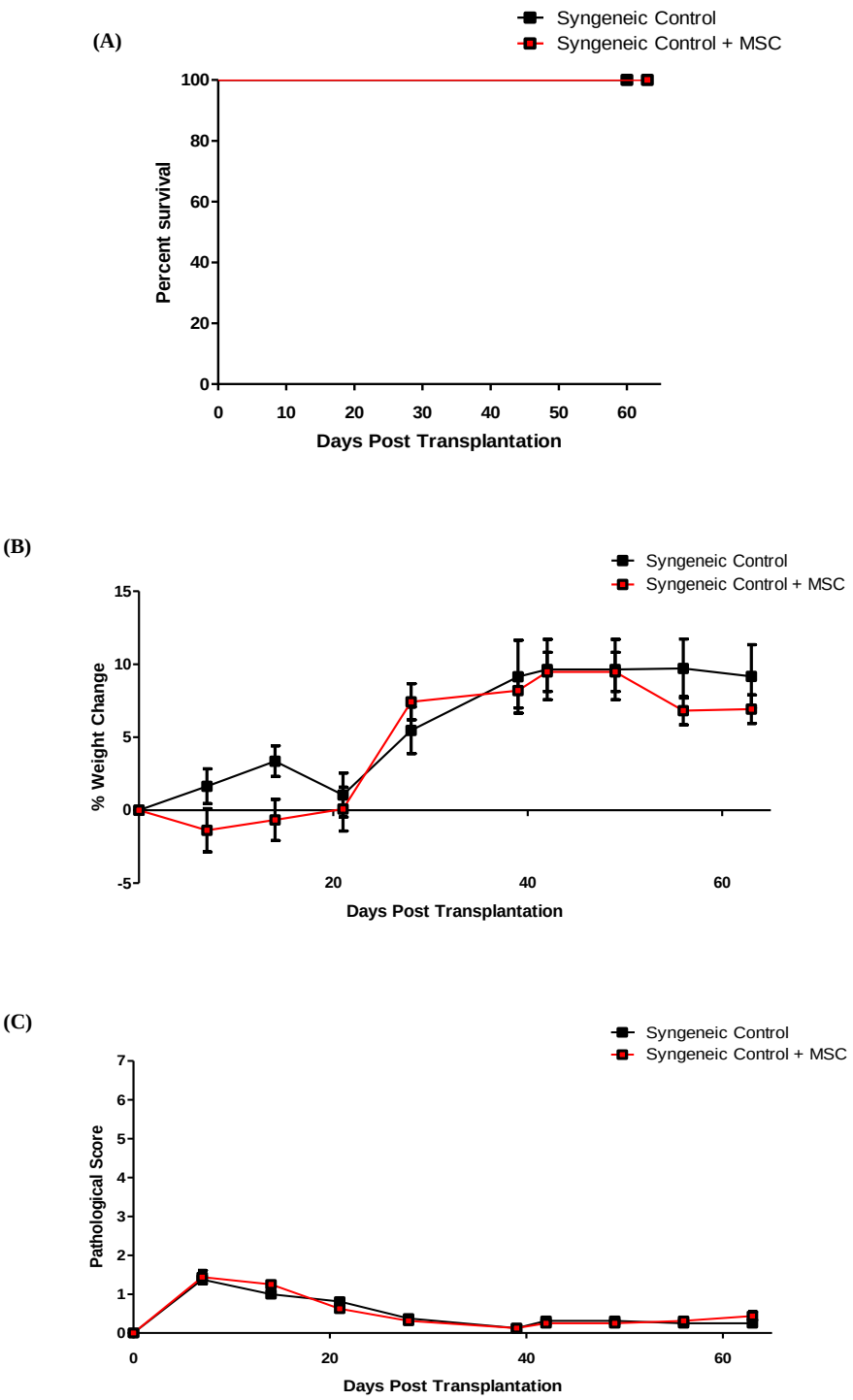

Figure 4.2. Human MSC had no adverse effect on survival, weight gain or clinical score of syngeneic control mice. Graphical representation of (A) survival, (B) percentage weight change and (C) pathological score of syngeneic transplant mice (black line) and MSC treated syngeneic transplant mice (red line). 5 x 10^6 bone marrow cells and whole spleen cells (limited to 1 x 10^6 $CD4^+$ cells) from BALB/c mice were administered to irradiated BALB/c mice. 1 x 10^6 human MSC were given as a cell therapy on days 1 and 3. Transplanted mice were monitored every 7 days for the duration of the experiment. n=6.

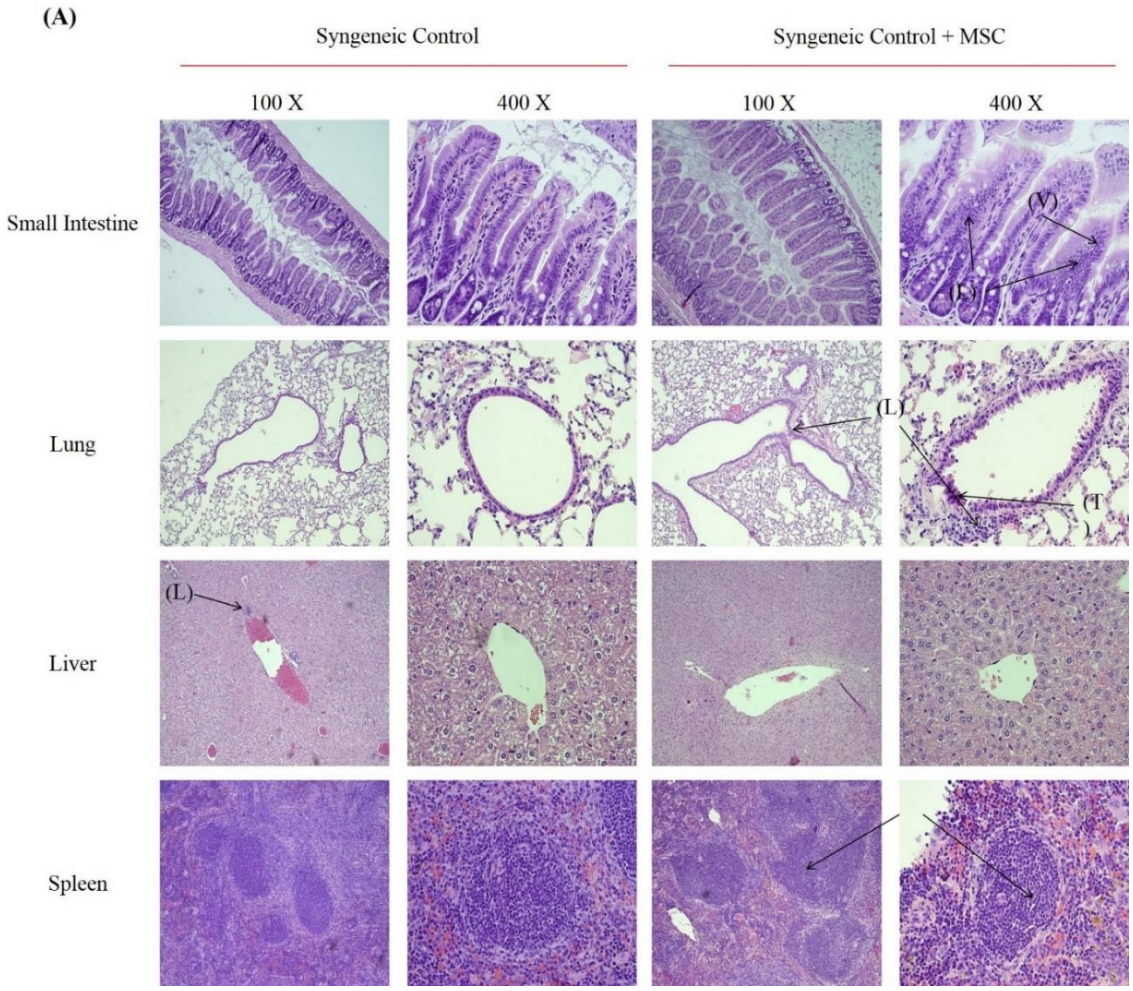
(A)
Syngeneic Control
Syngeneic Control + MSC
100 X
400 X
100 X
400 X
Small Intestine
Lung
Liver
Spleen
(V)
(L)
(L)
(L)

(B)

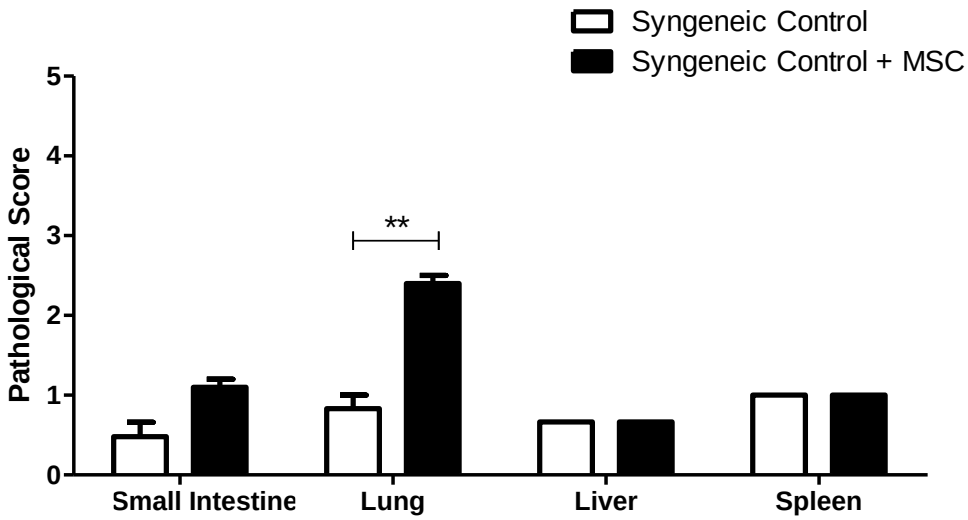

Figure 4.3. Human MSC significantly increased pathology in the lung of syngeneic control mice. 5 x 10^6 bone marrow cells and whole spleen cells (limited to 1 x 10^6 $CD4^+$ cells) from BALB/c mice were administered to irradiated BALB/c mice. 1 x 10^6 human MSC were given as cell therapy on days 1 and 3. Mice were sacrificed on day 28 and small intestine, lung, liver and spleen harvested and tissue sections were analysed by (A) H&E staining and (B) a defined scoring system. (A) Tissue samples were processed and stained with H&E and analysed for lymphocyte infiltration (L), villi destruction (V), thickening of epithelial airways (T) or germinal centre formation (GC). Pathological score determined by 2 independent researchers. Tissues samples were stained using H&E and images captured at 100X and 400X. (B) Graphical representation of combined pathological score for syngeneic control mice (white bars) and human MSC treated syngeneic mice (black bars). n=3 per group. Statistical analysis was carried out using a paired student *t* test. ** < 0.01.

4.3 XENOGENEIC MSC SIGNIFICANTLY INCREASED $CD4^+$ T CELLS IN THE LUNGS OF ALL TRANSPLANT MODELS TESTED.

This experiment was designed to determine the capacity of human MSC to increase survival and lower pathological score in murine models of chronic and acute GvHD. Human MSC were administered to syngeneic bone marrow transplant mice to control for effects associated with xenogeneic responses. Analysis of bronchoalveolar lavage (BAL) fluid recovered from the lungs of human MSC treated syngeneic mice subsequently demonstrated a significant increase in $CD4^+$ T cells 28 days post transplantation (Figure 4.4 A). However, after 63 days, syngeneic mice which had not received human MSC had a similar level of $CD4^+$ infiltration in the lungs compared to syngeneic mice which had received human MSC (Figure 4.4 B).

The administration of human MSC to chronic GvHD mice resulted in a significant increase in $CD4^+$ T cells recovered from BAL fluid 28 days (Figure 4.4 C) and 63 days (Figure 4.4 D) post transplantation. The administration of human MSC to chronic GvHD mice also resulted in increased $CD8^+$ T cell populations in the lungs by day 63 (Figure 4.4 D), which was not observed in syngeneic control mice (Figure 4.4 B).

As observed for both syngeneic control mice and chronic GvHD mice, the administration of human MSC to acute GvHD mice resulted in a significant increase in $CD4^+$ T cells recovered from BAL fluid at 28 days (Figure 4.4 E) and 63 days (Figure 4.4 F) post transplantation. The total number of $CD8^+$ T cells was also increased 28 days after transplantation (Figure 4.4 E). Interestingly this increase in $CD8^+$ T cell number was lost by day 63 (Figure 4.4 F).

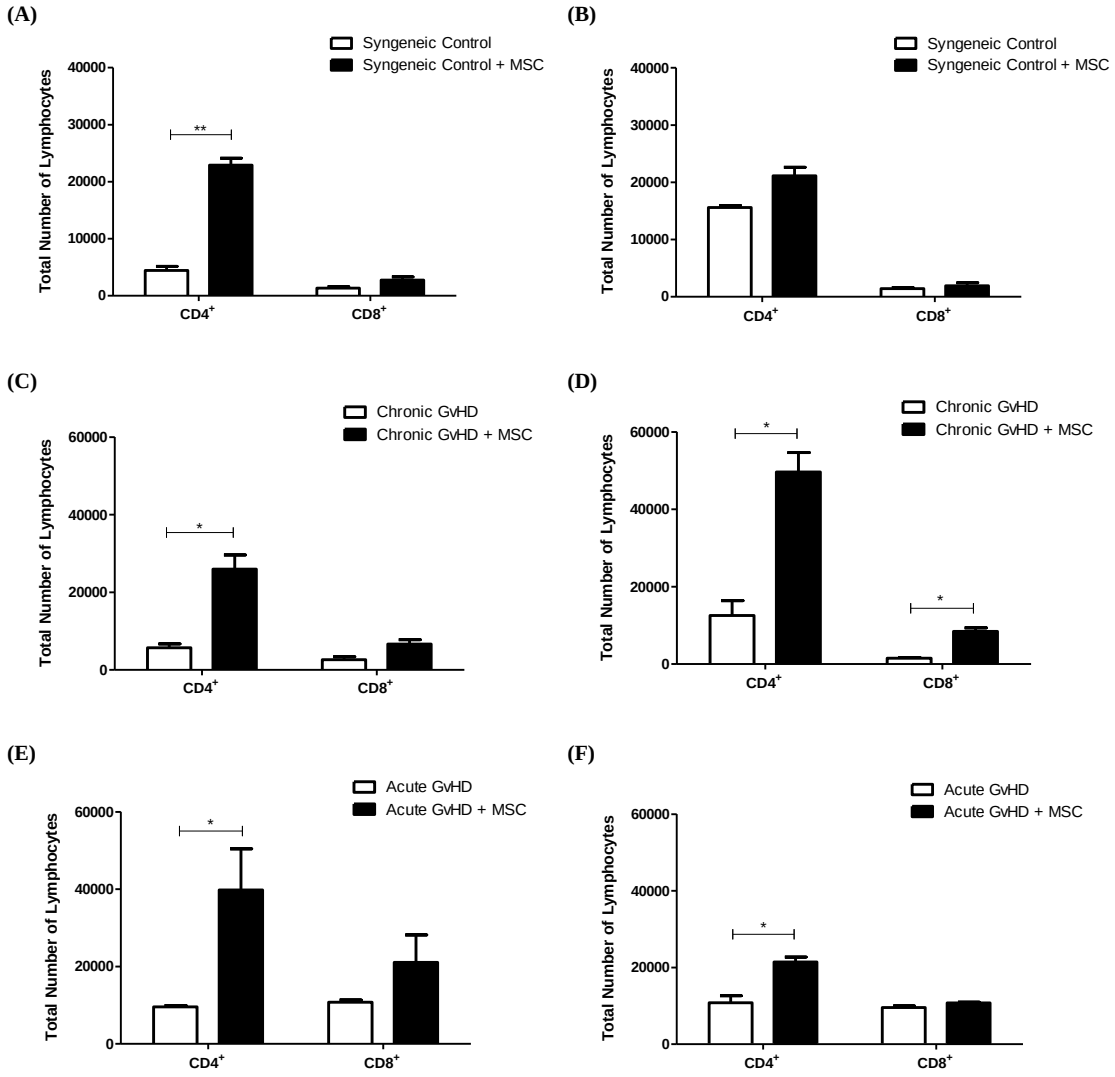

Figure 4.4. Human MSC therapy significantly increased CD4$^+$ T cells in the lung. Graphical representation of total CD4$^+$ and CD8$^+$ T cell numbers recovered from bronchoalveolar lavage fluid from (A) syngeneic mice on day 28, (B) syngeneic mice on day 63, (C) chronic GvHD mice on day 28, (D) chronic GvHD mice on day 63, (E) acute GvHD mice at day 28 and (F) acute GvHD mice at day 63 as measured by flow cytometry. Non-treated mice represented by white bars and MSC treated mice represented by black bars. n=3 per group. Statistical analysis was carried out using the students paired T test. * < 0.05, ** < 0.01.

4.4 HUMAN MSC REDUCED PATHOLOGY IN THE GUT OF CHRONIC GVHD MICE

Chronic GvHD (cGvHD) is a major cause of morbidity and mortality in long term survivors of HSCT. The model of cGvHD used in this study was established using a minor MHC mismatched transplant, originally developed by Korngold and Sprent (Korngold & Sprent 1978). BALB/c mice were sub-lethally irradiated (7 Gy) and transplanted with $5x10^6$ bone marrow cells and whole splenocytes limited to $1x10^6$ $CD4^+$ cells isolated from B10/D2 mice. Human MSC were administered to mice at days 1 and 3 post transplantation (Figure 4.1). As before the mice were monitored on a regular basis and the development of GvHD was defined as previously described (Table 4.1). Mice which received a combined pathological score of 6 from 8 or displayed weight loss in excess of 25% were considered to have severe GvHD and sacrificed humanely.

cGvHD had not yet fully developed in any of the mice within the 63 days duration of this experiment (this model of cGvHD would normally be run for 120 days, however, the duration of this experiment was reduced to facilitate a 3 month laboratory visit to Case Western Reserve University, Cleveland). Although the mice were beginning to display symptoms characteristic of GvHD, there were no fatalities in either the human MSC treated or non-treated chronic GvHD mice 63 days after transplantation (Figure 4.5). cGvHD mice which received human MSC had greater protection from weight loss than non-treated mice, which was particularly evident by day 63 (Figure 4.5). Human MSC treated mice also displayed a lower pathological score during the later stages of the experiment, evident from day 40 onwards, however this was not statistically different (Figure 4.5).

As before, the level of GvHD pathology in target organs of chronic GvHD mice was analysed using H&E staining of tissue sections from the small intestine, lung, liver and spleen. Human MSC therapy significantly reduced the pathological score in the gut

of cGvHD mice as measured by less destruction of villi and less lymphocyte infiltration to the small intestine (Figure 4.6 A&B). Non-treated mice presented large localised accumulations of lymphocytes and villous destruction in the small intestine (Figure 4.6 A). cGvHD mice treated with human MSC did not display these large accumulations of lymphocytes but smaller aggregations of lymphocytes were sporadically present at the base of villi throughout the organ (Figure 4.6 A).

cGvHD mice had a significant increase in peribronchial inflammation and much greater airway epithelium thickening than syngeneic control mice in the lung (Figure 4.6 A). As before, the administration of human MSC to murine chronic GvHD mice increased lung pathology compared to non-treated mice. Human MSC treated mice had increased lymphocyte infiltration, particularly around bronchi, and more profound airway epithelium thickening than non-treated mice (Figure 4.6 A). Similar to results observed with the syngeneic transplant mice, the administration of human MSC exacerbated lung pathology in cGvHD mice.

Although the liver is a major target for GvHD, very little pathology was observed in cGvHD mice by day 28 (Figure 4.6 A&B). cGvHD mice displayed lymphocyte infiltration around periportal areas (Figure 4.6 A). The administration of human MSC reduced lymphocyte infiltration in the livers of cGvHD mice (Figure 4.6 A).

cGvHD mice displayed impaired germinal centre formation and overall presence of lymphocytes within the spleen (Figure 4.6 A). The administration of human MSC therapy did not restore germinal centre formation or significantly reduce spleen pathology (Figure 4.6 A). This may suggest impaired B cell engraftment after transplantation or a complication associated with chronic GvHD (Figure 4.6 A). These results suggest that xenogeneic transplant of human MSC may offer some protection against damage to the

spleen in models of cGvHD, but that these may become more pronounced during latter stages of disease progression.

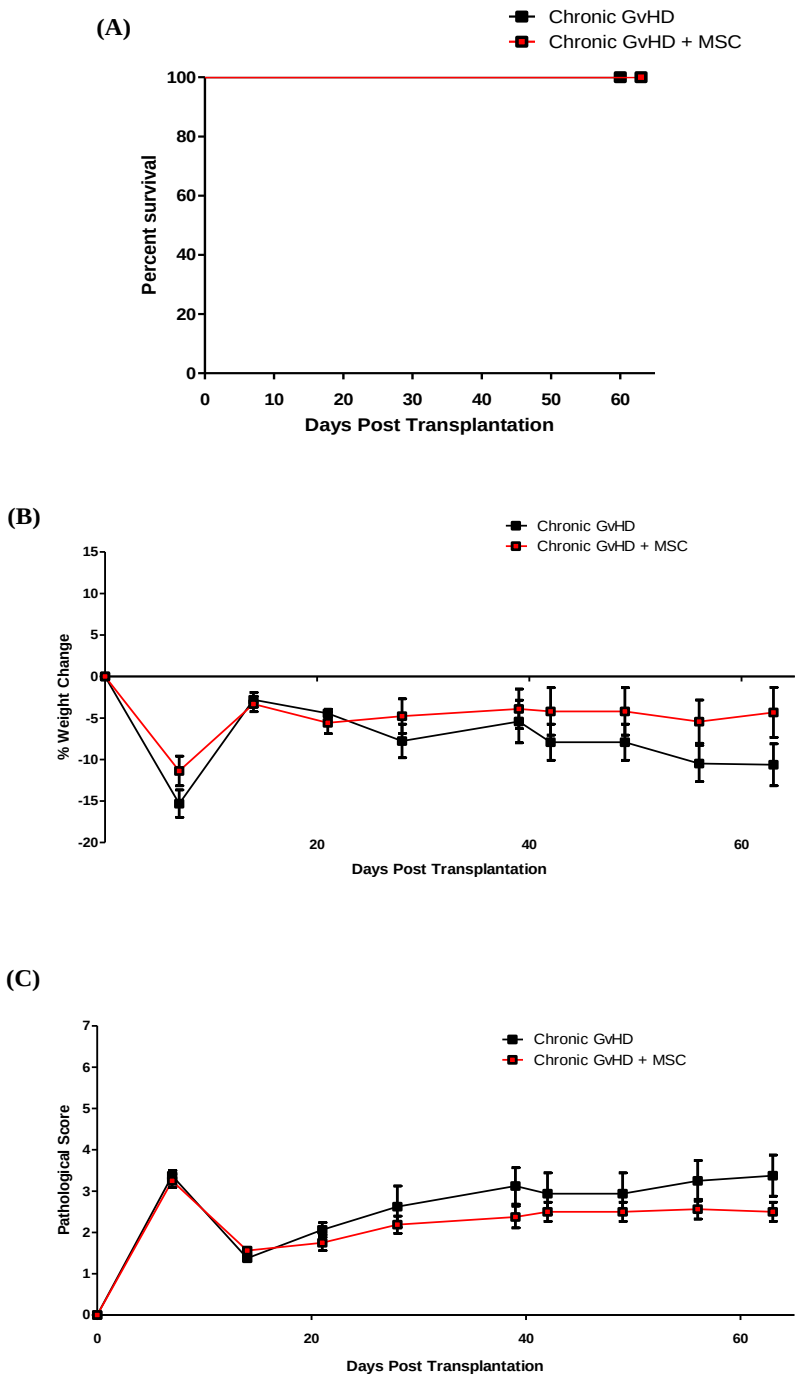

Figure 4.5. Human MSC reduced weight loss and pathology in chronic GvHD mice. Graphical representation of (A) survival, (B) percentage weight change and (C) pathological score of syngeneic transplant mice (black line) and MSC treated syngeneic transplant mice (red line). 5 x 10^6 bone marrow cells and whole spleen cells (limited to 1 x 10^6 $CD4^+$ cells) from B10.D2 mice were administered to irradiated BALB/c mice. 1 x 10^6 human MSC were given as cell therapy on days 1 and 3. Transplanted mice were monitored every 7 days for the duration of the experiment. Chronic GvHD mice are represented by the black line and chronic GvHD mice which received human MSC therapy are represented by red line. n=6.

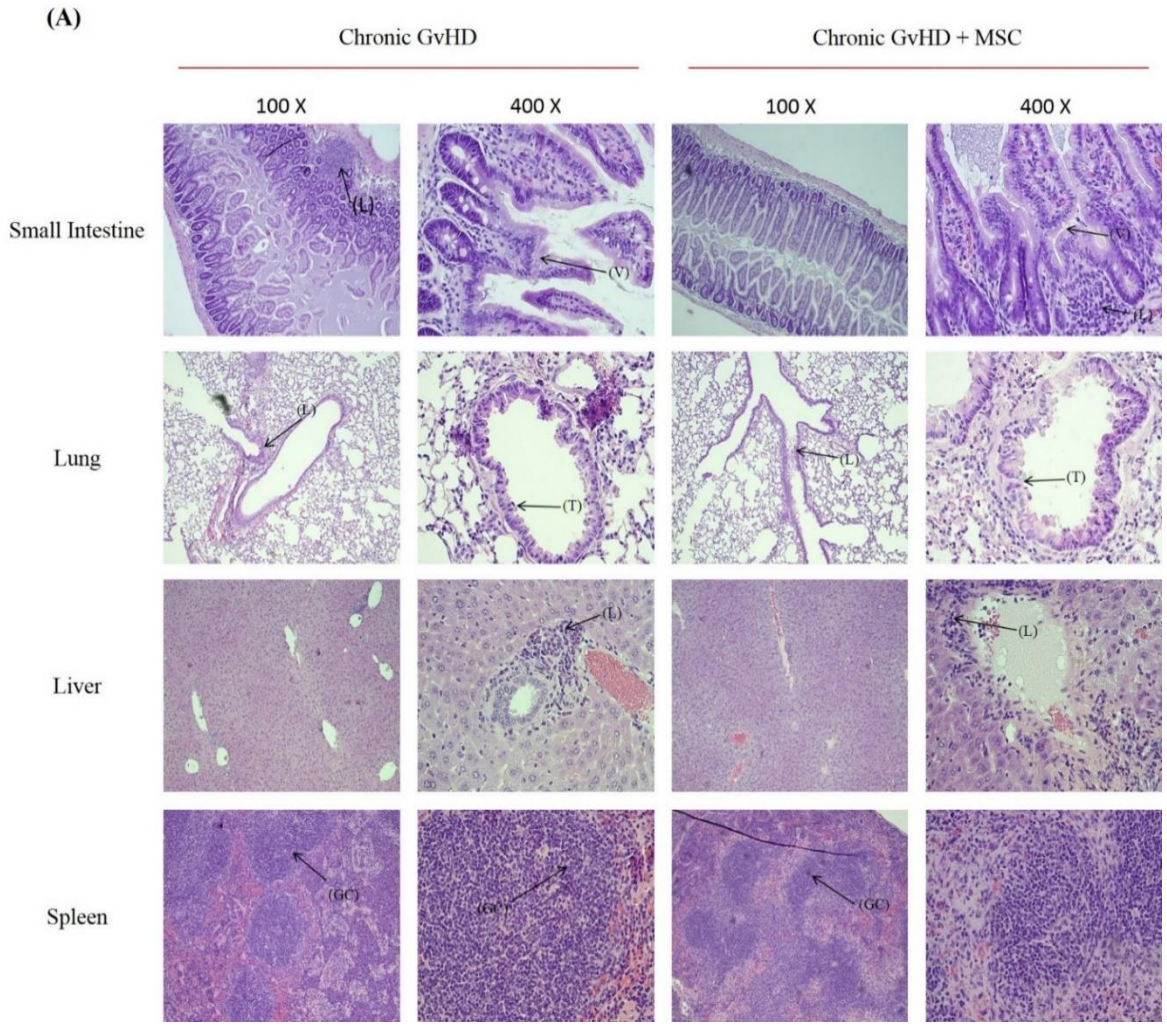
(A)
Chronic GvHD
Chronic GvHD + MSC
100 X
400 X
100 X
400 X
Small Intestine
Lung
Liver
Spleen
(L)
(V)
(T)
(GC)

(B)

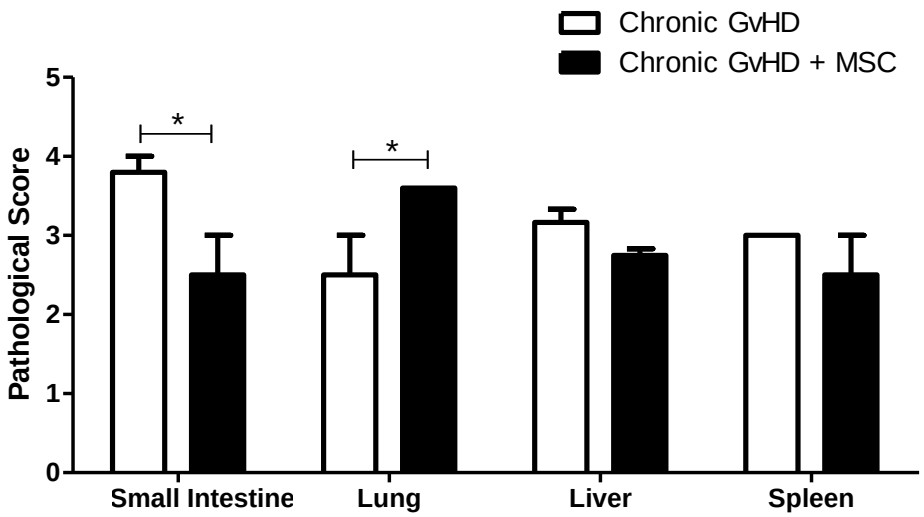

Figure 4.6. Human MSC significantly lowered the pathological score of small intestine but increased lymphocyte infiltration to the lungs of chronic GvHD mice. 5 x 10^6 bone marrow cells and whole spleen cells (limited to 1 x 10^6 $CD4^+$ cells) from B10.D2 mice were administered to irradiated BALB/c mice. 1 x 10^6 human MSC were given as cell therapy on days 1 and 3. Mice were sacrificed on day 28 and small intestine, lung, liver and spleen harvested and tissue sections were analysed by (A) H&E staining and (B) a defined scoring system. (A) Tissue samples were processed and stained with H&E and analysed for lymphocyte infiltration (L), villi destruction (V), thickening of epithelial airways (T) or germinal centre formation (GC). Pathological score determined by 2 independent researchers. Tissues samples were stained using H&E and images captured at 100X and 400X. (B) Graphical representation of combined pathological score for syngeneic control mice (white bars) and human MSC treated syngeneic mice (black bars). n=3 per group. Statistical analysis was carried out using a paired student T test. * < 0.05.

4.5 HUMAN MSC INCREASED SURVIVAL AND REDUCED PATHOLOGY IN MODELS OF ACUTE GVHD

Acute GvHD (aGvHD) is a life threatening complication following allogeneic HSCT which can occur in 30-50% of patients who receive sibling matched transplants. The model of aGvHD utilised in this experiment was established using a major MHC mismatched transplant. BALB/c mice were sub-lethally irradiated (7 Gy) and transplanted with $5x10^6$ bone marrow cells and whole splenocytes limited to $1x10^6$ $CD4^+$ cells isolated from C57BL/6 mice. Human MSC were administered to mice at days 1 and 3 post transplantation (Figure 4.1). As before, mice were monitored on a weekly basis and the development of aGvHD was defined as previously described (Table 4.1). Mice which received a combined pathological score of 6 from 8 or displayed weight loss in excess of 25% were considered to have severe aGvHD and sacrificed humanely.

The administration of human MSC significantly increased the survival of mice with aGvHD with 80% of mice surviving for the duration of this study while all non-treated mice succumbed to GvHD by day 57 (Figure 4.7 A). Human MSC therapy also resulted in reduced weight loss (Figure 4.7 B) and a lower clinical score compared to non-treated mice (Figure 4.7 C).

As before, the level of pathology in target organs was analysed through H&E staining of tissue sections from the small intestine, lung, liver and spleen. Human MSC therapy significantly reduced aGvHD associated pathology within the small intestine of aGvHD mice (Figure 4.8 A&B). Although the large accumulations of lymphocytes observed in cGvHD models were not present in the acute GvHD mice, significant destruction of the villi was clear throughout the organ (Figure 4.8 A). Healthy villi structure in MSC treated mice indicated the protective effect of human MSC in the small intestine (Figure 4.8 A).

Lower levels of lymphocyte infiltration were observed in the lungs of aGvHD mice (Figure 4.8 A) compared to chronic GvHD mice (Figure 4.6 A). However, there was much greater damage to lung architecture in aGvHD mice (Figure 4.8 A). In contrast to both syngeneic transplant and cGvHD mice, the administration of human MSC to mice did not significantly enhance lung pathology during aGvHD (Figure 4.8 A&B). Lower levels of lymphocyte infiltration may be caused by poor immune reconstitution in aGvHD mice and therefore an impaired immune response against human MSC.

Similar to pathology observed in the lung, human MSC had no significant effect on liver pathology during aGvHD (Figure 4.8 A&B). Significant lymphocyte infiltration around hepatic veins was observed in aGvHD mice, although to the same extent in cGvHD mice (Figure 4.6 A). Human MSC therapy did not lower pathological scores or significantly reduce lymphocyte infiltration in the liver during aGvHD (Figure 4.8 A&B).

Spleens taken from aGvHD mice completely lacked germinal centre formation 28 days post transplantation (Figure 4.8 A). This lack of germinal centre formation may be a result of a failure of B cells to engraft post transplantation. The expression of murine CD19 was also significantly reduced in the spleens of aGvHD mice (Figure 4.9). Overall human MSC therapy had no effect on pathological score, germinal centre formation or the expression of CD19 in the spleens of aGvHD mice (Figure 4.8 A; Figure 4.9).

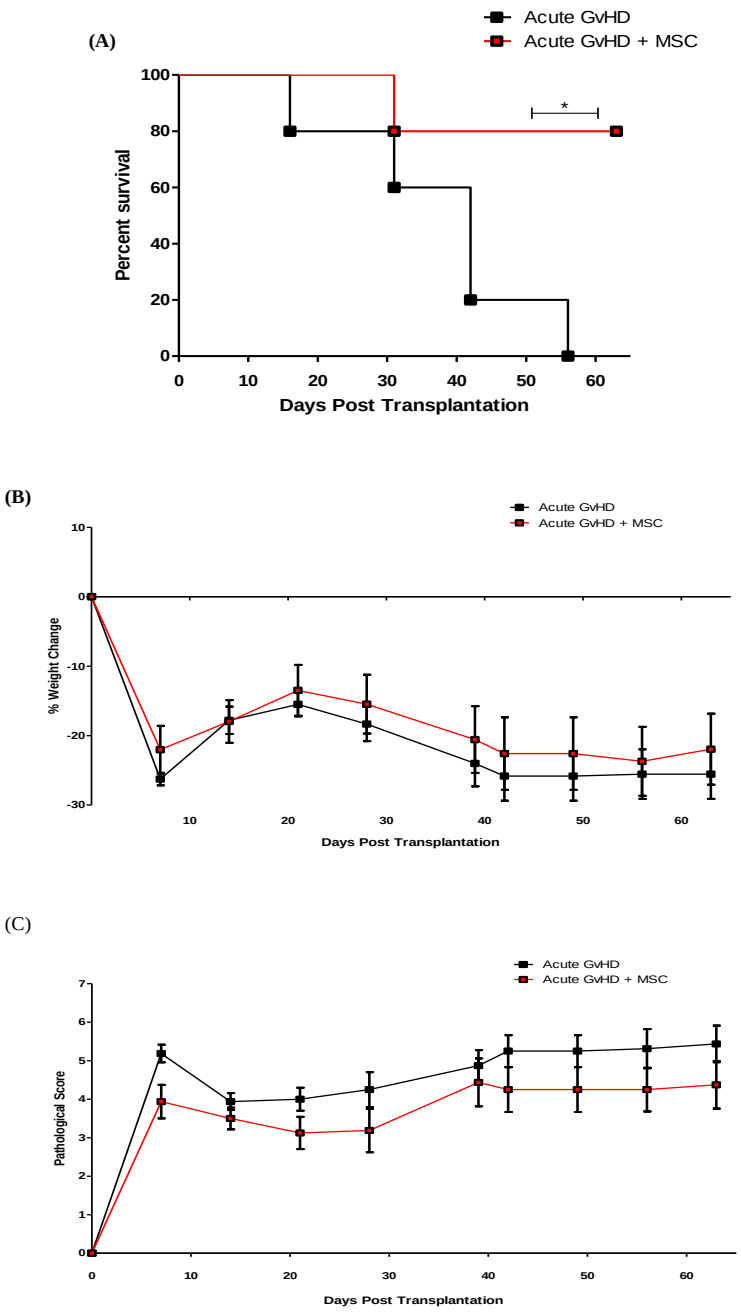

Figure 4.7. Human MSC significantly increased survival and reduced weight loss and clinical score in acute GvHD mice. Graphical representation of (A) survival, (B) percentage weight change and (C) pathological score of syngeneic transplant mice (black line) and MSC treated syngeneic transplant mice (red line). 5 x 10^6 bone marrow cells and whole spleen cells (limited to 1 x 10^6 $CD4^+$ cells) from C57BL/6 mice were administered to irradiated BALB/c mice. 1 x 10^6 human MSC were given as cell therapy on days 1 and 3. Transplanted mice were monitored every 7 days for the duration of the experiment. Non-treated mice (black line) and mice which received human MSC (red line). n=6. Statistical analysis was carried out using the un-paired student T test. * < 0.05.

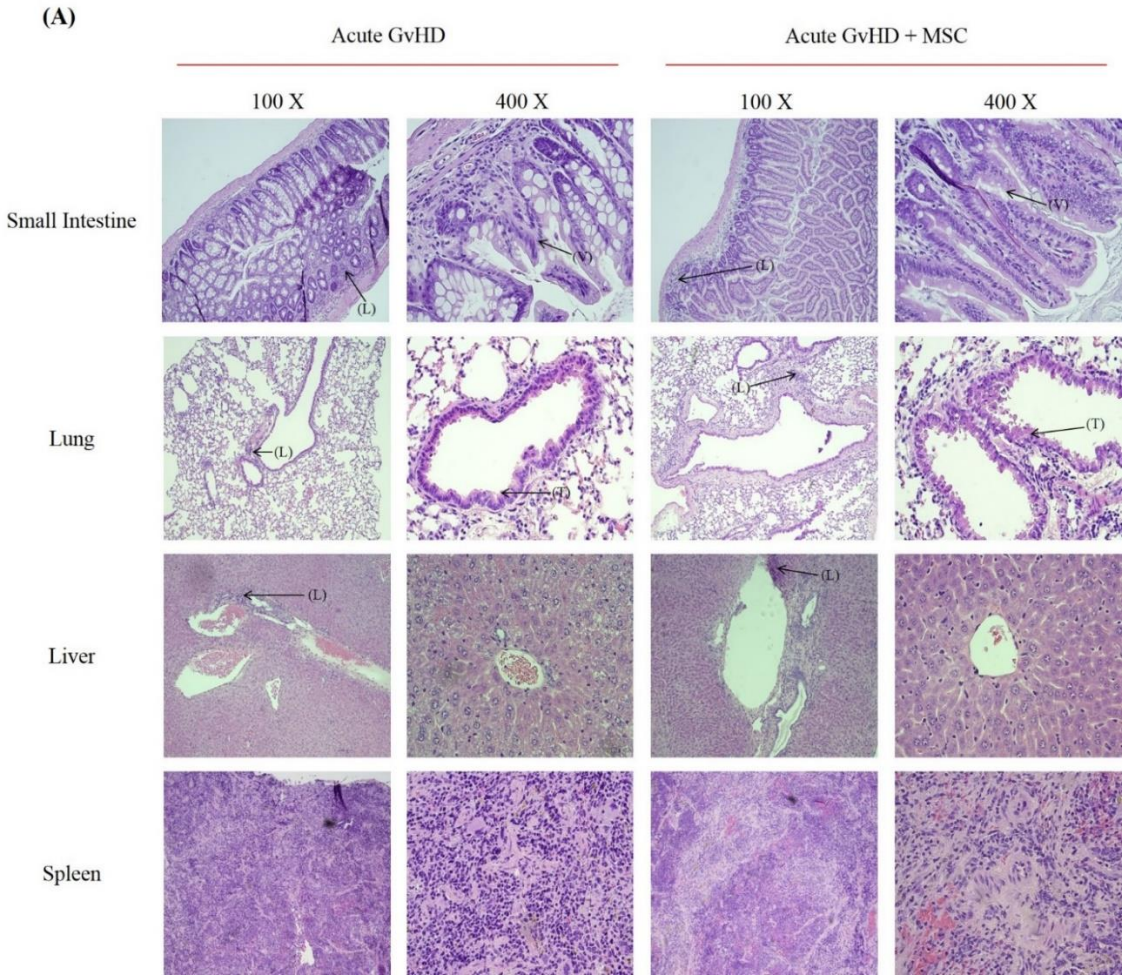
(A)
Acute GvHD
Acute GvHD + MSC
100 X
400 X
100 X
400 X
Small Intestine
Lung
Liver
Spleen
(L)
(V)
(T)

(B)

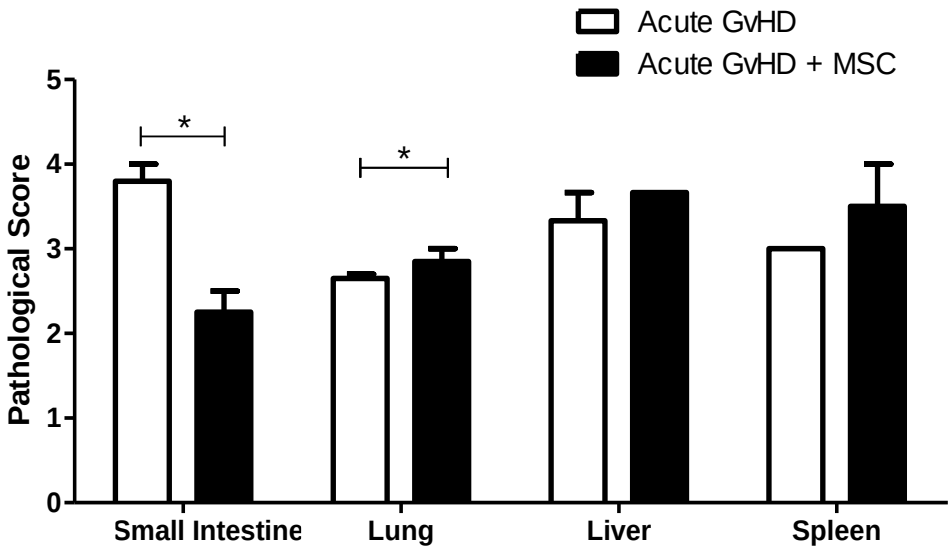

Figure 4.8. Human MSC significantly improved pathology in the small intestine of acute GvHD mice. 5 x 10^6 bone marrow cells and whole spleen cells (limited to 1 x 10^6 $CD4^+$ cells) from C57BL/6 mice were administered to irradiated BALB/c mice. 1 x 10^6 human MSC were given as cell therapy on days 1 and 3. Mice were sacrificed on day 28 and small intestine, lung, liver and spleen harvested and tissue sections were analysed by (A) H&E staining and (B) a defined scoring system. (A) Tissue samples were processed and stained with H&E and analysed for lymphocyte infiltration (L), villi destruction (V), thickening of epithelial airways (T) or germinal centre formation (GC). Pathological score determined by 2 independent researchers. Tissues samples were stained using H&E and images captured at 100X and 400X. (B) Graphical representation of combined pathological score for syngeneic control mice (white bars) and human MSC treated syngeneic mice (black bars). n=3 per group. Statistical analysis was carried out using a paired student T test. * < 0.05.

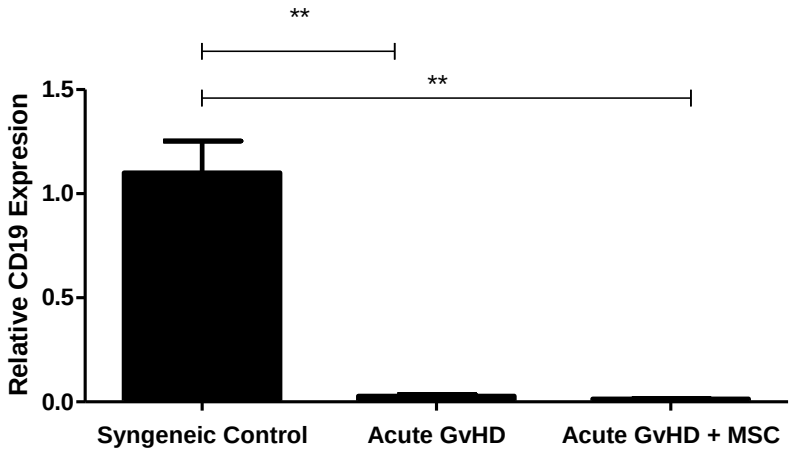

Figure 4.9. Human MSC did not protect B cell engraftment in the spleen. Graphical representation of murine CD19 mRNA expression in the spleens of syngeneic controls, non-treated acute GvHD mice and GvHD mice which received MSC therapy as measured by real time PCR at 28 days post transplantation. n=3 per group. Statistical analysis was carried out using the students paired *t* test. ** < 0.01.

4.6 HUMAN MSC DID NOT INHIBIT $CD4^+$ OR $CD8^+$ T CELL ENGRAFTMENT AFTER TRANSPLANTATION

After HSCT, it is essential that donor hematopoietic cells successfully engraft within the patient to provide a functional immune system and to eliminate any remaining tumour cells. This therefore requires that any potential new therapies against GvHD do not impair engraftment. To determine the effect of human MSC on the engraftment of murine $CD4^+$ and $CD8^+$ T cell populations, spleens were harvested from syngeneic mice, cGvHD mice and aGvHD mice at 28 and 63 days post transplantation. Lymphocyte populations were isolated from each spleen and analysed for the expression of $CD4^+$ and $CD8^+$ populations. The major MHC mismatch between the C57BL/6 donor cells and the BALB/c recipient mouse used in the acute model of GvHD also made it possible to distinguish T cells of donor origin ($H2^{b+}$) from recipient T cells ($H2^{d+}$) using flow cytometry.

Human MSC therapy had no effect on the total number of $CD4^+$ or $CD8^+$ T cells recovered from the spleen of syngeneic control mice 28 days post transplantation (Figure 4.10 A). However, significantly more $CD4^+$ T cells were recovered from the spleens of syngeneic control mice after human MSC therapy 63 days post transplantation (Figure 4.10 B).

The administration of human MSC to cGvHD mice resulted in approximately 50% more $CD4^+$ T cells being recovered from the spleens 28 days after transplantation (Figure 4.10 C), however there was no significant difference. This increase in $CD4^+$ T cells in human MSC treated mice was also evident 63 days post transplantation (Figure 4.10 D). Although there was a slight increase in $CD8^+$ T cells in cGvHD mice that received human MSC at both day 28 and 63, the results obtained were not significant (Figure 4.10 C&D).

The spleen is a primary target of acute GvHD and significant reductions in size as well as the development of extensive necrotic regions were observed in acute GvHD mice. This damage to splenic architecture was subsequently accompanied by a significant reduction in the numbers of viable lymphocytes recovered from the spleen. Similar to results observed in cGvHD models, human MSC therapy resulted in an increased engraftment of $CD4^+$ T cell populations when compared to non-treated mice at both 28 and 63 days after transplantation (Figure 4.10 E&F). A greater number of $CD8^+$ T cells were also recovered from the spleens of mice which received human MSC therapy (Figure 4.10 E&F). All $CD4^+$ and $CD8^+$ T cells recovered from the spleens of both human MSC treated and non-treated aGvHD mice were positive for the MHC class I haplotype K^b and were therefore of C57BL/6 origin (Figure 4.11). These data suggest the administration of human MSC to murine models of chronic or acute GvHD does not impair the engraftment of transplanted cells.

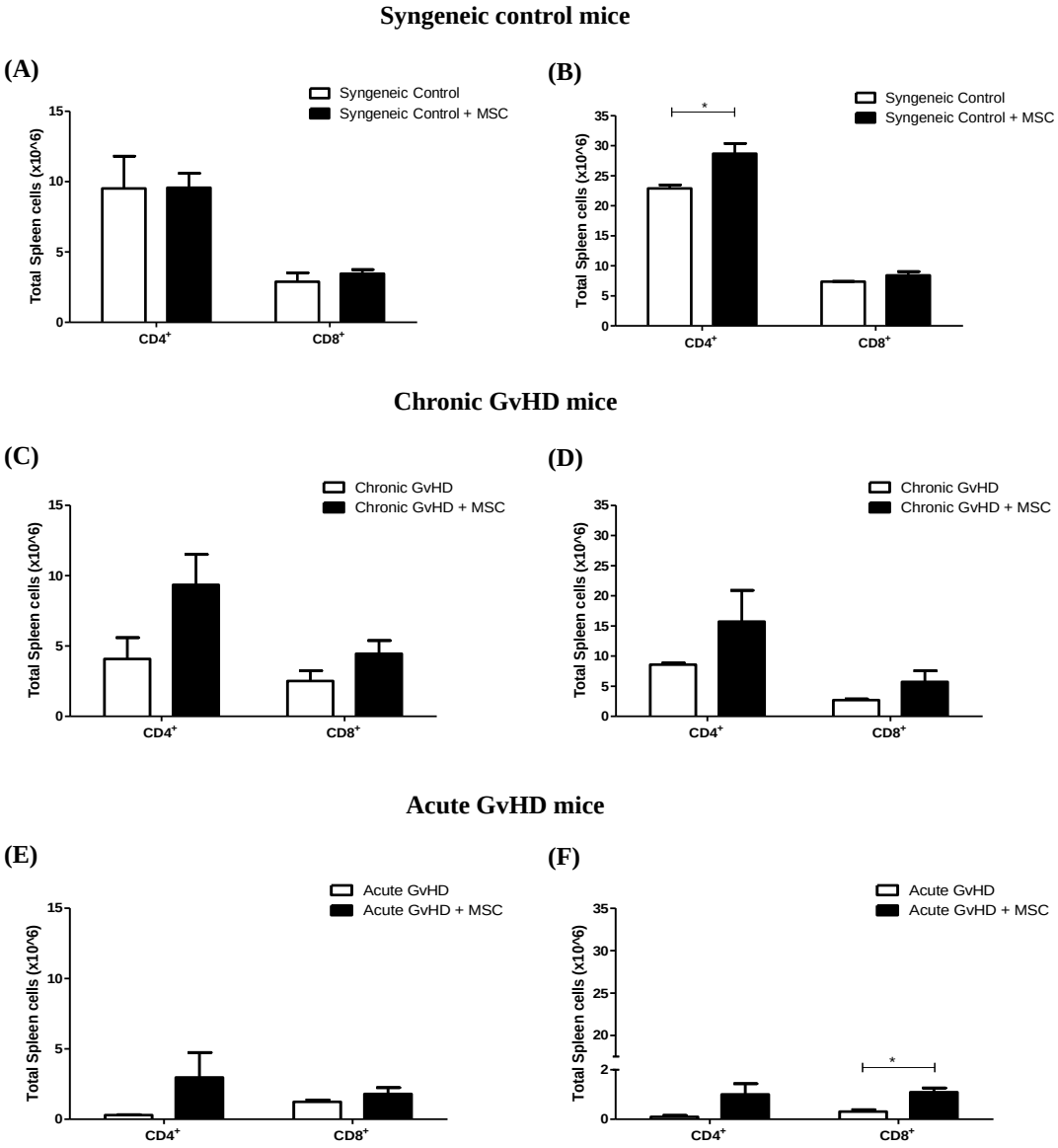

Figure 4.10. Human MSC therapy increased engraftment of $CD4^+$ and $CD8^+$ T cells post transplantation. Graphical representation of total $CD4^+$ and $CD8^+$ T cell numbers recovered from spleens of syngeneic control mice (A & B, chronic GvHD models (C & D) and acute GvHD models (E & F) which did not receive treatment (white bars) or received human MSC therapy (black bars) as measured by flow cytometry on days 28 (A, C & E) and 63 (B, D & F). n=3 per group. Statistical analysis was carried out using the students paired T test. * < 0.05, ** < 0.01.

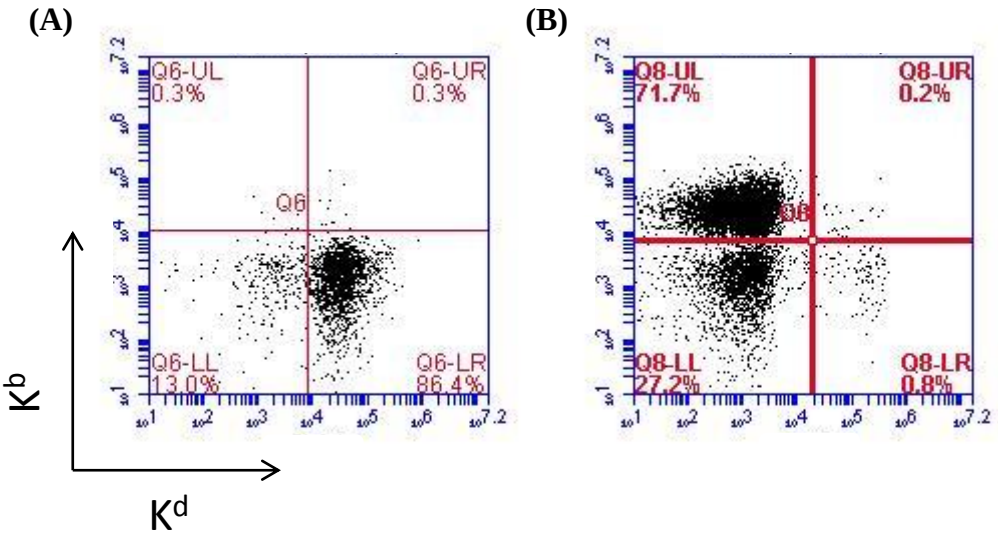

Figure 4.11. Reconstituted lymphocytes in acute GvHD are donor derived. Representative image comparing the expression of MHC class I haplotypes K^d and K^b on live $CD4^+$ lymphocytes recovered from the spleens of (A) syngeneic transplant mice and (B) acute GvHD mice as measured by flow cytometry 28 days after transplantation. n=3 per group.

4.7 SUMMARY

The main aims of this chapter were to (1) determine whether human (xenogeneic) MSC therapies can be assessed in murine models of acute or chronic GvHD, (2) to investigate the capacity for human MSC to promote survival in GvHD mice and (3) to examine the effect of human MSC on pathology, weight loss and engraftment. Transplantation of xenogeneic MSC into syngeneic control mice had no adverse effect on survival, weight gain or pathology (Figure 4.2); however human MSC significantly increased lymphocyte infiltration and thickening of the airway epithelial wall within the lungs of these mice (Figure 4.3). Syngeneic control mice which received human MSC also contained significantly more $CD4^+$ T cells in BAL fluid recovered from the lungs than non-treated mice after 28 days (Figure 4.4). Human MSC therapy had no effect on splenic T cell populations 28 days after transplantation but did however result in significantly more splenic $CD4^+$ T cells at day 63 (Figure 4.4). The administration of human MSC to cGvHD mice resulted in a slightly lower clinical score and reduced weight loss than non-treated mice 63 days post transplantation (Figure 4.5 A-C). Human MSC therapy reduced lymphocyte infiltration and overall pathological score in the small intestine of cGvHD mice (Figure 4.6 A&B). The administration of human MSC to cGvHD mice resulted in increased lymphocyte infiltration to the lungs, particularly around bronchi, and more profound airway epithelium thickening compared to non-treated mice (Figure 4.6 A). Human MSC therapy reduced the level of infiltrating lymphocytes around periportal areas in the livers of cGvHD mice (Figure 4.6 A).

Human MSC significantly increased survival and reduced pathological score and weight loss during aGvHD (Figure 4.7). Moreover, human MSC therapy significantly reduced pathology in the small intestine and provided protection from villous destruction when compared to non-treated mice (Figure 4.8 A&B). In contrast to results presented

for syngeneic control mice and cGvHD mice, the administration of human MSC did not exacerbate lung pathology in aGvHD mice (Figure 4.8 A&B).

CHAPTER 5

HUMAN MSC SIGNIFICANTLY PROLONG SURVIVAL IN A HUMANISED MOUSE MODEL OF AGVHD

5.1 INTRODUCTION

In the previous chapter, a number of limitations in the murine GvHD animal models were identified. This study highlighted the importance of developing novel animal models of aGvHD to further extend the understanding of aGvHD and to elucidate how human MSC might control the disease progression. The series of experiments conducted in chapter 4 demonstrated that human (xenogeneic) MSC therapies can be assessed in murine models of aGvHD, and provided a platform from which to investigate how human MSC modulate aGvHD. However, the major limitations, which included an immune response against the human MSC and the fact that the effector cells are murine rather than human, led to the development of a more clinically relevant model of aGvHD.

The development of humanised mice has yielded exciting new methods of studying human haematopoiesis and immunity *in vivo* and over the last number of years the development of humanised mouse models of disease has grown substantially (Shultz *et al.* 2012). Previous work within our research group has focussed on developing a robust and reproducible humanised mouse model of aGvHD by administering human PBMC to the NOD-SCID IL-2 receptor gamma null (NOD-SCID IL-2rγ^{null})(NSG) mouse, first developed by Pearson *et al.* (Pearson *et al.* 2008). The NSG model of aGvHD offers a more clinically relevant model of disease than those developed in chapter 4 as the disease is triggered and sustained by human immune cells. The development of this humanised mouse model of aGvHD allowed the identification that human MSC prolonged survival and reduced pathology of aGvHD mice through the inhibition of cell proliferation *in vivo* (Tobin *et al.* 2013).

PBMC isolated from freshly drawn blood were used to establish the NSG model of a GvHD; however, the use of PBMC from freshly extracted blood is extremely limiting in the amount of cells which can be isolated and therefore impacting the scale of the

experiments possible. Therefore, this chapter aimed to establish a consistent and reproducible humanised mouse model of aGvHD from PBMC isolated from buffy-packs. Isolating PBMC from buffy-packs provides significantly more PBMC and facilitates larger scale *in vivo* experiments to probe further into how MSC prolong the survival of aGvHD mice. This chapter will then use the aGvHD model as a platform to test therapeutic interventions. Specifically the efficacy of *Fasciola hepatica* tegumental antigen as a novel therapy against aGvHD will be investigated.

The objectives of this chapter were broken down as follows:

(1) Develop a robust and reproducible humanised mouse model of acute GvHD using PBMC isolated from buffy-packs.
(2) Identify potential mechanisms behind MSC protection against aGvHD.
(3) Determine whether the administration of γMSC therapy was more efficient than resting MSC therapy on day 7.
(4) Investigate whether multiple dose MSC therapy is more efficacious than single dose therapy.
(5) Utilise the humanised mouse model of aGvHD as a platform to test a novel immunomodulatory therapy (*Fasciola hepatica*).

5.2 Optimisation of the humanised mouse model of aGvHD using buffy pack derived lymphocytes

Previous work from our research group had developed a humanised mouse model of GvHD using PBMC isolated from freshly drawn blood (Tobin *et al.* 2013) from the protocol originally described by Pearson *et al.* (2008). The main limiting factor with these studies was the number of PBMC which could be recovered from freshly isolated blood. Therefore this study sought to advance this model to allow larger scale *in vivo* experiments. It was hypothesised that PBMC isolated from buffy-packs would be capable of provoking aGvHD in irradiated NSG mice. Using the studies by Pearson *et al.* and Tobin *et al.* as guidelines, a humanised mouse model of aGvHD was developed. This model is described in chapter 2.10.4. Briefly, after conditioning by low dose whole body irradiation (2.4 Gy), human PBMC were injected via the tail vein and the progression of GvHD was monitored. In accordance with the local ethical committee the development of GvHD was defined as total body weight loss of >20% of original starting weight with a series of clinical manifestations including posture, reduction in activity, fur condition and diarrhoea. These parameters were scored as described in Table 4.1, where any mouse which fell below 80% of their starting body weight or accumulated a clinical score of 6 or more was sacrificed humanely.

5.2.1 DETERMINATION OF OPTIMAL PBMC DOSE TO INDUCE AGVHD

Pearson *et al.* suggest a total dose of 2 x 10^7 PBMC was sufficient for consistent development of aGvHD in a humanised mouse model (Pearson *et al.* 2008). However, the previous work conducted by our research group had found that the administration of 2 x 10^7 PBMC resulted in inconsistent aGvHD development and instead suggested a dose of 6.3 x 10^5 PBMC $gram^{-1}$ from freshly drawn blood. PBMC isolated from freshly drawn blood are more responsive than those isolated from buffy packs and therefore it was hypothesised that a higher dose would be required. At the time of initial experiments in this model, the information on dose adjusted to mouse body weight was not available and so a total dose of 3 x 10^7 human PBMC was chosen to establish aGvHD in irradiated NSG mice.

To investigate whether 3 x 10^7 PBMC would trigger aGvHD, NSG mice were sub-lethally irradiated (2.4 Gy) and transplanted with either 3 x 10^7 human PBMC or PBS via tail vein injections. The survival and percentage weight loss were monitored throughout the experiment. The reproducibility of administering 3 x 10^7 PBMC was determined by examining the development of aGvHD using 4 different PBMC donors. Transplanted mice were monitored regularly and the development of aGvHD determined as described above (Table 4.1). As expected, all irradiated mice which received PBS survived until the conclusion of the experiment (Figure 5.1 A). PBS mice remained healthy and gained weight throughout the duration of the experiment (Figure 5.1 B). The administration of 3 x 10^7 PBMC to irradiated NSG mice successfully established aGvHD in all mice. However, administering 3 x 10^7 PBMC to irradiated NSG mice resulted in rapid and aggressive aGvHD symptoms. Notably all the mice which received PBMC lost over 20% body weight by day 11 (Figure 5.1 B). The aggressive nature of aGvHD induced by administering 3 x 10^7 PBMC was not suitable for future studies examining the effect of MSC therapy, suggesting that a lower PBMC dose was required.

While the work of Pearson *et al.* suggested a standard PBMC dose of 2 x 10^7 PBMC per mouse, the model of aGvHD previously established in our research group was designed as an individual dose of 6.3 x 10^5 PBMC $gram^{-1}$. Therefore a similar approach was taken while optimising the dose of buffy pack PBMC and it was hypothesised that the administration of 8 x 10^5 PBMC $gram^{-1}$ would consistently initiate aGvHD in irradiated NSG mice. NSG mice were irradiated as before and were then injected with 8 x 10^5 PBMC $gram^{-1}$. The consistency of GvHD development was determined using PBMC isolated from 4 different donors. One group of irradiated mice received PBS to act as a control. The mice were monitored and aGvHD determined as before. Initial optimisation studies mice which had suffered over 20% weight loss or accumulated a total score greater than 6 (Table 4.1) were sacrificed humanely. However, it was agreed with the NUIM ethics committee that in subsequent studies mice which had suffered over 15% weight loss over successive days or accumulated a score of 6 or more would be sacrificed.

Control mice which received PBS in place of PBMC had a survival rate of 100% at the conclusion of the experiment (Figure 5.2 A). The sub-lethal radiation dose administered as pre-conditioning regiment results in slight weight loss in all experimental groups (Figure 5.2 B); however PBS control mice remain asymptomatic and returned to their starting weight by day 28 (Figure 5.2 B). Mice which received PBMC from 3 of the donors developed GvHD during the desired period. aGvHD was established in these mice from day 10, as illustrated by the significant weight loss after this day, and all of the mice had succumbed to aGvHD by day 16 (Figure 5.2 A). However, the establishment of aGvHD in mice which received PBMC from donor 007 was not as robust. Weight loss was delayed in these mice and 50% survived until day 28 (Figure 5.2). These results suggest that the administration of 8 x 10^5 PBMC, isolated from buffy-packs, was capable of initiating aGvHD but the variation between human donors indicated that some PBMC donors or preparations might not be suitable.

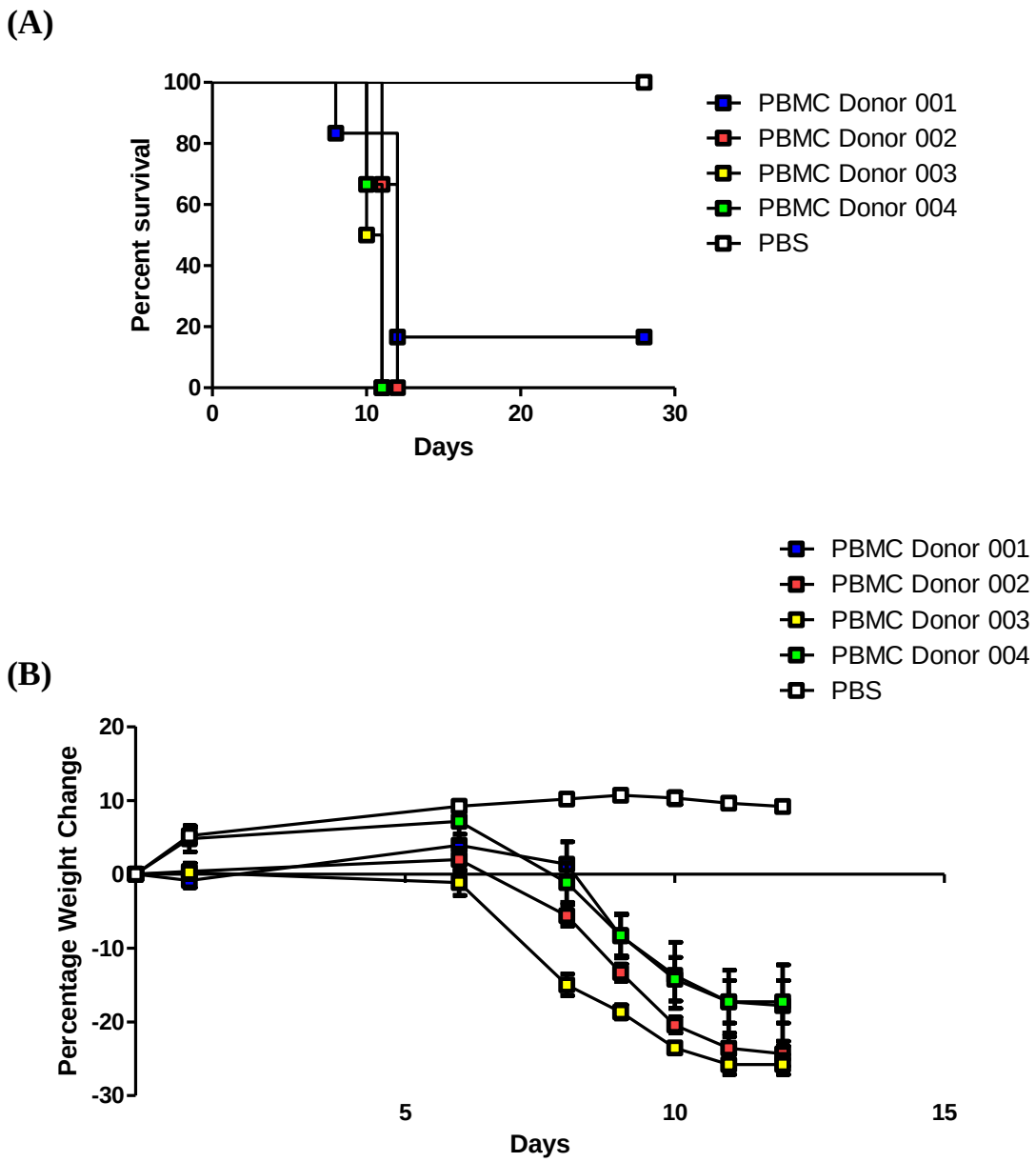

Figure 5.1. 3 x 10^7 PBMC results in aggressive aGvHD. Graphical representation of (A) survival and (B) percentage weight change of irradiated NSG mice which have received 3 x 10^7 human PBMC from donors 001 (blue), 002 (red), 003 (yellow), 004 (green) or PBS control mice (white). Transplanted mice were monitored every 2 days until day 9 and then every day for the duration of the experiment. n = 6 mice per group. Statistical analysis was carried out using the un-paired student *t*-test.

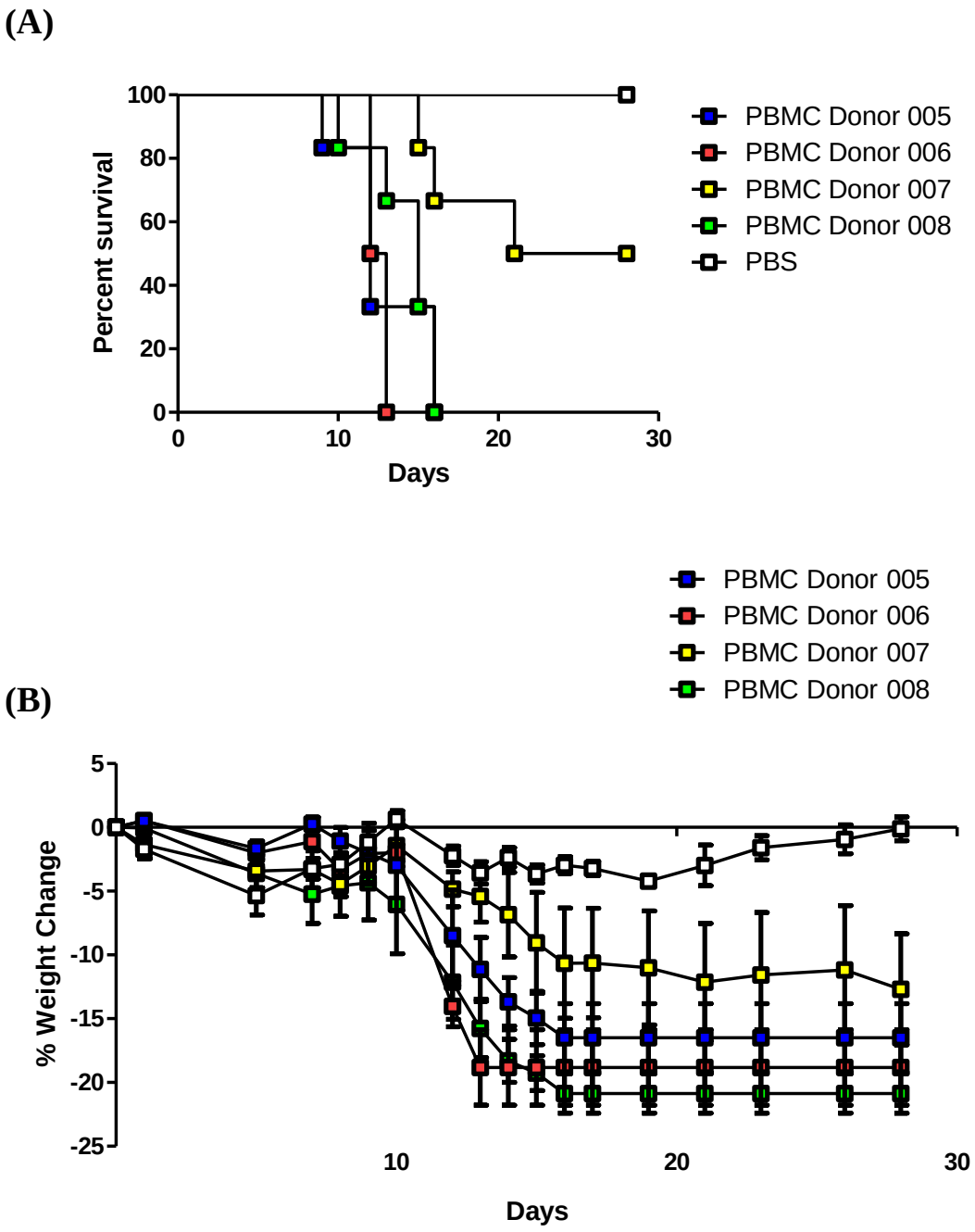

Figure 5.2. Administration of 8 x 10^5 PBMC $gram^{-1}$ results in a reproducible model of aGvHD. Graphical representation of (A) survival and (B) percentage weight change of irradiated NSG mice which have received 8 x 10^5 human PBMC $gram^{-1}$ from donors 005 (blue), 006 (red), 007 (yellow), 008 (green) or PBS control mice (white). Transplanted mice were monitored every 2 days until day 9 and then every day for the duration of the experiment. n = 6 mice per group. Statistical analysis on survival curve was carried out using a Mantel-Cox test. * < 0.05.

5.2.2 OPTIMISING AGVHD MODEL FOR CRYOPRESERVED PBMC

As highlighted from figure 5.2, the variability in PBMC responsiveness between donors can significantly impair the efficacy of this model. Therefore it was hypothesised that a bank of responsive PBMC populations could be amassed and stored in liquid nitrogen. PBMC were isolated from buffy packs as before and cryopreserved as described in chapter 2.3.4. In order to create a bank of reactive PBMC, it was first necessary to determine whether PBMC recovered from cryopreservation were capable of consistently inducing aGvHD. It was thought that PBMC recovered from liquid nitrogen storage would be less effective than freshly isolated PBMC and therefore higher doses were investigated. NSG mice were irradiated as before and then received a total dose of 3 x 10^7 thawed PBMC, 9.3 x 10^5 PBMC gram^{-1} or 1 x 10^6 PBMC gram^{-1}. Control mice were also established by administrating PBS to irradiated NSG mice. Mice were monitored and aGvHD determined as previously described. As before, mice which had suffered over 20% weight loss or accumulated a total score greater than 6 (Table 4.1) were sacrificed humanely.

Unlike the previous experiments, one of the PBS control mice began to lose weight and had to be sacrificed after 8 days of the study. However, none of the remaining PBS mice displayed any aGvHD symptoms and all recovered to their starting weight by day 12. When each irradiated mouse was given a total dose of 3 x 10^7 PBMC, aGvHD was established using both thawed PBMC donors; however the development of aGvHD was not consistent for the two donors. aGvHD mice which received PBMC from donor 002 began to display pathological signs of GvHD early and all of these mice were sacrificed by day 11 (Figure 5.3 A). Mice which received PBMC from donor 004 showed more delayed weight loss and the onset of aGvHD was more similar to the desired model of aGvHD (Figure 5.3). These results suggested that tailoring the dose of thawed PBMC to each individual mouse may result in a more consistent model of aGvHD.

The ability of 9.3 x 10^5 thawed PBMC $gram^{-1}$ to establish aGvHD in irradiated NSG mice was subsequently investigated. As seen with figure 5.3, variability between PBMC donors 002 and 004 resulted in differences in the development of aGvHD. Mice which received PBMC from donor 002, demonstrated steady weight loss and aGvHD development between days 10 and 16; with 84% of mice being sacrificed by day 16 (Figure 5.4 A). However, mice which were given PBMC from donor 004 developed aGvHD later but did however display steady weight loss and all mice which received PBMC from donor 004 had to be sacrificed by day 28 (Figure 5.4 B). These results suggested that administrating 9.3 x 10^5 thawed PBMC $gram^{-1}$ was better than a total dose of 3 x 10^7 PBMC but might still be lower than optimal.

To determine the reliability of establishing aGvHD with 1 x 10^6 $gram^{-1}$ thawed PBMC, PBMC were isolated from buffy-packs obtained from 4 different healthy donors. All PBS control mice survived until the conclusion of the experiment and steadily gained weight throughout the 28 days. Similar to the results presented in figure 5.2, 3 of the 4 PBMC donors generated aGvHD. Mice which received PBMC from donors 001, 002 or 004 all began to gradually lose weight between days 9 and 15 with all of the mice developing aGvHD and being sacrificed by day 18 (Figure 5.5 A). The variability associated with human donors was again witnessed in mice which received PBMC from donor 003. Administering 1 x 10^6 $gram^{-1}$ thawed PBMC from donor 003 resulted in an overly aggressive form of aGvHD where mice rapidly lost weight and all mice from this group had to be sacrificed by day 11 (Figure 5.5). These results indicate that it is possible to establish a robust and reproducible model of aGvHD from a frozen bank of responsive PBMC with a dose of 1 x 10^6 $gram^{-1}$ PBMC.

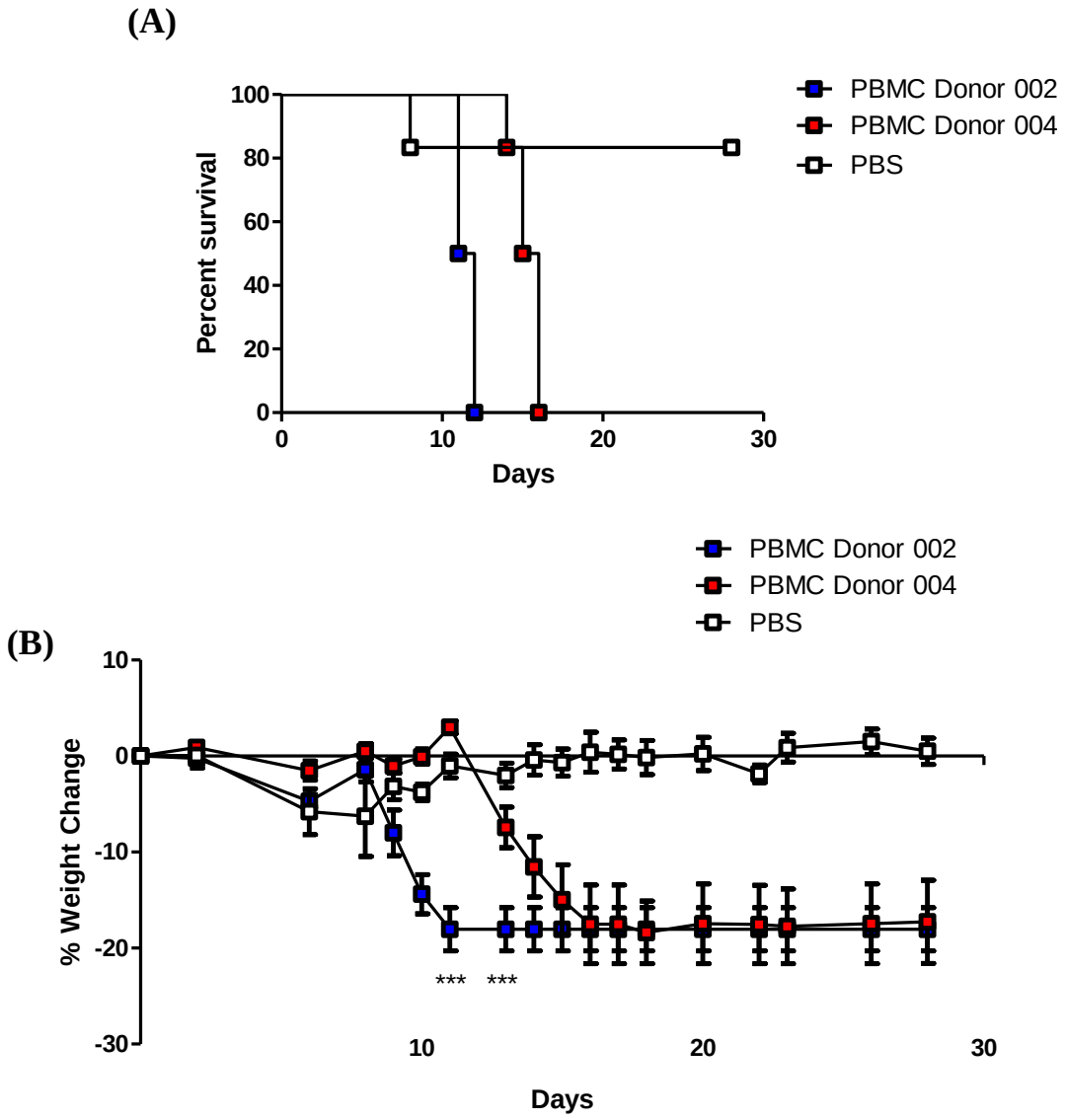

Figure 5.3. Administration of 3 x 10^7 thawed PBMC resulted in inconsistent aGvHD development. Graphical representation of (A) survival and (B) percentage weight change of irradiated NSG mice which have received 3 x 10^7 thawed human PBMC from donors 002 (blue) or 004 (red). PBS control mice are represented by white boxes. Transplanted mice were monitored every 2 days until day 9 and then every day for the duration of the experiment. n = 6 mice per group. Statistical analysis was performed using student *t*-test where *** < 0.001 between blue and red boxes.

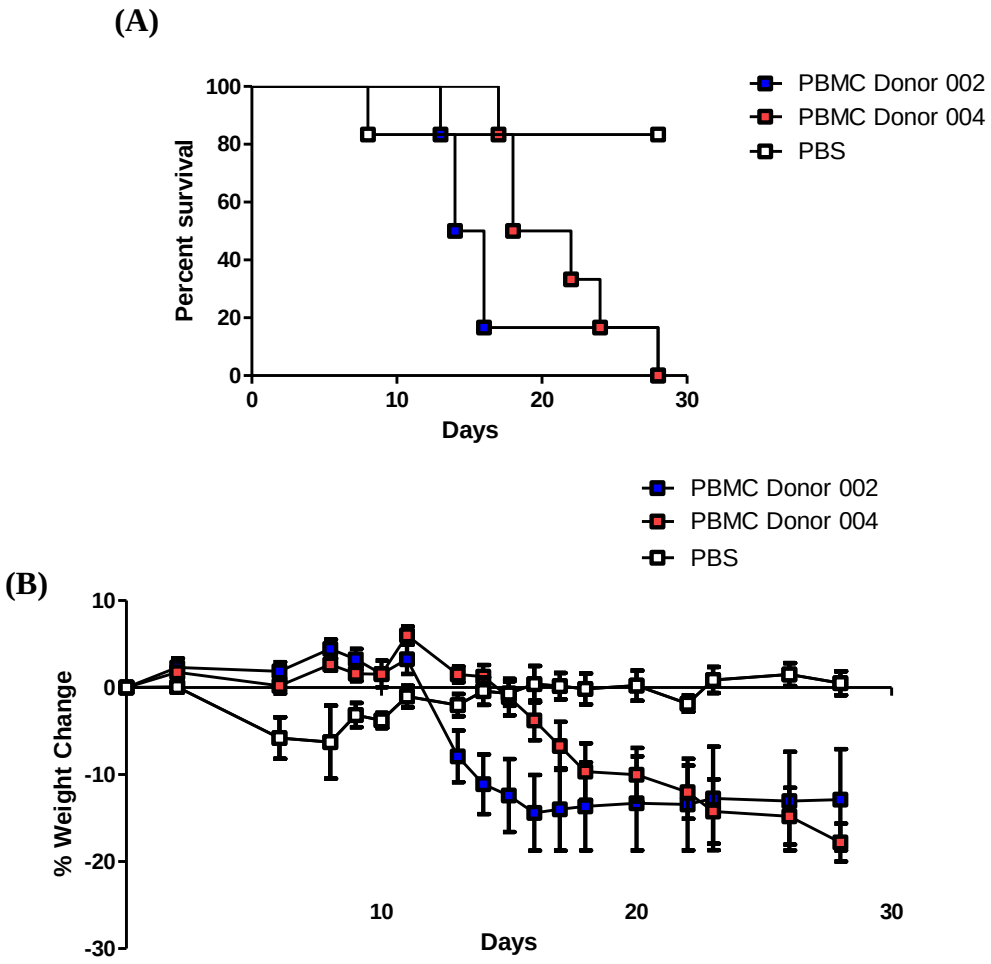

Figure 5.4. aGvHD was less severe following administration of 9.3 x 10^5 thawed PBMC $gram^{-1}$. Graphical representation of (A) survival and (B) percentage weight change of irradiated NSG mice which have received 9 x 10^5 thawed human PBMC $gram^{-1}$ from donors 002 (blue) or 004 (red). PBS control mice are represented by white boxes. Transplanted mice were monitored every 2 days until day 9 and then every day for the duration of the experiment. n = 6 mice per group.

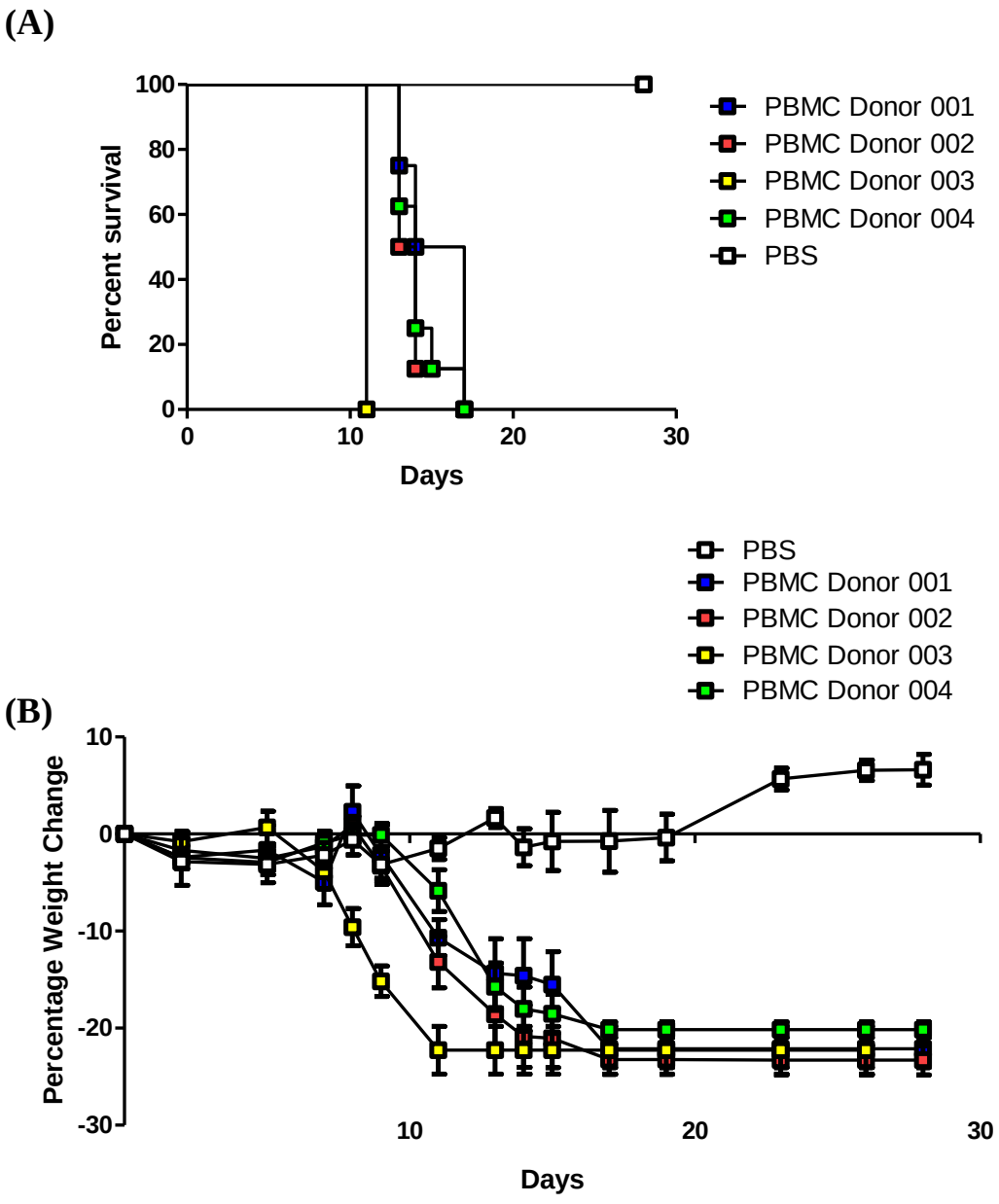

Figure 5.5. Administration of 1 x 10^6 thawed PBMC $gram^{-1}$ results in a reproducible model of aGvHD. Graphical representation of (A) survival and (B) percentage weight change of irradiated NSG mice which have received 1 x 10^6 human PBMC $gram^{-1}$ from donors 001 (blue), 002 (red), 003 (yellow) or 004 (green). PBS control mice are represented by white boxes. Transplanted mice were monitored every 2 days until day 9 and then every day for the duration of the experiment. n = 6 mice per group.

5.2.3 Optimisation of Busulfan as a conditioning agent for aGvHD model

Other research groups which have utilised the NSG mouse for models of aGvHD, have administered human PBMC without the use of a pre-conditioning regimen. These models of GvHD require the administration of 6 x 10^7 PBMC and can take up to 30 days before the mice developed GvHD (Hippen *et al.* 2012). The development of sub-lethal whole body irradiation (2.4 Gy) as a pre-conditioning regimen in this study significantly reduces the amount of PBMC required as well as shortening the duration of the experiment. However, future collaborative projects required a chemical pre-conditioning regimen and therefore the potential use of the chemotherapeutic agent Busulfan as a pre-conditioning agent was investigated. Busulfan was administered by I.P. injection (25 mg/kg) in two doses, on day -2 and day -1. A separate group of mice were irradiated on day 0 as before. Mice which received Busulfan or irradiation then received 8 x 10^5 PBMC $gram^{-1}$ via tail vein injection. Control groups of mice pre-conditioned with Busulfan or irradiation were also given sterile PBS. The mice were monitored and aGvHD determined as before where mice which had suffered over 20% weight loss or accumulated a total score greater than 6 (Table 4.1) were sacrificed humanely.

There was one irradiated PBS control mouse which had to be sacrificed in the first few days of the study. This was due to the mouse not moving around the cage or responding to stimuli and did not seem related to aGvHD but most likely to the manipulation of the tail during the administration of agents. Pre-conditioning of NSG mice with Busulfan prior to PBMC administration resulted in a very similar survival curve to mice which were pre-conditioned with irradiation (Figure 5.6 A). However, mice which were pre-conditioned with Busulfan appeared to be ill for a number of days after receiving Busulfan. This was illustrated by the significantly higher weight loss in Busulfan treated mice on day 1 compared to irradiated mice (Figure 5.6 B). However, Busulfan treated mice recovered their weight loss and were very similar to irradiated mice

between days 3 and 9. Mice which received irradiation appeared to develop GvHD slightly earlier and had significantly higher weight loss on days 10 and 11 (Figure 5.6 B). Despite this, there was no difference in survival between mice which received Busulfan and mice which were irradiated suggesting that the chemical pre-conditioning of NSG mice with Busulfan could provide a viable alternative to irradiation. Hereafter the dose of PBMC from buffy packs derived from a single donor of 8×10^5 PBMC $gram^{-1}$ was used as the most reliable protocol for further study.

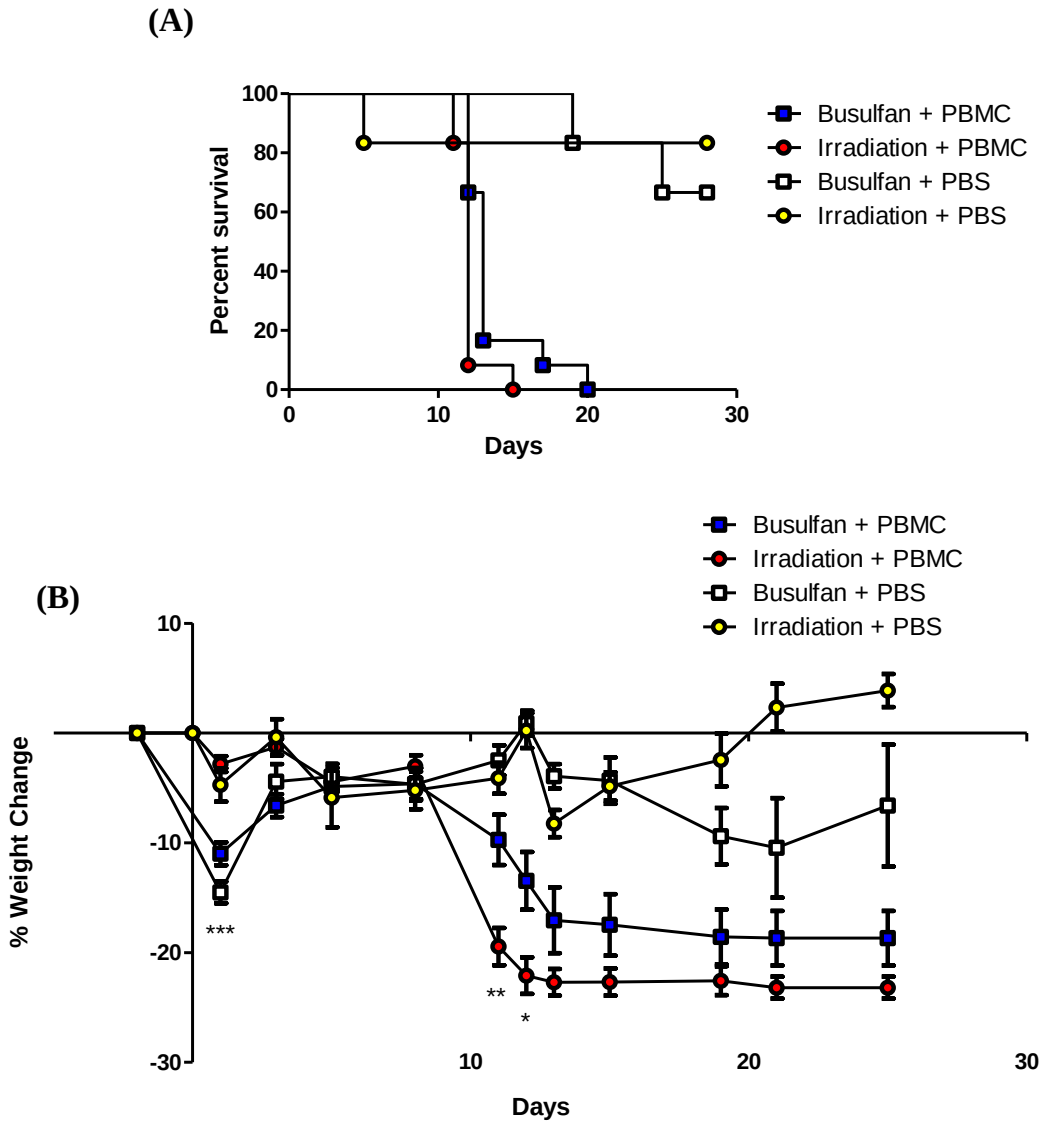

Figure 5.6. Pre-conditioning with Busulfan is comparable to irradiation in the humanised mouse model of aGvHD. Graphical representation of (A) survival and (B) percentage weight change of irradiated NSG mice which have received 8 x 10^5 human PBMC $gram^{-1}$ from after 25 mg/kg Busulfan on day -2 and day -1 (blue boxes) or irradiation on day 0 (red circles). PBS control mice which received 25 mg/kg Busulfan on day -2 and day -1 are represented by white boxes while PBS mice which received irradiation on day 0 are represented by yellow circles. Transplanted mice were monitored every 2 days until day 9 and then every day for the duration of the experiment. Graph represents 2 PBMC donors with n = 6 mice per donor. Statistical analysis was carried out using the un-paired student *t*-test where * < 0.05, ** < 0.01 and *** < 0.001.

5.3 HUMAN MSC SIGNIFICANTLY INCREASED SURVIVAL AND REDUCED WEIGHT LOSS OF AGVHD MICE

Following optimisation of the model, this study sought to determine whether human MSC suppressed acute GvHD in this model. PBMC were isolated from buffy-packs and administered to irradiated (2.4 Gy) NSG mice via tail vein injection ($8x10^5$ PBMC $gram^{-1}$). Control groups were also established by administrating sterile PBS to irradiated NSG mice. All mice were monitored on a regular basis and the development of GvHD was defined as previously described (Table 4.1). Mice which received a combined pathological score higher than 6 or displayed weight loss in excess of 15% were considered to have severe GvHD and sacrificed humanely (in accordance with local ethics committee recommendations at NUI Maynooth).

After PBMC administration, the survival and weight loss of each mouse was monitored every 2 days until day 9 and then every day for the duration of the experiment (Figure 5.7). As expected, the administration of PBS to irradiated NSG mice had no effect on survival and did not result in any weight loss of PBS mice (Figure 5.8 A). NSG mice which received PBMC developed acute GvHD with only 10% surviving until day 15 and none surviving past day 19 (Figure 5.8 A). The administration of MSC therapy to PBMC mice on day 7 significantly prolonged the survival of aGvHD mice with 50% of mice surviving past day 15 and 26% of MSC treated mice surviving the duration of the experiment (Figure 5.8 A). aGvHD mice which received MSC therapy also displayed significantly less weight loss between days 14 and 20 (Figure 5.8 B). After day 20 however, the difference in weight loss was no longer significant and all MSC treated mice demonstrated signs of developing aGvHD by day 22 (Figure 5.8 B).

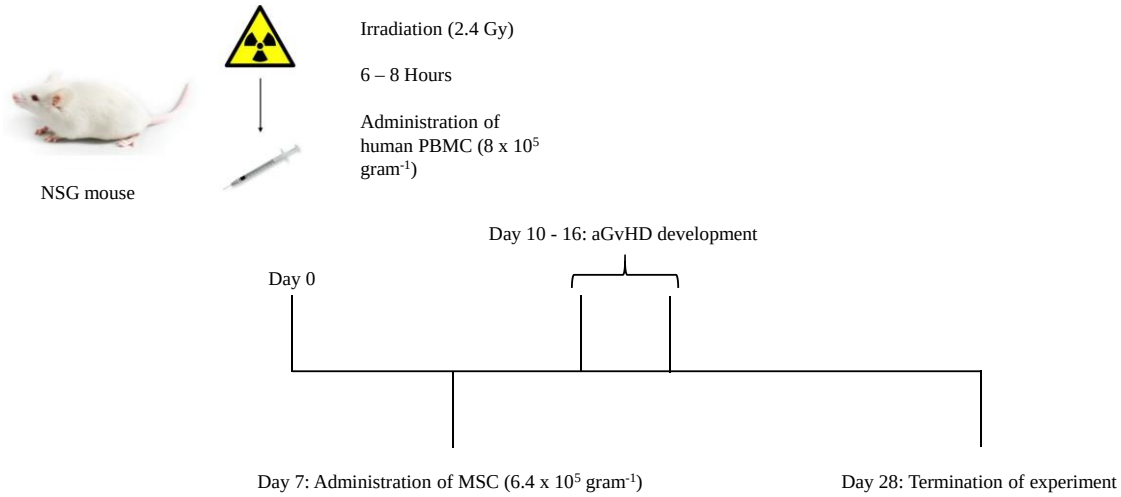

Figure 5.7. Development of a humanised mouse model of aGvHD. NOD-SCID IL-2rγ^{null} (NSG) mice were exposed to a sub-lethal dose of gamma irradiation (2.4 Gy). 8 x 10^5 PBMC gram^{-1} or sterile PBS was then administered intravenously (300 µl) to each mouse via the tail vein. Mesenchymal stromal cells (6.4 x 10^4 gram^{-1}) were administered intravenously on day 7. The development of aGvHD was monitored every second day until day 9 and then everyday thereafter by recording weight loss, fur texture, posture, activity and diarrhoea.

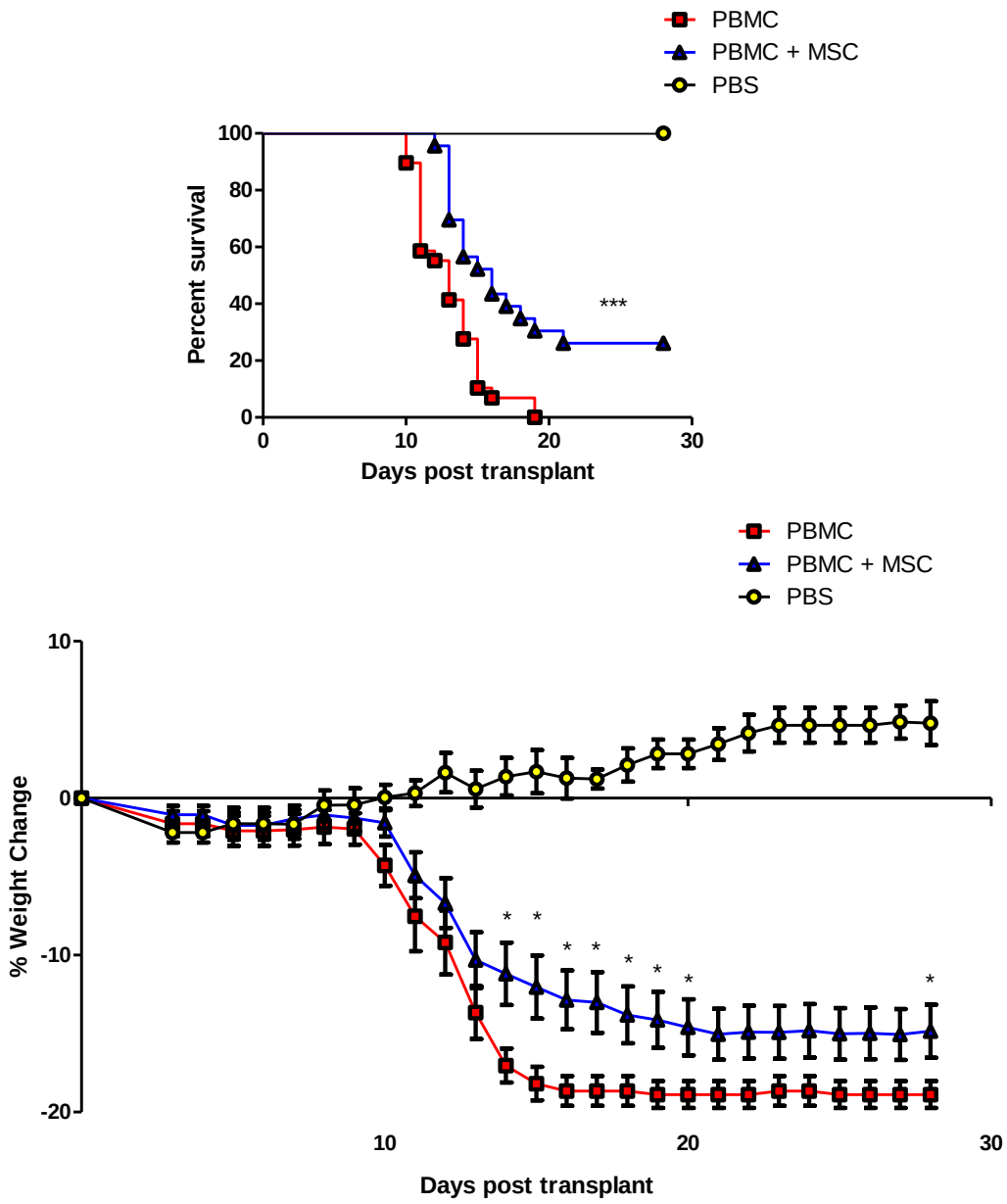

Figure 5.8. MSC significantly prolong survival and reduce weight loss in aGvHD mice. (A) survival curve, and (B) percentage weight change of aGvHD mice (blue line) and MSC treated aGvHD mice (red line). PBS control mice are represented by the yellow line. 8 x 10^5 human PBMC $gram^{-1}$ were administered to irradiated NSG mice (2.4 Gy). 6.4 x 10^4 human MSC $gram^{-1}$ were given as cell therapy on day 7. Transplanted mice were monitored every 2 days until day 9 and then every day for the duration of the experiment. n=29 for PBMC mice, n=23 for PBMC + MSC mice and n=10 for PBS mice. Statistical analysis was carried out using a Mantel-Cox test for the survival curve and un-paired student *t*-test for weight change where * < 0.05 and *** < 0.001.

5.4 ADMINISTRATION OF HUMAN MSC DID NOT REDUCE THE ENGRAFTMENT OF PBMC

The administration of MSC to acute GvHD mice resulted in significantly prolonged survival, reduced weight loss and lower pathological scores. However, GvHD mice which received MSC eventually developed typical acute GvHD symptoms from 16 days post transplantation and most of these mice developed GvHD by the end of the study. The engraftment of transplanted HSC is essential for the recovery of HSCT patients after transplantation and novel cell therapies designed to control aGvHD should not impair this process. To examine whether the increased survival observed in MSC treated aGvHD mice (Figure 5.8) was associated with impaired PBMC engraftment, irradiated NSG mice were given PBMC (8×10^5 gram^{-1}) and treated with MSC 7 days later. On day 12, mice were sacrificed and the engraftment of human $CD45^+$ lymphocytes in the spleen was determined by flow cytometry (Figure 5.9). The engraftment of human $CD45^+$ lymphocytes was unaffected by MSC therapy (Figure 5.10 A). Neither the percentages nor total numbers of human $CD45^+$ lymphocytes recovered from the spleens of aGvHD mice were reduced in mice which had received MSC therapy.

Although antigen presenting cells (APC) have previously been reported to be essential in the development of GvHD, recent studies have indicated that T cells are the main drivers of GvHD pathology (Li *et al.* 2012). Therefore the effect of MSC on the engraftment of $CD4^+$, $CD8^+$ and $CD4^+CD8^+$ cells was investigated. Live cells were gated for human CD45 and the expression of human $CD4^+$, $CD8^+$ or $CD4^+CD8^+$ was determined. There was no difference in the percentage of human $CD4^+$, $CD8^+$ or $CD4^+CD8^+$ populations in the spleens of aGvHD mice after MSC treatment (Figure 5.10 B). Interestingly, the total number of human $CD45^+CD4^+$ cells was significantly higher when aGvHD mice received MSC compared to mice that received PBMC alone (Figure 5.10 B). Total numbers of human $CD8^+$ and $CD4^+CD8^+$ cell populations were unaffected by MSC therapy.

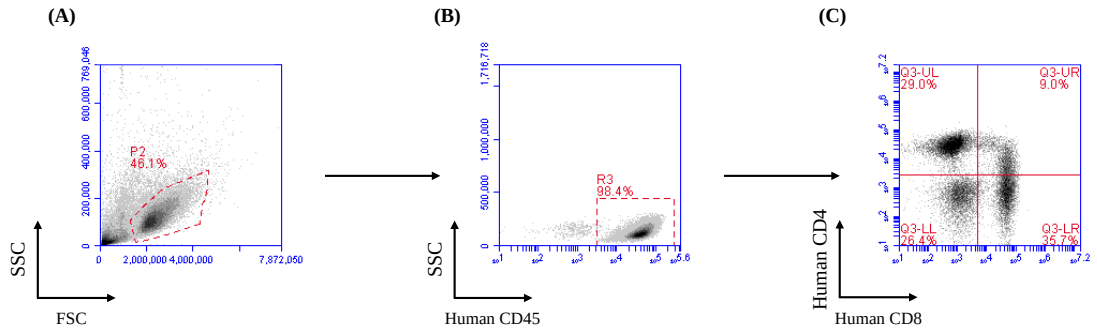

Figure 5.9: Representative example of gating strategies used to define human CD4$^+$ and CD8$^+$ T cells from the tissues of GvHD mice. (A) Illustrates the gated lymphocyte population from SSC against FSC plot, (B) represents the gating position for human CD45$^+$ (APC) expression within the CD4$^+$ lymphocyte population and (C) illustrates the gating position for CD4 (FITC) and CD8 (PE) expression within the CD45$^+$ population. All gating positions were determined using matching isotype controls.

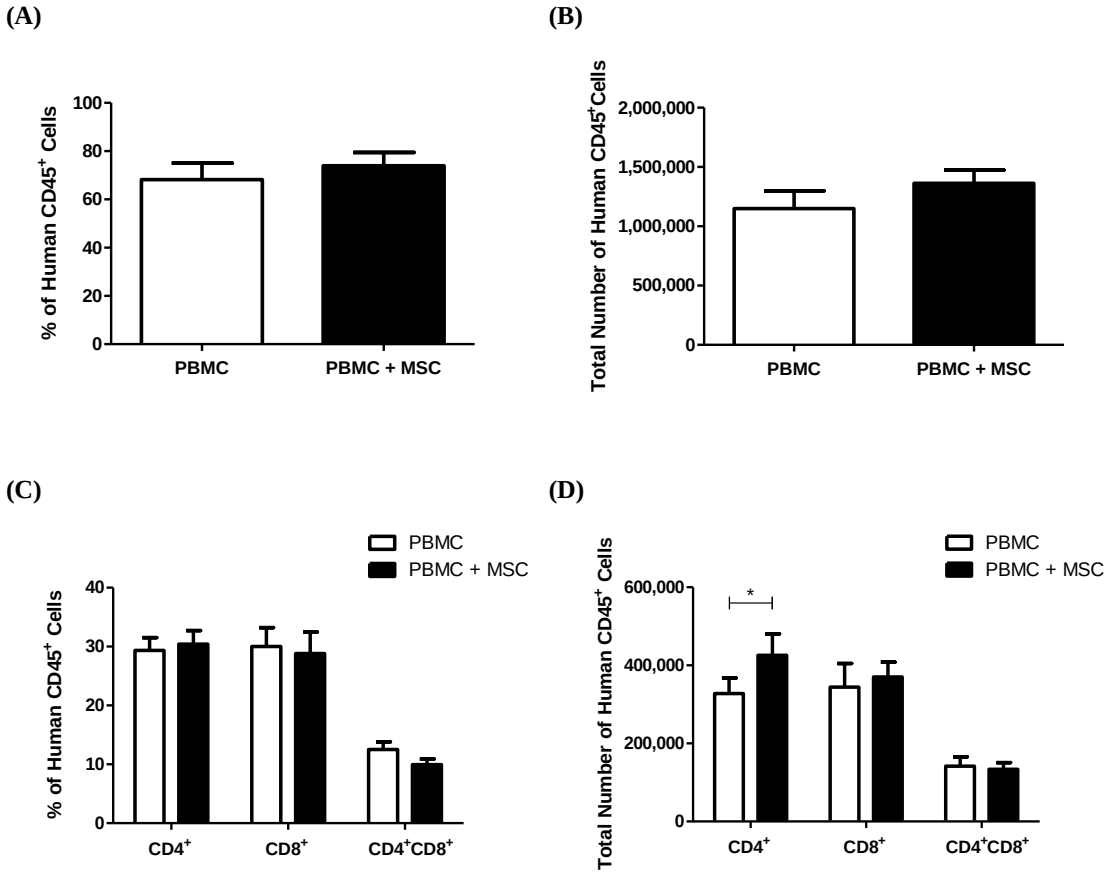

Figure 5.10. MSC did not impair the engraftment of human lymphocytes in the spleens of aGvHD mice. NSG mice which were sub-lethally irradiated (2.4 Gy) and given PBMC (8 x 10^5 per $gram^{-1}$) via tail vein injection were analysed on day 12 by flow cytometry. (A) Analysis of the percentage of human $CD45^+$ lymphocytes recovered from the spleen of aGvHD mice using 2 different PBMC donors with 2 different MSC donors (n=6 for each). (B) The total number of human $CD45^+$ lymphocytes recovered from the spleens of aGvHD mice using 2 different PBMC donors with 2 different MSC donors (n=6 for each). (C) The percentage of human $CD4^+$, $CD8^+$ or $CD4^+CD8^+$ cells recovered from the spleens of aGvHD mice using 2 different PBMC donors with 2 different MSC donors (n=6 for each). (D) The total cell number of human $CD4^+$, $CD8^+$ or $CD4^+CD8^+$ cells recovered from the spleens of aGvHD mice using 2 different PBMC donors with 2 different MSC donors (n=6 for each). Non-treated aGvHD mice are represented by white bars and aGvHD mice which received MSC therapy are represented by black bars. The total number of human lymphocytes was assessed using counting beads during flow cytometry. Statistical significance was determined using student *t*-test where * < 0.05.

5.5. HUMAN MSC THERAPY DID NOT PREVENT THE ENGRAFTMENT OF PBMC IN THE LIVER OR LUNGS OF AGVHD MICE

GvHD is characterised by the infiltration of effector lymphocytes and subsequent destruction of specific target organs including the liver and the lungs. Therefore, the ability of MSC to prevent the migration of effector T cells to these organs was identified as a possible mechanism by which they prolonged survival of aGvHD mice (Figure 5.8). To examine this hypothesis, it was necessary to develop a method of recovering comparatively pure human lymphocyte populations from the tissues of aGvHD mice. As described in detail in Chapter 2, the liver and lungs of aGvHD mice were harvested under sterile conditions and mechanically digested. Human lymphocytes were isolated using density gradient centrifugation and examined for the expression of human CD45, CD4 and CD8 by flow cytometry using the gating strategy illustrated in figure 5.9.

The administration of MSC therapy had no significant effect on the percentages or total number of human $CD45^+$, $CD4^+$, $CD8^+$ or $CD4^+CD8^+$ cells recovered from the liver of aGvHD mice, 12 days after PBMC transplantation (Figure 5.11 A & B). The engraftment of human lymphocytes in the lungs of aGvHD mice was also unaffected by the administration of MSC therapy. There was a slight increase in the total number of human $CD45^+$ and $CD4^+$ lymphocytes recovered from the lungs of aGvHD mice (Figure 5.11 C & D). However, these increases were not significant. These results suggest that MSC therapy does not impair the engraftment of human lymphocytes in the lungs or livers of aGvHD mice.

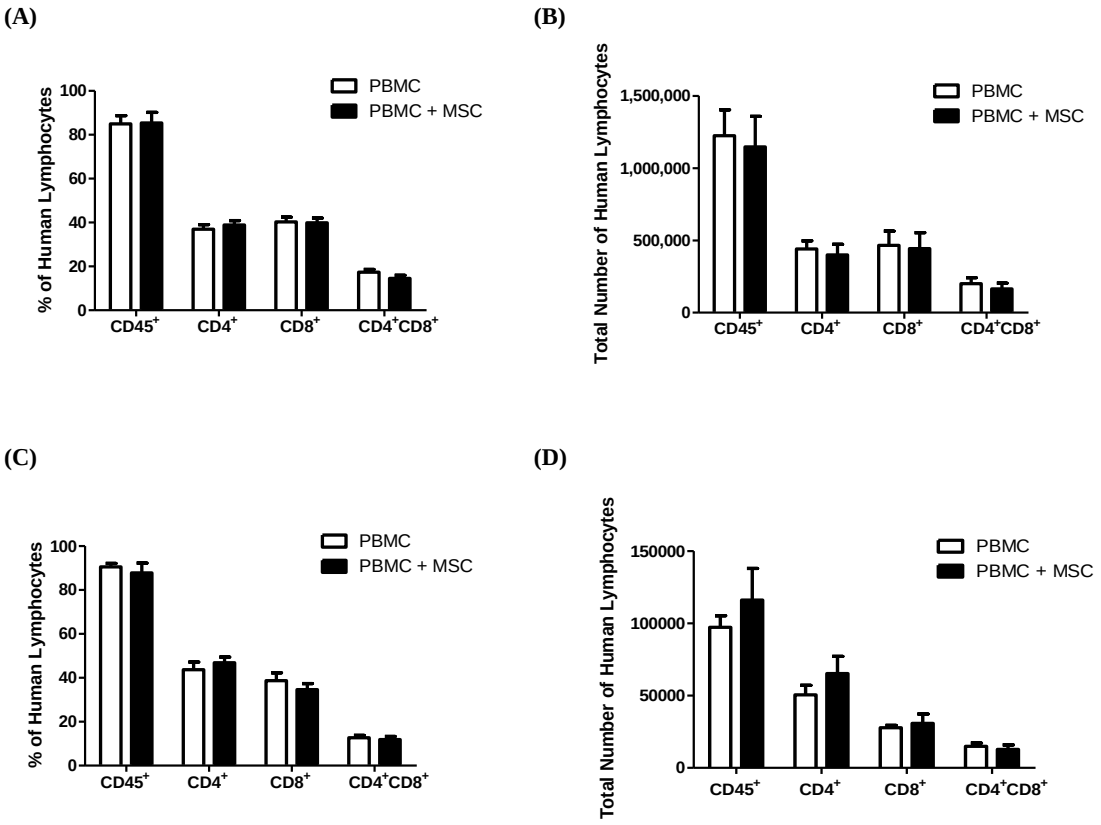

Figure 5.11. MSC did not inhibit the engraftment of human lymphocytes in the liver or lungs of aGvHD mice. NSG mice which were sub-lethally irradiated (2.4 Gy) and given PBMC (8 x 10^5 per $gram^{-1}$) via tail vein injection were analysed on day 12 by flow cytometry. (A) Analysis of the percentage of human $CD45^+$, $CD4^+$, $CD8^+$ and $CD4^+CD8^+$ lymphocytes recovered from the liver of aGvHD mice using 2 different PBMC donors with 2 different MSC donors (n=6 for each). (B) The total number of human $CD45^+$, $CD4^+$, $CD8^+$ and $CD4^+CD8^+$ lymphocytes recovered from the liver of aGvHD mice using 2 different PBMC donors with 2 different MSC donors (n=6 for each). (C) Analysis of the percentage of human $CD45^+$, $CD4^+$, $CD8^+$ and $CD4^+CD8^+$ lymphocytes recovered from the lungs of aGvHD mice using 2 different PBMC donors with 2 different MSC donors (n=6 for each). (D) The total number of human $CD45^+$, $CD4^+$, $CD8^+$ and $CD4^+CD8^+$ lymphocytes recovered from the lungs of aGvHD mice using 2 different PBMC donors with 2 different MSC donors (n=6 for each). Non-treated aGvHD mice are represented by white bars and aGvHD mice which received MSC therapy are represented by black bars. The total number of human lymphocytes were assessed using counting beads during flow cytometry.

5.6. MSC DID NOT PREVENT T CELL POLARISATION TO EFFECTOR OR MEMORY T CELL PHENOTYPES

The phenotypic characterisation of naïve, central (Tcm) and effector memory (Tem) T cell populations from post-BMT patients can provide valuable information and help to define the immunological basis of GvHD (Ali *et al.* 2012). The characterisation of these T cell sub-populations is essential in understanding the nature of the immune response associated with xenogeneic models of GvHD and may help to further understand the immune response in GvHD patients. It was hypothesised that the prolonged survival of aGvHD mice which received MSC therapy may be caused by impaired polarisation to effector T cell populations. Anti-human CD45RO, CD27 and CD62L antibodies were combined with either anti-human CD4 or CD8 antibodies to characterise naïve ($CD45RO^{-}CD27^{+}$), central memory ($CD45RO^{+}CD27^{+}CD62L^{+}$) or effector memory ($CD45RO^{+}CD27^{+}CD62L^{-}$) T cell populations within $CD4^{+}$ populations in the spleen, liver and lung. Representative example of gating strategies used to define T cell subsets from murine tissues are shown in figure 5.12.

The administration of MSC, 7 days after PBMC injection, had no effect on the presence of effector or memory T cells within the spleens (Figure 5.13 A & B), livers (Figure 5.13 C & D) or lungs (Figure 5.13 E & F) of aGvHD mice. The percentages and total numbers of naïve, Tcm and Tem human $CD4^{+}$ cells were unaffected by the administration of MSC therapy in each of the organs tested. These results suggest that the increased survival observed in MSC treated aGvHD mice was not mediated by preventing the development of $CD4^{+}$ Tem or the ability of these cells to migrate to target organs.

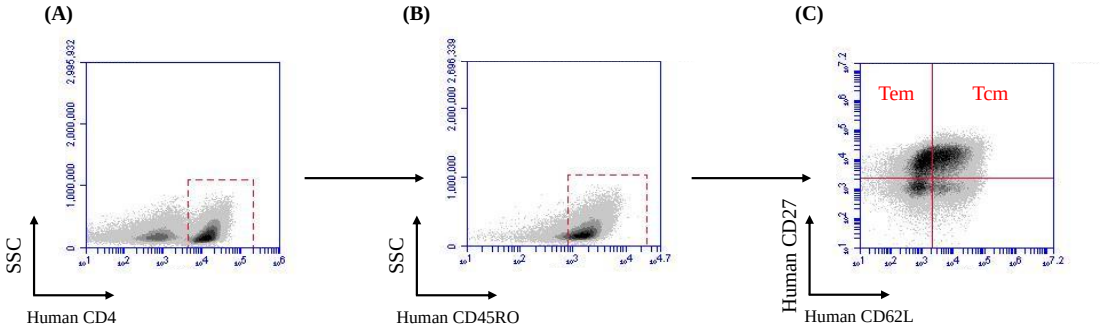

Figure 5.12: Representative example of gating strategies used to define human Tem and Tcm subsets from the tissues of aGvHD mice. (a) illustrates the gating position for human $CD4^+$ (PercP) expression, (b) represents the gating position for human $CD45RO^+$ (APC) expression within the $CD4^+$ population and (c) illustrates the gating position for CD27 (FITC) and CD62L (PE) expression within the $CD4^+CD45RO^+$ population. All gating positions were determined using matching isotype controls.

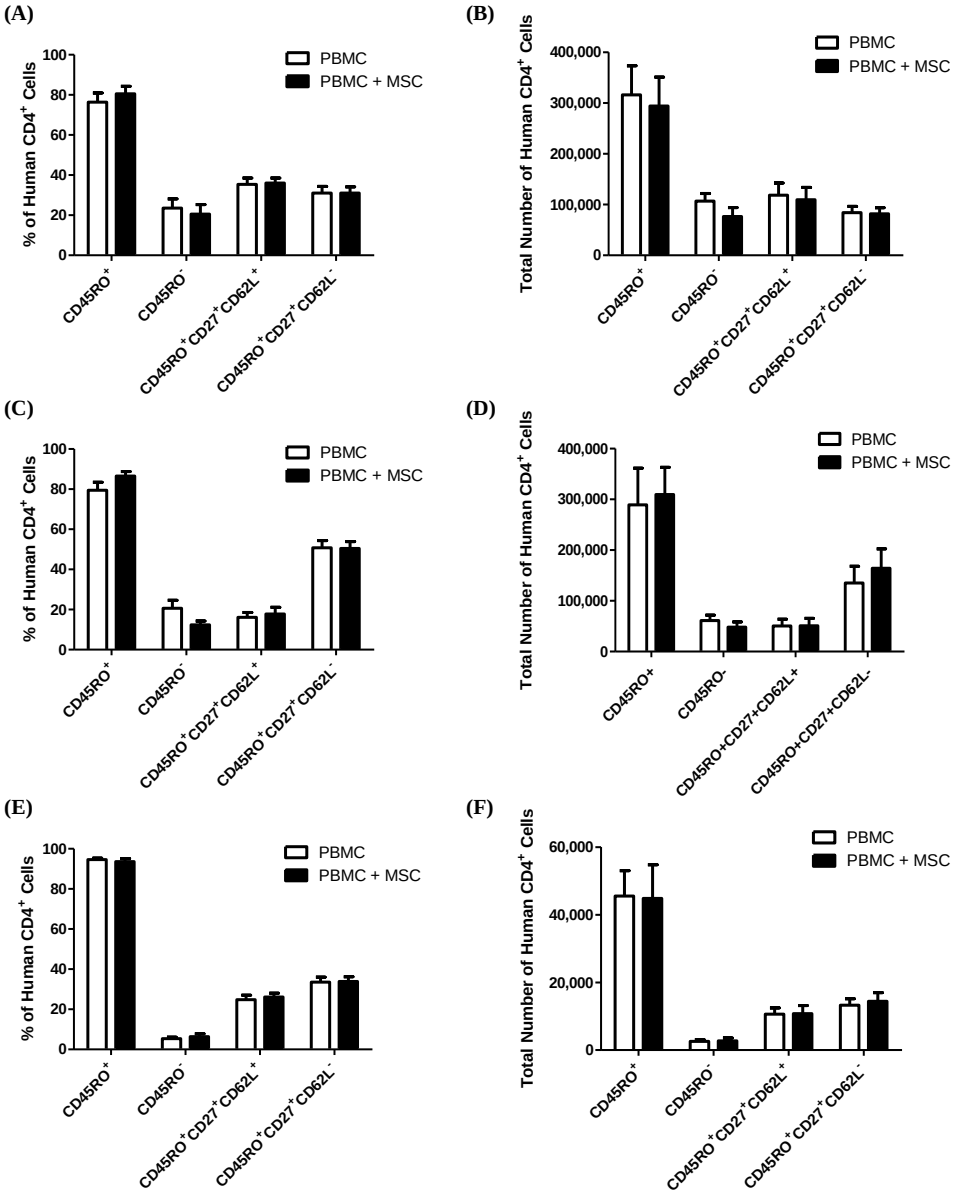

Figure 5.13. MSC do not reduce the percentage or number of activated (CD45RO$^+$), naïve (CD45RO$^-$), Tem (CD45RO$^+$CD27$^+$) and Tcm (CD45RO$^+$CD27$^+$CD62L$^+$) human CD4$^+$ T cells in acute GvHD mice. NSG mice which were sub-lethally irradiated (2.4 Gy) and given PBMC (8 x 10^5 per gram^{-1}) via tail vein injection were analysed on day 12 by flow cytometry. Graphical representation of the percentage of activated, naïve, Tem and Tcm CD4$^+$ cells recovered from the spleen (A), livers (C) and lungs (E) of non-treated aGvHD mice (white bar) or aGvHD mice which received MSC therapy (black bar). Accumulated data illustrating the total number of activated, naïve, Tem and Tcm CD4$^+$ cells recovered from the spleen (B), livers (D) and lungs (F) of non-treated aGvHD mice or aGvHD mice which received MSC therapy. n=6 per group (2 PBMC donors with 2 MSC donors). The total number of human CD45+ lymphocytes was assessed using counting beads via flow cytometry.

5.7. MSC THERAPY DID NOT REDUCE LEVELS OF PRO-INFLAMMATORY CYTOKINES IL-2, IFN-γ OR IL-1 IN AGVHD MICE

Acute GvHD is a systemic disorder driven by the recognition of patient HLA by the transplanted graft. One of the key drivers of pathology is the production of pro-inflammatory cytokines such as IL-1β, IFN-γ and IL-2. Therefore, it was hypothesised that the reduced mortality observed in aGvHD mice which received human MSC (Figure 5.8) may be a result of impaired human IL-2, IFN-γ or IL-1β production by human T cells after MSC therapy. The levels of circulating human IFN-γ, IL-2 and IL-1β were analysed from serum samples obtained through facial bleeds taken from aGvHD mice 12 days after transplantation and analysed by bead array cytokine assay or ELISA. The ability of human $CD4^+$ and $CD8^+$ T cells to produce IFN-γ or IL-2 was also determined using intra-cellular cytokine staining and analysed by flow cytometry.

Contrary to the hypothesis, the administration of human MSC to aGvHD mice had no effect on the serum levels of human IL-1β on day 12, as measured by ELISA (Figure 5.14). MSC therapy, administered 7 days after PBMC administration, did not reduce the levels of circulating human IL-1β when compared to aGvHD mice which received no cell therapy (Figure 5.14).

Surprisingly, aGvHD mice which received human MSC therapy on day 7 had enhanced serum levels of human IFN-γ compared to aGvHD mice which did not receive MSC (Figure 5.15 A). In fact the total number of IFN-γ producing $CD4^+$ cells in the spleen of aGvHD mice was slightly increased after MSC therapy (Figure 5.15 B); however the total number of $CD8^+$ T cells producing IFN-γ was significantly lowered after MSC administration (Figure 5.15 C).

The level of circulating IL-2 was also unaffected by the administration of human MSC therapy when compared to non-treated aGvHD (Figure 5.16 A). MSC therapy

resulted in a slight increase in the total number of human IL-2 producing $CD4^+$ and $CD8^+$ T cells recovered from the spleens of aGvHD mice (Figure 5.16 B & C). However, these increases were not significant.

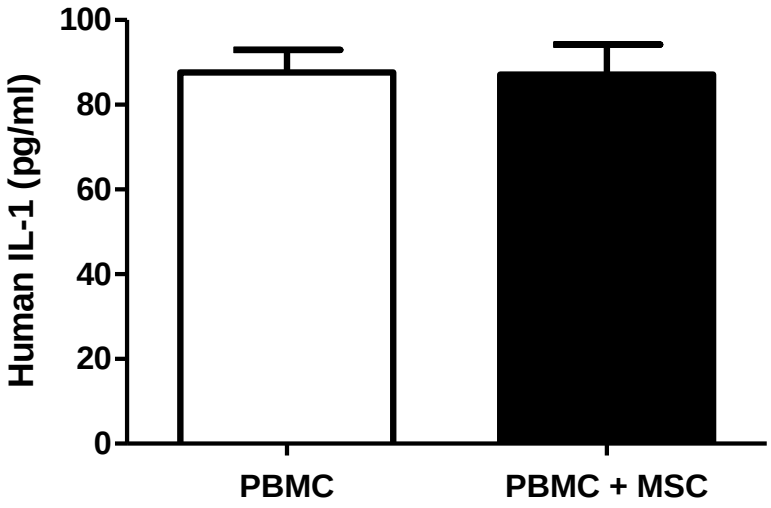

Figure 5.14. Human MSC therapy had no effect on levels of human IL-1β in the serum of aGvHD mice. NSG mice which were sub-lethally irradiated (2.4 Gy) and given PBMC (8 x 10^5 $gram^{-1}$) via tail vein injection. On day 12, post transplantation, facial bleeds were performed on PBS control mice (not detected), aGvHD mice (white bar) and aGvHD mice which received MSC therapy (black bar) and the presence of human IL-1β was determined using ELISA. n=20 per group (4 PBMC donors). Statistical significance was analysed using Student *t* test.

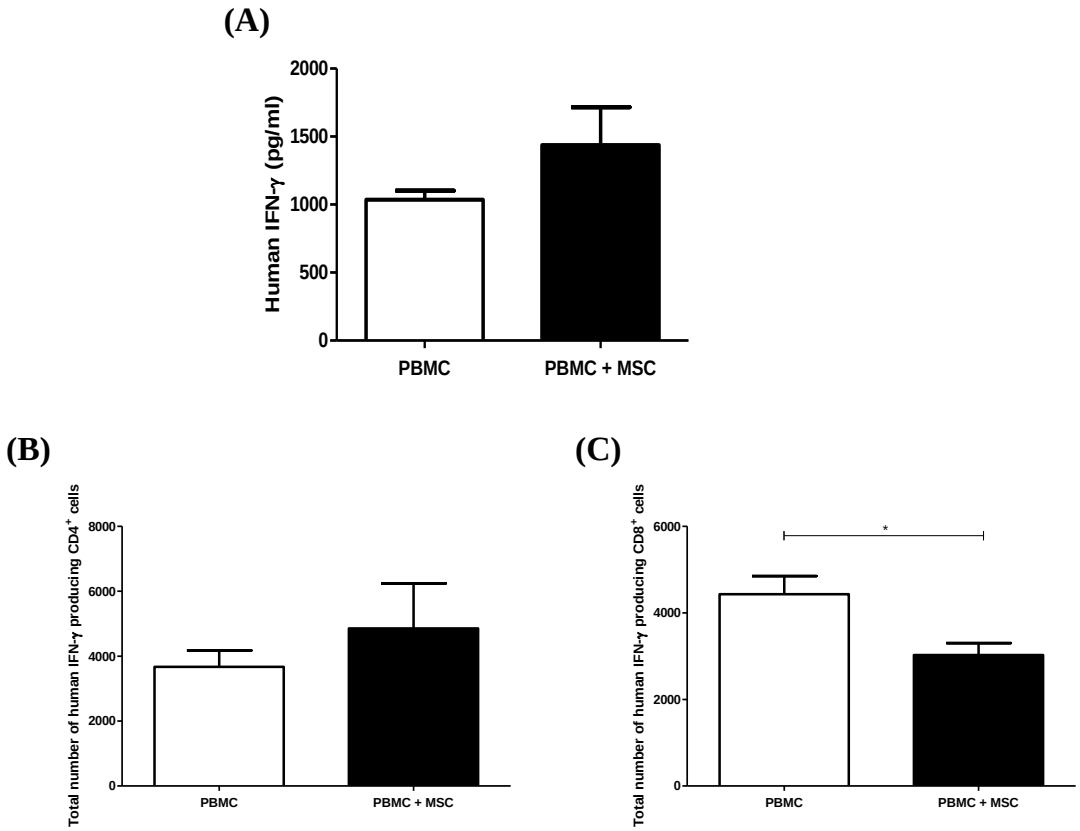

Figure 5.15. Human MSC therapy did not reduce the levels of IFN-γ in the serum of aGvHD mice. NSG mice which were sub-lethally irradiated (2.4 Gy) and given PBMC (8 x 10^5 $gram^{-1}$) via tail vein injection. On day 12, post transplantation, facial bleeds were performed on PBS control mice (not detected), aGvHD mice (white bar) and aGvHD mice which received MSC therapy (black bar). (A) The total level of circulating human IFN-γ was analysed in the serum of aGvHD mice using ELISA. n=20 per group (4 PBMC donors). The total number of human IFN-γ producing $CD4^+$ (B) and $CD8^+$ (C) T cells was determined from the spleens of aGvHD by intra-cellular flow cytometry. n=4 for (B) and (C). Statistical significance was analysed using student *t*-test where * < 0.05.

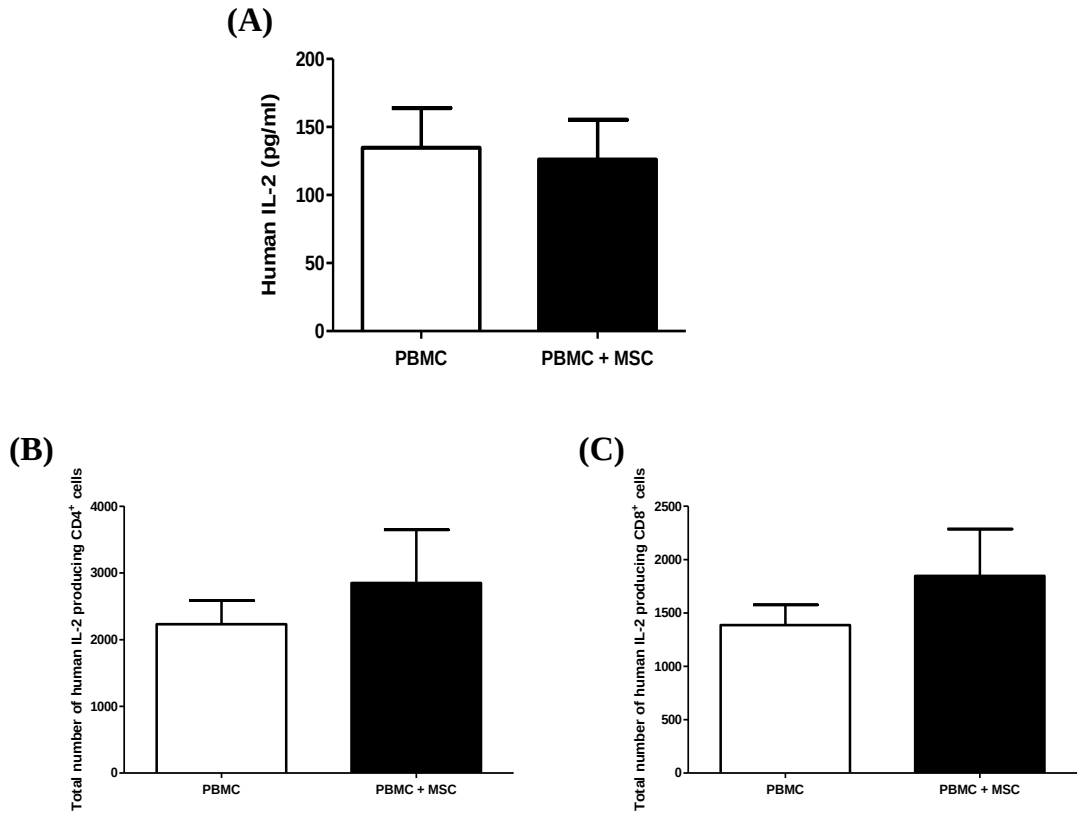

Figure 5.16. Human MSC therapy did not reduce the levels of IL-2 in the serum of aGvHD mice. NSG mice which were sub-lethally irradiated (2.4 Gy) and given PBMC (8 x 10^5 $gram^{-1}$) via tail vein injection. On day 12, post transplantation, facial bleeds were performed on PBS control mice (not detected), aGvHD mice (white bar) and aGvHD mice which received MSC therapy (black bar). (A) The total level of circulating human IL-2 was analysed in the serum of aGvHD mice using ELISA. n=20 per group (4 PBMC donors). The total number of human IL-2 producing $CD4^+$ (B) and $CD8^+$ (C) T cells was determined from the spleens of aGvHD by intra-cellular flow cytometry. n=4 for (B) and (C). Statistical significance was analysed using student *t*-test.

5.8. MSC SIGNIFICANTLY REDUCED TNF-α PRODUCING T CELLS

The role of TNF-α as one of the main drivers of pathogenesis in aGvHD has been well characterised (Ferrara *et al.* 2009). The ability of human MSC to prevent the development of human TNF-α producing $CD4^+$ and $CD8^+$ T cells during aGvHD was analysed in the spleens of aGvHD mice using intra-cellular flow cytometry. The effect of MSC therapy on the ability of human TNF-α producing T cells to engraft in the liver or lungs of aGvHD mice was also investigated.

Human $CD4^+$ and $CD8^+$ T cells were recovered from the spleens of both MSC treated and non-treated aGvHD mice 12 days after PBMC administration. The potential for TNF-α production was investigated in these cells via intra-cellular flow cytometry. As hypothesised, MSC therapy significantly reduced the total number of human TNF-α producing $CD4^+$ and $CD8^+$ T cells in the spleens of aGvHD mice (Figure 5.17 B). In addition to this, the ability of human TNF-α producing T cells within the liver and lungs of aGvHD mice was also investigated. As hypothesised, human TNF-α producing $CD4^+$ and $CD8^+$ T cells were observed in both the liver and lungs of aGvHD mice. Interestingly, the administration of human MSC therapy significantly reduced the total number of TNF-α producing $CD4^+$ and $CD8^+$ T cells in the lungs, but not the liver of aGvHD mice (Figure 5.18). These results suggest that MSC therapy protection against mortality in aGvHD mice may involve the reduction of TNF-α production.

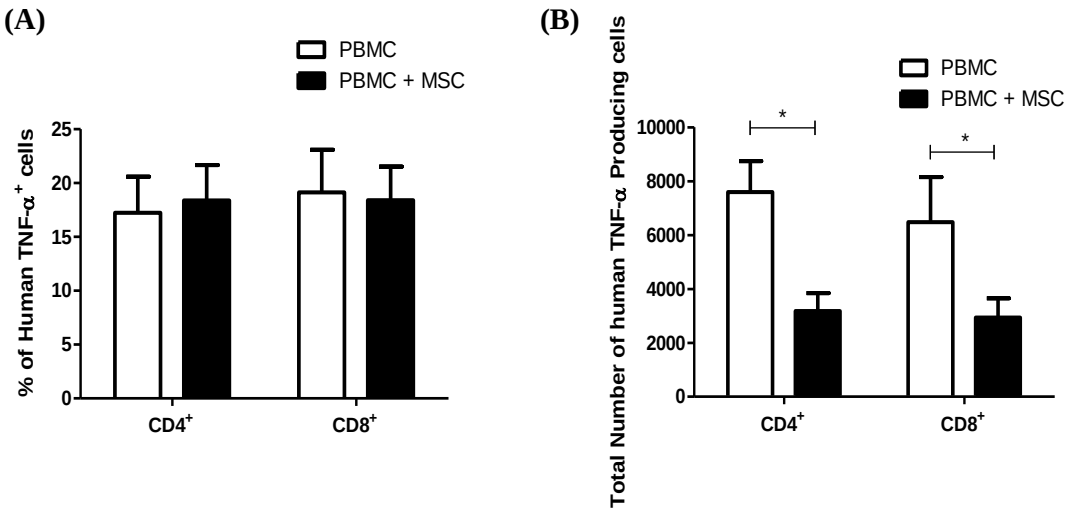

Figure 5.17. MSC significantly reduced the total number of human TNF-α producing $CD4^+$ and $CD8^+$ T cells in the spleens of aGvHD mice. NSG mice were sub-lethally irradiated (2.4 Gy) and given PBMC ($8x10^5$ $gram^{-1}$) via tail vein injection were analysed on day 12 by intra-cellular flow cytometry. Graphical representation of the percentage of human TNF-α, producing $CD4^+$ T and $CD8^+$ T cells recovered from the spleen (A). Accumulated data for total cell number of human TNF-α producing $CD4^+$ T and $CD8^+$ T cells recovered from the spleen (B). n=6 per group (2 PBMC donor with 2 MSC donors). White bars represent non-treated aGvHD mice while black bars represent aGvHD mice which have received MSC therapy. The total number of human lymphocytes was assessed using counting beads during flow cytometry. Statistical significance was determined using student *t*-test where * < 0.05.

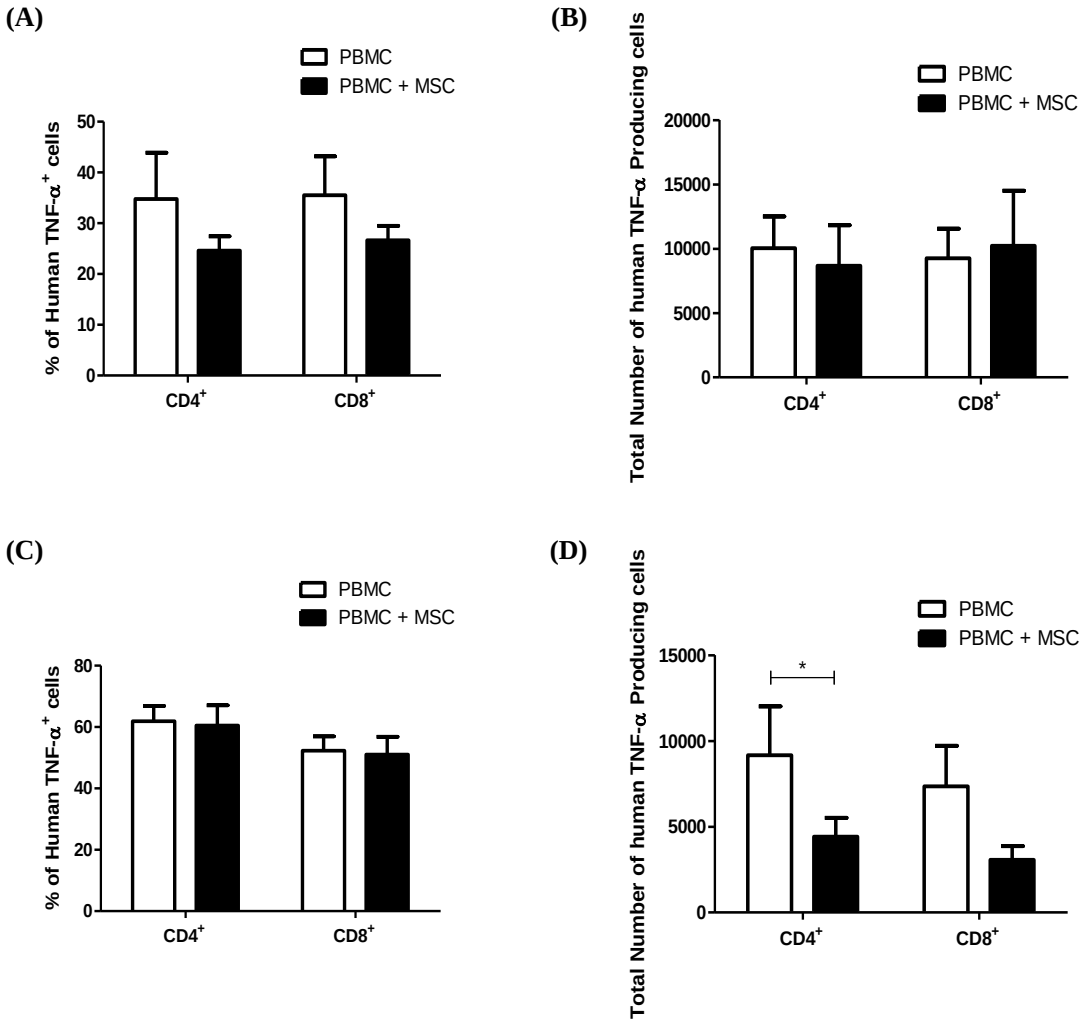

Figure 5.18. MSC reduced the total number of TNF-α producing CD4$^+$ and CD8$^+$ T cells in the livers and lungs of aGvHD mice. NSG mice were sub-lethally irradiated (2.4 Gy) and given PBMC ($8x10^5$ gram^{-1}) via tail vein injection were analysed on day 12 by intra-cellular flow cytometry. Graphical representation of the percentage of human TNF-α, producing CD4$^+$ T and CD8$^+$ T cells recovered from the liver (A) and the lungs (C) of aGvHD mice. Accumulated data for total cell number of human TNF-α producing CD4$^+$ T and CD8$^+$ T cells recovered from the liver (B) and lungs (D) of aGvHD mice. n=6 per group (2 PBMC donor with 2 MSC donors). White bars represent non-treated aGvHD mice while black bars represent aGvHD mice which have received MSC therapy. The total number of human lymphocytes was assessed using counting beads during flow cytometry. Statistical significance was determined using student *t*-test where * < 0.05.

5.9. MSC THERAPY SIGNIFICANTLY INCREASED REGULATORY T CELLS DURING AGVHD

Regulatory T cells (Treg) are potent regulators of the immune system and their potential to control aGvHD is one of the main methods of treatment currently being investigated. Previous work from our research group had published that Treg cells did not engraft in the NSG model of aGvHD (Tobin *et al.* 2013). However, the work carried out in the present study utilised a more sensitive method of recovering human lymphocytes from murine tissue. This resulted in a purer cell population with less non-specific background which allowed the detection of human Treg cells in the spleens, livers and lungs of aGvHD mice. Therefore the ability for human MSC therapy to modulate Treg cells during aGvHD was investigated under the hypothesis that MSC increase the survival of aGvHD in part due to the induction, expansion or maintenance of Treg cells.

MSC treated and non-treated aGvHD mice were sacrificed on day 12 and the spleens, lungs and livers harvested under sterile conditions. Human Treg cells were defined as human $CD4^{+}CD25^{+}FoxP3^{+}$ and determined by intra-cellular flow cytometry. Very small populations of Treg cells were recovered from the spleens of GvHD mice which had not received MSC therapy; however the administration of human MSC on day 7 resulted in a significant increase in the total number of Treg cells recovered from the spleen of aGvHD mice (Figure 5.19 B). Interestingly, the total number of human Treg cells was also significantly increased in the lungs and livers of aGvHD mice which received human MSC therapy (Figure 5.19 D & F). These results suggest that MSC therapy results in increased Treg cells during aGvHD and that these Treg cells are capable of engrafting within areas of inflammation associated with GvHD.

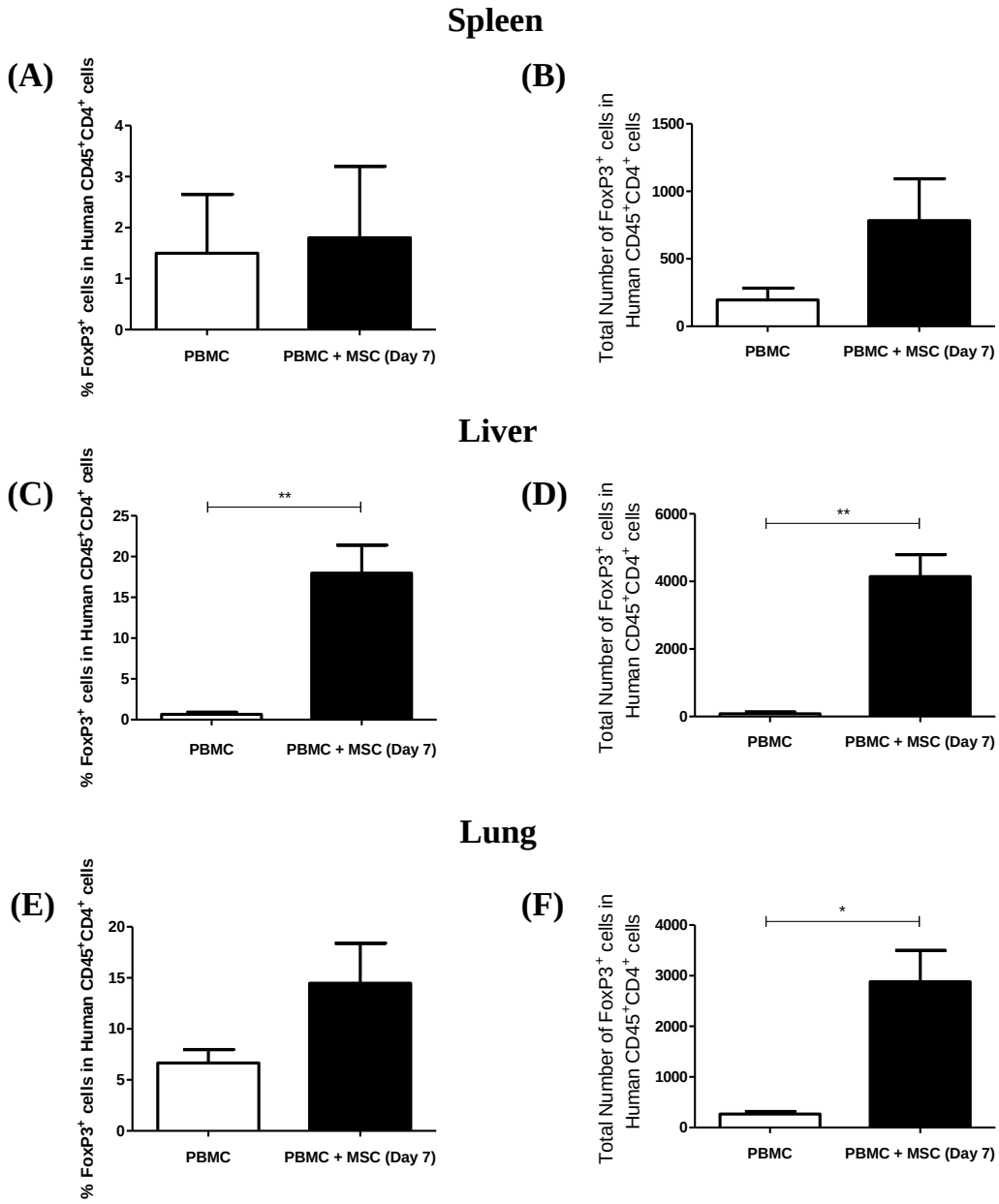

Figure 5.19. MSC therapy significantly increased the number of Treg cells during aGvHD. NSG mice were sub-lethally irradiated (2.4 Gy) and given PBMC (8×10^5 gram^{-1}) via tail vein injection were analysed on day 12 by intra-cellular flow cytometry. Graphical representation of the Treg cells recovered from the spleen (A), liver (C) and lung (E) from non-treated aGvHD mice (white bar) or aGvHD mice which received MSC therapy (black bar) mice. Accumulated data for total cell number of Treg cells recovered from the spleen (B), liver (D) and lung (F). n=6 per group (2 PBMC donor with 2 MSC donors). The total number of human lymphocytes was assessed using counting beads during flow cytometry. Statistical significance was determined using student *t*-test where * < 0.05, ** <0.005.

5.10. MSC PRESERVE REGULATORY T CELLS RATHER THAN INDUCE OR ENHANCE THEM *IN VITRO*

Treg cells are potent mediators of the immune response and the significant increase in the number of Treg cells observed after MSC therapy offers a potential mechanism by which MSC therapy prolongs survival in aGvHD mice. However, the mechanism behind how MSC generate Treg cells remains a contentious issue. A number of *in vitro* experiments were designed to try to shed some light on how MSC increase Treg cells *in vivo*. Some research groups have published data suggesting that MSC can directly induce the polarisation of naïve $CD4^+$ T cells into Treg cells. Other research groups, including our own, have published data which suggests that MSC do not induce but expand resident Treg populations. However, a third method by which MSC generate Treg cells may be by promoting the survival of resident Treg populations. To determine whether MSC induced or expanded Treg populations, PBMC were isolated from buffy-packs and sorted into $CD4^+CD25^+$ or $CD4^+CD25^-$ populations using a BD FACS Aria cell sorter under the premise that resident Treg cells should be contained in the $CD4^+CD25^+$ T cell population. Both populations of cells were then cultured with or without MSC for 72 hours and the presence of Treg cells was then analysed by flow cytometry. Treg cells were defined as $CD4^+CD25^+FoxP3^+$ cells.

The number of $CD4^+CD25^+FoxP3^+$ cells recovered from the $CD4^+CD25^-$ population after 72 hours was very low and culturing $CD4^+CD25^-$ cells in the presence of MSC did not increase the number of $CD4^+CD25^+FoxP3^+$ cells (Figure 5.20). This result suggests that MSC were not capable of inducing Treg populations from $CD4^+CD25^-$ cell populations. After 72 hours, the number of $CD4^+CD25^+FoxP3^+$ cells recovered from the $CD4^+CD25^+$ population was much higher. In addition, culturing $CD4^+CD25^+$ cells in the

presence of MSC enhanced the total number of $CD4^+CD25^+FoxP3^+$ cells (Figure 5.20). These results suggested that MSC were not capable of inducing Treg populations but this approach in isolation could not distinguish whether MSC were enhancing or preserving the residual Treg population. Therefore, the proliferation marker KI-67 was used to determine whether Treg cells were actively expanding when cultured in the presence of MSC (Figure 5.21). For this experiment, $CD4^+$ T cells were isolated from whole PBMC using MACS beads (Miltenyi Biotec). Isolated $CD4^+$ T cells were then cultured with or without MSC for 72 hours. Treg cells were defined as $CD4^+CD25^+FoxP3^+$ cells and the proliferation marker KI-67 was used to distinguish expanding cells from resting cells. As expected isolated $CD4^+$ T cells cultured without stimulus did not express the proliferation marker KI-67 after 72 hours (Figure 5.22 B). When $CD4^+$ T cells were cultured in the presence of MSC there was indeed a significant increase in the total number of Treg cells compared to $CD4^+$ T cells cultured alone (Figure 5.22 A); however Treg cells cultured in the presence of MSC did not express the proliferation marker KI-67 (Figure 5.22 C & D). Taken together, these results suggest that MSC did not induce or expand Treg populations and that the increase in number of Treg cells was due to MSC preserving the original Treg population.

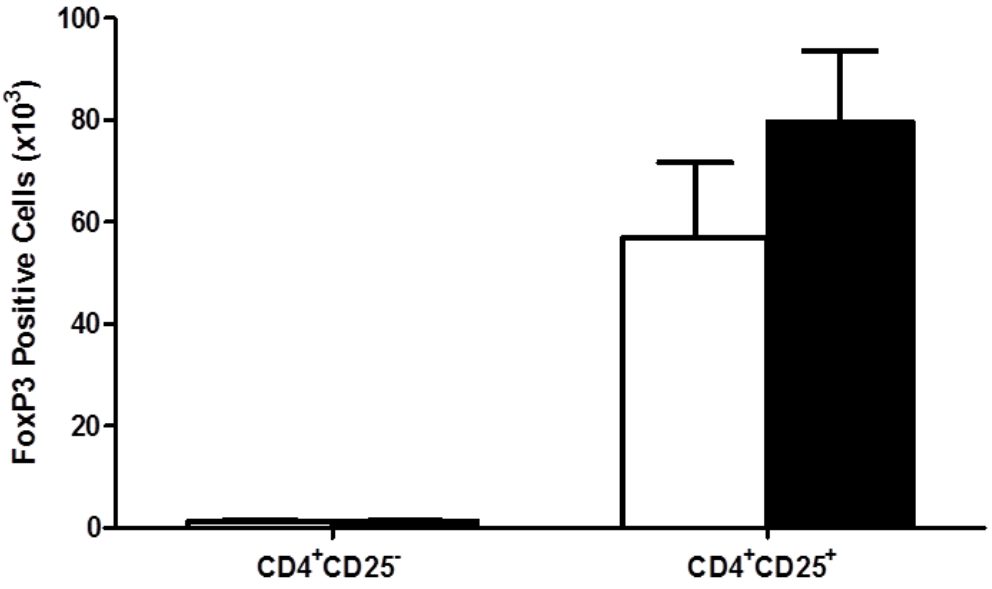

Figure 5.20. MSC did not induce Treg cells from $CD4^+CD25^-$ populations. PBMC were isolated from buffy packs and sorted into $CD4^+CD25^-$ or $CD4^+CD25^+$ populations using FACS Aria cell sorter. $CD4^+CD25^-$ or $CD4^+CD25^+$ cells were cultured in the presence or absence of MSC (3 PBMC: 1 MSC) for 72 hours. The total number of Treg cells was determined using flow cytometry. n=4 PBMC donors with 2 MSC donors. White bars represent T cell populations cultured alone while black bars represent T cell populations cultured in the presence of human MSC. The total number of human lymphocytes was assessed using counting beads during flow cytometry.

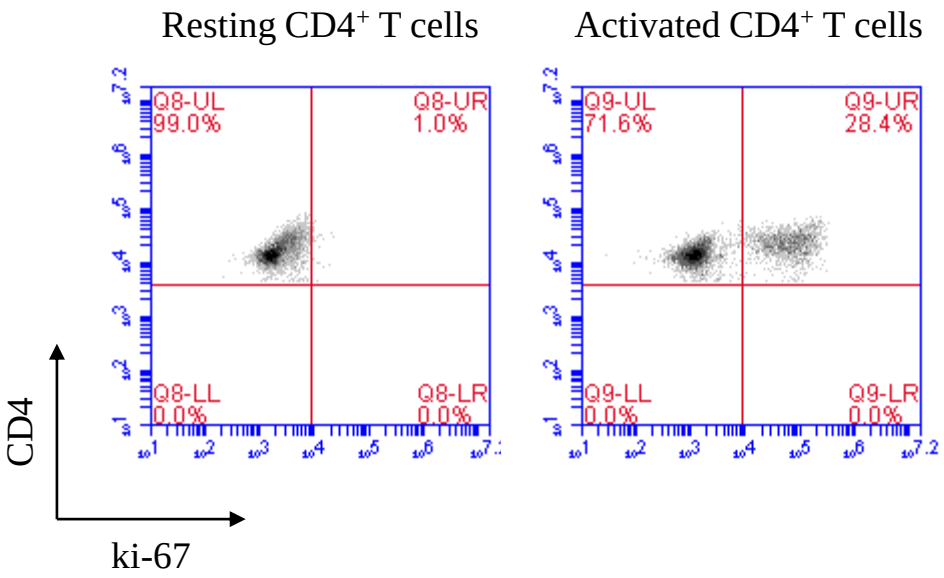

Figure 5.21. Representative image of KI-67 antibody optimisation. PBMC were isolated from buffy packs and $CD4^+$ T cells were purified using MACS beads. $CD4^+$ T cells were cultured in the presence or absence of T cell activating beads and the expression of KI-67 was determined using flow cytometry.

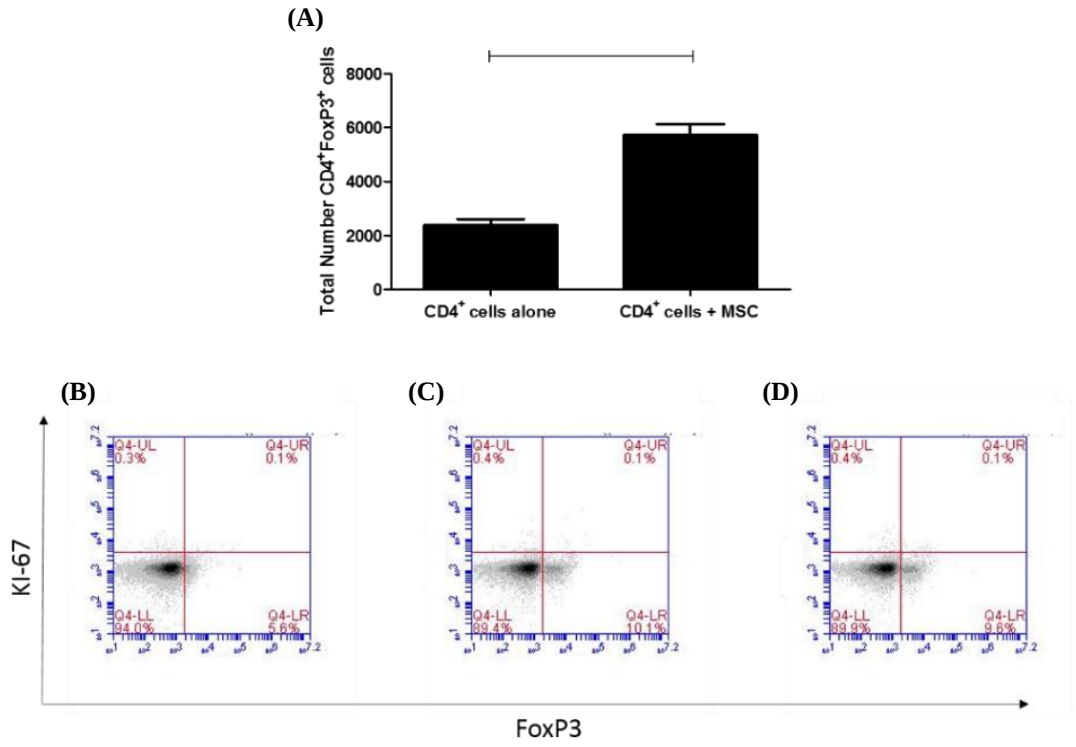

Figure 5.22. MSC co-culture did not result in the expansion of Treg cells. PBMC were isolated from buffy packs and $CD4^+$ T cells were purified using MACS beads. $CD4^+$ T cells were cultured in the presence or absence of MSC (3 PBMC: 1 MSC) for 72 hours. (A) The total number of Treg cells recovered from co-culture was determined using flow cytometry. Treg cells were characterised as CD4+CD25+FoxP3+ and the expression of KI-67 was determined on $CD4^+$ T cells alone (B) and CD4+ T cells co-cultured with two different MSC donors (C) and (D). n=4 per group (2 PBMC donor with 2 MSC donors). The total number of human lymphocytes was assessed using counting beads during flow cytometry. Statistical significance was determined using student *t*-test where * < 0.05.

5.11. MSC INCREASED iNKT CELL POPULATIONS DURING aGvHD

Invariant natural killer T (iNKT) cells are a very rare auto-reactive CD1d restricted T cell sub-population characterised by the expression of an invariant T cell receptor alpha chain (Vα24^{-}Jα18) (Montoya *et al.* 2007). The ability of iNKT cells to modulate their micro-environment and interact with a wide range of immune cells has resulted in their association with a number of diseases including aGvHD (Schneidawind *et al.* 2014). Recent analysis of patient data has suggested that the post-transplant recovery of iNKT cells correlates with a lower risk of aGvHD development (Rubio *et al.* 2012). Therefore it was hypothesised that the administration of human MSC therapy resulted in increased engraftment of iNKT cells during aGvHD. To examine this hypothesis, aGvHD mice were sacrificed on day 12 and the spleens, livers and lungs were harvested under sterile conditions. Human lymphocytes were isolated as described in section 2 and iNKT cells were characterised as human CD3^{+}Vα24^{-}Jα18^{+} by flow cytometry.

The administration of human MSC therapy resulted in a significantly higher percentage of human CD3^{+}Vα24^{-}Jα18^{+} lymphocytes in the spleens of aGvHD mice. There was no difference in the percentage of human CD3^{+}Vα24^{-}Jα18^{+} recovered from the livers of aGvHD after MSC therapy; however the percentage of human CD3^{+}Vα24^{-}Jα18^{+} cells was significantly increased in the spleens of aGvHD mice which received MSC therapy (Figure 5.23 A). There was also a slight, but not significant, increase in the percentage of human CD3^{+}Vα24^{-}Jα18^{+} cells recovered from the lungs of aGvHD mice which received MSC therapy (Figure 5.23 C). These results suggest that human MSC therapy may have a beneficial effect on the post-transplant engraftment of donor iNKT cells in the spleen.

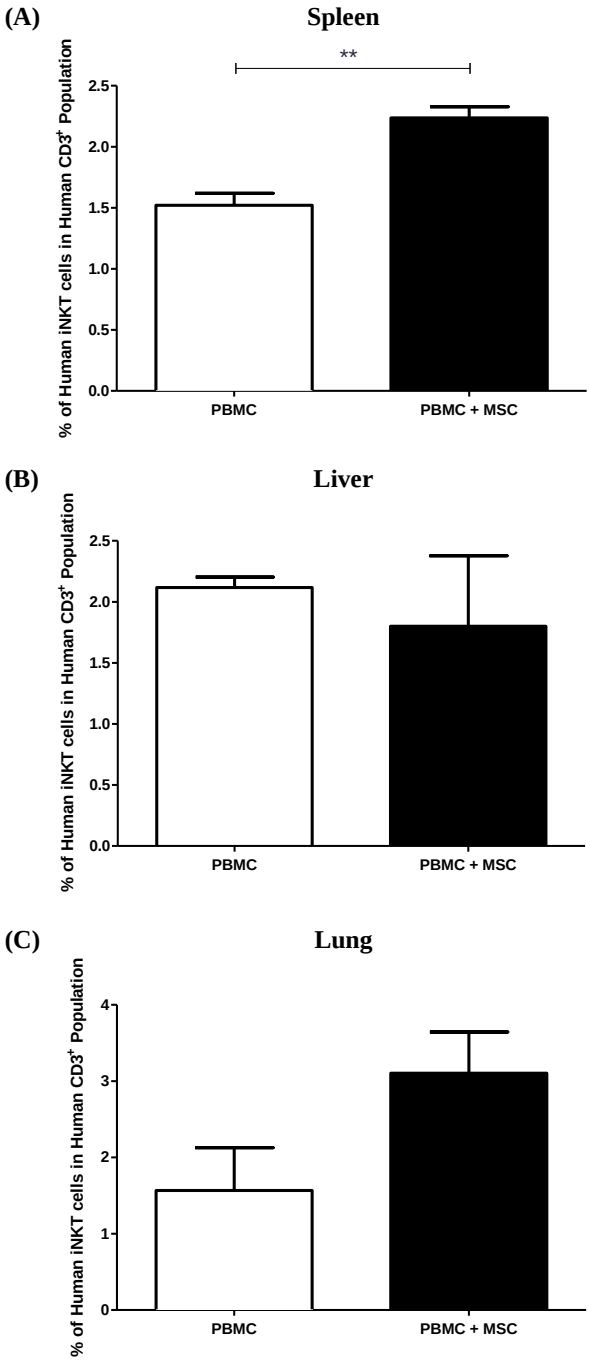

Figure 5.23. MSC therapy resulted in increased iNKT populations during aGvHD. NSG mice which were sub-lethally irradiated (2.4 Gy) and given PBMC (8 x 10^5 per gram^{-1}) via tail vein injection were analysed on day 12 by flow cytometry. iNKT cells were characterised as CD3+Vα24$^-$Jα18$^+$ using flow cytometry. Graphical representation of the percentage of iNKT cells recovered from the spleen (A), livers (B) and lungs (C) of non-treated aGvHD mice (white bar) or aGvHD mice which received MSC therapy (black bar). n=4 per group (2 PBMC donors with 1 MSC donors). The total number of human lymphocytes was assessed using counting beads via flow cytometry. Statistical significance was determined using student *t*-test where ** < 0.01.

5.12. THE ADMINISTRATION OF IFN-γ STIMULATED MSC ON DAY 7 DID NOT FURTHER IMPROVE SURVIVAL OF AGVHD MICE COMPARED TO THE ADMINISTRATION OF RESTING MSC.

As mentioned before, previous research from our laboratory has demonstrated that the administration of IFN-γ stimulated MSC (γMSC) on day 0 resulted in increased survival and reduced pathology of aGvHD mice while the administration of resting MSC on day 0 did not protect against aGvHD. Therefore this study investigated whether administering γMSC on day 7 would demonstrate increased efficacy compared to resting MSC.

NSG mice were irradiated and PBMC were administered as before. MSC or γMSC therapies were then administered 7 days later and the survival and weight loss of mice was monitored (Figure 5.24). NSG mice which received human MSC demonstrated significantly higher survival and lower weight loss compared to non-treated mice. Mice which received γMSC therapy also demonstrated significantly higher survival and lower weight loss than non-treated mice (Figure 5.25). However, the use of γMSC therapy did not significantly prolong survival or prevent weight loss compared to resting MSC therapy (Figure 5.25).

As previously demonstrated, the administration of human MSC therapy on day 7 did not reduce T cell engraftment within GvHD mice. However, γMSC are more potent regulators of T cell proliferation and therefore the effect of γMSC, on day 7, on T cell engraftment in target organs was also investigated. The administration of resting MSC therapy on day 7 did not inhibit T cell engraftment as measured by the total number of $CD4^+$ and $CD8^+$ cells recovered from the spleens of GvHD mice (Figure 5.26 A). γMSC therapy on day 7 also did not inhibit the engraftment of $CD4^+$ or $CD8^+$ T cells in the spleens of GvHD mice (Figure 5.26 A). The ability of γMSC to prevent the migration of

$CD4^+$ or $CD8^+$ T cells to the lungs and livers of GvHD mice was not affected by the administration of resting MSC. The ability of γMSC to prevent the engraftment of $CD4^+$ or $CD8^+$ T cells within the livers and lungs of GvHD mice was subsequently investigated. The numbers of $CD4^+$, $CD8^+$ or $CD4^+CD8^+$ cells recovered from the livers of GvHD mice were not significantly reduced by the administration of either resting MSC or γMSC on day 7 (Figure 5.26 B). In contrast to the hypothesis, the administration of MSC and γMSC had increased the amount of cells infiltrating the lungs of aGvHD mice (Figure 5.26 C).

The ability of γMSC to reduce the TNF-α production by human $CD4^+$ and $CD8^+$ T cells during aGvHD was analysed by intra-cellular flow cytometry. GvHD mice were sacrificed on day 12 and spleens, livers and lungs were harvested under sterile conditions. Human cells were recovered from the tissues and the number of human TNF-α producing $CD4^+$ and $CD8^+$ T cells were determined by flow cytometry. The administration of resting MSC resulted in a significant decrease in the number of human TNF-α producing $CD4^+$ and $CD8^+$ T cells found in the spleen, liver and lungs of GvHD mice (Figure 5.27). While the administration of γMSC also resulted in significant reductions in human TNF-α producing cells in comparison to non-treated GvHD mice, the numbers of human TNF-α producing cells were not lower than observed when resting MSC therapy was used (Figure 5.27).

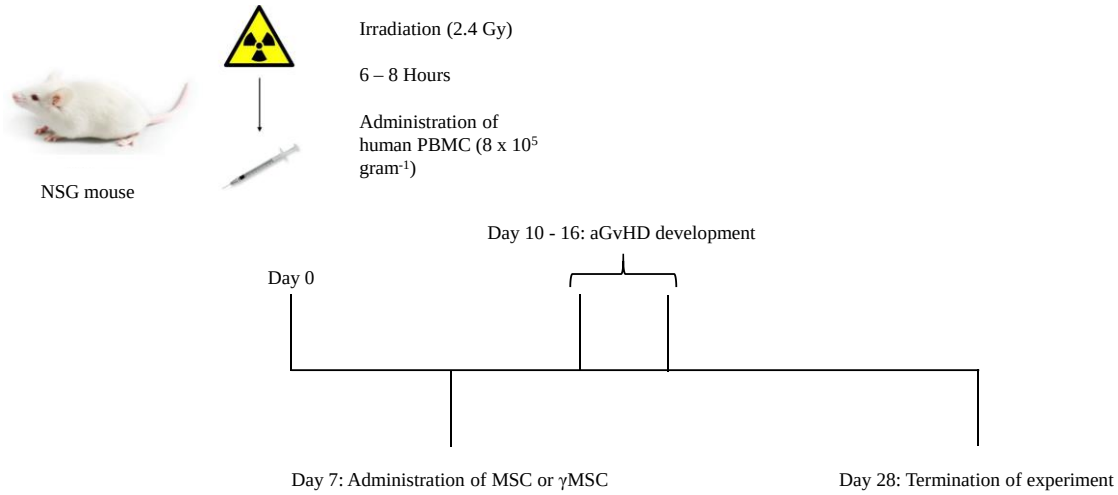

Figure 5.24. Development of a humanised mouse model of aGvHD to compare MSC and γMSC therapies. NOD-SCID IL-2rγ^{null} (NSG) mice were exposed to a sub-lethal dose of gamma irradiation (2.4 Gy). 8 x 10^5 PBMC gram^{-1} or sterile PBS was then administered intravenously (300 µl) to each mouse via the tail vein. MSC or γMSC (6.4 x 10^4 gram^{-1}) were administered intravenously on day 7. The development of aGvHD was monitored every second day until day 9 and then everyday thereafter by recording weight loss, fur texture, posture, activity and diarrhoea.

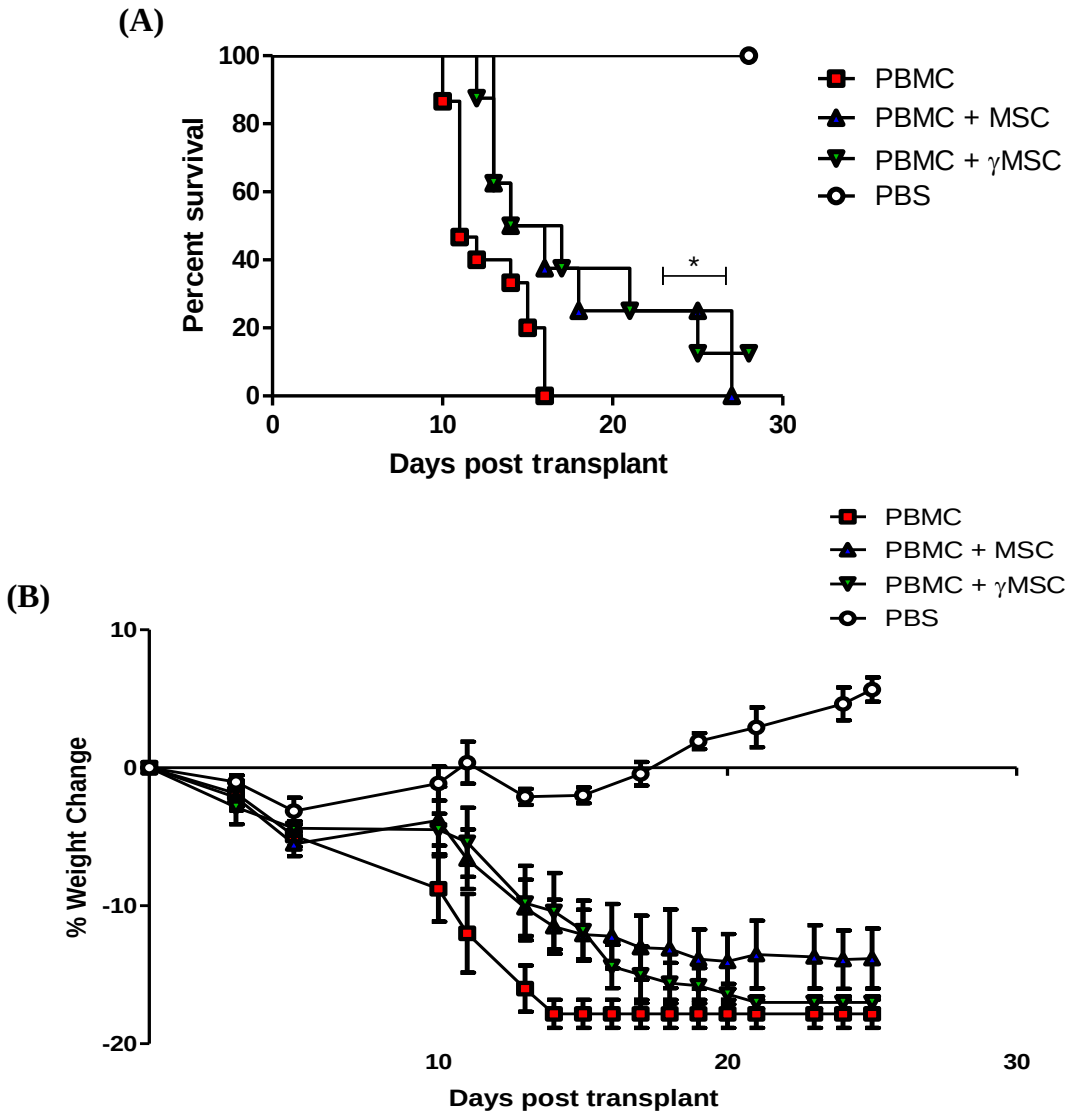

Figure 5.25. Both γMSC and resting MSC significantly prolonged survival and lowered weight loss in aGvHD mice. (A) Survival curve and (B) percentage weight change of aGvHD mice (red square), MSC treated aGvHD mice (blue triangle) and γMSC (green triangle). PBS control mice are represented by the white circles. 8 x 10^5 human PBMC $gram^{-1}$ were administered to irradiated NSG mice (2.4 Gy). 6.4 x 10^4 human $gram^{-1}$ MSC or γMSC were given as cell therapy on day 7. Transplanted mice were monitored every 2 days until day 9 and then every day for the duration of the experiment. n=6 mice per group. Statistical analysis was carried out using the un-paired student *t*-test.

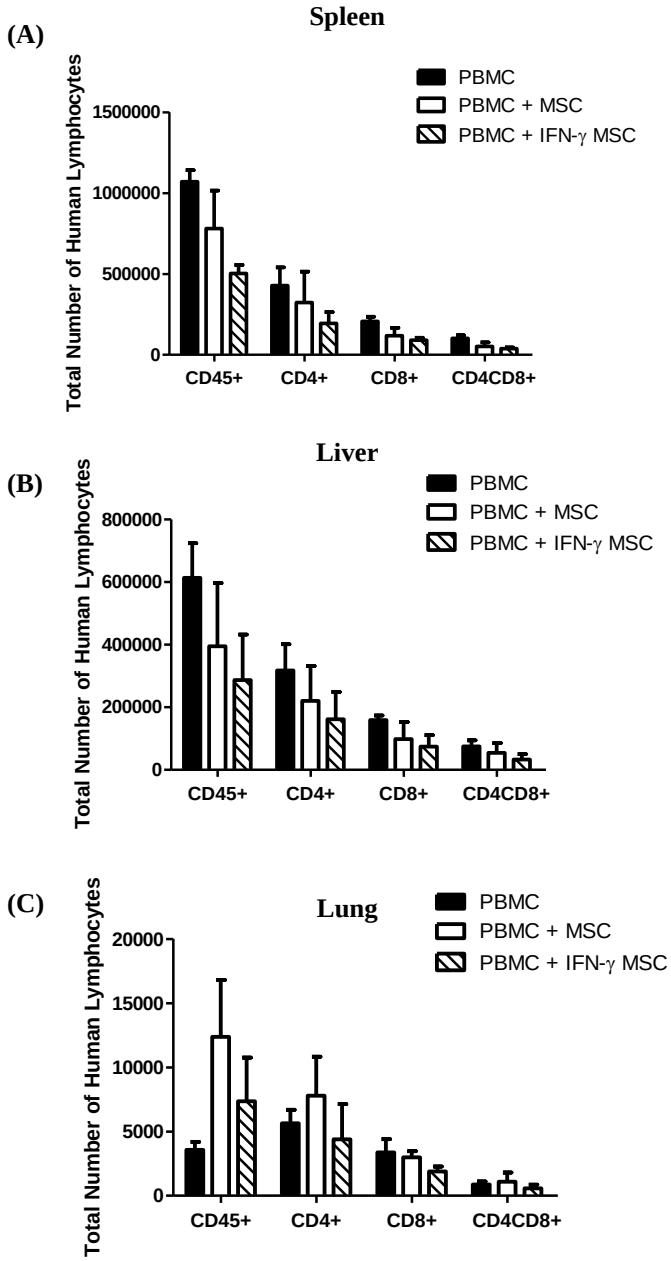

Figure 5.26. γMSC therapy did not impair the engraftment of human lymphocytes in aGvHD mice. NSG mice which were sub-lethally irradiated (2.4 Gy) and given PBMC (8 x 10^5 per $gram^{-1}$) via tail vein injection were analysed on day 12 by flow cytometry. (A) The total number of human $CD45^+$, $CD4^+$, $CD8^+$ and $CD4^+CD8^+$ lymphocytes recovered from the spleen of aGvHD mice. (B) The total number of human $CD45^+$, $CD4^+$, $CD8^+$ and $CD4^+CD8^+$ lymphocytes recovered from the livers of aGvHD mice. (C) The total number of human $CD45^+$, $CD4^+$, $CD8^+$ and $CD4^+CD8^+$ lymphocytes recovered from the livers of aGvHD mice. n=6 for each. Non-treated aGvHD mice are represented by black bars, aGvHD mice which received MSC therapy are represented by white bars and aGvHD mice which received γMSC therapy are represented by striped bars. The total number of human lymphocytes was assessed using counting beads during flow cytometry. Statistical significance was determined using paired student *t*-test.

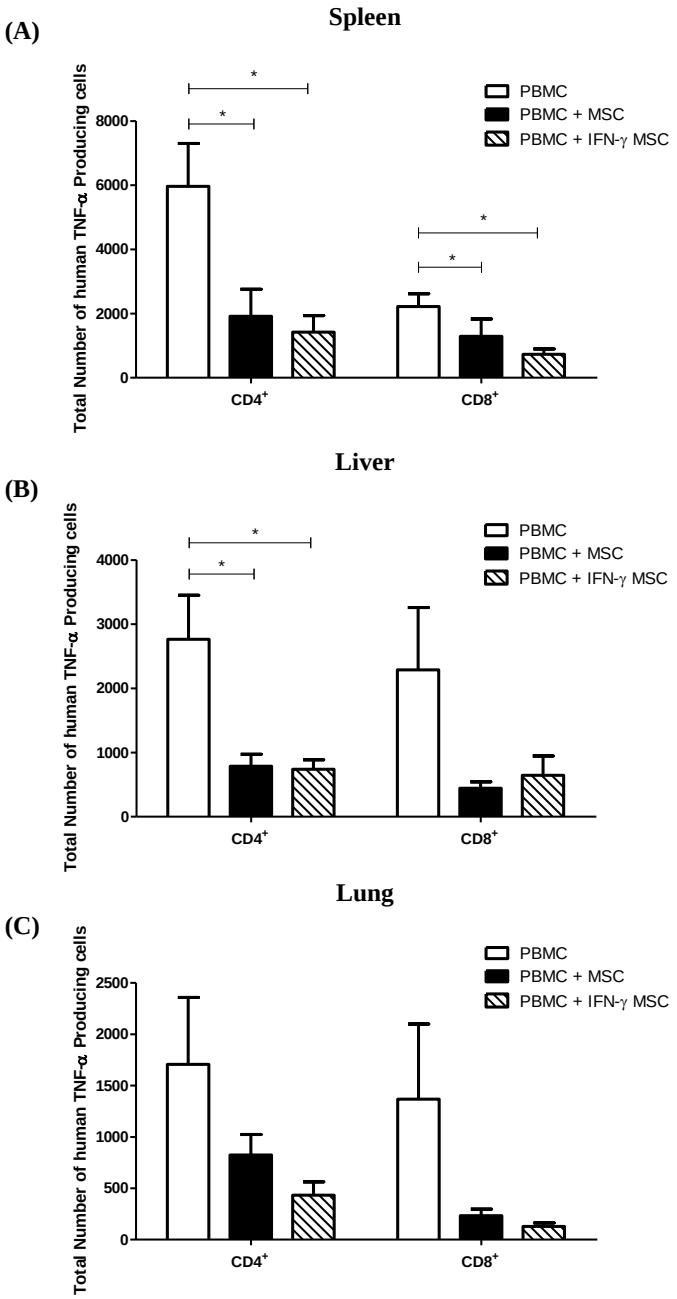

Figure 5.27. MSC and γMSC therapies reduced the total number of TNF-α producing CD4$^+$ and CD8$^+$ T cells in the spleens, livers and lungs of aGvHD mice. NSG mice were sub-lethally irradiated (2.4 Gy) and given PBMC ($8x10^5$ gram^{-1}) via tail vein injection were analysed on day 12 by intra-cellular flow cytometry. Graphical representation of accumulated data for total cell number of human TNF-α producing CD4$^+$ T and CD8$^+$ T cells recovered from the spleen (A), liver (B) and lungs (C) of aGvHD mice. n=6 per group (2 PBMC donor with 2 MSC donors). White bars represent non-treated aGvHD mice, black bars represent aGvHD mice which have received MSC therapy and striped bars represent aGvHD mice which have received γMSC therapy. The total number of human lymphocytes was assessed using counting beads during flow cytometry. Statistical significance was determined using student *t*-test where * < 0.05.

5.13. ADMINISTRATION OF TWO MSC THERAPEUTIC DOSES DID NOT FURTHER ENHANCE SURVIVAL OR PREVENT WEIGHT LOSS COMPARED TO SINGLE DOSE MSC TREATMENT

As demonstrated throughout this chapter, the administration of human MSC therapy significantly prolonged survival and reduced weight loss in a humanised mouse model of aGvHD. However, MSC therapy does not prevent aGvHD development and by the end of each study almost all of the mice which received MSC had succumbed to or at least exhibited symptoms associated with aGvHD. Therefore, the next step was to investigate whether the administration of multiple doses of MSC therapy would further prolong survival and prevent aGvHD progression. To achieve this, NSG mice were irradiated (2.4 Gy) and injected with human PBMC (8×10^5 gram^{-1}) or PBS via tail vein injection. As before, one group of mice received a single dose of human MSC (6.4×10^4 gram^{-1}) on day 7. Another group of mice received two doses of human MSC (6.4×10^4 gram^{-1}) on days 7 and 9. Transplanted mice were closely monitored as before and the survival and weight loss of each mouse was recorded (Figure 5.28).

The administration of 8×10^5 gram^{-1} human PBMC resulted in consistent aGvHD development in non-treated mice. aGvHD mice which received no cell therapy began to exhibit gradual but significant weight loss from day 10 and all non-treated aGvHD mice were sacrificed by day 17. The administration of human MSC therapy on day 7 resulted in significantly prolonged survival and reduced weight loss in aGvHD mice (Figure 5.29 A). aGvHD mice which received two doses of human MSC (day 7 and day 9) also demonstrated significantly prolonged survival and reduced weight loss compared to aGvHD mice which did not receive cell therapy (Figure 5.29 A). However, the survival of aGvHD mice which received two doses of MSC therapy was not enhanced compared to aGvHD mice which received a single dose of MSC. Surprisingly, weight loss was

slightly increased after the administration of the second MSC dose compared to mice which received MSC on day 7 only (Figure 5.29 B).

The effect of administering two doses of human MSC on the TNF-α production was also analysed by intra-cellular flow cytometry after 12 days. GvHD mice were sacrificed on day 12 and spleens, livers and lungs were harvested under sterile conditions. Human cells were recovered from the tissues and the number of human TNF-α producing $CD4^+$ and $CD8^+$ T cells were determined by flow cytometry. The administration of a single MSC dose on day 7 resulted in the reduction of number of human TNF-α producing $CD4^+$ and $CD8^+$ T cells found in the liver and lungs of GvHD mice; however there was no reduction of human TNF-α producing $CD4^+$ and $CD8^+$ T cells detected in the spleen (Figure 5.31 A). Interestingly, the administration of 2 doses of MSC therapy, day 7 and day 9, seemed to further reduce the number of human TNF-α producing $CD4^+$ and $CD8^+$ T cells in the lungs and liver compared to aGvHD mice which received a single dose of MSC, although these reductions were not determined to be significant (Figure 5.31 B & C). These results suggest that while the administration of two separate doses of MSC resulted in a slight reduction in TNF-α producing cells, there was no difference in the survival or weight loss when compared to single dose MSC therapy. At present a beneficial effect for multiple doses cannot be ruled out, but examination of TNF-α as a marker might be a useful diagnostic for optimising a timing of further doses.

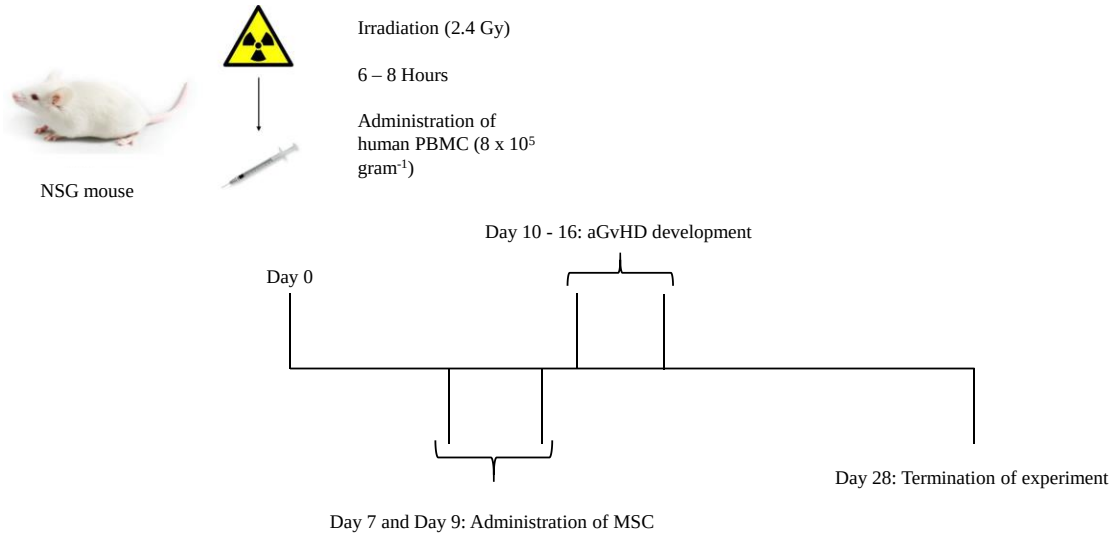

Figure 5.28. Development of a humanised mouse model of aGvHD to investigate double doses of MSC therapy. NOD-SCID IL-2rγ^{null} (NSG) mice were exposed to a sub-lethal dose of gamma irradiation (2.4 Gy). 8 x 10^5 PBMC gram^{-1} or sterile PBS was then administered intravenously (300 µl) to each mouse via the tail vein. Mesenchymal stromal cells (6.4 x 10^4 gram^{-1}) were administered intravenously as either a single dose on day 7 or as a multiple dose therapy on days 7 and 9. The development of aGvHD was monitored every second day until day 9 and then everyday thereafter by recording weight loss, fur texture, posture, activity and diarrhoea.

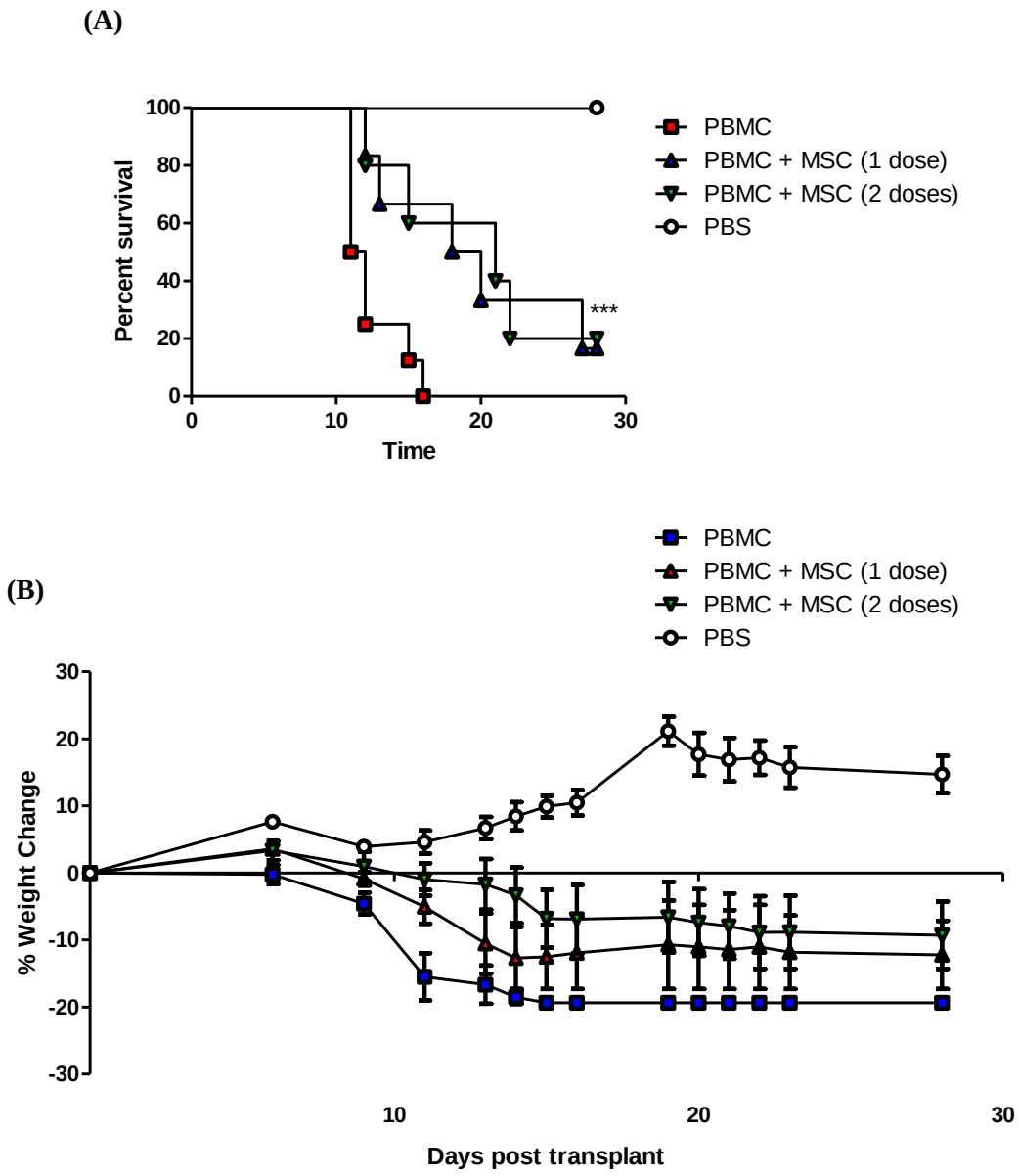

Figure 5.29. Single dose was comparable to double dose MSC therapy in aGvHD mice. (A) Survival curve and (B) percentage weight change of aGvHD mice (red square), single dose MSC treated aGvHD mice (blue triangle) and multiple dose MSC (green triangle). PBS control mice are represented by the white circles. 8 x 10^5 human PBMC $gram^{-1}$ were administered to irradiated NSG mice (2.4 Gy). 6.4 x 10^4 human $gram^{-1}$ MSC were given as cell therapy on day 7 and day 9. Transplanted mice were monitored every 2 days until day 9 and then every day for the duration of the experiment. n=6 mice per group. Statistical analysis was carried out using the un-paired student *t*-test where *** < 0.001 between red square and blue triangle, and also between the red square and green triangle.

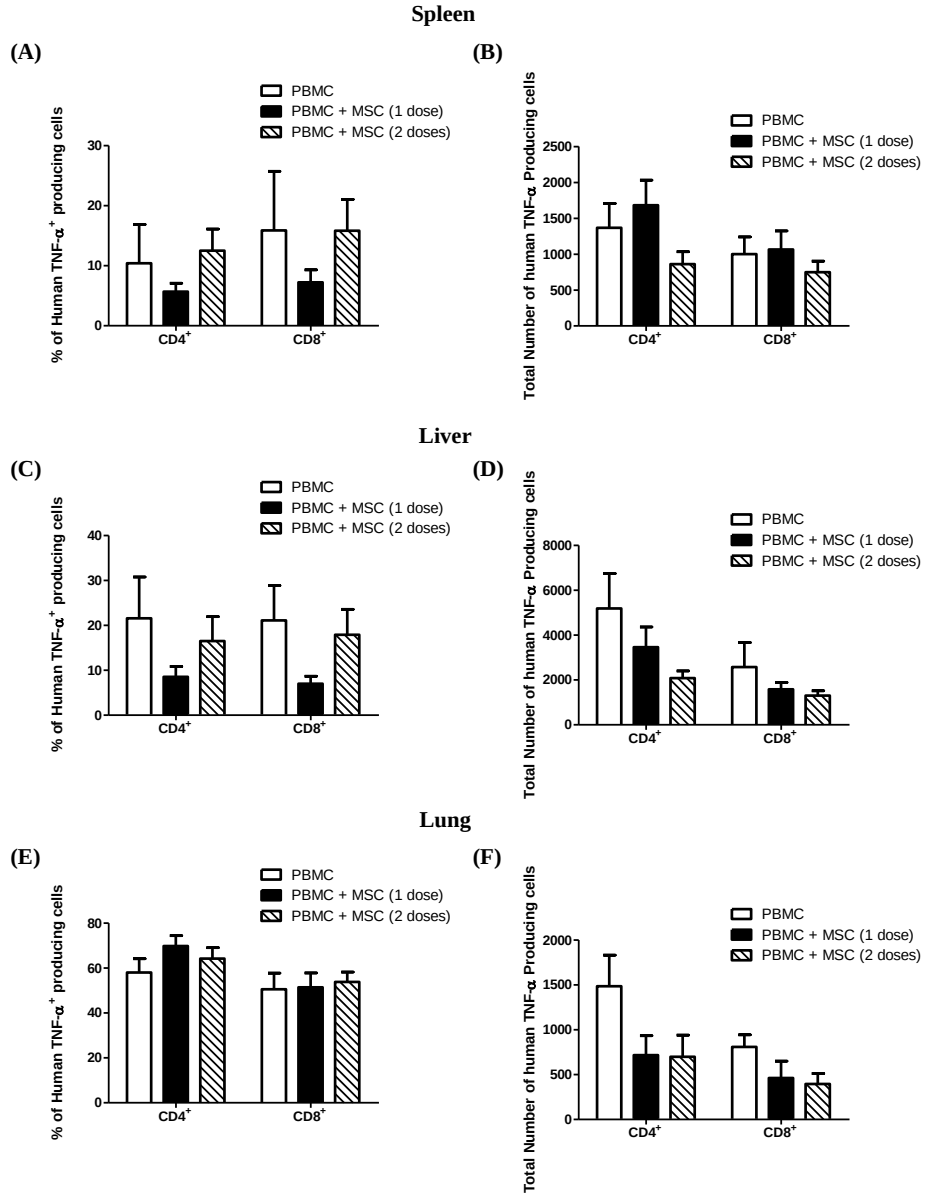

Figure 5.30. Both single and double dose MSC therapy reduced the total number of TNF-α producing CD4$^+$ and CD8$^+$ T cells in the spleens, livers and lungs of aGvHD mice. NSG mice were sub-lethally irradiated (2.4 Gy) and given PBMC ($8x10^5$ gram^{-1}) via tail vein injection were analysed on day 12 by intra-cellular flow cytometry. Graphical representation of the human TNF-α producing T cells recovered from the spleen (A), liver (C) and lung (E) from aGvHD mice. Accumulated data for total cell number human TNF-α producing CD4$^+$ T and CD8$^+$ T cells recovered from the spleen (B), liver (D) and lungs (F) of aGvHD mice. n=6 per group (2 PBMC donor with 2 MSC donors). White bars represent non-treated aGvHD mice, black bars represent aGvHD mice which have received MSC therapy and striped bars represent aGvHD mice which have received 2 doses of MSC therapy. The total number of human lymphocytes was assessed using counting beads during flow cytometry. Statistical significance was determined using student *t*-test where * < 0.05.

5.14. Summary I

The main objectives of this section were to (1) to develop a robust and reproducible humanised mouse model of acute GvHD using PBMC isolated from buffy-packs, (2) investigate how MSC effect human PBMC *in vivo*, (3) compare the efficacy of γMSC to resting MSC after day 7 administration and (4) to determine whether administering double doses of MSC increased protection from aGvHD compared to single dose. The Nod Scid IL-2rγ^{null} model of aGvHD initially designed by Pearson *et al.* (2008); using this as a guideline an optimised and consistent model of aGvHD was developed for use with PBMC isolated from buffy packs. This chapter also presents an optimised model of aGvHD for use with buffy pack PBMC which were thawed from a frozen stock and demonstrates the possibility of using the chemotherapeutic agent Busulfan as a conditioning agent in situations where irradiation is not possible.

Using this optimised and consistent model of aGvHD, the administration of human MSC therapy on day 7 was shown to significantly prolong the survival and reduce weight loss during aGvHD. MSC therapy did not inhibit the engraftment of human lymphocytes within the spleens, lungs or livers of aGvHD mice. The addition of human MSC therapy did not prevent the polarisation of PBMC to effector or central memory T cells. The production of human IL-1β, IL-2 or IFN-γ were not reduced in aGvHD mice which received human MSC therapy. However, administration of human MSC on day 7 resulted in the significant reduction in human TNF-α producing $CD4^+$ and $CD8^+$ T cells in aGvHD mice. This chapter also demonstrates that human MSC therapy significantly increases the number of Treg cells in the liver and lungs of aGvHD 12 days after PBMC administration.

The next step was to investigate whether the administration of γMSC on day 7 were more beneficial than resting MSC. While the administration of γMSC on day 7

resulted in prolonged survival and reduced weight loss when compared to non-treated aGvHD mice, there was no significant difference compared to resting MSC. Similarly, aGvHD mice which received two doses of MSC, day 7 and day 9, did not display enhanced survival or reduced weight loss when compared to aGvHD mice which received a single dose of MSC. Taken together these results demonstrate a beneficial effect of MSC therapy against aGvHD in a humanised mouse model. The beneficial effect of MSC therapy may be a result of reduced TNF-α production and an increase in Treg populations.

5.15. *FASCIOLA HEPATICA*

Fasciola hepatica is a parasitic flatworm which can cause chronic liver infection (fascioliasis) in mammals (Collins *et al.* 2004) with over 2 million reported cases in humans worldwide (McManus & Dalton 2006). *F. hepatica* have the ability to modulate the immune response of its host organism and can subsequently avoid clearance. Recent studies into how *F. hepatica* modulate their host's immune system have focussed around antigens embedded on the tegumental coat which is shed every 2-3 hours. *F. hepatica* tegumental antigen (Fh-Teg) has been shown to suppress LPS induced expression of DC maturation markers CD80, CD86 and CD40, as well as the production of pro-inflammatory cytokines IFN-γ and IL-12p70 by DC in mouse models of septic shock (Hamilton *et al.* 2009; Dowling *et al.* 2010). Fh-Teg did not detrimentally affect the survival of DC after LPS stimulation (Hamilton *et al.* 2009). Fh-Teg have also been shown to inhibit murine mast cells ability to drive Th1 immune responses by inhibiting the release of TNF-α, IL-6, IFN-γ and IL-10 (Vukman *et al.* 2013). These studies have focused on the ability of Fh-Teg to modulate murine immune cells and to date there is no data available as to whether Fh-Teg can suppress human immune cells in a similar manner. Therefore this study was designed to investigate whether Fh-Teg could suppress human T cell function in humanised mouse model of GvHD.

The main aims of this section were to examine (1) whether Fh-Teg treatment of PBMC could promote survival in GvHD mice, (2) to investigate the effect of Fh-Teg on the engraftment of PBMC within NSG mice and (3) to determine the effect of Fh-Teg on human T cell function *in vivo* as measured by the expression of memory T cell markers and the ability of T cells to produce pro-inflammatory cytokines in response to xenogeneic stimulation.

5.16. FH-TEG INCREASED SURVIVAL AND LOWERED PATHOLOGICAL SCORE IN AGVHD MICE

The ability of Fh-Teg to suppress the immune system has previously been described in mice; however the effect of Fh-Teg on human immune cells has not yet been characterised. In order to examine whether Fh-Teg were capable of supressing human immune cells, Fh-Teg stimulated PBMC were administered to the humanised mouse model of GvHD. The ability for xenogeneic recognition and subsequent GvHD induction of Fh-Teg stimulated PBMC compared to PBMC was used as an indicator of an immune suppressive effect. PBMC were isolated from buffy packs and either rested (PBMC) or stimulated with Fh-Teg (Fh-Teg PBMC) (10µg/ml) overnight. The following day PBMC and Fh-Teg PBMC were counted and administered to irradiated (2.4 Gy) NSG mice via tail vein injection ($1x10^6$ PBMC per gram). As before the mice were monitored on a regular basis and the development of GvHD was defined as previously described (Table 4.1). Mice which received a combined pathological score of 6 from 8 or displayed weight loss in excess of 15% were considered to have severe GvHD and sacrificed humanely.

After PBMC administration, the survival, weight loss and GvHD pathological score of each mouse was monitored every 2 days until day 9 and then every day for the duration of the experiment (Figure 5.31). PBMC mice developed acute GvHD as expected as PBMC mice did not survive past day 14; however the survival of Fh-Teg PBMC mice was significantly longer with 50% of mice surviving past day 15 (Figure 5.31 A). The accumulative pathological score of Fh-Teg PBMC mice was significantly lower than PBMC mice from day 10 until the end of the experiment (Figure 5.31 B). Weight loss in Fh-Teg PBMC mice was significantly lower until day 14; after which it was similar to PBMC mice (Figure 5.31 C). After day 15 however, the pathological score and weight loss of Fh-Teg PBMC mice increased and all Fh-Teg PBMC mice either succumbed to or showed signs of developing GvHD by day 22 (Figure 5.31).

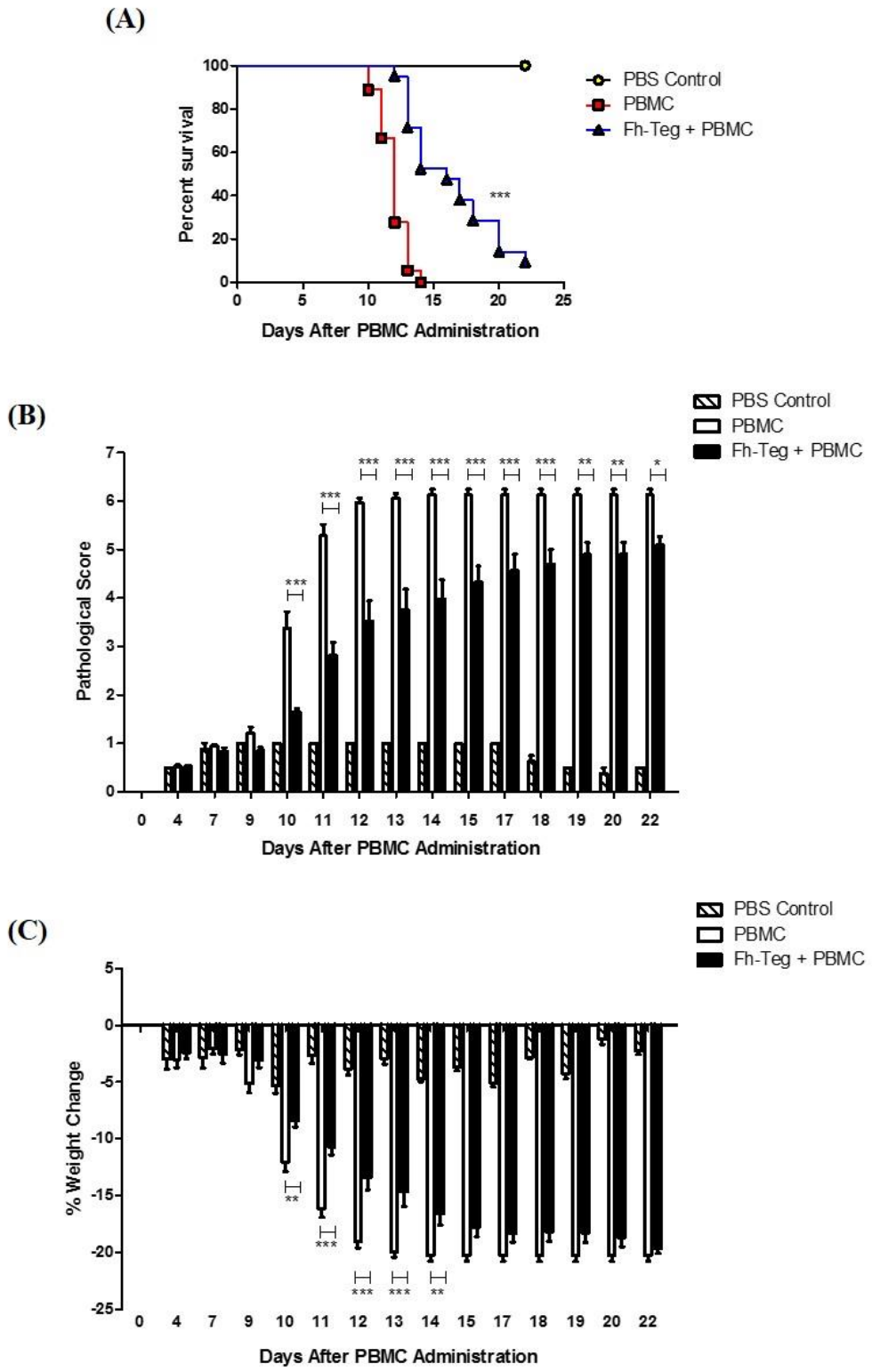

Figure 5.31. Fh-Teg PBMC significantly prolonged survival and reduced pathological score in aGvHD mice. PBS control mice are represented by diagonally lined bars, mice which received PBMC are represented by white bars and mice which received Fh-Teg PBMC are represented by black bars. Statistical significance was determined using a Martel-Cox test for (A) and student *t*-test for (B) where * < 0.05, ** < 0.005 and *** < 0.001. n=5 for PBS, n=18 for PBMC, n=21 for Fh-Teg PBMC.

5.17. FH-TEG SIGNIFICANTLY IMPAIRED PBMC ENGRAFTMENT

The data presented in section 5.18 suggest a mechanism by which pre-stimulation of PBMC with Fh-Teg overnight can delay the onset of acute GvHD (Figure 5.31). In order to confirm that overnight stimulation with Fh-Teg did not result in apoptosis of the PBMC, EB/AO staining was used to examine cell viability. The percentage of live PBMC following Fh-Teg stimulation was not significantly different compared to PBMC which were not stimulated with Fh-Teg (Figure 5.32). Despite these results, all Fh-Teg PBMC mice began to develop typical acute GvHD symptoms from 15 days post transplantation and most of these mice developed GvHD by the end of the study. Therefore it was hypothesised that pre-treating PBMC with Fh-Teg impaired the ability of the PBMC to engraft within the mouse. To examine this hypothesis, irradiated NSG mice were given PBMC or Fh-Teg PBMC (1×10^6 per gram) and monitored as before. On day 12, the mice were sacrificed and the engraftment of human $CD45^+$ lymphocytes in the spleen was determined by flow cytometry. There was a significant reduction in the percentage of human $CD45^+$ lymphocytes recovered from the spleens of Fh-Teg PBMC mice when the results from all 4 PBMC donors were combined (Figure 5.33 I). The total number of human $CD45^+$ lymphocytes was also significantly reduced in the spleens of Fh-Teg PBMC mice (Figure 5.33 J).

Although APCs have previously been reported to be essential in the development of GvHD, recent studies have indicated that T cells are the main drivers of GvHD pathology (Li *et al.* 2012). Therefore it was hypothesised that the reduction in mortality and pathological score observed in Fh-Teg PBMC mice (Figure 5.31) could be a result of impaired engraftment of human T cells *in vivo*. Therefore live cells were gated for human CD45 and their expression of human $CD4^+$, $CD8^+$ or $CD4^+CD8^+$ populations was determined. While there was no difference in the percentage of $CD45^+$ cells which were $CD4^+$, $CD8^+$ or $CD4^+CD8^+$ between PBMC and Fh-PBMC mice, the total number of

$CD4^+$, $CD8^+$ and $CD4^+CD8^+$ T cell populations was significantly reduced in Fh-Teg PBMC mice (Figure 5.34 A&B).

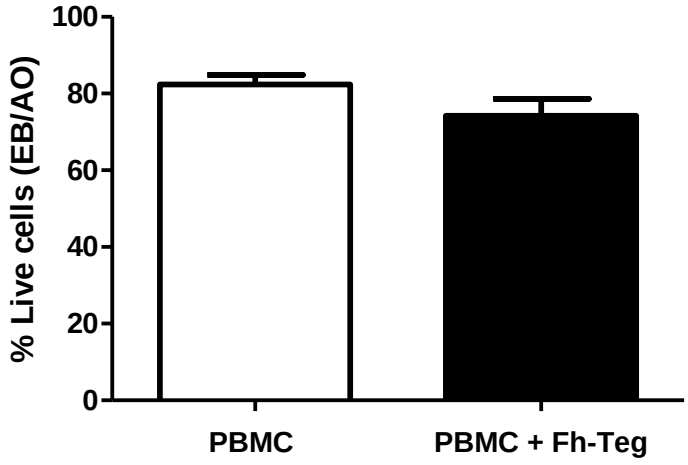

Figure 5.32. Overnight stimulation with Fh-Teg did not affect PBMC viability. Prior to administration to NSG mice, PBMC were cultured overnight in the presence or absence of Fh-Teg (10 µg/ml). Ethidium Bromide/ Acrylamide Orange staining was used to determine the viability of PBMC following Fh-Teg stimulation (n=4 PBMC donors). PBMC are represented by white bars and Fh-Teg PBMC mice are represented by black bars.

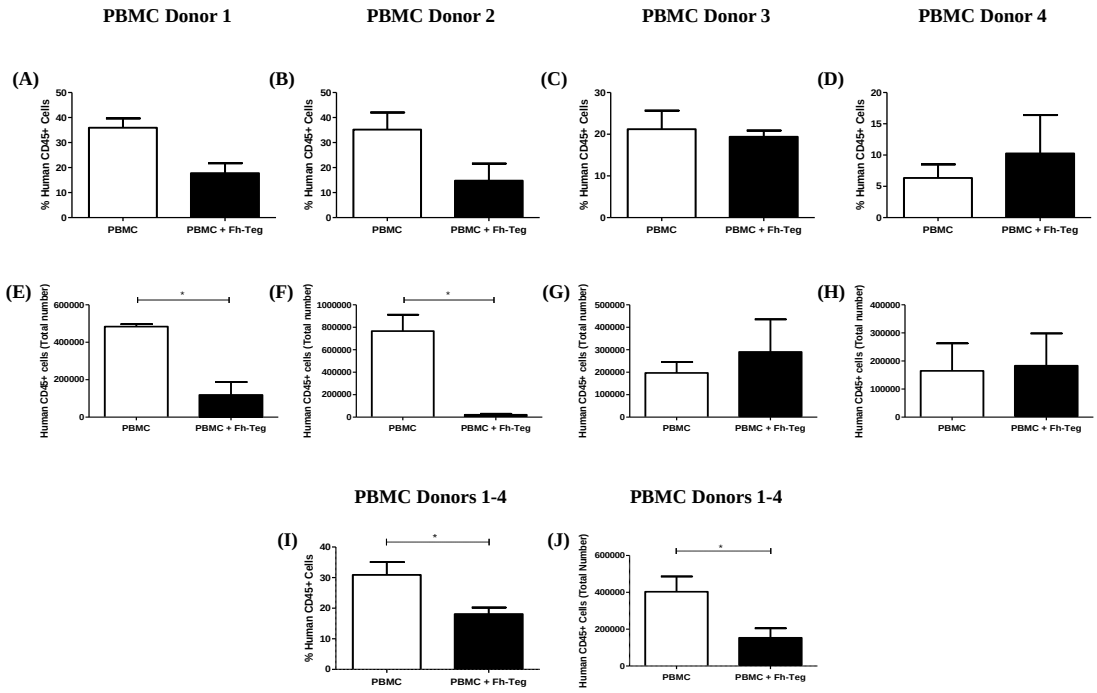

Figure 5.33. Fh-Teg PBMC significantly reduced the percentage and total number of human CD45$^+$ lymphocytes in the spleens of acute aGvHD mice. NSG mice which were sub-lethally irradiated (2.4 Gy) and given PBMC or Fh-Teg PBMC (1x10^6 per gram) via tail vein injection were analysed on day 12 by flow cytometry. (A)-(D) Analysis of the percentage of human CD45$^+$ lymphocytes recovered from the spleen of GvHD mice using 4 different PBMC donors (n=3 for each). (E)-(F) The total number of human CD45$^+$ lymphocytes recovered from the spleens of GvHD mice using 4 different PBMC donors (n=3 for each). (I) The accumulated data analysing the percentage of human CD45$^+$ lymphocytes from all 4 PBMC donors (n=12) and (J) the accumulated data of the total number of human CD45$^+$ lymphocytes from all 4 PBMC donors (n=12). PBMC are represented by white bars and Fh-Teg PBMC mice are represented by black bars. The total number of human CD45$^+$ lymphocytes was assessed using counting beads during flow cytometry. Statistical significance was determined using student *t*-test where * < 0.05.

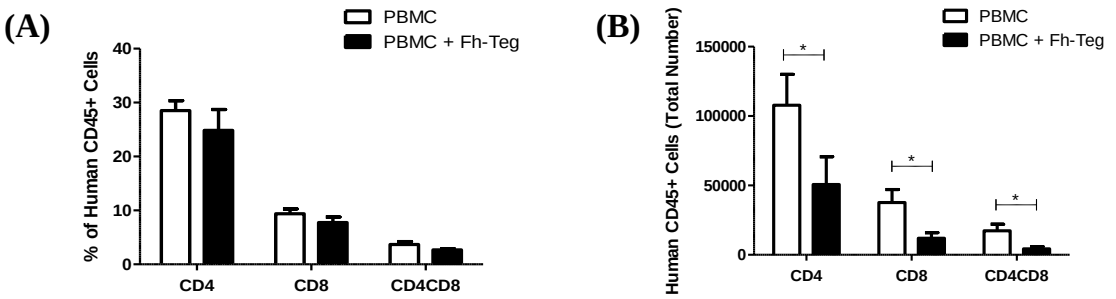

Figure 5.34. Fh-Teg significantly reduced the total number of human CD4$^+$, CD8$^+$ and CD4$^+$CD8$^+$ lymphocytes in the spleens of aGvHD mice. Graphical representation of percentage and total number of human CD4$^+$, CD8$^+$ and CD4+CD8$^+$ cell populations as measured by flow cytometry. NSG mice were sub-lethally irradiated (2.4 Gy) and given PBMC or Fh-Teg PBMC (1x10^6 per gram) via tail vein injection. (A) The accumulated data analysis of the percentage of human CD4$^+$, CD8$^+$ or CD4+CD8+ cells recovered from the spleens of PBMC (white bar) and Fh-Teg PBMC (black bar) mice. (B) The total cell number of human CD4$^+$, CD8$^+$ or CD4$^+$CD8$^+$ cells recovered from the spleens of PBMC and Fh-Teg PBMC mice. The total number of human CD4$^+$ and CD8$^+$ lymphocytes were determined using counting beads during flow cytometry. n=12 per group (4 PBMC donors). Statistical significance was determined using student *t*-test where * < 0.05.

5.18. Fh-Teg significantly reduces the infiltration of human lymphocytes to the liver and lung of GvHD mice

GvHD is characterised by the tissue specific destruction of target organs by infiltrating lymphocytes. Therefore it was hypothesised that the reduction in GvHD pathological score and mortality when PBMC were pre-treated with Fh-Teg (Figure 5.31) was caused by impaired migration of human lymphocytes to the organs of humanised mice. To examine this hypothesis, PBMC and Fh-Teg PBMC treated groups were sacrificed on day 12 and liver and lungs were harvested. Both organs were mechanically digested and PBMC recovered by density gradient centrifugation. Isolated cells were then examined for the expression of human CD45 by flow cytometry. There was a small but significant reduction in the percentage of human $CD45^+$ cells recovered from the liver (Figure 5.35 A) and in the lung (Figure 5.35 C) of Fh-Teg PBMC mice. The actual number of $CD45^+$ cells recovered from the liver (Figure 5.35 B) and the lungs (Figure 5.35 D) of Fh-Teg PBMC mice was significantly reduced. Human $CD45^+$ lymphocytes recovered from the liver and the lung of GvHD mice were also analysed for human $CD4^+$, $CD8^+$ and $CD4^+CD8^+$ populations. The percentage of human $CD4^+$ and $CD4^+CD8^+$ cell populations were significantly reduced in the liver of Fh-Teg PBMC mice but no significant change in the percentage of human $CD8^+$ cells was detected (Figure 5.36 A). Similar to results observed in the spleen, significantly less human $CD4^+$, $CD8^+$ or $CD4^+CD8^+$ cells were recovered from the livers of Fh-Teg PBMC mice during GvHD (Figure 5.36 B). The expression of human $CD4^+$, $CD8^+$ or $CD4^+CD8^+$ was also determined in the lung of PBMC and Fh-Teg PBMC mice. Fh-Teg PBMC mice had a significantly lower percentage of $CD4^+$, $CD8^+$ and $CD4^+CD8^+$ cells than mice which had received PBMC (Figure 5.36 C). Similar to results observed in the liver (Figure 5.36 B), there was a significant reduction in the total number of human $CD4^+$, $CD8^+$ or $CD4^+CD8^+$ T cells recovered from the lungs of Fh-Teg PBMC mice (Figure 5.36 D).

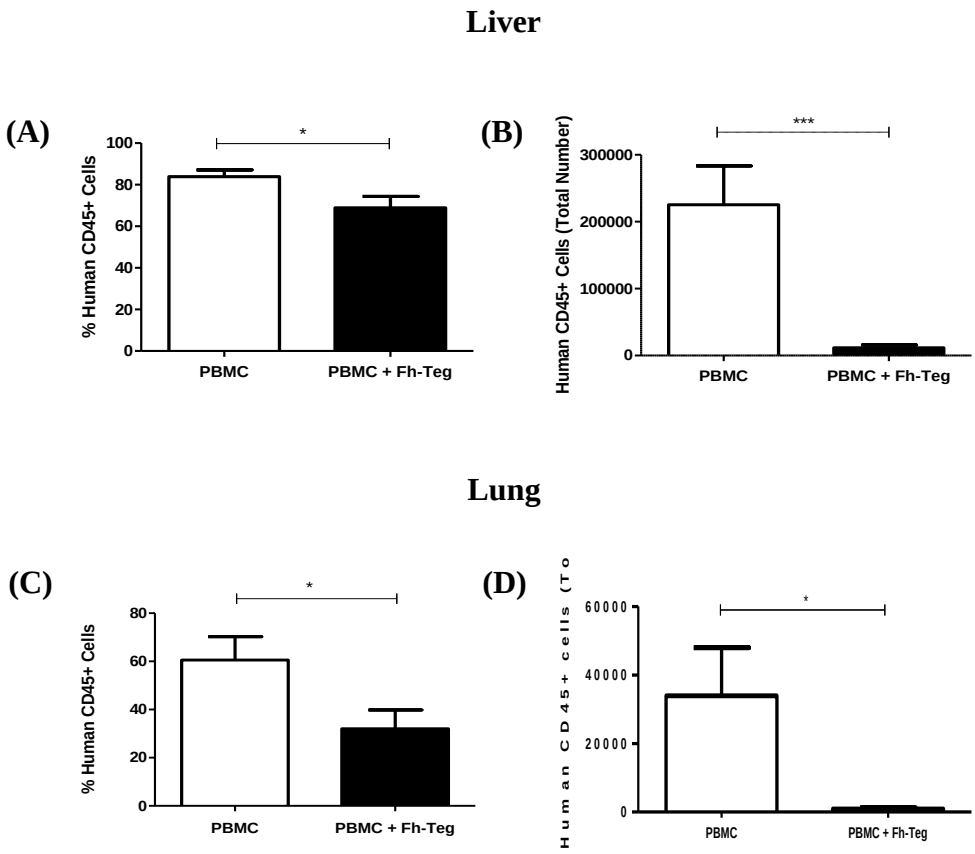

Figure 5.35. Fh-Teg significantly reduced the percentage and total number of CD45$^+$ lymphocytes in liver and lungs of GvHD mice. NSG mice which were sub-lethally irradiated (2.4 Gy) and given PBMC or Fh-Teg PBMC (1x10^6 per gram) via tail vein injection were analysed on day 12 by flow cytometry. Analysis of the percentage of human CD45$^+$ lymphocytes recovered from (A) the liver and (C) the lungs of PBMC (white bar) and Fh-Teg PBMC (black bar) mice. Accumulated data analysing the total number of human CD45$^+$ lymphocytes recovered from (B) the liver and (D) the lungs of acute GvHD mice. n=12 per group (4 PBMC donors). The total number of human CD45$^+$ lymphocytes was assessed using counting beads during flow cytometry Statistical significance was determined using student *t*-test where * < 0.05, *** < 0.001.

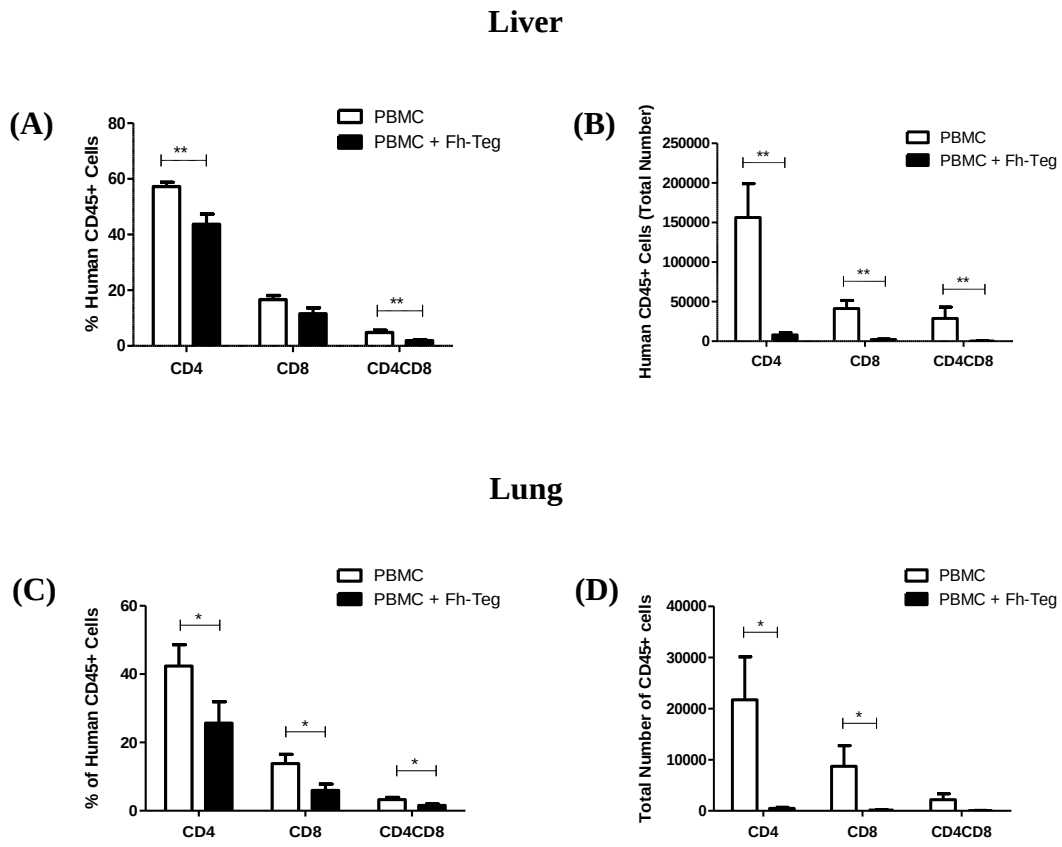

Figure 5.36. Fh-Teg significantly reduced the percentage and total number of human CD4$^+$, CD8$^+$ and CD4$^+$CD8$^+$ cells in GvHD mice. Graphical representation of percentage and total number of human CD4$^+$, CD8$^+$ and CD4+CD8$^+$ cell populations recovered from the livers and lungs of GvHD mice and measured on day 12 by flow cytometry. NSG mice were sub-lethally irradiated (2.4 Gy) and given PBMC or Fh-Teg PBMC (1x10^6 per gram) via tail vein injection. Analysis of the percentage of human CD4$^+$, CD8+ and CD4$^+$CD8$^+$ lymphocytes recovered from (A) the liver and (C) the lungs of PBMC (white bar) and Fh-Teg PBMC (black bar) mice. Accumulated data analysing the total number of human CD4$^+$, CD8+ and CD4$^+$CD8$^+$ lymphocytes recovered from (B) the liver and (D) the lungs of acute GvHD mice. n=12 per group (4 PBMC donors). The total number of human CD4$^+$ and CD8$^+$ lymphocytes were determined using counting beads during flow cytometry. Statistical significance was determined using student *t*-test where * < 0.05, ** < 0.005.

5.19. FH-TEG SIGNIFICANTLY REDUCES THE NUMBER OF HUMAN CENTRAL AND EFFECTOR MEMORY LYMPHOCYTES IN THE SPLEEN, LIVER AND LUNG OF GVHD MICE

The phenotypic characterisation of naïve, central (Tcm) and effector memory (Tem) T cell populations from post-BMT patients can provide valuable information and help to define the immunological basis of GvHD (Ali *et al.* 2012). The characterisation of these T cell sub-populations is essential in understanding the nature of the immune response associated with xenogeneic models of GvHD and may help to further understand the immune response in GvHD patients. It was hypothesised that the reduced mortality and pathology observed using Fh-Teg PBMC (Figure 5.31) may be caused by impaired polarisation to effector T cell populations after stimulation with Fh-Teg. Anti-human CD45RO, CD27 and CD62L antibodies were combined with either anti-human CD4 or CD8 antibodies to characterise naïve ($CD45RO^{-}CD27^{+}$), central memory ($CD45RO^{+}CD27^{+}CD62L^{+}$) or effector memory ($CD45RO^{+}CD27^{+}CD62L^{-}$) T cell populations within $CD4^{+}$ or $CD8^{+}$ populations in the spleen, liver and lung. The characterisation of T cell sub-populations from the spleens of GvHD mice demonstrated that pre-treating PBMC with Fh-Teg did not significantly affect the percentage of human naïve, Tem or Tcm populations within either the $CD4^{+}$ (Figure 5.37 A) or $CD8^{+}$ populations (Figure 5.38 A). One PBMC donor expressed a significantly higher proportion of Tcm within both the $CD4^{+}$ and $CD8^{+}$ populations; however, this increase in Tcm was not replicated across the other PBMC donors and the accumulated data from all 4 PBMC donors showed no difference in naïve, Tem or Tcm populations between PBMC and Fh-Teg PBMC mice. Similar to the results presented above, there was a significant reduction in the total number of $CD4^{+}$ (Figure 5.37 B) and $CD8^{+}$ (Figure 5.38 B) naïve, Tem and Tcm populations recovered from the spleen from mice which had received Fh-Teg PBMC.

The ability of Tcm and Tem cells to home to and infiltrate the liver and lungs of GvHD mice was also analysed. T cell sub-populations recovered from the livers of GvHD mice showed that Fh-Teg PBMC had no effect on the percentages of naïve, Tem or Tcm cells within either the $CD4^+$ (Figure 5.37 C) or $CD8^+$ (Figure 5.38 C) gates. As for the spleen, significantly less cells were recovered from each T cell sub-population. Fh-Teg PBMC mice had significantly reduced amounts of naïve, Tem and Tcm cells within both $CD4^+$ (Figure 5.38 D) and $CD8^+$ (Figure 5.39 D) cells.

Spleen

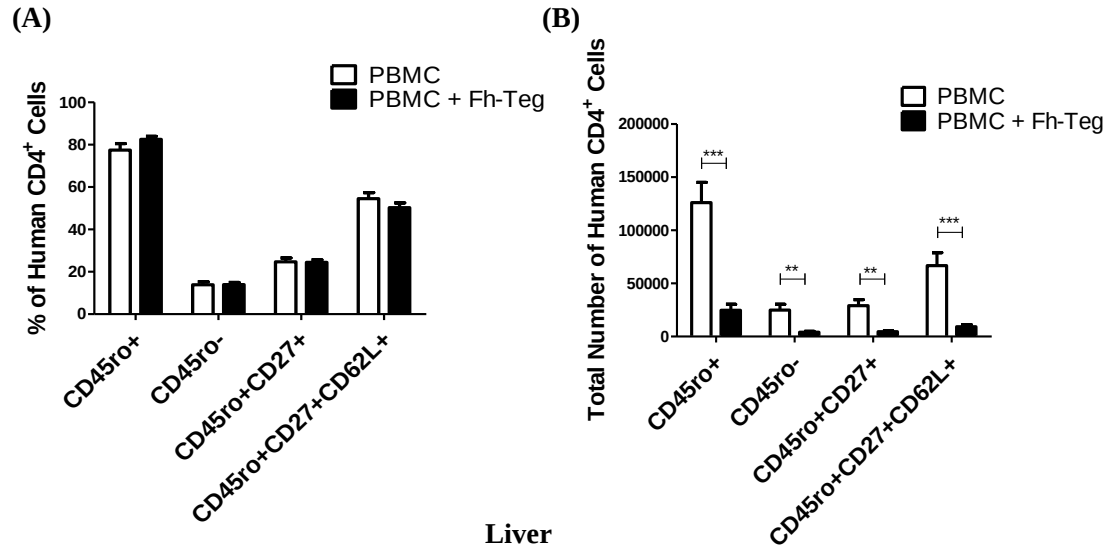

Liver

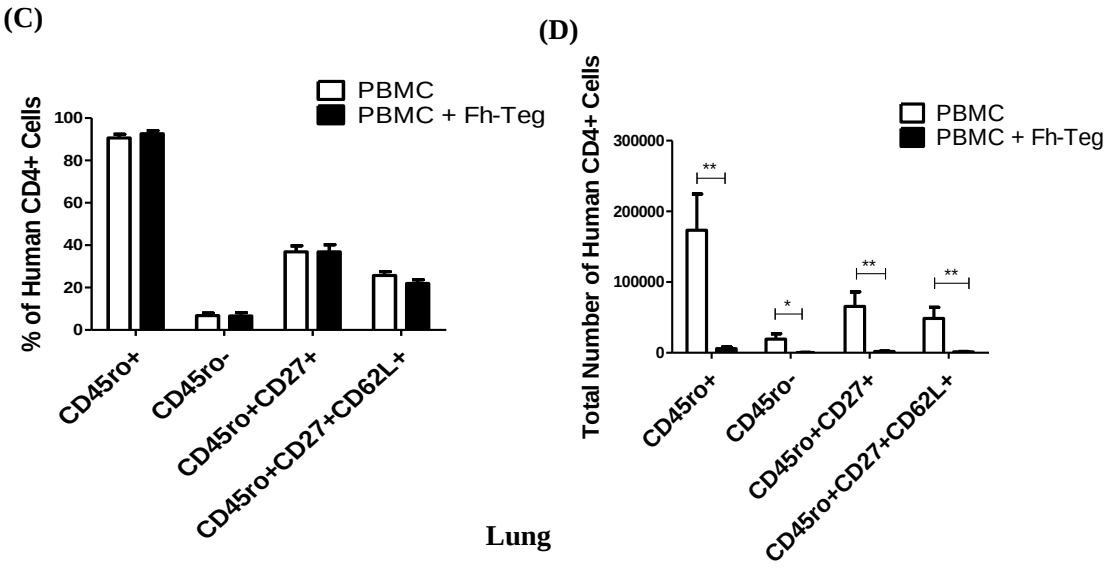

Lung

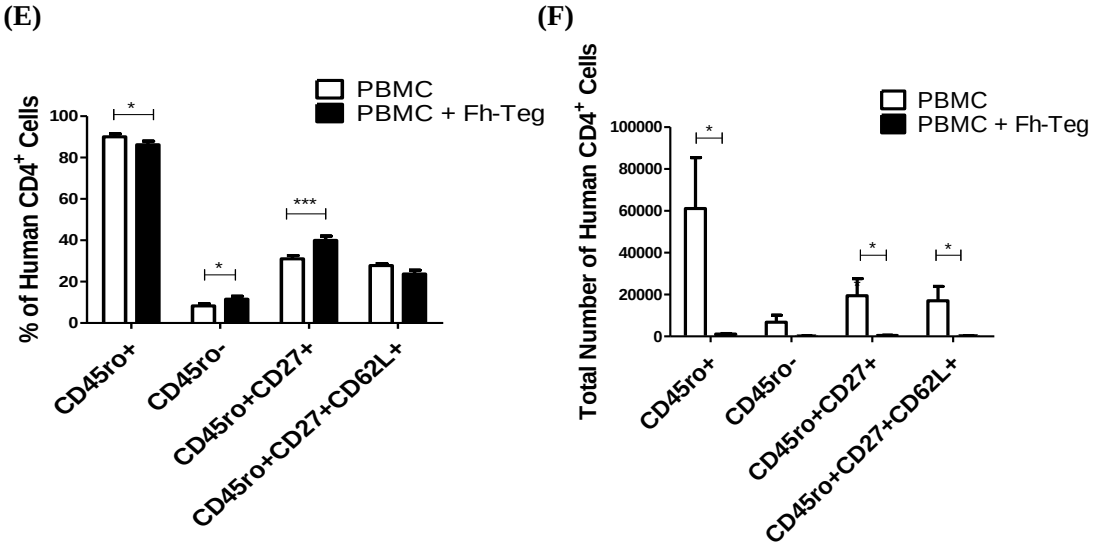

Figure 5.37. Fh-Teg significantly reduced the number of activated ($CD45RO^+$), naïve ($CD45RO^-$), Tem ($CD45RO^+CD27^+$) and Tcm ($CD45RO^+CD27^+CD62L^+$) human $CD4^+$ T cells in aGvHD mice. NSG mice which were sub-lethally irradiated (2.4 Gy) and given PBMC or Fh-Teg PBMC ($1x10^6$ per gram) via tail vein injection were analysed after 12 days. Graphical representation of the percentage of activated, naïve, Tem and Tcm $CD4^+$ cells recovered from the spleen (A), livers (C) and lungs (E) of PBMC (white bar) or Fh-Teg PBMC (black bar) mice. Accumulated data illustrating the total number of activated, naïve, Tem and Tcm $CD4^+$ cells recovered from the spleen (B), livers (D) and lungs (F) of PBMC or Fh-Teg PBMC mice. n=12 per group (4 PBMC donors). The total number of human lymphocytes was assessed using counting beads during flow cytometry. Statistical significance was determined using student *t*-test where * < 0.05, ** < 0.005, *** < 0.001.

Spleen

(A)

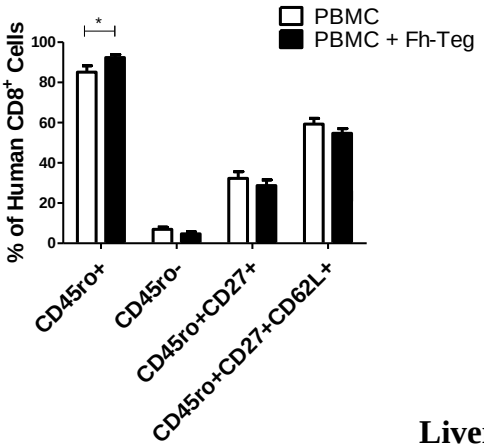

(B)

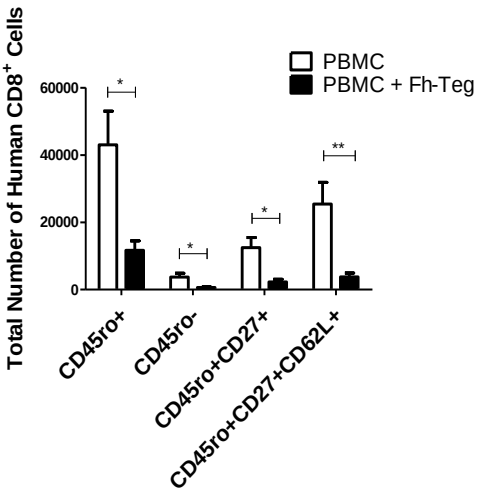

Liver

(C)

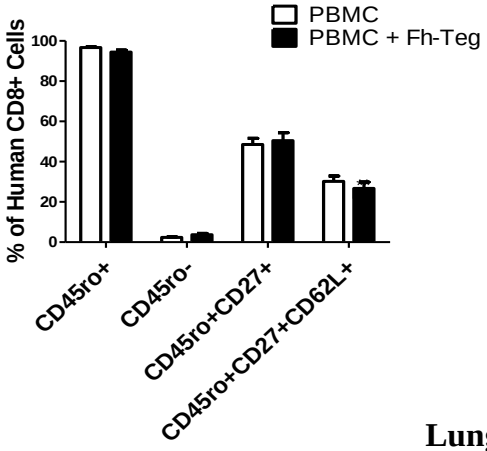

(D)

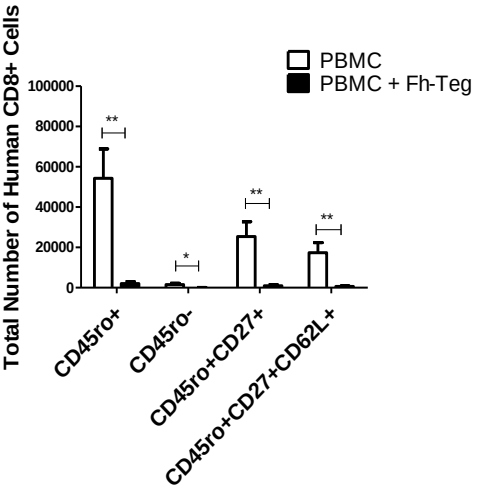

Lung

(E)

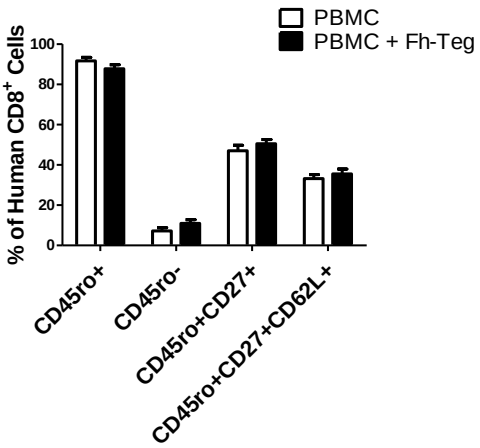

(F)

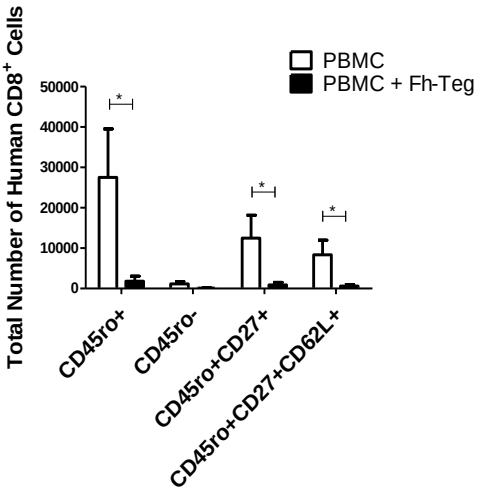

Figure 5.38. Fh-Teg significantly reduced the number of activated ($CD45RO^+$), naïve ($CD45RO^-$), Tem ($CD45RO^+CD27^+$) and Tcm ($CD45RO^+CD27^+CD62L^+$) human $CD8^+$ T cells in aGvHD mice. NSG mice which were sub-lethally irradiated (2.4 Gy) and given PBMC or Fh-Teg PBMC ($1x10^6$ per gram) via tail vein injection were analysed after 12 days. Graphical representation of the percentage of activated, naïve, Tem and Tcm $CD8^+$ cells recovered from the spleen (A), livers (C) and lungs (E) of PBMC (white bar) or Fh-Teg PBMC (black bar) mice. Accumulated data illustrating the total number of activated, naïve, Tem and Tcm $CD8^+$ cells recovered from the spleen (B), livers (D) and lungs (F) of PBMC or Fh-Teg PBMC mice. n=12 per group (4 PBMC donors). The total number of human lymphocytes was assessed using counting beads during flow cytometry. Statistical significance was determined using student *t*-test where * < 0.05, ** < 0.005.

5.20. FH-TEG SIGNIFICANTLY REDUCES THE ENGRAFTMENT OF PRO- INFLAMMATORY CYTOKINE PRODUCING HUMAN T CELLS

One of the key characteristics of aGvHD is the production of pro-inflammatory cytokines such as TNF-α, IFN-γ and IL-2 (Ferrara *et al.* 2009). Therefore, it was hypothesised that stimulation of PBMC with Fh-Teg before administration may impair the ability of PBMC to produce these cytokines *in vivo* and subsequently result in the reduced mortality and GvHD pathological score observed in figure 5.31.

The level of circulating human TNF-α was analysed in serum obtained through facial bleeds taken from PBMC and Fh-Teg PBMC mice 10 days after transplantation and analysed by ELISA. There was a significant reduction in the amount of human TNF-α detected from mice which received Fh-Teg PBMC during acute GvHD (Figure 5.39). Control mice, which were transplanted with PBS rather than PBMC, had no detectable levels of human TNF-α.

In order to determine the underlying factor behind the reduction of human TNF-α in the serum of Fh-Teg PBMC mice, intra-cellular flow cytometry was performed on human T cells recovered from PBMC and Fh-PBMC mice for the production of TNF-α, IFN-γ and IL-2. Human $CD4^+$ and $CD8^+$ lymphocytes were isolated from the spleens, livers and lungs of PBMC and Fh-Teg PBMC and analysed for the expression of human TNF-α, IFN-γ and IL-2. Analysis of human $CD4^+$ lymphocytes from the spleen demonstrated that pre-stimulation of PBMC with Fh-Teg before administration had no effect on the percentages of $CD4^+$ lymphocytes producing human TNF-α, IFNγ or IL-2 (Figure 5.40 A); however a significant reduction in the total number of human TNF-α, IFN-γ and IL-2 producing $CD4^+$ lymphocytes recovered from the spleens of mice was observed in Fh-Teg PBMC mice (Figure 5.40 B). Apart from one PBMC donor, which had a significantly higher percentage of IFN-γ producing $CD8^+$ cells, there were no

detectable differences in the percentages of human TNF-α, IFN-γ or IL-2 producing $CD8^+$ lymphocytes recovered from the spleen (5.41 A). The total number of human $CD8^+$ lymphocytes which were producing TNF-α, IFN-γ and IL-2 was also significantly lower in Fh-Teg PBMC mice (Figure 5.41 B).

As mentioned above the systemic pathology associated with aGvHD is driven by the ability of donor T cells to migrate to target organs such as the liver and the lungs. Another key factor to consider is whether these infiltrating T cells are producing pro-inflammatory cytokines. Therefore the ability of infiltrating $CD4^+$ and $CD8^+$ T lymphocytes to produce human TNF-α, IFN-γ and IL-2 was analysed on lymphocytes recovered from the liver and the lungs of GvHD mice. Pre-treating PBMC with Fh-Teg had no significant effect on the percentage of human TNF-α, IFN-γ or IL-2 producing $CD4^+$ T cells which had infiltrated the liver (Figure 5.40 C). Similar to the spleen however, the total number of human TNF-α, IFN-γ or IL-2 producing $CD4^+$ T cells recovered from the liver was significantly reduced in Fh-Teg PBMC mice (Figure 5.40 D). The percentages of human TNF-α, IFN-γ or IL-2 producing $CD8^+$ T cells in the liver was also unaffected by pre-stimulating the PBMC with Fh-Teg (Figure 5.41 C). The total number of infiltrating $CD8^+$ T cells capable of producing TNF-α, IFN-γ or IL-2 was significantly reduced in the livers of Fh-Teg PBMC mice (Figure 5.41 D). The pre-treatment of PBMC with Fh-Teg had no effect on the percentages of human TNF-α, IFN-γ or IL-2 producing $CD4^+$ T cells which had infiltrated the lung (Figure 5.40 E). The total number of human TNF-α, IFN-γ or IL-2 producing $CD4^+$ T cells recovered from the lung was significantly reduced in Fh-Teg PBMC mice (Figure 5.40 F). The percentages of human TNF-α, IFN-γ or IL-2 producing $CD8^+$ T cells recovered from the lung was also unaffected by pre-stimulating the PBMC with Fh-Teg (Figure 5.41 E). The total number of infiltrating $CD8^+$ T cells capable of producing TNF-α, IFN-γ or IL-2 was significantly reduced in the lungs of Fh-Teg PBMC mice (Figure 5.41 F).

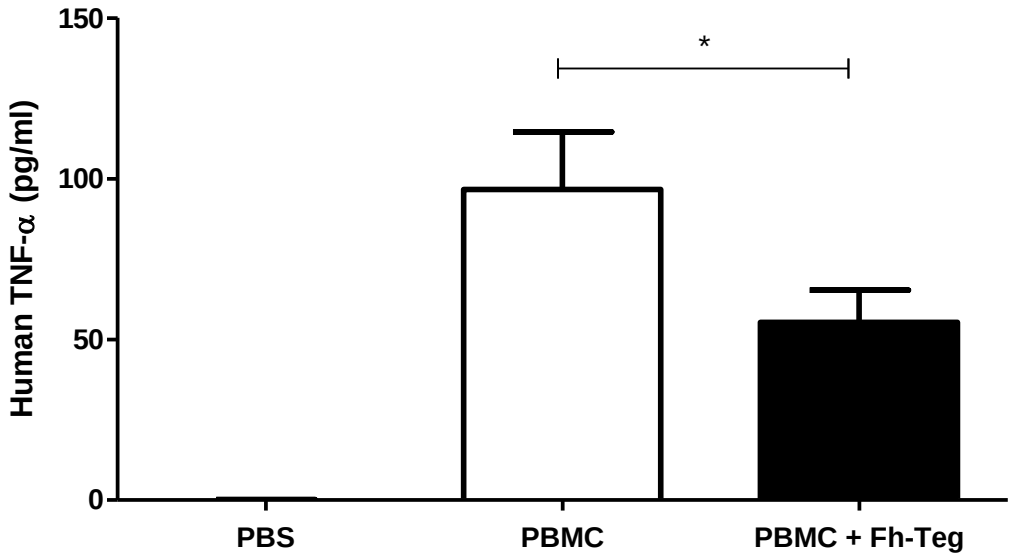

Figure 5.39. Fh-Teg stimulation significantly reduced levels of human TNF-α in the serum of aGvHD mice. NSG mice which were sub-lethally irradiated (2.4 Gy) and given PBMC or Fh-Teg PBMC ($1x10^6$ per gram) via tail vein injection. On day 10, post transplantation, facial bleeds were performed on PBS control mice (not detected), PBMC mice (white bar) and Fh-Teg PBMC mice (black bar) and the presence of human TNF-α was determined using ELISA. n=20 per group (4 PBMC donors). Statistical significance was determined using student *t*-test where * < 0.05.

Spleen

(A)

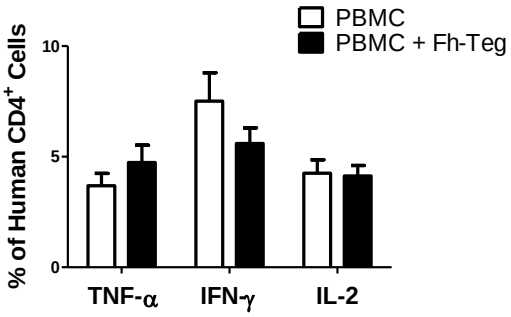

(B)

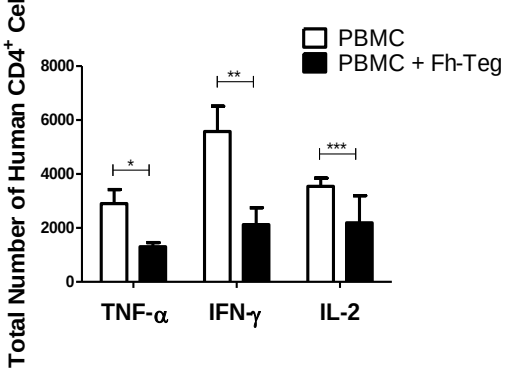

Liver

(C)

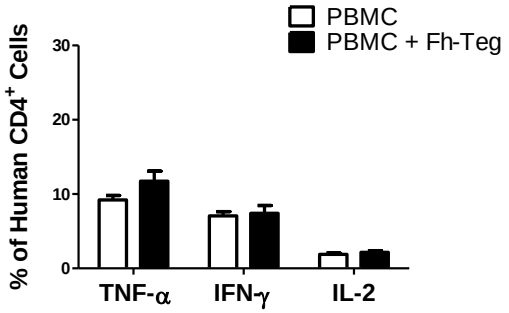

(D)

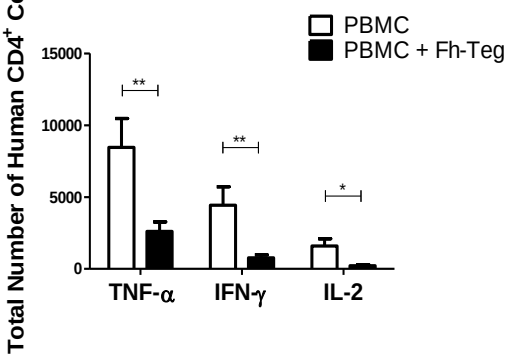

Lung

(E)

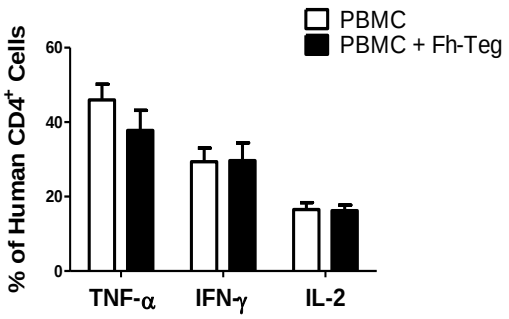

(F)

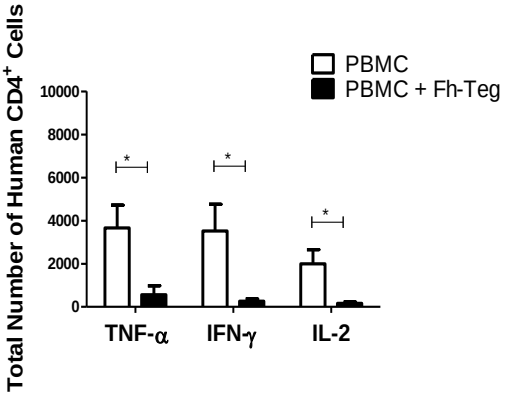

Figure 5.40. Fh-Teg significantly reduced the number of human TNF-α, IFN-γ and IL-2 producing $CD4^+$ T cells in aGvHD mice. NSG mice were sub-lethally irradiated (2.4 Gy) and given PBMC or Fh-Teg PBMC ($1x10^6$ per gram) via tail vein injection were analysed on day 12 by intra-cellular flow cytometry. Graphical representation of the TNF-α, IFN-γ and IL-2 producing $CD4^+$ T cells recovered from the spleen (A), liver (C) and lung (E) from PBMC (white bar) or Fh-Teg PBMC (black bar) mice. Accumulated data for total cell number of cytokine producing $CD4^+$ T cells recovered from the spleen (B), liver (D) and lung (F). n=12 per group (4 PBMC donor). The total number of human $CD4^+$ lymphocytes was assessed using counting beads during flow cytometry. Statistical significance was determined using student *t*-test where * < 0.05, ** <0.005 and *** < 0.001.

Spleen

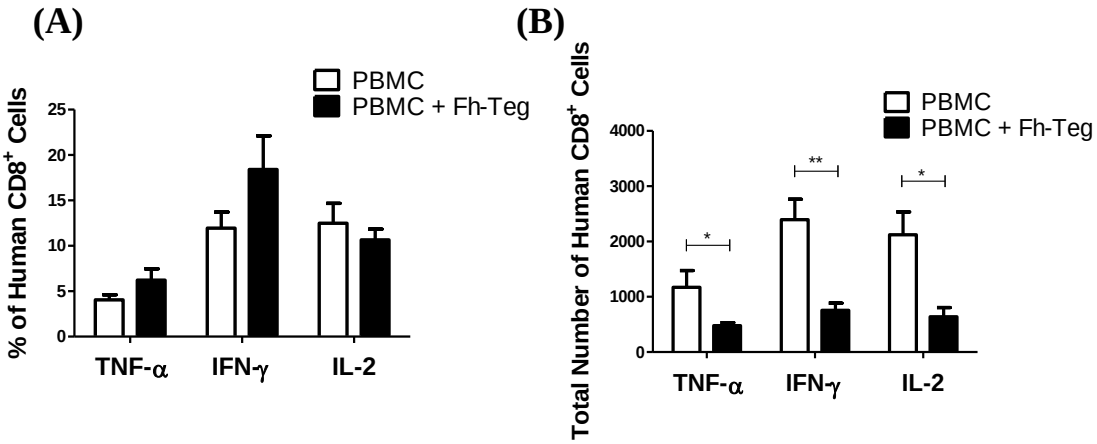

Liver

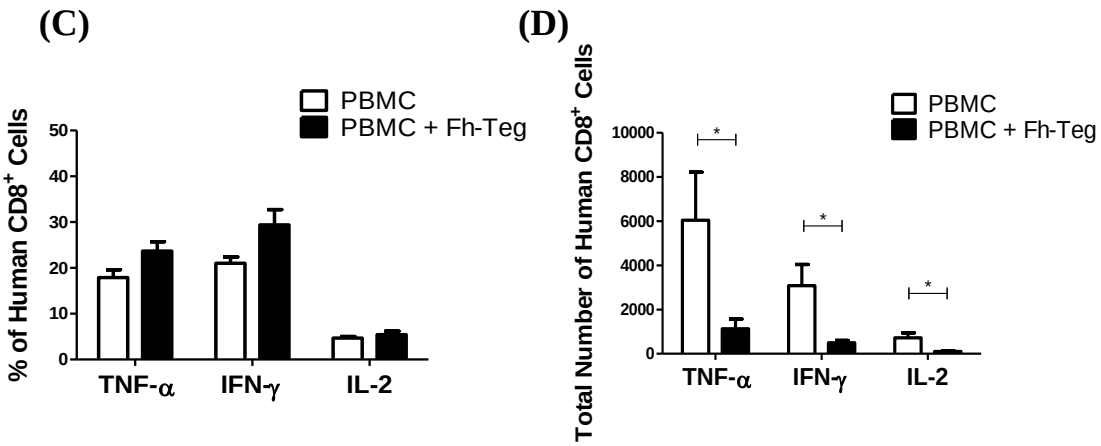

Lung

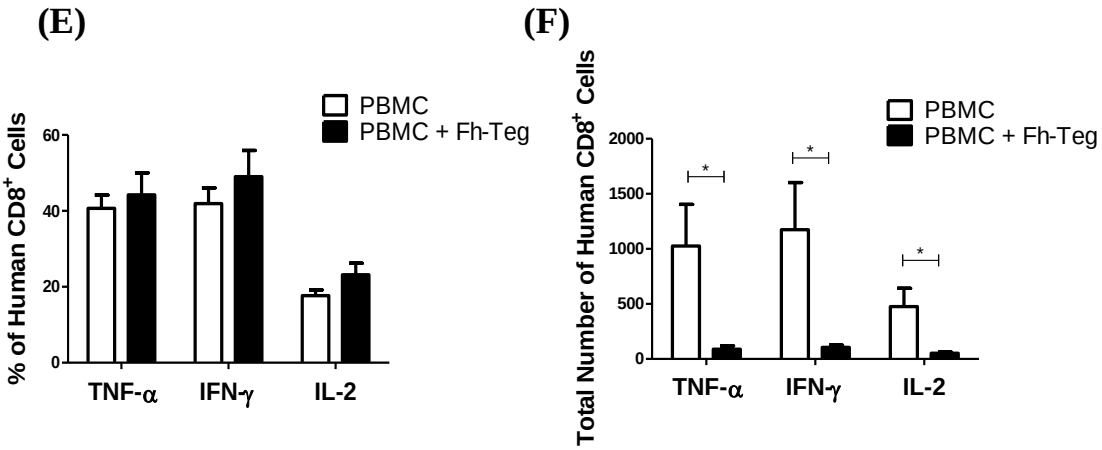

Figure 5.41. Fh-Teg significantly reduced the number of human TNF-α, IFN-γ and IL-2 producing $CD8^+$ T cells in aGvHD mice. NSG mice were sub-lethally irradiated (2.4 Gy) and given PBMC or Fh-Teg PBMC ($1x10^6$ per gram) via tail vein injection were analysed on day 12 by intra-cellular flow cytometry. Graphical representation of the TNF-α, IFN-γ and IL-2 producing $CD8^+$ T cells recovered from the spleen (A), liver (C) and lung (E) from PBMC (white bar) or Fh-Teg PBMC (black bar) mice. Accumulated data for total cell number of cytokine producing $CD8^+$ T cells recovered from the spleen (B), liver (D) and lung (F). n=12 per group (4 PBMC donor). The total number of human $CD8^+$ lymphocytes was assessed using counting beads during flow cytometry. Statistical significance was determined using student *t*-test where * < 0.05, ** <0.005.

5.21. Fh-Teg significantly reduces pathology in aGvHD mice

The target organs involved in acute GvHD pathology include the liver, spleen gut and lung. As seen in Figure 5.31, PBMC which had been pre-treated with Fh-Teg resulted in significantly lower pathological scores. Therefore, histological analysis was carried out on GvHD target organs to compare the effect of PBMC to Fh-Teg PBMC on GvHD pathology.

Irradiation and PBS administration did not adversely affect the lung architecture of control mice or induce pathology as measured by lymphocyte inflammation around peribronchial areas (L) or airway epithelium thickening (T) (Figure 5.42). PBMC mice had large accumulations of lymphocytes around peribronchial areas and demonstrated distinct epithelium thickening around the airways in the lungs (Figure 5.42). In accordance with the flow cytomtetry data presented above, Fh-Teg PBMC mice demonstrated reduced lymphocyte infiltration in the lung. Despite the reduction in lymphocyte infiltration there was no observable difference in airway epithelium thickening when compared to PBMC mice (Figure 5.42).

PBS control mice demonstrated no adverse effect on liver pathology, as measured by lymphocyte infiltration (L) and damage to the structural integrity of the liver (D). Although the liver is a major target for GvHD, very little pathology was observed in PBMC or Fh-Teg PBMC mice on day 12. However PBMC mice did display large amounts of lymphocyte infiltration around periportal areas of the liver (Figure 5.42). The administration of Fh-Teg PBMC resulted in a significant decrease in the level of infiltrating lymphocytes in the liver, particularly at periportal ducts (Figure 5.42). GvHD pathology of the small intestine was determined by lymphocyte infiltration (L) and villous destruction (V). The administration of PBS to irradiated mice did not result in any pathology within the gut (Figure 5.42). PBMC mice demonstrated a significant increase

in gut pathology. There was a significant increase in the frequency of villous destruction which was accompanied by the infiltration of human lymphocytes (Figure 5.42). There was no significant difference in pathology observed in the gut of Fh-Teg PBMC (Figure 5.42). There was a similar level of destruction to villi and also with a similar level of lymphocyte infiltration as was observed in PBMC mice (Figure 5.42). Irradiated control mice treated with PBS had very little structural architecture of the spleen (Figure 5.42). While the red pulp (RP) and white pulp (WP) of the spleen was clearly visible there were no resident lymphocytes. The administration of PBMC resulted in lymphocyte infiltration to the spleen and human lymphocytes can be clearly seen in the red pulp of the spleen (Figure 5.42). As seen with the spleen and the liver, there was a visible reduction in the amount of lymphocytes present in the spleens of Fh-Teg mice (Figure 5.42). Lymphocytes present in the spleens of Fh-Teg mice were found only in the red pulp.

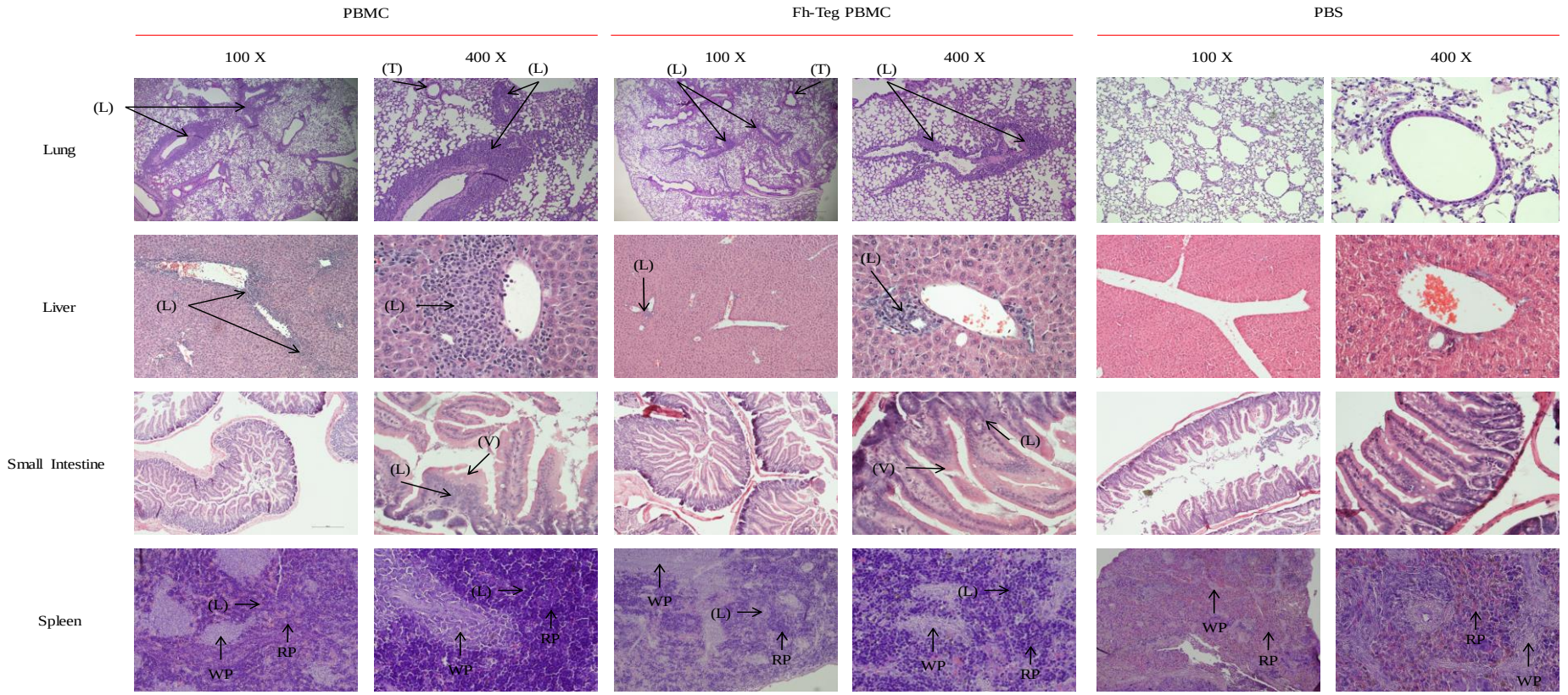

Figure 5.42. Fh-Teg PBMC resulted in reduced pathology and lowered lymphocyte infiltration in the lung, liver and spleens of aGvHD mice. NSG mice which were sub-lethally irradiated (2.4 Gy) and given PBMC or Fh-Teg PBMC ($1x10^6$ per gram) via tail vein injection, on day 12. Tissue samples were paraffin embedded and stained with H&E and representative images analysed for lymphocyte infiltration (L), villi destruction (V), thickening of epithelial airways (T) or red pulp (RP) and white pulp (WP) in the spleen and representative images are displayed for each group. n=12 per group (4 PBMC donors). Tissues samples were stained using H&E and images captured at 100X and 400X.

5.22. SUMMARY II

The main aims of this section were to examine (1) whether Fh-Teg treatment of PBMC could promote survival in GvHD mice, (2) to investigate the effect of Fh-Teg on the engraftment of PBMC within NSG mice and (3) to determine the effect of Fh-Teg on T cell function *in vivo* as measured by the expression of memory T cell markers and the ability of T cells to produce pro-inflammatory cytokines in response to xenogeneic stimulation. The pre-treatment of PBMC with Fh-Teg significantly reduced mortality and GvHD pathological score in xenogeneic mouse model (Figure 5.31). The administration of Fh-Teg PBMC also resulted in the detection of significantly lower levels of human TNF-α in the serum of GvHD mice after 10 days (Figure 5.39). Moreover, the engraftment of human $CD45^+$ lymphocytes within NSG mice was significantly impaired after PBMC were treated with Fh-Teg (Figure 5.32). As previously described, the number of PBMC which engraft within irradiated NSG mice correlates with the development of GvHD in this model. Therefore the increase in survival and reduced pathological score observed in Fh-Teg PBMC mice was a result of the impaired engraftment of human T cells and subsequently delayed the development of GvHD (Figure 5.31). The detection of significantly lower levels of human TNF-α in the serum of Fh-Teg PBMC mice can also be explained by the presence of fewer cytokine producing T cells in the mouse rather than the ability of Fh-Teg to prevent TNF-α production per se (Figure 5.39). This data demonstrates the usefulness of the model as a platform to test novel immunomodulatory agents.

CHAPTER 6

DISCUSSION

6.1 MSC support B cell survival through cell contact dependent up-regulation of VEGF

In 1991, Arnold Caplan predicted a major role for MSC therapy in regenerative medicine, particularly in terms of the replacement or regeneration of damaged tissue (Caplan 1991). However, over the past decade, the focus of MSC therapies has shifted away from the regeneration of damaged tissues and towards the development of a cell therapy capable of modulating inflammation and immune mediated disease. The idea that trophic factors produced by MSC could be used to modulate the immune system was proposed (Haynesworth *et al.* 1996) before initial studies examining the administration of autologous MSC therapy proved feasible and safe (Koç *et al.* 2000). However it was not until the ability of MSC to modulate inflammation and immune cell function in an allogeneic setting was determined (Bartholomew *et al.* 2002; Aggarwal & Pittenger 2005) that the field of MSC therapy garnered the attention of the scientific community. The ability to bypass allogeneic immune recognition facilitates the clinical transfusion of allogeneic MSC therapy without rejection, facilitating the development of a standardised, regulatable "off the shelf" cell therapy against inflammatory and immune mediated diseases.

Clinical trials have demonstrated the beneficial potential of MSC as a novel cell therapy, particularly against GvHD, Crohn's disease and myocardial infarction (Duijvestein *et al.*, 2010; Hare *et al.*, 2009; Prasad *et al.*, 2011). Despite these recent advances, there are outstanding questions which need to be addressed before the full potential of MSC therapy can be realised. The main unresolved issues include the optimal conditions for large scale manufacturing of MSC, the persistence and bio-distribution of MSC *in vivo* and the widespread clinical use of MSC therapy without a complete understanding of their mechanisms of action. To address these outstanding issues and develop an optimised MSC therapy for routine clinical use, it is essential to take a step

back from clinical administration and develop novel models of disease designed to characterise how MSC therapy perform mechanistically in clinically relevant systems.

The ability of MSC to suppress the adaptive immune system is a key feature in the development of MSC therapy, however the progress in elucidating the mechanisms by which MSC modulate T cells and B cells has not progressed at the same rate. The mechanism by which MSC attract and suppress activated T cells has been thoroughly characterised and is mediated through a combination of chemokines (Ren *et al.* 2008), cell contact signals and immunosuppressive soluble factors (Di Nicola 2002). The expression of CXCR3 on MSC attracts T cells (Ren *et al.* 2008) before binding via the expression of ICAM-1 and VCAM-1 (Ren *et al.* 2010). The immunosuppressive soluble factors secreted by MSC are known to include HGF, TGF-β (Di Nicola 2002), IDO (Meisel *et al.* 2004), PGE_2 (Németh *et al.* 2009), IL-10 (Yang *et al.* 2009), IL-6 (Najar *et al.* 2009), semaphorin-3A, Galectin-1 (Lepelletier *et al.* 2010), Galectin-9 (Gieseke *et al.* 2013), adenosine (Sattler *et al.* 2011) and TSG-6 (Lee *et al.* 2009; Oh *et al.* 2010; Prockop & Oh 2012). In addition to directly suppressing effector T cells, MSC are also capable of promoting the generation of Treg cells (Maccario *et al.* 2005; Di Ianni *et al.* 2008) as well as inducing T cell apoptosis (Akiyama *et al.* 2012). The characterisation of how MSC modulate T cell function *in vitro* has led to hypothesis driven experiments (in animal models of T cell mediated disease) to examine the immuno-suppressive ability of MSC *in vivo*. These studies successfully demonstrated impaired T cell responses (González *et al.* 2009b; Chiesa *et al.* 2011; Tobin *et al.* 2013) and expansion of Treg cell populations (Boumaza *et al.* 2009; Madec *et al.* 2009) in models of GvHD, colitis and diabetes. However, under certain conditions, MSC have the potential to support T cell proliferation and sustain disease through IL-7 production (Nemoto *et al.* 2013), highlighting the necessity to fully understand how MSC therapy will respond following clinical

administration. In stark contrast to the detailed characterisation of T cell suppression by MSC, the effect of MSC on B cell function remains less clear (Franquesa *et al.* 2012).

B cells are major regulators of the adaptive immune system and the activation and rapid proliferation of peripheral B cells in response to antigen recognition is essential to the development of a functional immune response (Pieper *et al.* 2013). Accordingly, to develop a complete understanding of how MSC therapy will respond following administration it is essential to elucidate exactly how MSC interact with and modulate B cell function. Therefore chapter 3 of this thesis was dedicated to determining how MSC affect B cell biology in terms of activation, proliferation and survival and to elucidating the mechanisms involved.

Studies on the effect of MSC on B cell biology *in vitro* have reported conflicting results (Corcione *et al.* 2006; Tabera *et al.* 2008; Rasmusson *et al.* 2007; Traggiai *et al.* 2008; Franquesa *et al.* 2012). The majority of the major *in vitro* published data suggest that MSC inhibit the proliferation and antibody production of adult B cells (Corcione *et al.* 2006; Comoli *et al.* 2008; Tabera *et al.* 2008); contrary to this however, a number of published studies suggest that MSC support proliferation and antibody production (Rasmusson *et al.* 2007; Traggiai *et al.* 2008). The reasons for such conflicting results is likely due to variability among experimental protocols used between different laboratories resulting in very varied B cell populations. In the aforementioned studies, starting B cell populations vary between whole PBMC (Comoli *et al.* 2008; Traggiai *et al.* 2008) and purified B cells (Corcione *et al.* 2006; Rasmusson *et al.* 2007; Tabera *et al.* 2008). The ratio of MSC to B cells also varies from 1:1 to 1:20 and a single defined B cell activating protocol was not implemented throughout these studies. In support of this theory, a recent publication has demonstrated that MSC have the potential to either inhibit or support B cell proliferation depending on the presence of T cells in the co-culture (Rosado *et al.* 2014). In addition to the variability of experimental protocol, a significant

inhibitory factor to determining how MSC modulate B cells is that the mechanism by which MSC support or suppress B cell biology has not yet been established. In the previous studies, Rasmusson *et al.* and Traggiai *et al.* demonstrate the requirement for cell contact to support B cell antibody production (Rasmusson *et al.* 2007; Traggiai *et al.* 2008) while the work published by both Corcionne *et al.* and Comoli *et al.* demonstrate that inhibition of B cell proliferation and antibody production was mediated through soluble factors (Corcione *et al.* 2006; Comoli *et al.* 2008). Given that T cell contact signals are required for B cell help, and that activated T cells bind to MSC it is possible that confounding factors have influenced these data and their interpretation.

The initial experiments of this project were designed to identify the effect of MSC on a purified population of human $CD19^+$ B cells. In chapter 3, we demonstrated that MSC enhanced the activation and proliferation of purified $CD19^+$ B cell populations through a contact dependent mechanism. This parallels previous observations reported by Traggiai *et al.* (Traggiai *et al.* 2008), but importantly identifies that enhanced B cell activation was not influenced by allogeneic recognition of MSC; B cells cultured in the presence of MSC without cytokine activation did not significantly increase CD69, CD80, CD86 or CD25 expression. As described in section 1.3, the clonal expansion of activated B cells is essential for the development of antibody producing effector B cells and generally occurs within secondary lymphoid tissues. It is now clear that transplanted MSC have the capacity to migrate to lymph nodes (Schwarz *et al.*, 2014). Thus the administration of MSC in concurrence with B cell activation may lead to enhanced expansion of B cells; which in the case of B cell driven or idiopathic disease may be detrimental to the patient. This premise is consistent with experimental data; the administration of allogeneic MSC in a murine model of lupus resulted in exacerbated disease (Youd *et al.* 2010) and is a good example of the potential adverse effects

associated with MSC therapy if promoted without adequate experimental understanding of the functional mechanisms.

Antibody production by activated B cells is one of the hallmarks of B cell mediated disease; however the ability of MSC to support or inhibit antibody production is also a contentious issue. The studies conducted by Traggiai *et al.* observed increased IgG and IgM when B cells from lupus patients were cultured in the presence of MSC, while Rasmusson *et al.* reported increased IgG production by healthy B cells following culture with MSC (Traggiai *et al.* 2008; Rasmusson *et al.* 2007). In contrast to these studies, our data showed that MSC had no effect on the IgG or IgM production by purified $CD19^+$ B cells. These differential findings might be caused by variances in experimental setup as the ratio of B cell to MSC, activating molecules and the purity of B cell populations all differ between our studies. Some of these studies used ratios of 1:1 or 1:2, however, these ratios are extremely unlikely to occur *in vivo*. In an attempt to create a more physiologically relevant system, our study utilised a B cell:MSC co-culture ratio of 5:1. Although total levels of IgG and IgM are commonly analysed by ELISA, it may also be possible that the ELISA kit used in our experiments became completely saturated making it impossible to determine any differences between samples. Another possibility is that the cytokine cocktail used to activate B cells in this experiment may have been sufficient to maximise B cell production of IgG and IgM. IL-21 is a known to induce plasma cell differentiation and IgG production (Ettinger *et al.* 2005) and is notably absent from the studies which reported increased IgG (Rasmusson *et al.* 2007; Traggiai *et al.* 2008). Therefore, the activation cocktail used to stimulate B cells in this study may have maximised IgG and IgM production, making it impossible to detect any increases in the presence of MSC.

In vivo, MSC function as stromal cells and are essential for maintaining the haematopoietic stem cell niche within the bone marrow (Mendez-Ferrer *et al.*, 2010;

Tokoyoda *et al.*, 2010). In adults, B cell development occurs within this MSC supported environment (Uccelli *et al.* 2006) and we hypothesised that *in vitro* B cell:MSC co-cultures mimic the HSC niche where MSC support the survival of B cells. Indeed, B cell viability was significantly increased in the presence of MSC and this was mediated through a cell contact dependent mechanism (Section 3.6). This result supports previous work by Tabera *et al.* (2008), but further demonstrates MSC influence on purified B cell populations and highlights the requirement for cell contact. In contrast to this study however, Tabera *et al.* demonstrated inhibition of B cell proliferation during MSC co-culture (Tabera *et al.*, 2008). The difference in results between these two studies likely lies in the activation status if the B cells. In our study B cells were activated with CD40L and CpG in the presence of B cell supportive cytokines IL2, IL-10 and IL-21, while the study of Tabera *et al.* used anti-Ig and IL-4 in conjunction with CD40L and CpG during B cell activation. The B cell supportive cytokines IL-2, IL-10 and IL-21 were included in our study in an attempt to create a similar micro-environment to that encountered by B cells during an activating immune response (Ettinger *et al.* 2005) and may be more supportive of B cell viability than anti-Ig and IL-4. Increased B cell survival when exposed to MSC may well offer an explanation to the increased activation and proliferation, as more viable population of B cells would be more responsive to the activation cytokines. Thus the B cell:MSC interaction is likely to be further modulated by T cells *in vivo*; but the major effect of MSC on activated B cells is supportive of expansion when mature T cells are absent. This finding has consequences for cell therapy in terms of disease targets and especially the route and timing of administration.

While a requirement for cell contact has previously been identified for MSC support of B cell proliferation (Rasmusson *et al.* 2007; Traggiai *et al.* 2008) no further advances in defining how MSC modulate B cell biology have been reported. Identifying the mechanisms behind MSC modulation of T cell function has provided a platform from

which to design effective MSC therapies. Therefore, it was hypothesised that identifying the mechanism involved in MSC support of B cell survival would further our understanding of how MSC interact with B cells and provide valuable information regarding the development of future *in vivo* studies. With cell contact dependency already established, a detailed review of the literature identified a number of potential cell surface proteins which may have a role in signalling between MSC and B cells. The first standout target identified was B cell activating factor (BAFF). Under normal physiological conditions, BAFF signalling is a potent inducer of B cell expansion and survival (Schneider *et al.*, 1999). In addition to this, the expression of BAFF on the surface of adipocyte derived MSC has been described (Wang *et al.*, 2011). Therefore, the possibility that BAFF signalling was mediating MSC support on B cell survival and proliferation was investigated. Although low levels of constitutive BAFF expression were detected on our bone marrow derived MSC, this expression was significantly up-regulated following stimulation with pro-inflammatory cytokines IFN-γ or TNF-α suggesting that in the presence of the correct signals our MSC could express high levels of BAFF. However, neutralising BAFF signalling in our system did not prevent MSC from enhancing B cell proliferation, indicating that MSC support of B cell *in vitro* expansion was not dependent on BAFF.

An alternative cell contact dependent signalling pathway known to have a role in B cell survival is notch. Notch signalling is a highly conserved immune regulatory pathway with established roles in immune cell development, proliferation, differentiation and survival (Fiuza and Arias, 2007). The development of peripheral B cells is dependent on notch signalling (Thomas *et al.*, 2007) and the importance of the notch signalling pathway in immune modulation by MSC has been established. The ability for MSC to inhibit DC maturation and antigen presentation (Chen *et al.*, 2007) as well as the induction of regulatory T cells (Del Papa *et al.*, 2013) are mediated through notch signalling. The

role of notch signalling during interactions between MSC and both innate and adaptive immune cells and the dependence on notch for B cell development highlighted notch as a potential candidate for the contact signal mediating MSC support of B cell survival. In addition, MSC have previously been shown to support the survival of B acute lymphocyte leukemia (B-all) cells through signalling through notch 3/4 (Nwabo Kamdje *et al.* 2011). However, blocking studies, described in section 3.8, demonstrated that notch signalling was not essential for MSC support of B cell survival in our study.

To elucidate the cell contact dependent mechanism behind MSC modulation of B cell biology it was necessary to explore more indirect pathways. MSC are known to modulate immune cells through the secretion of a wide range of immune-modulatory soluble factors (Barry *et al.* 2005). Hence, it was hypothesised that cell contact between MSC and B cells was triggering the production of a soluble anti-apoptotic signal by the MSC which in turn was promoting B cell survival. As before, a comprehensive review of existing literature was used to identify potential candidates and identified VEGF as an interesting target. VEGF has been described as one of the most important factors controlling angiogenesis (Leung *et al.* 1989; Keck *et al.* 1989) but an important role for VEGF in anti-apoptotic signalling has also been established (Abid *et al.*, 2004; Xia *et al.*, 2009). In fact, the addition of recombinant VEGF to TNF-α induced apoptotic epithelial cells *in vitro* was sufficient to induce survival in 80 - 90% of cells (Spyridopoulos *et al.*, 1997). Interestingly, VEGF production by MSC has also been identified as a major contributor to MSC support of angiogenesis (Beckermann *et al.* 2008). Therefore it was hypothesised that B cell contact stimulated VEGF production by the MSC and that increased levels of VEGF induced anti-apoptotic signalling in the B cell in our system. In agreement with published data, resting MSC constitutively produced VEGF (Section 3.9). Interestingly, a significant up-regulation in VEGF was detected following MSC contact with B cells. The level of VEGF production by MSC was also very similar to the

previously published concentrations of recombinant VEGF capable of protecting endothelial cells from apoptosis (Spyridopoulos *et al.,* 1997). The physiological relevance of this VEGF up-regulation was investigated using a blocking antibody. Significant differences between the levels of B cell survival with or without the VEGF inhibitor were noted. MSC support of B cell survival was completely abrogated when VEGF signalling was blocked. The anti-apoptotic signalling pathway associated with VEGF signalling is mediated through the phosphorylation of AKT and results in a reduction in caspase 3 cleavage (Abid *et al.,* 2004; Xia *et al.,* 2009; Zhou *et al.,* 2000). MSC support of B cell survival mirrored this increase in phosphorylated AKT (pAKT) and dramatically reduced levels of cleaved caspase 3; these levels were completely restored by the addition of the VEGF inhibitor. At this stage we had a strong indication of a mechanism driving MSC support of B cell survival; however the cell contact signal required to initiate the process had yet to be identified.

Following the same approach as before, we studied the literature in search of cell contact signals associated with cell survival and VEGF production. CXCR4-CXCL12 binding has previously been reported to result in the up-regulation of VEGF production (Liang *et al.,* 2007) and in addition to this the constitutive expression of CXCR4 by B cells and the expression of its ligand CXCL12 by the MSC (Nakao *et al.* 2010) identified CXCR4-CXCL12 as an attractive candidate for the contact signal required for MSC production of VEGF. However, inhibiting CXCR4 binding in our system had no effect on the ability of MSC to promote B cell survival, suggesting that CXCR4 is not essential for MSC support of B cell viability.

An interesting alternative to CXCR4-CXCL12 signalling involved stimulation of the EGFR, a member of the tyrosine kinase family of receptors which play an important role in cell survival and proliferation (Wells, 1999). The expression of the EGFR on human bone marrow derived MSC has previously been reported and its activation results

in significant up-regulation of pro-angiogenic factors including VEGF (De Luca *et al.* 2011). The EGFR is stimulated by a range of ligands, many of which are expressed by peripheral B cells, and so a specific neutralising antibody targeting EGFR on the MSC was used in our system. The EGFR was determined to be essential for MSC viability and therefore the highest dose of inhibitor which did not kill the MSC was used. The addition of the EGFR inhibitor to MSC and B cell co-cultures did not prevent MSC support of B cell survival. However, the concentration of EGFR used may not have been sufficient to completely neutralise signalling (this could not be demonstrated) and therefore stimulation through the EGFR cannot be ruled out as the contact signal between MSC and B cells.

Chapter 3 was designed to determine how MSC affect the activation, proliferation and survival of peripheral $CD19^+$ B cells and to elucidate the mechanisms by which MSC modulate B cell biology. Although the critical cell contact signal between MSC and B cells remains to be elucidated, the data presented here represents a step forward in understanding the mechanism by which MSC support the activation, proliferation and survival of purified $CD19^+$ B cells. This study reveals that cell contact between purified B cells and MSC induces a significant up-regulation of VEGF production by the MSC. VEGF induces the up-regulation of pAKT and inhibits caspase 3 mediated $CD19^+$ B cell apoptosis (Figure 6.1).

The lack of a unique surface profile for MSC has limited the identification of MSC function *in vivo*; however, the information which has been gathered to date suggests that *in vivo* MSC support the HSC niche within the bone marrow (Méndez-Ferrer *et al.* 2010; Anthony & Link 2014). In addition to this long lived memory B and T cells reside in the bone marrow, and more specifically in the presence of IL-7 producing $CXCL12^+$ stromal cells (Tokoyoda *et al.* 2009). MSC production of the pro-survival factor IL-7 has been previously characterised (Chen *et al.* 2006) along with the surface expression of CXCL12

(Nakao *et al.* 2010). Despite the potent suppression of T cell activation and proliferation, MSC have also been shown to support T cell survival *in vitro* (Benvenuto *et al.* 2007). Therefore it is reasonable to suggest that support of B cell survival described in this study may be a reflection of the natural stromal properties of MSC.

An emerging hypothesis from the field of B cell immune regulation is that the generation of an immunosuppressive subpopulation of B cells termed regulatory B cells contributes to immune regulation (Fillatreau *et al.* 2002). Regulatory B cells represent a very rare population, they lack a unique surface marker profile, are characterised by expression of $CD1d^{high}CD5^{+}$ and IL-10 production (Wang *et al.* 2014). A recent publication has suggested that MSC are capable of generating regulatory B cells *in vitro* (Franquesa *et al.* 2014). In terms of our study it would be interesting to examine if the support of B cell survival and proliferation observed here contributes to the generation or expansion of a regulatory B cell population.

In order to further the development of MSC towards clinical application it is essential to clarify exactly how MSC interact with all cells of the immune response and design more tailored approaches to MSC treatment. This study has furthered our understanding of how MSC interact directly with peripheral B cell populations *in vitro* and has provided key information for future studies into the relationship between MSC and B cells. The limitation associated with all *in vitro* experiments is that *in vitro* experiments are manufactured systems designed to mimic a naturally occurring environment and this can lead to inconsistencies in results following progression to animal models. Therefore while this study represents a major step forward in identifying how MSC interact with B cells, it is essential to remember that from here we can merely hypothesise what might happen *in vivo*.

Pre-clinical studies examining the potential of MSC therapy to treat B cell mediated autoimmune diseases have provided conflicting results. The majority of studies examining MSC therapy in SLE and MS have demonstrated beneficial effects (Zhou *et al.* 2008; Gu *et al.* 2010; Zappia *et al.* 2005; Rafei *et al.* 2009); however studies carried out by Glenn *et al.* and Youd *et al.* have reported increased pathology after MSC therapy in models of EAE and SLE respectively (Glenn *et al.* 2014; Youd *et al.* 2010). Youd *et al.* reported significantly increased pathology mediated by increased proliferation of autoimmune B cells during murine models of SLE (Youd *et al.* 2010). The increased B cell survival and enhanced proliferation observed in this thesis supports the increased B cell proliferation described by Youd *et al.*, however we did not observe the increased antibody production reported in their study. Whether MSC therapy is beneficial or harmful during B cell mediated disease may be dependent on the stage of disease at the time of administration. Our data suggest that administering MSC during a stage of B cell activation and extensive proliferation would support this process and potentially exacerbate disease. Alternatively, administering MSC therapy during a different phase of disease progression may have beneficial effects, however without substantial *in vivo* evidence we can only speculate on what may happen. Despite conflicting results and the absence of clear mechanistic data on how MSC modulate B cell function, phase I clinical trials examining the effect of MSC therapy on B cell mediated diseases RA (Wang *et al.* 2013) and SLE (Sun *et al.* 2010; Sun *et al.* 2009; D. Wang *et al.* 2014) have already been completed and have progressed to phase II. While these phase I trials were primarily designed to investigate the feasibility and safety of MSC therapy in RA or SLE, the authors have also suggested slight improvements in patient condition after MSC therapy after 18 months. There are some potential explanations as to the variation between what our results predict and what has been observed in patients. The main reason being that our system was designed to examine the direct effect of MSC on B cell function.

Following *in vivo* administration the MSC will encounter a complete immune system and an extensive range of cytokines. The recent publication by Rosado *et al.* (2014) demonstrated that MSC were capable of either supporting or inhibiting B cell proliferation depending on the presence of T cells. Although RA and SLE are primarily B cell mediated diseases, T cell help is still an essential component. Therefore, MSC therapy may indirectly inhibit B cell function through the inhibition of T cell proliferation.

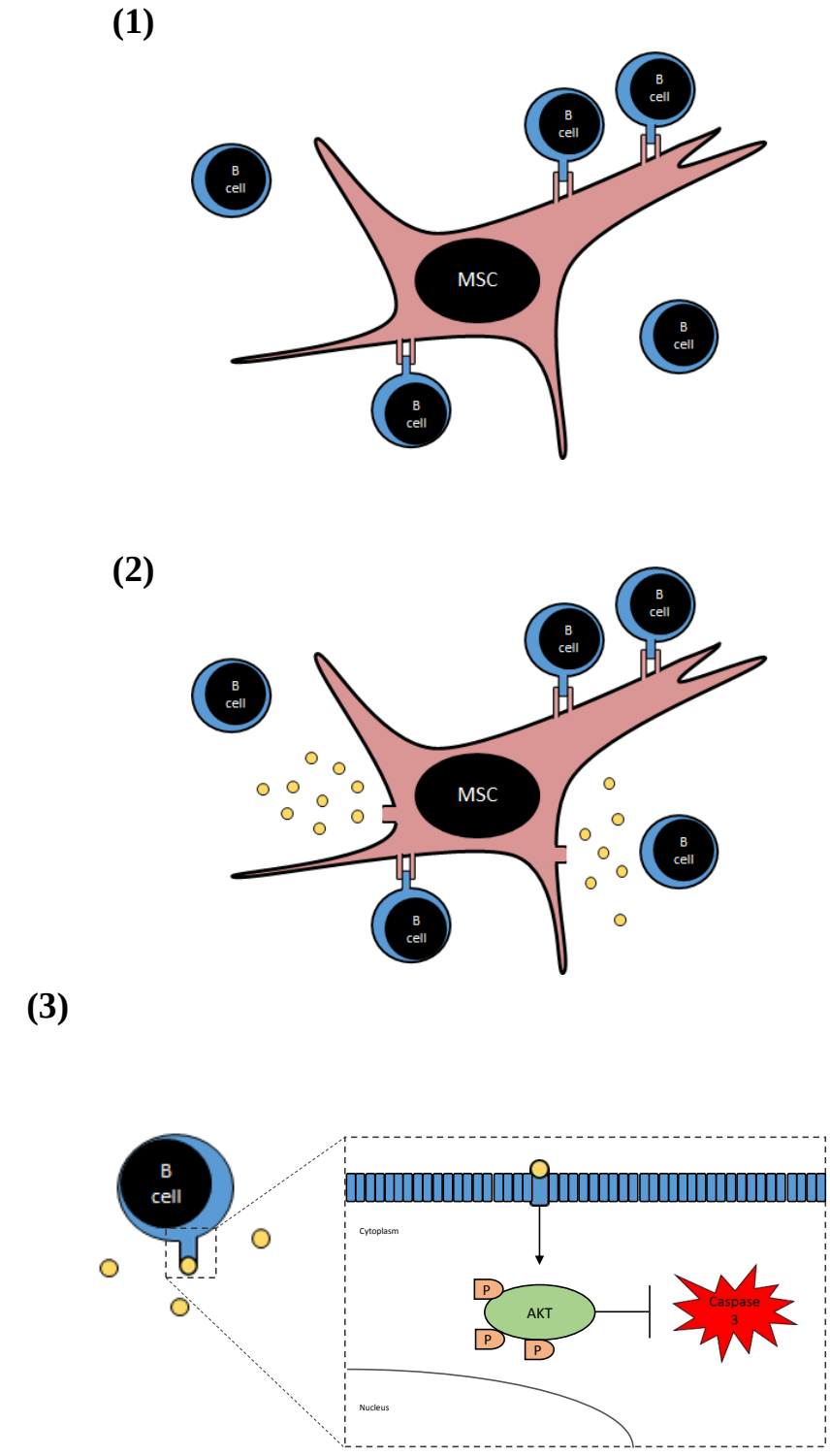

Figure 6.1. Model of mechanism of action in MSC promotion of B cell survival. Graphical depiction of proposed mechanism of action behind MSC support of B cell survival. (1) In our system, MSC bind to $CD19^{+}$ peripheral B cells (contact signal yet to be identified). (2) Cell contact signal induces a significant up-regulation of VEGF production by MSC. (3) Soluble VEGF is bound by VEGFR on $CD19^{+}$ B cells and induces phosphorylation of AKT. pAKT inhibits the pro-apoptotic caspase cascade significantly inhibiting caspase 3 cleavage and B cell apoptosis.

6.2 The development of novel models of GvHD to elucidate the mechanism of action by which MSC attenuate disease progression

MSC therapy has rapidly progressed through phase I and II clinical trials, but has yet to successfully complete large scale phase III trials. The most high profile of these trials has been a phase III trial completed by Osiris therapeutics (Martin *et al.* 2010). A number of possible reasons as to the failure of MSC therapy to progress to routine clinical application have been put forward; however it is fast becoming apparent that the lack of standardised approaches and conceptual understanding of MSC action is inhibiting progress and application. The advancement of MSC therapy from animal models of disease to clinical application has progressed rapidly with over 400 ongoing clinical trials investigating the efficacy of MSC therapy for a wide range of clinical application. One of the problems associated with such a rapid progression to clinical trials is the application of this cellular therapy without fully understanding exactly how it works. The application of MSC therapy on the grounds of compassionate use in patients with acute steroid resistant GvHD is an example. However, the failure to completely characterise how the MSC therapy regulates disease progression makes it almost impossible to determine optimal treatment dose, timing or importantly the identification of patients with underlying conditions where MSC therapy may not be suitable. This thesis contends that attaining a complete understanding of how MSC therapy modulates the immune response during GvHD will enable the development of more targeted and specific hypotheses resulting in a more tailored and successful approach to treating GvHD. Understanding the mechanism behind MSC modulation of aGvHD may allow the development of bio-markers specific to MSC treatment of aGvHD. With this in mind, Chapters 4 and 5 of this thesis were dedicated to the development of novel animal models designed to progress our understanding of the mechanisms of action utilised by MSC in the treatment

of acute and chronic GvHD and to provide more focused hypothesis driven clinical applications for MSC therapy.

In chapter 4, the capacity to assess human MSC therapies in murine (xenogeneic) models of acute or chronic GvHD was investigated. A number of studies have examined the effect of murine MSC on the pathophysiology of acute and chronic GvHD using murine models of disease and these studies have been hugely beneficial in identifying potential mechanisms by which MSC inhibit GvHD progression (Polchert *et al.* 2008). However, the functional chemokine repertoire and mechanisms of immunosuppression are different between murine and human MSC (Chamberlain *et al.* 2008; Ren *et al.* 2009) and therefore may not provide a true reflection of how human MSC therapy respond during GvHD. Therefore, it was hypothesised that the development of murine models of both acute and chronic GvHD in which human MSC therapy could be used to control disease progression might offer a more relevant comparison to how human MSC therapy might function in the clinic. The use of xenogeneic MSC therapy in animal models of disease has been performed before (Pal *et al.* 2010; Guan *et al.* 2012), however not all attempts to examine human MSC in the murine setting have been successful (Lin *et al.* 2012). The main reasons behind the failure of xenogeneic MSC in murine models of disease is the relatively poor survival rate of human MSC in immune-competent mice (Grinnemo *et al.* 2004; Grinnemo *et al.* 2006). In this study however, experimental mice are immune-compromised and it was considered that this would increase the survival rate of xenogeneic MSC therapy.

Firstly, the effect of transplanting human MSC into syngeneic control mice was investigated to identify any potential adverse effects associated with administering xenogeneic MSC therapy. Mice receiving transplantation of genetically identical syngeneic (control) immune cells did not develop GvHD and the administration of human MSC to syngeneic control mice did not adversely affect their survival or pathological

score. To ensure the pathological score of each mouse was reproducible and attained without bias, two researchers were tasked with independently determining the pathological score of each mouse. Each researcher was provided with sufficient training to confidently distinguish between the different stages of each category of pathology (Table 4.1). In cases where the pathological scores from each researcher differed significantly, the opinion of a third researcher was requested; thus resulting in a robust and reproducible GvHD scoring system between the experiments. Interestingly, administering human MSC therapy to syngeneic control mice resulted in significant infiltration of murine $CD4^+$ and $CD8^+$ cells into the lung as well as increased lung pathology. This infiltration of immune cells indicates a strong inflammatory response against the xenogeneic cell therapy. It is well established that the intravenous administration of MSC results in the entrapment of cells in the lung for up to 24 hours (Schrepfer *et al.* 2007) and the administration of BALB/c immune cells to BALB/c mice likely resulted in a competent immune system capable of mounting an immune response against the human MSC. These results suggest that the ability of human MSC to modulate allogeneic immune responses (Aggarwal & Pittenger 2005; Ryan *et al.* 2005) may not be conserved for xenogeneic immune cells. There are many possible reasons as to why MSC may not evade xenogeneic recognition but one suggestion is that the trophic factors secreted by human MSC to escape allogeneic rejection are not functional against murine immune cells. This may also explain the poor engraftment of human MSC reported in previous xenogeneic animal models (Grinnemo *et al.* 2004; Grinnemo *et al.* 2006). However, published evidence suggests that human MSC do not engraft for a prolonged period of time *in vivo* (Kidd *et al.* 2009; Lee *et al.* 2009) and therefore it is unlikely that the lymphocyte infiltration observed in the lung are part of an ongoing immune response against human MSC. The immune response observed in the lung may actually represents an initial phase of repair and remodelling in response to damage caused following the

xenogeneic recognition of human MSC. In response to lung endothelial cell damage, MCP-1 mediated infiltration of $CD4^+$ T cells has been shown to contribute to pulmonary vascular remodelling (Cuttica *et al.* 2011). Another important issue is the disparity between doses of MSC therapy administered to patients compared to the doses currently used in animal models of disease. Clinical administration of MSC to GvHD patients has varied significantly between studies, however in general has not exceeded 9×10^6 kg^{-1} (Le Blanc *et al.* 2008). Although the number of human MSC administered in our study was significantly lower than similar publications (Sudres *et al.* 2006; Li *et al.* 2014), infusing 2 separate doses of 1×10^6 MSC is significantly higher than the standard dose in humans. For a 25g mouse, this dose of MSC correlates to 40×10^6 kg^{-1} per infusion. It may also be possible that the inflammatory response and damage to the lungs following xenogeneic MSC therapy would be reduced after administrating a lower MSC dose. Hence, to increase the clinical relevance of this disease model, it may be necessary to lower the dose of MSC therapy administered to murine models of GvHD.

In comparison to aGvHD, relatively few clinical studies investigating the administration of MSC therapy (as a potential alternative to the immunosuppressive steroids currently used) for treating cGvHD have been published (Zhou *et al.* 2010; Weng *et al.* 2010). In 2010, Weng *et al.*, published the results of a small scale clinical study where 19 refractory cGvHD patients were treated with MSC (Weng *et al.* 2010). Despite the relatively small treatment group and lack of placebo controlled patients, the results from the study were very promising. The authors reported that 14 of the 19 cGvHD patients demonstrated a partial or complete response to MSC therapy with no observable adverse effects. Furthermore, of the 14 responding patients, 5 were able to discontinue their immune-suppressive steroid regimen (Weng *et al.* 2010). Similar to the data presented from the Prochymal phase III clinical study (Osiris) in aGvHD, MSC therapy was more protective in selective organs rather than systemically (Martin *et al.* 2010;

Weng *et al.* 2010). The responsiveness of cGvHD patients suffering from GI symptoms was approximately 90%, yet patients displaying symptoms in the lungs were non-responsive to MSC treatment (Weng *et al.* 2010). Despite the promising results reported from this clinical study, many open questions on the use of MSC therapy against cGvHD remain to be answered before MSC therapy can be considered routine therapy. The optimal dose, timing and number of MSC administrations as well as the extent of MSC expansion prior to administration all remain to be determined before MSC therapy can be used on a larger scale. The ability to analyse the efficacy of human MSC therapy in murine models of cGvHD would provide a useful tool which could begin to answer these questions and further the development of a clinically relevant MSC therapy. Unfortunately, restrictions on time available at Case Western Reserve University resulted in the model of cGvHD being stopped before the development of cGvHD; however the data recorded up to this time (Section 4.4) was promising. cGvHD mice which had received human MSC displayed reduced pathology and weight loss on day 63 when the experiment was finished, however whether human MSC would have resulted in increased survival remains inconclusive. As observed with the syngeneic control mice, the administration of human MSC to cGvHD mice resulted in significantly increased lymphocyte infiltration and pathology within the lungs of cGvHD mice which received human MSC therapy. As described above, this may have been a result of the xenogeneic recognition and immune response against the human MSC which had become trapped in the lungs. Interestingly however, human MSC therapy significantly reduced villus destruction and lymphocyte infiltration in the small intestine of cGvHD mice. The observed protection of the small intestine but increased damage to the lungs of cGvHD mice following human MSC therapy is in line with the observations of Weng *et al.* after MSC administration to cGvHD patients (Weng *et al.* 2010), suggesting comparisons between the model and clinical data. While the ability of MSC to increase survival of

cGvHD mice could not be determined, the results presented here support the possibility of analysing the efficacy of human MSC therapy in murine models of cGvHD. A fully optimised model of cGvHD in which to analyse human MSC therapy could be used to address outstanding issues regarding the optimal dose, timing and expansion of MSC prior to infusion. In addition to this, it would provide a platform to elucidate the mechanisms involved in MSC modulation of cGvHD.

The potential of MSC therapy in aGvHD has been studied in greater detail than cGvHD in both animal models and the clinic. Since the pioneering work of Le Blanc *et al.* demonstrated that MSC therapy was beneficial for the treatment of steroid resistant aGvHD in paediatric patients (Le Blanc *et al.* 2004), there have been a number of successful small scale clinical studies which have highlighted the potential of MSC therapy for aGvHD (Le Blanc *et al.* 2008). However, despite the relative success observed in these clinical studies, the progression to large scale blinded trials have proved unsuccessful (Martin *et al.* 2010). As mentioned above, a number of reasons which might explain the failure of the large scale trials have been put forward; however one of the major problems associated with MSC therapy for aGvHD is the absence of a clear understanding of how MSC modulate disease progression on a mechanistic level. The development of novel animal models which more closely mimic the aGvHD micro-environment is essential to the progression of our understanding and the development of a more targeted and effective MSC therapy. As a result, this study was designed to determine whether a murine model of aGvHD could be used to examine the efficacy of human MSC therapy and subsequently provide a platform from which future studies could investigate the mechanisms behind MSC protection during aGvHD. As expected, all aGvHD mice resulted in full donor chimerism, developed aGvHD and succumbed to the disease by day 56. In contrast, there was a significant increase in the survival of aGvHD mice after human MSC administration with 80% of the mice surviving the

duration of the experiment. The administration of human MSC also resulted in significant protection against lymphocyte infiltration and villi destruction in the small intestine. The protection against gut pathology is in agreement with results presented from the Prochymal™ clinical trial (Martin *et al.* 2010). Similar to the results from the Prochymal™ clinical study, MSC therapy was selectively rather than systemically protective and the protection observed in the gut was not evident in every tissue. In fact, lung pathology was significantly higher in aGvHD mice which received human MSC. In line with the results presented for syngeneic control and cGvHD mice, the increased pathology in the lungs was probably a result of xenogeneic recognition and immune response to the human MSC. These results suggest that human MSC are capable of controlling the development of aGvHD in mouse models and offer a potential new method of progressing our knowledge on how MSC therapies protect against aGvHD.

In contrast to the results from this study, other research groups have reported no beneficial role for MSC therapy in this model of aGvHD (Sudres *et al.* 2006; Jeon *et al.* 2010). Sudres *et al.* also transplanted bone marrow from C57Bl/6 mice into sub-lethally irradiated BALB/c mice; however in their study, Sudres *et al.*, administered murine MSC therapy at the same time as the bone marrow transplant (Sudres *et al.* 2006). Jeon *et al.* administered human MSC therapy to sub-lethally irradiated BALB/c mice 7 days after the transplantation of bone marrow from C57Bl/6 mice (Jeon *et al.* 2010). Neither of these studies reported the increase in survival or reduction in pathology observed after MSC therapy in our study. One of the key factors which may explain the disparities between the 3 studies is the timing of MSC administration. Previous research from our group has demonstrated the critical nature of the time of MSC administration and especially that the administration of resting MSC at the same time as PBMC had no beneficial effect (Tobin *et al.* 2013). This may explain why the study of Sudres *et al.* did not find an increase in survival after MSC therapy. The study of Joen *et al.* delayed MSC

administration until 7 days after bone marrow transplantation, whereas our study administered 2 doses of MSC on day 1 and day 3. The transplantation of C57Bl/6 derived immune cells to irradiated BALB/c mice is characterised by a severe cytokine storm induced by the major MHC mismatch between donor immune cells and host tissue. The cytokine storm peaks at day 7 and therefore the administration of MSC therapy at this stage may be too late to prevent significant damage. On the other hand, administration of human MSC on days 1 and 3 may limit the effects of this cytokine storm and result in the protection observed, in particular of the small intestine, during our study.

This study clearly indicates that human MSC are capable of modulating aGvHD within murine models of disease; however the results presented in this thesis also highlight the limitations associated with using xenogeneic disease models to study human MSC therapy. The murine models of aGvHD were designed to examine the effect of human MSC; however, within these models the effector cells are murine and may respond differently to human MSC. The immune response to the human MSC therapy suggests that mechanisms utilised by human MSC to evade allogeneic rejection were not functional in the xenogeneic setting. The differential mechanisms by which human MSC interact with murine and human immune cells may restrict the clinical relevance of results obtained from xenogeneic models of GvHD. Another limitation of the aGvHD model is the time frame associated with disease progression. The aGvHD model required 63 days to confidently determine that human MSC therapy was successful in prolonging survival and reducing disease pathology. Prolonged *in vivo* studies require a lot of time and money and therefore we decided to shift our focus to the development of a humanised mouse model of aGvHD in which to investigate potential mechanisms of immune modulation by MSC therapy.

While the immunomodulatory ability of MSC highlights their potential as a useful cell therapy, there are a number of inhibitory factors surrounding the development of

MSC therapy. Firstly, generating sufficient numbers of MSC to treat aGvHD or cGvHD patients without compromising the immune-modulatory ability of these cells remains an issue. The number of MSC delivered to aGvHD patients has varied from 0.4 to 9 x 10^6 cells kg^{-1} per infusion (Le Blanc *et al.* 2008). The generation of these quantities of MSC from a single donor requires extensive *ex vivo* expansion, which is known to negatively affect the immune-suppressive capacity of these cells. The donor to donor variability in MSC growth kinetics, gene expression and immunomodulatory ability is another major inhibiting factor to the development of a standardised MSC therapy (Siddappa *et al.* 2007; Jansen *et al.* 2010; Menard *et al.* 2013). The range of contributing factors to donor variability already identified, including age (Choudhery *et al.* 2014), gender (Siegel *et al.* 2013), and underlying medical conditions (Nie *et al.* 2010) suggest that the development of stringent expansion protocols may not be sufficient to create a standardised cell therapy for clinical administration. The establishment of a standardised immune suppression potency assay would ensure the infusion of functional and comparable doses of MSC therapy (Menard *et al.* 2013). The proliferation kinetics, differentiation ability and immunosuppressive capacity of freshly isolated MSC could be screened against this profile before clinical administration.

The development of humanised mouse models to study aGvHD has provided the most clinically relevant system by which to study the pathophysiology of disease. The humanised mouse model of aGvHD facilitates the engraftment of adult human immune cells within the mouse. These transplanted immune cells become active and proliferate in response to the xenogeneic recognition of murine MHC molecules, providing a system which mimics the basis of aGvHD development. The humanised mouse model of aGvHD also exhibits a number of experimental advantages over the mouse-mouse model of aGvHD used in the previous section. Importantly the pathogenesis in these models is mediated by human immune cells and therefore provides a system to investigate the

ability of a human cell therapy to control disease. In addition, disease progression is faster in humanised models of aGvHD significantly reducing the time and cost associated with large scale *in vivo* experiments. Therefore this thesis focused on the optimisation of a humanised model of aGvHD for the determination of how MSC modulate aGvHD.

There are a number of humanised mouse models available to study aGvHD (Shultz *et al.* 2012), however the NSG model is at the cutting edge (Ali *et al.* 2012). In a direct comparison with another frequently used humanised mouse model of aGvHD, the BALB/c-Rag2^{null}IL-2Rγ^{null} (BRG) humanised mouse, the NSG mouse displayed faster expansion of human CD45$^+$ lymphocytes and higher engraftment of human CD3$^+$ T cells within the peripheral blood, spleens, lymph nodes and bone marrow compared to BRG mice (Ali *et al.* 2012). The increased human lymphocyte engraftment and function *in vivo* allows for the faster development and progression of aGvHD. This system facilitates the study of human cell therapy in an aGvHD model driven by human T cells and thus represents a more clinically relevant system.

Using the NSG mouse model, this thesis set out to build on and enhance previous work from our research group which sought to elucidate the mechanisms by which MSC control aGvHD. Tobin *et al.* developed an aGvHD NSG mouse model using human lymphocytes obtained from freshly drawn blood and based on a protocol published by Pearson *et al.* (Tobin *et al.* 2013; Pearson *et al.* 2008). The original protocol developed by Pearson *et al.* suggested that the administration of 2 x 10^7 PBMC, isolated from buffy packs, to irradiated NSG mice resulted in consistent aGvHD development (Pearson *et al.* 2008). However, previous attempt to replicate this protocol within the Mahon lab were unsuccessful and resulted in inconsistent aGvHD development between mice of the same group; hence the focus was switched to developing the humanised model from freshly isolated blood where the dose of PBMC was normalised to the weight of each mouse (Tobin *et al.* 2013). While this approach facilitated consistent aGvHD development, the

relatively low numbers of PBMC which can be isolated from laboratory scale sampling of fresh blood significantly restricted the number of mice which could be used in each experiment. The progression of this model to PBMC isolated from buffy packs, while still retaining robust and reproducible aGvHD development, would facilitate the performance of large scale *in vivo* experiments; subsequently enhancing the investigation of how MSC attenuate aGvHD development. In order to determine the optimal PBMC dose required to consistently induce aGvHD, two separate approaches were taken. The first approach was designed to overcome the inconsistent aGvHD development previously observed within the Mahon lab by administering a higher dose of PBMC. However, this higher dose of PBMC resulted in the development of an extremely aggressive aGvHD. The sudden onset of aGvHD made it impossible to study the effect of MSC therapy on disease progression. The second approach investigated whether administering a dose of PBMC tailored to each particular mouse would result in a more consistent disease model. The PBMC dose for each NSG mouse was calculated based on the weight of each mouse, extending the work of Tobin *et al.* (Tobin *et al.* 2013). In 3 of the 4 PBMC donors tested, the results were very promising. All of the mice within these groups displayed a gradual weight loss pattern while still developing aGvHD. However, the development of aGvHD was not consistent in mice which received the PBMC from the fourth donor. Inconsistent development of aGvHD within an experimental group is likely to be associated with the quality or level of responsiveness of the PBMC acquired from a particular donor. A link between the physical health of individuals and the functional ability of their immune cells has been reported (Amar *et al.* 2007; O'Shea *et al.* 2010). Therefore it is possible that despite the 'healthy donors' used in this study being clear of disease or infection, obesity, sub-clinical infection or other environmental factors can reduce the responsiveness of PBMC. Less responsive PBMC would not respond to the xenogeneic recognition of mouse MHC at the same rate and/or scale as

healthier cells; which may result in a reduced severity, delayed onset or complete absence of disease and may explain the observed results. Despite the disparity associated with one donor, the robust and reproducible nature of the other 3 donors was adequate to determine that 8 x 10^5 PBMC $gram^{-1}$ per mouse was the optimal dose required to induce aGvHD in irradiated NSG mice using PBMC obtained from buffy packs.

Failure of PBMC from a particular donor to engraft and induce aGvHD is extremely costly in terms of time and reagents but also presents an ethical issue in terms of use of the NSG mice. To overcome this issue, it was hypothesised that PBMC thawed from liquid nitrogen storage could also be used to induce aGvHD in NSG mice. This would allow batches of PBMC to be tested for efficacy in small pilot studies and only PBMC batches which reliably cause aGvHD would be used for large scale studies. To test this, PBMC were isolated from buffy packs as before and stored in liquid nitrogen. To account for a reduction in responsiveness and proliferative capacity which may have been lost by PBMC during liquid nitrogen storage (freezing and thawing process), irradiated NSG mice were given a higher dose of PBMC than optimised for freshly isolated PBMC. Similar to the results observed above, this dose was too high and the onset and progression of aGvHD was too sudden. Next, we decided not only to reduce the overall PBMC dose but also to take a similar approach as above by calculating the dose of PBMC for each mouse based on weight. The reduced dose of PBMC resulted in a more gradual disease progression and weight loss than observed with the higher dose; however the timing of disease onset was later than desired. Therefore, the dose of PBMC was increased slightly and was subsequently administered to irradiated NSG mice. The administration of 1 x 10^6 PBMC $gram^{-1}$ to irradiated NSG mice resulted in a robust and reproducible model of aGvHD in 3 of the 4 donors tested. In the fourth PBMC donor analysed, the disease progression was too aggressive. Interestingly the aggressive disease progression observed with this donor was also observed when these PBMC were used

directly after isolation and further emphasises that PBMC obtained from one donor can respond differently to others. This sequence of experiments demonstrate the possibility of inducing aGvHD in NSG mice using thawed PBMC. This has led to ongoing experiments in the English lab to identify "useable" PBMC donors, creating a bank of PBMC cells which can consistently produce aGvHD. The presence of this bank of PBMC would address the experimental and ethical issues associated with PBMC donor variability surrounding this model, and may allow future characterisation of donors to discover what makes a PBMC donor "useable".

The current pre-conditioning regimen of sub-lethal irradiation is a robust and reproducible technique; however, many labs do not have access to an irradiator and future collaborative projects will need to be carried out in centres without irradiation facilities. Therefore the ability to induce aGvHD after chemical immune-depletion was investigated using the chemotherapeutic agent Busulfan. The use of Busulfan as part of a pre-conditioning regiment in the clinic has become common practice (Kanakry *et al.* 2014; Patel *et al.* 2014; Raida *et al.* 2014) and therefore was selected for use in the NSG system. The development of aGvHD in NSG mice was compared between groups of mice which received Busulfan or irradiation in side by side experiments. Busulfan was administered in 2 doses at a concentration of 25 mg/kg, 48 and 24 hours before PBMC administration. Overall the onset of aGvHD was similar between mice which were irradiated and mice which received Busulfan. The survival curves were very similar between the 2 sets of mice. However, mice which received Busulfan displayed significant weight loss for 3 days after administration. This dramatic loss in body weight was not observed after irradiation and suggests that Busulfan is a much harsher method of immunodepletion. Despite this, Busulfan treated mice recovered their weight loss and appeared very similar to irradiated mice before the onset of disease. Interestingly however, the survival rate of PBS control mice which received Busulfan was affected at later stages in the experiment

compared to irradiated PBS mice. Although one of the irradiated PBS mice died early during the study, this mouse did not exhibit aGvHD symptoms and instead may have died in similar circumstances to those highlighted earlier. These results demonstrate that it is possible to substitute sub-lethal irradiation for the chemotherapeutic agent Busulfan as the pre-conditioning regimen without sacrificing the reproducibility of the NSG model. The use of Busulfan is much more severe than irradiation and the mice require daily monitoring until at least day 5. Other research within the English lab is currently being carried out to determine the lowest possible dose of Busulfan capable of facilitating the same level of PBMC engraftment observed in this study. The lowest effective dose of Busulfan will then be used throughout future collaborative research projects.

The model of aGvHD optimised in this thesis describes a clinically relevant system in which to investigate how MSC therapy responds to the aGvHD micro-environment and subsequently modulates the inflammatory immune response associated with aGvHD. The first step in doing so was to confirm that MSC therapy was effective in protecting against aGvHD in this particular model. To this end, the study demonstrates the capacity for MSC to prolong survival in this optimised model of aGvHD when administered on day 7 (Section 5.3). Following this, we tested a number of hypothesis exploring the mechanisms utilised by MSC in prolonging survival in aGvHD including the engraftment kinetics, memory phenotypes, cytokine profiles and Treg cell expansion of aGvHD mice.

The engraftment of the transplanted cells after HSCT is essential to the development of a functional immune system and also holds anti-tumour properties; therefore potential cell therapies which inhibit the engraftment of transplanted cells are not suitable candidates for the treatment of aGvHD. aGvHD is a systemic disease characterised by the migration of donor T cells to target organs including the skin, liver, lungs and small intestine resulting in extensive tissue damage (Duffner *et al.* 2003; Fu *et*

al. 2014). MSC are known to inhibit T cell proliferation and function *in vitro* and *in vivo* (Di Nicola 2002; Meisel *et al.* 2004; Németh *et al.* 2009; González *et al.* 2009a; Tobin *et al.* 2013) and therefore may attenuate the ability of T cells to engraft in aGvHD target organs. It has been established that the use of MSC therapy does not inhibit the engraftment of transplanted cells in aGvHD patients (Lee *et al.* 2002; Le Blanc *et al.* 2008); however it was necessary to determine the effects of MSC therapy on engraftment in the NSG model. In our system, aGvHD onset occurs between days 10 and 14; therefore the effect of MSC therapy on PBMC engraftment at day 12 was investigated. In correlation with the data provided from clinical studies (Lee *et al.* 2002; Le Blanc *et al.* 2008), the total number of human $CD45^+$ lymphocytes engrafted in the spleens of aGvHD mice was unaffected by MSC therapy. In fact the engraftment of human $CD4^+$ T cells was significantly higher in aGvHD mice which received MSC therapy, suggesting that MSC therapy in the NSG mouse is in line with clinical data (Le Blanc *et al.* 2008). The administration of human MSC therapy did not reduce the total number of human $CD45^+$ lymphocytes recovered from the livers or lungs of aGvHD mice, suggesting that human MSC therapy does not affect the ability of PBMC to engraft in target organs during aGvHD pathogenesis.

Following exposure to lymphopenic conditions, naïve T cells develop a memory phenotype (Ali *et al.* 2012). Memory T cells are primarily classed as effector memory T cells (Tem) or central memory T cells (Tcm) (King *et al.* 2008). Tem cells represent the effector arm of memory T cell populations and are characterised by the migration to inflamed tissue (Sallusto *et al.* 1999; Weninger *et al.* 2001; Sallusto *et al.* 2004). Tcm cells are primarily located in the secondary lymphoid organs (Sallusto *et al.* 1999; Weninger *et al.* 2001; Sallusto *et al.* 2004) and are responsible for the long term memory against foreign antigens (Zaph *et al.* 2004). Tcm are capable of responding to repeated antigenic stimulation by undergoing self-renewal and generating Tem (Zheng *et al.*

2009). Compared to Tcm, Tem cells are characterised by rapid proliferation and production of perforin and IFN-γ while Tcm maintain a greater proliferative capacity. It is becoming apparent that central memory T cells mediate aGvHD development (Zheng *et al.* 2009). While the MHC mismatched transplantation of effector memory T cells to irradiated mice was not sufficient to sustain a GvHD response, it is believed that a role for effector memory T cells exists during aGvHD (Zhang *et al.* 2012). Given that the number of engrafted PBMC was not reduced by MSC, this study examined the effect of MSC on the expression of naïve and memory phenotypes in the engrafted PBMC. The administration of MSC therapy did not reduce the percentage or total number of $CD4^+$ Tcm or Tem cells recovered from the organs of aGvHD mice. The tissue specific distribution of Tem and Tcm cells is comparable to the results obtained from previous studies (Ali *et al.* 2012). Spleen samples were rich with Tcm populations whereas samples obtained from lungs and livers of aGvHD mice displayed more Tem cells. These results suggest that enhanced survival in the aGvHD model is not associated with MSC impairment of Tcm or Tem cell development or engraftment in target organs.

Pro-inflammatory cytokine production is one of the driving forces behind the development of aGvHD. The presence of the pro-inflammatory cytokines IFN-γ, IL-1, IL-2 and TNF-α are essential for the progression of the disease (Ferrara *et al.* 2009). IL-1β is an important member of the initial cytokine storm which is essential during phase 1 of aGvHD pathogenesis (Ferrara *et al.* 2009). IL-1β is also product of the NLRP3 inflammasome which is currently being investigated as a potential mediator of inflammation during aGvHD (Jankovic *et al.* 2013). We utilised our model of aGvHD to examine the effect of MSC on the production of these cytokines by human PBMC. The effect of MSC treatment on the production of IL-1β is not very well documented and was investigated under the hypothesis that MSC therapy reduces the levels of circulating human IL-1β which may impair aGvHD progression. However, the level of human IL-

1β detected in the serum of aGvHD mice production day 12 was unaffected by MSC therapy. In fact MSC therapy had no significant effect on the serum levels of any of the human cytokines examined (IL-1β, IL-2 or IFN-γ) after 12 days in aGvHD NSG mice. Notably, the role for IL-1β has been established as an integral mediator of phase 1 aGvHD pathology and therefore is important very early in disease. Therefore, the administration of MSC therapy on day 7 may be too late to have an effect on IL-1β production.

Although, measuring cytokine levels in serum provides an overall view of circulating cytokine concentrations, this assay does not provide any detail of cytokines being produced at the cellular level. It may be the case that although no changes are evident in total serum cytokine level, there may be important differences in the type or number of cells producing cytokines. In line with the total serum levels of IL-2 and IFN-γ, the total number of human T cells producing these cytokines was not reduced following MSC therapy. The failure of MSC to reduce IL-2 production was not surprising considering there was no reduction in PBMC engraftment, however the slight increase in levels of human IFN-γ in the serum of aGvHD following MSC therapy was not expected. MSC inhibition of T cell proliferation *in vitro* also corresponds to reduced IFN-γ (Patel *et al.* 2010; Zinöcker & Vaage 2012) and infusion of MSC therapy to murine models of colitis reduced production of Th1 cytokines including IFN-γ (González *et al.* 2009a). The increased levels of IFN-γ are difficult to explain and whilst it might be an additional allogeneic (effector T cell vs MSC) effect, it certainly reflects the complexity of the model.

The production of TNF-α is a hallmark of aGvHD and the ability of MSC to prevent the production of human TNF-α during NSG models of aGvHD may be one method by which survival is increased. We have previously reported the reduction in total TNF-α in the serum of aGvHD mice (Tobin *et al.* 2013), but whether this reduction was caused by T cells or another cell type remained unanswered. This study showed that

MSC administration significantly reduced the total number of human TNF-α producing T cells in the spleen and lungs of aGvHD mice. The failure of MSC therapy to reduce the number of TNF-α producing $CD4^+$ or $CD8^+$ T cells in the livers of aGvHD mice was unexpected but this result is in line with the organ specific rather than systemic effect of MSC therapy during aGvHD. This result supports our previous observation than MSC therapy reduced the total levels of TNF-α in the serum of aGvHD mice and may offer a potential mechanism by which MSC support survival. Targeting the production of TNF-α as a treatment for aGvHD has already provided encouraging results. A study carried out by King *et al.* demonstrated that blocking of TNF-α production using Etanercept resulted in prolonged survival of NSG aGvHD mice (King *et al.* 2009). The correlation between elevated serum levels of TNF-α and aGvHD development has also been reported in humans (Holler *et al.* 1990; Kitko *et al.* 2008) which has led to suggestions that serum levels of TNF-α could be used as a bio-marker of aGvHD (Paczesny *et al.* 2009).

Studies dedicated to the discovery of novel cell therapies capable of regulating aGvHD development have identified the potential for Treg cells (Taylor *et al.* 2002; Hoffmann *et al.* 2002; Edinger *et al.* 2003). The reduced engraftment or depletion of Treg cells results in increased aGvHD progression and severity (Taylor *et al.* 2002). In addition, the infusion of donor derived Treg cells at the time of allogeneic BMT increased survival and reduced pathology in murine models of aGvHD through an IL-10 dependent mechanism (Hoffmann *et al.* 2002; Edinger *et al.* 2003). The correlation between reduced Treg cell engraftment and aGvHD development has also been identified in the peripheral blood of HSCT patients (Magenau *et al.* 2010). Interestingly, we observed significantly increased engraftment of Treg cells in the spleens, livers and lungs of aGvHD mice which received MSC therapy. These results are in line with previous *in vivo* studies which also report the increase in Treg cells in aGvHD mice after MSC transfusion (Joo *et al.*, 2010; Hao *et al.*, 2011). However, this result is in contrast to previous reports from our

laboratory which did not find any increase in Treg cells within murine tissues (Tobin *et al.,* 2013). The differences are likely caused by the improved recovery of lymphocytes using a more optimised protocol. The previous experiments mechanically digested the organs and then stained samples for flow cytometry. In this study, the mechanically digested organs were then purified using density gradient centrifugation. This allowed the recovery of a purer lymphocyte population which resulted in less artefacts or non-specific staining during the analysis. Although the total number of Treg cells is modest, the potent nature of the cell means that the presence of these Treg cells may be playing a role in the regulation of aGvHD pathogenesis. It would be interesting to ablate the Treg cells from PBMC before administration or during the model to determine whether or not the increased Treg cells were protective. Another interesting target for future studies on the relationship between MSC therapy and Treg cells during aGvHD is the expression levels of the anti-inflammatory cytokine IL-35. While a role for MSC in the induction of IL-35 production has not yet been characterised *in vitro* or *in vivo*, a recently published study has demonstrated that increased IL-35 production by Treg cells is capable of controlling aGvHD while preserving GvL effects (Liu *et al.* 2014). The authors also demonstrate a significant correlation between the expression of IL-35 and reduced aGvHD progression in aGvHD patients (Liu *et al.* 2014). Therefore it would be interesting to investigate whether the increased Treg cells detected after MSC therapy also resulted in increased human IL-35 production during aGvHD.

Although the increase in Treg cells has been established as one of the primary mechanisms employed by MSC to regulate the immune response, it is not clear exactly how MSC therapy results in increased Treg cells. One hypothesis is that MSC directly induce the differentiation of Treg cells from naïve $CD4^+$ T cells (Del Papa *et al.,* 2012; Luz-Crawford *et al.*, 2013). In this thesis we determined that MSC were unable to induce Treg cells from a $CD4^+CD25^-$ population, however co-culturing MSC with $CD4^+CD25^+$

populations resulted in increased FoxP3 expression which suggested that MSC were not inducing but more likely expanding Treg populations. In order to determine whether MSC were enhancing Treg populations or promoting the survival of original Treg populations, KI-67 was used as a marker of proliferation (Section 5.10). Absence of KI-67 expression in the $CD4^+CD25^+FoxP3^+$ Treg cells would suggest that MSC were simply promoting survival of existing Treg cells as opposed to enhancing their proliferation. Treg cells did not express KI-67 after co-culture with MSC, suggesting that MSC promote the survival rather than induce or enhance Treg cells *in vitro*. However, while KI-67 is an established marker for proliferative cells it only represents one snapshot of the experiment. The use of CFSE would provide a more detailed description of Treg cell proliferation including the number of completed division cycles. In addition, *in vitro* analysis is a simplified system and is not always a true reflection of *in vivo* interactions. The presence of other cell types or the particular micro-environment during aGvHD progression may influence how MSC increase T cell numbers *in vivo*.

So far this thesis has demonstrated that the administration of human MSC on day 7 results in increased survival, increased Treg cell numbers (in target organs) and reduced TNF-α production in aGvHD mice. The next step was to investigate whether the potency of MSC therapy in aGvHD could be enhanced through licensing (pre-stimulation) with IFN- γ. Our lab has previously shown that administering γMSC on the same day as PBMC significantly prolonged survival and reduced aGvHD pathology in a similar manner to the administration of resting MSC on day 7 (Tobin *et al.,* 2013). It was hypothesised that resting MSC therapy required activation upon delivery by human IFN-γ produced during aGvHD development and therefore act as a treatment rather than preventative of aGvHD. Therefore the delivery of pre-stimulated MSC on day 7 may offer a more rapid, potent suppression of cytotoxic T cell activity resulting in enhanced survival of aGvHD mice. However there were no differences between γMSC and MSC therapy

administered on day 7. Similar to resting MSC therapy, γMSC therapy did not inhibit PBMC engraftment and also reduced the total number of TNF-α producing T cells in the spleen, liver and lungs of aGvHD mice. Delivery of γMSC therapy on day 7 was of no more benefit than administering resting MSC, suggesting that the level of human IFN-γ present in the mouse on day 7 is sufficient to activate resting MSC. It may be interesting to investigate whether the administration of γMSC at an earlier time-point (but later than day 0) may be more efficient in reducing TNF-α production and the subsequent prevention of aGvHD.

Although the delivery of a single dose of human MSC therapy successfully prolonged the survival of aGvHD mice; it does not prevent the development of aGvHD. This phenomenon reflects the results of MSC therapy in the clinic (Le Blanc *et al.* 2004). In this situation aGvHD patients have received and responded to a second infusion of MSC therapy (Le Blanc *et al.* 2004; Ringdén *et al.* 2006; Müller *et al.* 2008; Ball *et al.* 2013). It was hypothesised that administering a second dose of human MSC therapy prior to the onset of aGvHD symptoms would further prolong the survival and prevent weight loss than single dose MSC therapy. The second dose of MSC therapy was delivered on day 9 as it represents the period when aGvHD symptoms begin to become prominent. The administration of 2 doses of MSC significantly prolonged the survival of aGvHD mice compared to non-treated mice; however the survival of aGvHD mice was not significantly greater than aGvHD mice which received a single dose of MSC therapy. Whilst there was an improvement in weight loss reduction immediately after the second dose of MSC therapy, this increase was not statistically significant. The reduction in TNF-α production by human T cells was also similar between mice which received a single or double dose of MSC therapy. These results suggest that administering 2 doses of MSC therapy did not enhance protection from aGvHD when compared to administering a single MSC therapy. The delayed weight loss is noteworthy however and

it may be interesting to analyse the survival of aGvHD mice after administering a third dose of human MSC on day 12. Another strategy which would be worth exploring is to administer MSC therapies on day 4 and 7 and compare with day 7 alone. A clinical study by Ball *et al.* suggests that patients who received their first MSC dose earlier responded better (Ball *et al.* 2013). The earlier delivery of the extra MSC dose may further reduce TNF-α production or possibly increase the number of Treg cells present in aGvHD mice. On the other hand, the recognition of re-administered MSC therapy could lead to rapid clearance by the patient's immune system before the MSC can have an effect.

This thesis explored many aspects of MSC immune regulation both *in vitro* and *in vivo*. Following MSC therapy *in vivo*, significantly increased numbers of Treg cells were present in the organs of aGvHD mice. In addition to this, the total number of human TNF-α producing $CD4^+$ and $CD8^+$ T cells were also reduced (Figure 6.2). Whether the reduction in TNF-α production is linked to the increase in Treg cells or independently mediated by the MSC remains to be determined, however it is hypothesised that the increase in Tregs and reduction of TNF-α play an important role in aGvHD survival. TNF-α is one of the key inflammatory signals in the progression of aGvHD in both murine models and in the clinical setting. During the early stages of aGvHD, leakage of LPS from the gut activates donor monocytes/macrophage and DC to produce high levels of TNF-α (Ferrara *et al.* 2009) and it was hypothesised that MSC induced reduction in serum levels of TNF-α was achieved by interfering with this process. While this may still be the case, this thesis has determined a role for MSC therapy in reducing TNF-α produced by human T cells within the NSG mouse. Excessive TNF-α production can result in the proliferation of donor DC and T cells and result in the direct apoptosis of patient's tissue cells or the activation of donor DC and cytotoxic T lymphocytes and NK cells. TNF-α inflammatory responses are known to increase vascular permeability which in the case of aGvHD may promote the infiltration of activated donor lymphocytes to target organs

resulting in extensive tissue damage. The striking protective effect of MSC in the gut of both murine models and humanised models of aGvHD suggest that MSC therapy may protect the integrity of the gut which may limit the amount of LPS leakage. These finding are in line with results observed in the clinical setting (Le Blanc *et al.* 2004) and should be investigated thoroughly.

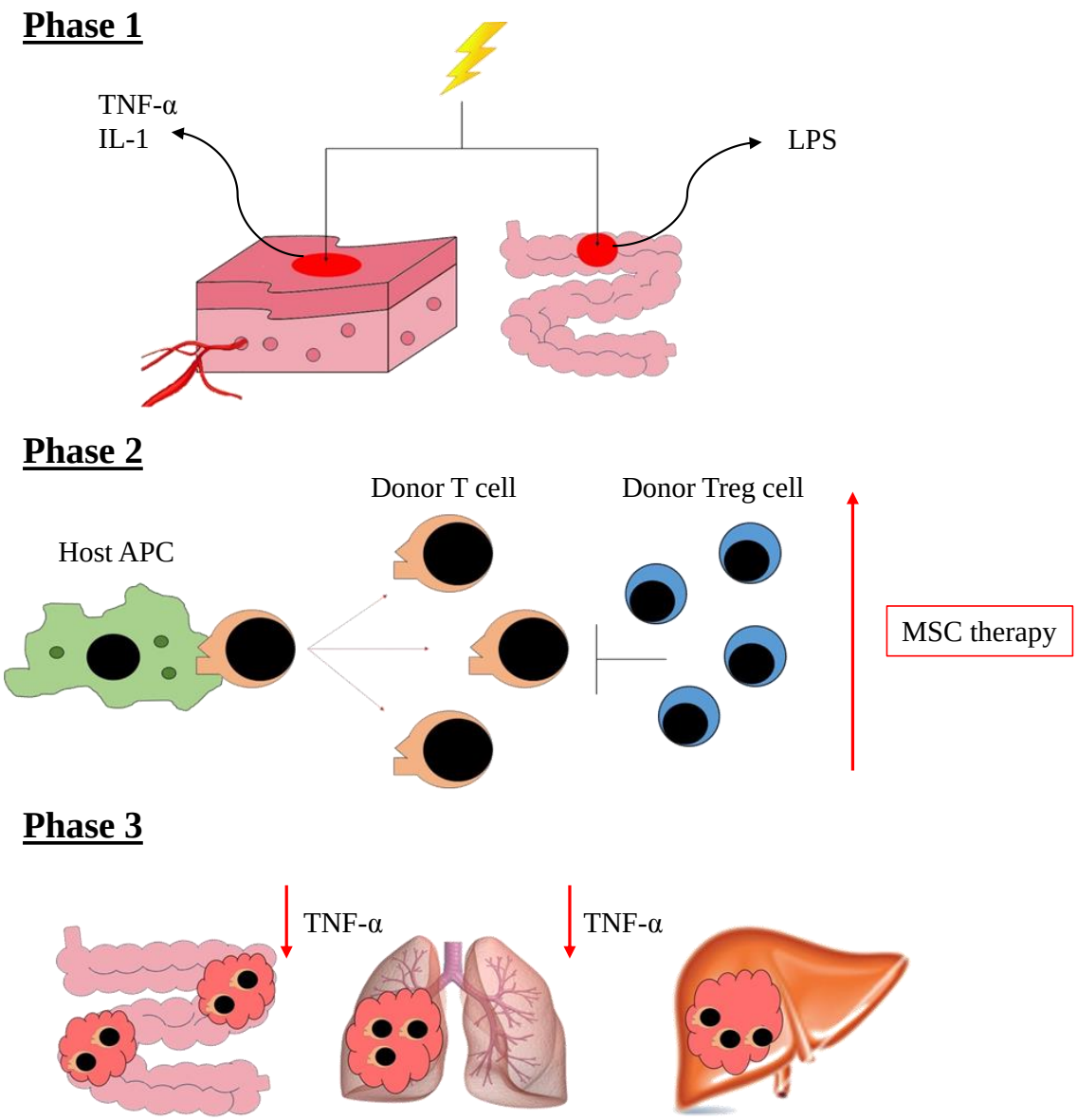

Figure 6.2. MSC modulation of aGvHD is mediated through enhanced Treg cell numbers and reduced TNF-α production in aGvHD target organs. Graphical representation detailing potential areas of MSC inhibition during aGvHD pathophysiology. In phase 1, although increased levels of TNF-α stimulate host APC, MSC administration is too late to reduce the effect of pre-conditioning regimen. During phase 2, activated host APC activate mature donor T cells. Following MSC therapy, increased Treg cells inhibit the activation of door T cells and the secretion of immunesuppressive cytokines reduce the inflammatory environment. In phase 3, MSC therapy does not reduce engraftment of effector T cells in the lungs or liver but significantly increases Treg cells and reduces the production of TNF-α, limiting necrosis and apoptosis.

An interesting concept currently being investigated in models of Crohn's disease is the role played by the microbiome in disease progression (Gevers *et al.* 2014). The ability of MSC to alter the microbiome has not yet been reported, however suppression of the gut microbiome has recently been shown to prevent aGvHD development (Vossen *et al.* 2014). Based on the consistent protection observed in the gut of aGvHD and Crohn's disease patients, alterations to the gut microbiome following MSC therapy is an interesting concept. Another possibility is that the increased number of Treg cells detected after MSC therapy promote a less inflammatory T cell population and reduces TNF-α production. Circulating levels of TNF-α have long been suggested as a potential bio-marker of aGvHD development (Holler *et al.* 1990); however increased TNF-α production is not specific to aGvHD (Chen & Cutler 2013). However, the reduction in TNF-α production following MSC therapy suggests a potential role for TNF-α as a possible indicator of treatment efficacy in aGvHD patients.

The final part of this thesis was designed to determine if our model of aGvHD could be used as a platform to investigate the immunomodulatory potential of non-MSC therapies. *F. hepatica* tegumental antigen (Fh-Teg) potently impairs the immune response of murine immune cells (Hamilton *et al.* 2009; Vukman *et al.* 2013; Adams *et al.* 2014) and ongoing collaborative research has demonstrated that Fh-Teg can also potently suppress human PBMC. Therefore, it was hypothesised, by our collaborators, that stimulating PBMC with Fh-Teg overnight before administration to irradiated NSG mice would reduce the inflammatory potential of these cells and prevent the development of aGvHD. Indeed, the administration of Fh-Teg PBMC resulted in significantly increased survival, lower pathological score and reduced weight loss compared to mice which received PBMC alone. These results were very promising and a larger scale *in vivo* experiment was designed to determine how Fh-Teg stimulation was reducing aGvHD. Similar to the MSC data, the effect of Fh-Teg stimulation on engraftment kinetics,

memory cell polarisation, pro-inflammatory cytokine production and pathology was investigated. However, it quickly became apparent that stimulating PBMC with Fh-Teg significantly inhibited engraftment within the mice. Subsequently, the number of effector or central memory T cells, number of pro-inflammatory cytokine producing cells and overall pathology were reduced. The failure of Fh-Teg PBMC to engraft suggests that stimulation with Fh-Teg significantly reduced the ability of the PBMC to recognise and proliferate in response to xenogeneic tissue, indicating the potency of suppression by Fh-Teg. At this stage, it is very difficult to hypothesise the mechanism by which Fh-Teg suppresses the immune response; although *in vitro* work carried out in the collaborative lab has suggested Fh-Teg stimulation does not induce T cell anergy. The key finding of our study is that Fh-Teg would not be a useful preconditioning regime for graft cells, as it impairs engraftment. The published studies to date have established the ability of Fh-Teg to potently inhibit DC maturation and antigen presentation ability (Hamilton *et al.* 2009) and may suggest an important role for DC mediated T cell priming in the early stages of our model. In murine models, Fh-Teg has been shown to skew the T cell balance in favour of a Th2 response (Dowling *et al.* 2010) and thus may reduce the cytotoxic ability of the T cells; however further studies are required to examine these hypotheses. The suppressive ability of Fh-Teg on adult immune cells is interesting and future experiments designed to identify which particular protein mediates immune suppression may have important implications in terms of immune regulation. These data further validated the humanised mouse model of aGvHD as a useful platform for testing novel immune modulatory therapies, and rejecting those that are unlikely to succeed in the clinic.

In conclusion, this thesis represents a step forward in understanding the relationship between human MSC and peripheral B cells. Chapter 3 identified a novel mechanism by which human MSC support the survival, proliferation and activation of

$CD19^+$ peripheral B cells. Developing a complete understanding of how MSC effect peripheral B cell biology will help to progress MSC therapy towards successful clinical application and the mechanism identified in chapter 3 significantly enhances our knowledge. This thesis also represents the optimisation of a humanised mouse model of aGvHD. Humanised mouse models are at the cutting edge of translational research and the development of this model allows in depth investigation into the pathogenesis of aGvHD and the mechanisms employed by MSC or other immune modulatory therapies to limit disease progression. Chapter 5 identified the reduction in TNF-α production by human T cells and the increase in Treg cells as potential mechanisms by which MSC modulate aGvHD development. This chapter also ruled out the possibility that MSC therapy reduced aGvHD by impairing PBMC engraftment, the polarisation to memory phenotypes or the production of pro-inflammatory cytokines IL-1β, IL-2 or IFN-γ. Overall this thesis has furthered our knowledge of human MSC biology and provided novel disease models to progress MSC therapy to a translational setting.

CHAPTER 7

BIBLIOGRAPHY

Abid, M.R. et al., 2004. Vascular endothelial growth factor activates PI3K/Akt/forkhead signaling in endothelial cells. *Arteriosclerosis, thrombosis, and vascular biology*, 24(2), pp.294–300.

Abreu, M.T. et al., 2009. Extracorporeal photopheresis for the treatment of refractory Crohn's disease: results of an open-label pilot study. *Inflammatory bowel diseases*, 15(6), pp.829–36.

Adams, P.N. et al., 2014. Fasciola hepatica tegumental antigens indirectly induce an M2 macrophage-like phenotype in vivo. *Parasite immunology*, 36(10), pp.531–9.

Aggarwal, S. & Pittenger, M.F., 2005. Human mesenchymal stem cells modulate allogeneic immune cell responses. *Blood*, 105(4), pp.1815–22.

Akiyama, K. et al., 2012. Mesenchymal-stem-cell-induced immunoregulation involves FAS-ligand-/FAS-mediated T cell apoptosis. *Cell stem cell*, 10(5), pp.544–55.

Aldinucci, A. et al., 2010. Inhibition of immune synapse by altered dendritic cell actin distribution: a new pathway of mesenchymal stem cell immune regulation. *Journal of immunology (Baltimore, Md. : 1950)*, 185(9), pp.5102–10.

Ali, N. et al., 2012. Xenogeneic graft-versus-host-disease in NOD-scid IL-2Rγnull mice display a T-effector memory phenotype. *PloS one*, 7(8), p.e44219.

Allman, D. et al., 2001. Resolution of three nonproliferative immature splenic B cell subsets reveals multiple selection points during peripheral B cell maturation. *Journal of immunology (Baltimore, Md. : 1950)*, 167(12), pp.6834–40.

Amar, S. et al., 2007. Diet-induced obesity in mice causes changes in immune responses and bone loss manifested by bacterial challenge. *Proceedings of the National Academy of Sciences of the United States of America*, 104(51), pp.20466–71.

Ankrum, J.A., Ong, J.F. & Karp, J.M., 2014. Mesenchymal stem cells: immune evasive, not immune privileged. *Nature biotechnology*, 32(3), pp.252–60.

Anthony, B.A. & Link, D.C., 2014. Regulation of hematopoietic stem cells by bone marrow stromal cells. *Trends in immunology*, 35(1), pp.32–7.

Antin, J.H. et al., 2002. A phase I/II double-blind, placebo-controlled study of recombinant human interleukin-11 for mucositis and acute GVHD prevention in allogeneic stem cell transplantation. *Bone marrow transplantation*, 29(5), pp.373–7.

Ashton, B.A. et al., 1980. Formation of bone and cartilage by marrow stromal cells in diffusion chambers in vivo. *Clinical orthopaedics and related research*, (151), pp.294–307.

Augello, A. et al., 2007. Cell therapy using allogeneic bone marrow mesenchymal stem cells prevents tissue damage in collagen-induced arthritis. *Arthritis & Rheumatism*, 56(4), pp.1175–1186.

Bai, L. et al., 2012. Hepatocyte growth factor mediates mesenchymal stem cell–induced recovery in multiple sclerosis models. *Nature neuroscience*, 15(6), pp.862–70.

Ball, L.M. et al., 2013. Multiple infusions of mesenchymal stromal cells induce sustained remission in children with steroid-refractory, grade III-IV acute graft-versus-host disease. *British journal of haematology*, 163(4), pp.501–9.

Barr, M.L. et al., 1998. Photopheresis for the prevention of rejection in cardiac transplantation. Photopheresis Transplantation Study Group. *The New England journal of medicine*, 339(24), pp.1744–51.

Barry, F.P. et al., 2005. Immunogenicity of adult mesenchymal stem cells: lessons from the fetal allograft. *Stem cells and development*, 14(3), pp.252–65.

Bartholomew, A. et al., 2002. Mesenchymal stem cells suppress lymphocyte proliferation in vitro and prolong skin graft survival in vivo. *Experimental hematology*, 30(1), pp.42–8.

Bauer, S. et al., 2001. Human TLR9 confers responsiveness to bacterial DNA via species-specific CpG motif recognition. *Proceedings of the National Academy of Sciences of the United States of America*, 98(16), pp.9237–42.

Baxter, A.G. & Cooke, A., 1993. Complement lytic activity has no role in the pathogenesis of autoimmune diabetes in NOD mice. *Diabetes*, 42(11), pp.1574–8.

Beckermann, B.M. et al., 2008. VEGF expression by mesenchymal stem cells contributes to angiogenesis in pancreatic carcinoma. *British journal of cancer*, 99(4), pp.622–31.

Benvenuto, F. et al., 2007. Human mesenchymal stem cells promote survival of T cells in a quiescent state. *Stem cells (Dayton, Ohio)*, 25(7), pp.1753–60.

Billingham, R.E., The biology of graft-versus-host reactions. *Harvey lectures*, 62, pp.21–78.

BILLINGHAM, R.E., BRENT, L. & MEDAWAR, P.B., 1953. Actively acquired tolerance of foreign cells. *Nature*, 172(4379), pp.603–6.

Biron, C.A., 1997. Activation and function of natural killer cell responses during viral infections. *Current opinion in immunology*, 9(1), pp.24–34.

Le Blanc, K. et al., 2008. Mesenchymal stem cells for treatment of steroid-resistant, severe, acute graft-versus-host disease: a phase II study. *Lancet*, 371(9624), pp.1579–86.

Le Blanc, K. et al., 2004. Treatment of severe acute graft-versus-host disease with third party haploidentical mesenchymal stem cells. *Lancet*, 363(9419), pp.1439–41.

Blazar, B.R., Carroll, S.F. & Vallera, D.A., 1991. Prevention of murine graft-versus-host disease and bone marrow alloengraftment across the major histocompatibility barrier after donor graft preincubation with anti-LFA1 immunotoxin. *Blood*, 78(11), pp.3093–102.

Boissel, L. et al., 2008. Umbilical cord mesenchymal stem cells increase expansion of cord blood natural killer cells. *Biology of blood and marrow transplantation : journal of the American Society for Blood and Marrow Transplantation*, 14(9), pp.1031–8.

Bosma, G.C., Custer, R.P. & Bosma, M.J., 1983. A severe combined immunodeficiency mutation in the mouse. *Nature*, 301(5900), pp.527–30.

Boumaza, I. et al., 2009. Autologous bone marrow-derived rat mesenchymal stem cells promote PDX-1 and insulin expression in the islets, alter T cell cytokine pattern and preserve regulatory T cells in the periphery and induce sustained normoglycemia. *Journal of autoimmunity*, 32(1), pp.33–42

Bradford, M.M., 1976. A rapid and sensitive method for the quantitation of microgram quantities of protein utilizing the principle of protein-dye binding. *Analytical biochemistry*, 72, pp.248–54.

Breitbart, E.A. et al., 2010. Mesenchymal stem cells accelerate bone allograft incorporation in the presence of diabetes mellitus. *Journal of orthopaedic research : official publication of the Orthopaedic Research Society*, 28(7), pp.942–9.

Brunstein, C.G. et al., 2011. Infusion of ex vivo expanded T regulatory cells in adults transplanted with umbilical cord blood: safety profile and detection kinetics. *Blood*, 117(3), pp.1061–70.

BURNET, M., 1959. Auto-immune disease. I. Modern immunological concepts. *British medical journal*, 2(5153), pp.645–50.

Caplan, A.I., 1991. Mesenchymal stem cells. *Journal of orthopaedic research : official publication of the Orthopaedic Research Society*, 9(5), pp.641–50.

Carpenter, E.L. et al., 2009. Activation of human B cells by the agonist CD40 antibody CP-870,893 and augmentation with simultaneous toll-like receptor 9 stimulation. *Journal of translational medicine*, 7(1), p.93.

Carpenter, P.A. et al., 2002. A humanized non-FcR-binding anti-CD3 antibody, visilizumab, for treatment of steroid-refractory acute graft-versus-host disease. *Blood*, 99(8), pp.2712–9.

Casellas, R. et al., 2007. Igkappa allelic inclusion is a consequence of receptor editing. *The Journal of experimental medicine*, 204(1), pp.153–60.

Casiraghi, F. et al., 2008. Pretransplant infusion of mesenchymal stem cells prolongs the survival of a semiallogeneic heart transplant through the generation of regulatory T cells. *Journal of immunology (Baltimore, Md. : 1950)*, 181(6), pp.3933–46.

Cerutti, A., 2008. The regulation of IgA class switching. *Nature reviews. Immunology*, 8(6), pp.421–34.

Chamberlain, G. et al., 2008. Murine mesenchymal stem cells exhibit a restricted repertoire of functional chemokine receptors: comparison with human. P. Sommer, ed. *PloS one*, 3(8), p.e2934.

Chen, C. et al., 1995. Immunoglobulin heavy chain gene replacement: a mechanism of receptor editing. *Immunity*, 3(6), pp.747–55.

Chen, L. et al., 2007. Effects of human mesenchymal stem cells on the differentiation of dendritic cells from CD34+ cells. *Stem cells and development*, 16(5), pp.719–31.

Chen, W. et al., 2003. Conversion of peripheral CD4+CD25- naive T cells to CD4+CD25+ regulatory T cells by TGF-beta induction of transcription factor Foxp3. *The Journal of experimental medicine*, 198(12), pp.1875–86.

Chen, X., Armstrong, M.A. & Li, G., 2006. Mesenchymal stem cells in immunoregulation. *Immunology and cell biology*, 84(5), pp.413–21.

Chen, Y.-B. & Cutler, C.S., 2013. Biomarkers for acute GVHD: can we predict the unpredictable? *Bone marrow transplantation*, 48(6), pp.755–60.

Chiesa, S. et al., 2011. Mesenchymal stem cells impair in vivo T-cell priming by dendritic cells. *Proceedings of the National Academy of Sciences of the United States of America*, 108(42), pp.17384–9.

Choudhery, M.S. et al., 2014. Donor age negatively impacts adipose tissue-derived mesenchymal stem cell expansion and differentiation. *Journal of translational medicine*, 12(1), p.8.

Christianson, S.W. et al., 1997. Enhanced human CD4+ T cell engraftment in beta2-microglobulin-deficient NOD-scid mice. *Journal of immunology (Baltimore, Md. : 1950)*, 158(8), pp.3578–86.

Claman, H.N. et al., 1985. Chronic graft-versus-host disease as a model for scleroderma. *Cellular Immunology*, 94(1), pp.73–84.

Clavert, A. et al., 2013. Safety and efficacy of rituximab in steroid-refractory chronic GVHD. *Bone marrow transplantation*, 48(5), pp.734–6.

Collins, P.R. et al., 2004. Cathepsin L1, the major protease involved in liver fluke (Fasciola hepatica) virulence: propetide cleavage sites and autoactivation of the zymogen secreted from gastrodermal cells. *The Journal of biological chemistry*, 279(17), pp.17038–46.

Collison, L.W. et al., 2007. The inhibitory cytokine IL-35 contributes to regulatory T-cell function. *Nature*, 450(7169), pp.566–9.

Comoli, P. et al., 2008. Human mesenchymal stem cells inhibit antibody production induced in vitro by allostimulation. *Nephrology, dialysis, transplantation : official publication of the European Dialysis and Transplant Association - European Renal Association*, 23(4), pp.1196–202.

Corcione, A. et al., 2006. Human mesenchymal stem cells modulate B-cell functions. *Blood*, 107(1), pp.367–72.

Couriel, D.R. et al., 2005. Sirolimus in combination with tacrolimus and corticosteroids for the treatment of resistant chronic graft-versus-host disease. *British journal of haematology*, 130(3), pp.409–17.

Cutler, C. et al., 2006. Rituximab for steroid-refractory chronic graft-versus-host disease. *Blood*, 108(2), pp.756–62.

Cuttica, M.J. et al., 2011. Perivascular T-cell infiltration leads to sustained pulmonary artery remodeling after endothelial cell damage. *American journal of respiratory cell and molecular biology*, 45(1), pp.62–71.

Cyster, J.G., 1999. Chemokines and cell migration in secondary lymphoid organs. *Science (New York, N.Y.)*, 286(5447), pp.2098–102.

DeClerck, Y., Draper, V. & Parkman, R., 1986. Clonal analysis of murine graft-vs-host disease. II. Leukokines that stimulate fibroblast proliferation and collagen synthesis in graft-vs. host disease. *Journal of immunology (Baltimore, Md. : 1950)*, 136(10), pp.3549–52.

Deeg, H.J., 2007. How I treat refractory acute GVHD. *Blood*, 109(10), pp.4119–26.

Degos, L., 2009. Jean Dausset a scientific pioneer: intuition and creativity for the patients (1916-2009). *Haematologica*, 94(9), pp.1331–2.

DelaRosa, O. et al., 2012. Human adipose-derived stem cells impair natural killer cell function and exhibit low susceptibility to natural killer-mediated lysis. *Stem cells and development*, 21(8), pp.1333–43.

Delgado, M. et al., 2006. Vasoactive intestinal polypeptide induces regulatory dendritic cells that prevent acute graft versus host disease and leukemia relapse after bone marrow transplantation. *Annals of the New York Academy of Sciences*, 1070, pp.226–32.

Dhir, S., Slatter, M. & Skinner, R., 2014. Recent advances in the management of graft-versus-host disease. *Archives of disease in childhood*, 99(12), pp.1150–1157.

Dieckmann, D. et al., 2001. Ex vivo isolation and characterization of CD4(+)CD25(+) T cells with regulatory properties from human blood. *The Journal of experimental medicine*, 193(11), pp.1303–10.

Dignan, F.L. et al., 2012. Efficacy of bimonthly extracorporeal photopheresis in refractory chronic mucocutaneous GVHD. *Bone marrow transplantation*, 47(6), pp.824–30.

Dignan, F.L. et al., 2012. Organ-specific management and supportive care in chronic graft-versus-host disease. *British journal of haematology*, 158(1), pp.62–78.

Djouad, F. et al., 2007. Mesenchymal stem cells inhibit the differentiation of dendritic cells through an interleukin-6-dependent mechanism. *Stem cells (Dayton, Ohio)*, 25(8), pp.2025–32.

Djouad, F. et al., 2005. Reversal of the immunosuppressive properties of mesenchymal stem cells by tumor necrosis factor alpha in collagen-induced arthritis. *Arthritis and rheumatism*, 52(5), pp.1595–603.

Doherty, P.C. & Zinkernagel, R.M., 1975a. A biological role for the major histocompatibility antigens. *Lancet*, 1(7922), pp.1406–9.

Doherty, P.C. & Zinkernagel, R.M., 1975b. H-2 compatibility is required for T-cell-mediated lysis of target cells infected with lymphocytic choriomeningitis virus. *The Journal of experimental medicine*, 141(2), pp.502–7.

Dominici, M. et al., 2006. Minimal criteria for defining multipotent mesenchymal stromal cells. The International Society for Cellular Therapy position statement. *Cytotherapy*, 8(4), pp.315–7.

Doney, K. et al., 1985. A randomized trial of antihuman thymocyte globulin versus murine monoclonal antihuman T-cell antibodies as immunosuppressive therapy for aplastic anemia. *Experimental hematology*, 13(6), pp.520–4.

Dowling, D.J. et al., 2010. Major secretory antigens of the helminth Fasciola hepatica activate a suppressive dendritic cell phenotype that attenuates Th17 cells but fails to activate Th2 immune responses. *Infection and immunity*, 78(2), pp.793–801.

Duffner, U. et al., 2003. Role of CXCR3-induced donor T-cell migration in acute GVHD. *Experimental hematology*, 31(10), pp.897–902.

Durie, F.H. et al., 1994. Antibody to the ligand of CD40, gp39, blocks the occurrence of the acute and chronic forms of graft-vs-host disease. *The Journal of clinical investigation*, 94(3), pp.1333–8.

Dutt, S. et al., 2007. Naive and Memory T Cells Induce Different Types of Graft-versus-Host Disease. *The Journal of Immunology*, 179(10), pp.6547–6554.

Edelson, R. et al., 1987. Treatment of cutaneous T-cell lymphoma by extracorporeal photochemotherapy. Preliminary results. *The New England journal of medicine*, 316(6), pp.297–303.

Edinger, M. et al., 2003. CD4+CD25+ regulatory T cells preserve graft-versus-tumor activity while inhibiting graft-versus-host disease after bone marrow transplantation. *Nature medicine*, 9(9), pp.1144–50.

Ehlers, S., 2005. Tumor necrosis factor and its blockade in granulomatous infections: differential modes of action of infliximab and etanercept? *Clinical infectious diseases : an official publication of the Infectious Diseases Society of America*, 41 Suppl 3, pp.S199–203.

English, K. et al., 2009. Cell contact, prostaglandin E(2) and transforming growth factor beta 1 play non-redundant roles in human mesenchymal stem cell induction of CD4+CD25(High) forkhead box P3+ regulatory T cells. *Clinical and experimental immunology*, 156(1), pp.149–60.

English, K. et al., 2007. IFN-gamma and TNF-alpha differentially regulate immunomodulation by murine mesenchymal stem cells. *Immunology letters*, 110(2), pp.91–100.

English, K., Barry, F.P. & Mahon, B.P., 2008. Murine mesenchymal stem cells suppress dendritic cell migration, maturation and antigen presentation. *Immunology letters*, 115(1), pp.50–8.

English, K. & Wood, K.J., 2013. Mesenchymal stromal cells in transplantation rejection and tolerance. *Cold Spring Harbor perspectives in medicine*, 3(5), p.a015560.

Ettinger, R. et al., 2005. IL-21 induces differentiation of human naive and memory B cells into antibody-secreting plasma cells. *Journal of immunology (Baltimore, Md. : 1950)*, 175(12), pp.7867–79.

Fassbender, M. et al., 2010. Cyclic adenosine monophosphate and IL-10 coordinately contribute to nTreg cell-mediated suppression of dendritic cell activation. *Cellular immunology*, 265(2), pp.91–6.

Fauriat, C. et al., 2010. Regulation of human NK-cell cytokine and chemokine production by target cell recognition. *Blood*, 115(11), pp.2167–76.

Ferrara, J.L. & Deeg, H.J., 1991. Graft-versus-host disease. *The New England journal of medicine*, 324(10), pp.667–74.

Ferrara, J.L.M. et al., 2009. Graft-versus-host disease. *Lancet*, 373(9674), pp.1550–61.

Fillatreau, S. et al., 2002. B cells regulate autoimmunity by provision of IL-10. *Nature immunology*, 3(10), pp.944–50.

Finkelman, F.D., Mond, J.J. & Metcalf, E.S., 1983. Effects of neonatal anti-delta antibody treatment on the murine immune system. I. Suppression of development of surface IgD+ B cells and expansion of a surface IgM+ IgD- B lymphocyte population. *Journal of immunology (Baltimore, Md. : 1950)*, 131(2), pp.593–600.

Fisher-Shoval, Y. et al., 2012. Transplantation of placenta-derived mesenchymal stem cells in the EAE mouse model of MS. *Journal of molecular neuroscience : MN*, 48(1), pp.176–84.

Fiúza, U.-M. & Arias, A.M., 2007. Cell and molecular biology of Notch. *The Journal of endocrinology*, 194(3), pp.459–74.

Fletcher, J.M. et al., 2009. CD39+Foxp3+ regulatory T Cells suppress pathogenic Th17 cells and are impaired in multiple sclerosis. *Journal of immunology (Baltimore, Md. : 1950)*, 183(11), pp.7602–10.

Flowers, M.E.D. et al., 2008. A multicenter prospective phase 2 randomized study of extracorporeal photopheresis for treatment of chronic graft-versus-host disease. *Blood*, 112(7), pp.2667–74.

Forquet, F. et al., 1999. Presentation of antigens internalized through the B cell receptor requires newly synthesized MHC class II molecules. *Journal of immunology (Baltimore, Md. : 1950)*, 162(6), pp.3408–16.

Francis, D.A. et al., 1995. Induction of the transcription factors NF-kappa B, AP-1 and NF-AT during B cell stimulation through the CD40 receptor. *International immunology*, 7(2), pp.151–61.

Franquesa, M. et al., 2014. Human adipose tissue-derived mesenchymal stem cells abrogate plasmablast formation and induce regulatory B cells independently of T helper cells. *Stem cells (Dayton, Ohio)*.

Franquesa, M. et al., 2012. Immunomodulatory effect of mesenchymal stem cells on B cells. *Frontiers in immunology*, 3, p.212.

Friedenstein, A.J. et al., 1968. Heterotopic of bone marrow. Analysis of precursor cells for osteogenic and hematopoietic tissues. *Transplantation*, 6(2), pp.230–47.

Friedenstein, A.J. et al., 1974. Stromal cells responsible for transferring the microenvironment of the hemopoietic tissues. Cloning in vitro and retransplantation in vivo. *Transplantation*, 17(4), pp.331–40.

Friedenstein, A.J., Piatetzky-Shapiro, I.I. & Petrakova, K. V, 1966. Osteogenesis in transplants of bone marrow cells. *Journal of embryology and experimental morphology*, 16(3), pp.381–90.

Fu, J. et al., 2014. T-bet Is Critical for the Development of Acute Graft-versus-Host Disease through Controlling T Cell Differentiation and Function. *Journal of immunology (Baltimore, Md. : 1950)*.

Gavin, A. et al., 2004. Peripheral B lymphocyte tolerance. *The Keio journal of medicine*, 53(3), pp.151–8.

Gay, D. et al., 1993. Receptor editing: an approach by autoreactive B cells to escape tolerance. *The Journal of experimental medicine*, 177(4), pp.999–1008.

Ge, W. et al., 2010. Regulatory T-cell generation and kidney allograft tolerance induced by mesenchymal stem cells associated with indoleamine 2,3-dioxygenase expression. *Transplantation*, 90(12), pp.1312–20.

Gevers, D. et al., 2014. The treatment-naive microbiome in new-onset Crohn's disease. *Cell host & microbe*, 15(3), pp.382–92.

Gieseke, F. et al., 2013. Proinflammatory stimuli induce galectin-9 in human mesenchymal stromal cells to suppress T-cell proliferation. *European journal of immunology*, 43(10), pp.2741–9.

Gill, R.G., 2010. NK cells: elusive participants in transplantation immunity and tolerance. *Current opinion in immunology*, 22(5), pp.649–54.

Giuliani, M. et al., 2014. TLR ligands stimulation protects MSC from NK killing. *Stem cells (Dayton, Ohio)*, 32(1), pp.290–300.

Glenn, J.D. et al., 2014. Mesenchymal stem cells differentially modulate effector CD8+ T cell subsets and exacerbate experimental autoimmune encephalomyelitis. *Stem cells (Dayton, Ohio)*, 32(10), pp.2744–55.

Gondek, D.C. et al., 2005. Cutting edge: contact-mediated suppression by CD4+CD25+ regulatory cells involves a granzyme B-dependent, perforin-independent mechanism. *Journal of immunology (Baltimore, Md. : 1950)*, 174(4), pp.1783–6.

González, M.A. et al., 2009a. Adipose-derived mesenchymal stem cells alleviate experimental colitis by inhibiting inflammatory and autoimmune responses. *Gastroenterology*, 136(3), pp.978–89.

González, M.A. et al., 2009b. Treatment of experimental arthritis by inducing immune tolerance with human adipose-derived mesenchymal stem cells. *Arthritis and rheumatism*, 60(4), pp.1006–19.

Goodnow, C.C. et al., 1988. Altered immunoglobulin expression and functional silencing of self-reactive B lymphocytes in transgenic mice. *Nature*, 334(6184), pp.676–82.

Gooley, T.A. et al., 2010. Reduced mortality after allogeneic hematopoietic-cell transplantation. *The New England journal of medicine*, 363(22), pp.2091–101.

Gorer, P.A., 1936. The Detection of Antigenic Differences in Mouse Erythrocytes by the Employment of Immune Sera. *British Journal of Experimental Pathology*, 17(1), p.42.

Gospodarowicz, D. & Lau, K., 1989. Pituitary follicular cells secrete both vascular endothelial growth factor and follistatin. *Biochemical and biophysical research communications*, 165(1), pp.292–8.

Götherström, C. et al., 2011. Fetal and adult multipotent mesenchymal stromal cells are killed by different pathways. *Cytotherapy*, 13(3), pp.269–78.

Grandien, A. et al., 1994. Negative selection of multireactive B cell clones in normal adult mice. *European journal of immunology*, 24(6), pp.1345–52.

Graubert, T.A. et al., 1997. Perforin/granzyme-dependent and independent mechanisms are both important for the development of graft-versus-host disease after murine bone marrow transplantation. *The Journal of clinical investigation*, 100(4), pp.904–11.

Graziani, F. et al., 2002. Treatment of acute graft versus host disease with low dose-alternate day anti-thymocyte globulin. *Haematologica*, 87(9), pp.973–8.

Greinix, H.T. et al., 2011. Progressive improvement in cutaneous and extracutaneous chronic graft-versus-host disease after a 24-week course of extracorporeal photopheresis--results of a crossover randomized study. *Biology of blood and marrow transplantation : journal of the American Society for Blood and Marrow Transplantation*, 17(12), pp.1775–82.

Grigoriadis, N. et al., 2011. Variable behavior and complications of autologous bone marrow mesenchymal stem cells transplanted in experimental autoimmune encephalomyelitis. *Experimental neurology*, 230(1), pp.78–89.

Grinnemo, K.H. et al., 2004. Xenoreactivity and engraftment of human mesenchymal stem cells transplanted into infarcted rat myocardium. *The Journal of thoracic and cardiovascular surgery*, 127(5), pp.1293–300.

Grinnemo, K.-H. et al., 2006. Human mesenchymal stem cells do not differentiate into cardiomyocytes in a cardiac ischemic xenomodel. *Annals of medicine*, 38(2), pp.144–53.

Grossman, W.J. et al., 2004. Human T regulatory cells can use the perforin pathway to cause autologous target cell death. *Immunity*, 21(4), pp.589–601.

Gu, Z. et al., 2010. Transplantation of umbilical cord mesenchymal stem cells alleviates lupus nephritis in MRL/lpr mice. *Lupus*, 19(13), pp.1502–14.

Guan, M. et al., 2012. Directing mesenchymal stem cells to bone to augment bone formation and increase bone mass. *Nature medicine*, 18(3), pp.456–62.

Guo, Y. et al., 2013. Human mesenchymal stem cells upregulate CD1dCD5(+) regulatory B cells in experimental autoimmune encephalomyelitis. *Neuroimmunomodulation*, 20(5), pp.294–303.

Gupta, K. et al., 1999. VEGF prevents apoptosis of human microvascular endothelial cells via opposing effects on MAPK/ERK and SAPK/JNK signaling. *Experimental cell research*, 247(2), pp.495–504.

Hakim, F.T. et al., 1991. Repopulation of host lymphohematopoietic systems by donor cells during graft-versus-host reaction in unirradiated adult F1 mice injected with parental lymphocytes. *Journal of immunology (Baltimore, Md. : 1950)*, 146(7), pp.2108–15.

Hall, B.M. et al., 1990. Specific unresponsiveness in rats with prolonged cardiac allograft survival after treatment with cyclosporine. III. Further characterization of the CD4+ suppressor cell and its mechanisms of action. *The Journal of experimental medicine*, 171(1), pp.141–57.

Halverson, R., Torres, R.M. & Pelanda, R., 2004. Receptor editing is the main mechanism of B cell tolerance toward membrane antigens. *Nature immunology*, 5(6), pp.645–50.

Hamilton, B.L., 1987. L3T4-positive T cells participate in the induction of graft-vs-host disease in response to minor histocompatibility antigens. *Journal of immunology (Baltimore, Md. : 1950)*, 139(8), pp.2511–5.

Hamilton, C.M. et al., 2009. The Fasciola hepatica tegumental antigen suppresses dendritic cell maturation and function. *Infection and immunity*, 77(6), pp.2488–98.

Hardy, R.R. & Hayakawa, K., 2001. B cell development pathways. *Annual review of immunology*, 19, pp.595–621.

Hartigan-O'Connor, D.J. et al., 2007. Human CD4+ regulatory T cells express lower levels of the IL-7 receptor alpha chain (CD127), allowing consistent identification and sorting of live cells. *Journal of immunological methods*, 319(1-2), pp.41–52.

Hartley, S.B. et al., 1991. Elimination from peripheral lymphoid tissues of self-reactive B lymphocytes recognizing membrane-bound antigens. *Nature*, 353(6346), pp.765–9.

Hartley, S.B. et al., 1993. Elimination of self-reactive B lymphocytes proceeds in two stages: Arrested development and cell death. *Cell*, 72(3), pp.325–335.

Hattori, K. et al., 1998. Differential effects of anti-Fas ligand and anti-tumor necrosis factor alpha antibodies on acute graft-versus-host disease pathologies. *Blood*, 91(11), pp.4051–5.

Haynesworth, S.E., Baber, M.A. & Caplan, A.I., 1996. Cytokine expression by human marrow-derived mesenchymal progenitor cells in vitro: effects of dexamethasone and IL-1 alpha. *Journal of cellular physiology*, 166(3), pp.585–92.

Hesselton, R.M. et al., 1995. High levels of human peripheral blood mononuclear cell engraftment and enhanced susceptibility to human immunodeficiency virus type 1 infection in NOD/LtSz-scid/scid mice. *The Journal of infectious diseases*, 172(4), pp.974–82.

Hill, G.R. et al., 1999. Differential roles of IL-1 and TNF-alpha on graft-versus-host disease and graft versus leukemia. *The Journal of clinical investigation*, 104(4), pp.459–67.

Hill, G.R. & Ferrara, J.L., 2000. The primacy of the gastrointestinal tract as a target organ of acute graft-versus-host disease: rationale for the use of cytokine shields in allogeneic bone marrow transplantation. *Blood*, 95(9), pp.2754–9.

Hingorani, S.R. et al., 2005. Acute renal failure after myeloablative hematopoietic cell transplant: incidence and risk factors. *Kidney international*, 67(1), pp.272–7.

Hippen, K.L. et al., 2012. Blocking IL-21 signaling ameliorates xenogeneic GVHD induced by human lymphocytes. *Blood*, 119(2), pp.619–28.

Hippen, K.L. et al., 2005. In Vivo Assessment of the Relative Contributions of Deletion, Anergy, and Editing to B Cell Self-Tolerance. *The Journal of Immunology*, 175(2), pp.909–916.

Ho, V.T. & Cutler, C., 2008. Current and novel therapies in acute GVHD. *Best practice & research. Clinical haematology*, 21(2), pp.223–37.

Hodgkin, P.D., Heath, W.R. & Baxter, A.G., 2007. The clonal selection theory: 50 years since the revolution. *Nature immunology*, 8(10), pp.1019–26.

Hoffmann, P. et al., 2002. Donor-type CD4(+)CD25(+) regulatory T cells suppress lethal acute graft-versus-host disease after allogeneic bone marrow transplantation. *The Journal of experimental medicine*, 196(3), pp.389–99.

Holler, E. et al., 1990. Increased serum levels of tumor necrosis factor alpha precede major complications of bone marrow transplantation. *Blood*, 75(4), pp.1011–6.

Horowitz, M.M. & Bortin, M.M., 1990. Current status of allogeneic bone marrow transplantation. *Clinical transplants*, pp.41–52.

Horwitz, E.M. et al., 2005. Clarification of the nomenclature for MSC: The International Society for Cellular Therapy position statement. *Cytotherapy*, 7(5), pp.393–5.

Howell, C.D. et al., 1989. Hepatic homing of mononuclear inflammatory cells isolated during murine chronic graft-vs-host disease. *Journal of immunology (Baltimore, Md. : 1950)*, 143(2), pp.476–83.

Hu, J. et al., 2013. Mesenchymal stem cells attenuate ischemic acute kidney injury by inducing regulatory T cells through splenocyte interactions. *Kidney international*, 84(3), pp.521–31.

Di Ianni, M. et al., 2008. Mesenchymal cells recruit and regulate T regulatory cells. *Experimental hematology*, 36(3), pp.309–18.

Di Ianni, M. et al., 2011. Tregs prevent GVHD and promote immune reconstitution in HLA-haploidentical transplantation. *Blood*, 117(14), pp.3921–8.

Jacobsohn, D.A. et al., 2009. Evaluation of pentostatin in corticosteroid-refractory chronic graft-versus-host disease in children: a Pediatric Blood and Marrow Transplant Consortium study. *Blood*, 114(20), pp.4354–60.

Jacobsohn, D.A. et al., 2003. Infliximab for steroid-refractory acute GVHD: a case series. *American journal of hematology*, 74(2), pp.119–24.

Jaffee, B.D. & Claman, H.N., 1983. Chronic graft-versus-host disease (GVHD) as a model for scleroderma. *Cellular Immunology*, 77(1), pp.1–12.

Jankovic, D. et al., 2013. The Nlrp3 inflammasome regulates acute graft-versus-host disease. *The Journal of experimental medicine*, 210(10), pp.1899–910.

Jansen, B.J.H. et al., 2010. Functional differences between mesenchymal stem cell populations are reflected by their transcriptome. *Stem cells and development*, 19(4), pp.481–90.

Jeon, M.-S. et al., 2010. Xenoreactivity of human clonal mesenchymal stem cells in a major histocompatibility complex-matched allogeneic graft-versus-host disease mouse model. *Cellular immunology*, 261(1), pp.57–63.

Jonuleit, H. et al., 2001. Identification and functional characterization of human CD4(+)CD25(+) T cells with regulatory properties isolated from peripheral blood. *The Journal of experimental medicine*, 193(11), pp.1285–94.

Jung, Y.-J. et al., 2007. MSC-DC interactions: MSC inhibit maturation and migration of BM-derived DC. *Cytotherapy*, 9(5), pp.451–8.

Kanakry, C.G. et al., 2014. Multi-Institutional Study of Post-Transplantation Cyclophosphamide As Single-Agent Graft-Versus-Host Disease Prophylaxis After Allogeneic Bone Marrow Transplantation Using Myeloablative Busulfan and Fludarabine Conditioning. *Journal of clinical oncology : official journal of the American Society of Clinical Oncology*, p.JCO.2013.54.0625–.

Karussis, D. et al., 2010. Safety and immunological effects of mesenchymal stem cell transplantation in patients with multiple sclerosis and amyotrophic lateral sclerosis. *Archives of neurology*, 67(10), pp.1187–94.

Kataoka, S. et al., 1983. Immunologic aspects of the nonobese diabetic (NOD) mouse. Abnormalities of cellular immunity. *Diabetes*, 32(3), pp.247–53.

Kavanagh, H. & Mahon, B.P., 2011. Allogeneic mesenchymal stem cells prevent allergic airway inflammation by inducing murine regulatory T cells. *Allergy*, 66(4), pp.523–31.

Kebriaei, P. et al., 2009. Adult human mesenchymal stem cells added to corticosteroid therapy for the treatment of acute graft-versus-host disease. *Biology of blood and marrow transplantation : journal of the American Society for Blood and Marrow Transplantation*, 15(7), pp.804–11.

Keck, P. et al., 1989. Vascular permeability factor, an endothelial cell mitogen related to PDGF. *Science*, 246(4935), pp.1309–1312.

Kidd, S. et al., 2009. Direct evidence of mesenchymal stem cell tropism for tumor and wounding microenvironments using in vivo bioluminescent imaging. *Stem cells (Dayton, Ohio)*, 27(10), pp.2614–23.

Kiel, M.J. & Morrison, S.J., 2008. Uncertainty in the niches that maintain haematopoietic stem cells. *Nature reviews. Immunology*, 8(4), pp.290–301.

Kilpinen, L. et al., 2013. Extracellular membrane vesicles from umbilical cord blood-derived MSC protect against ischemic acute kidney injury, a feature that is lost after inflammatory conditioning. *Journal of extracellular vesicles*, 2.

Kim, J. et al., 2008. Breaking of CD8+ T cell tolerance through in vivo ligation of CD40 results in inhibition of chronic graft-versus-host disease and complete donor cell engraftment. *Journal of immunology (Baltimore, Md. : 1950)*, 181(10), pp.7380–9.

King, M. et al., 2008. A new Hu-PBL model for the study of human islet alloreactivity based on NOD-scid mice bearing a targeted mutation in the IL-2 receptor gamma chain gene. *Clinical immunology (Orlando, Fla.)*, 126(3), pp.303–14.

King, M.A. et al., 2009. Human peripheral blood leucocyte non-obese diabetic-severe combined immunodeficiency interleukin-2 receptor gamma chain gene mouse model of xenogeneic graft-versus-host-like disease and the role of host major histocompatibility complex. *Clinical and experimental immunology*, 157(1), pp.104–18.

Kinnear, G., Jones, N.D. & Wood, K.J., 2013. Costimulation blockade: current perspectives and implications for therapy. *Transplantation*, 95(4), pp.527–35.

Kitko, C.L. et al., 2008. Plasma elevations of tumor necrosis factor-receptor-1 at day 7 postallogeneic transplant correlate with graft-versus-host disease severity and overall survival in pediatric patients. *Biology of blood and marrow transplantation : journal of the American Society for Blood and Marrow Transplantation*, 14(7), pp.759–65.

Koç, O.N. et al., 2000. Rapid hematopoietic recovery after coinfusion of autologous-blood stem cells and culture-expanded marrow mesenchymal stem cells in advanced breast cancer patients receiving high-dose chemotherapy. *Journal of clinical oncology : official journal of the American Society of Clinical Oncology*, 18(2), pp.307–16.

Korngold, R. & Sprent, J., 1978. Lethal graft-versus-host disease after bone marrow transplantation across minor histocompatibility barriers in mice. Prevention by removing mature T cells from marrow. *The Journal of experimental medicine*, 148(6), pp.1687–98.

Korngold, R. & Sprent, J., 1987. Variable capacity of L3T4+ T cells to cause lethal graft-versus-host disease across minor histocompatibility barriers in mice. *The Journal of experimental medicine*, 165(6), pp.1552–64.

Kovanen, P.E. & Leonard, W.J., 2004. Cytokines and immunodeficiency diseases: critical roles of the gamma(c)-dependent cytokines interleukins 2, 4, 7, 9, 15, and 21, and their signaling pathways. *Immunological reviews*, 202, pp.67–83.

Krampera, M. et al., 2003. Bone marrow mesenchymal stem cells inhibit the response of naive and memory antigen-specific T cells to their cognate peptide. *Blood*, 101(9), pp.3722–9.

Krampera, M. et al., 2006. Role for interferon-gamma in the immunomodulatory activity of human bone marrow mesenchymal stem cells. *Stem cells (Dayton, Ohio)*, 24(2), pp.386–98.

Kröger, N. et al., 2002. In vivo T cell depletion with pretransplant anti-thymocyte globulin reduces graft-versus-host disease without increasing relapse in good risk myeloid leukemia patients after stem cell transplantation from matched related donors. *Bone marrow transplantation*, 29(8), pp.683–9.

Kubota, E. et al., 1991. Role of T cells in the B-cell response: glutaraldehyde-fixed T-helper hybridoma cells synergize with the lymphokine IL-4 to induce B-cell activation and proliferation. *Immunology*, 72(1), pp.40–7.

Laemmli, U.K., 1970. Cleavage of structural proteins during the assembly of the head of bacteriophage T4. *Nature*, 227(5259), pp.680–5.

Lanzavecchia, A. & Bove, S., 1985. Specific B lymphocytes efficiently pick up, process and present antigen to T cells. *Behring Institute Mitteilungen*, (77), pp.82–7.

Lawton, A.R. et al., 1972. Suppression of immunoglobulin class synthesis in mice. I. Effects of treatment with antibody to -chain. *The Journal of experimental medicine*, 135(2), pp.277–97.

Lazarus, H.M. et al., 1995. Ex vivo expansion and subsequent infusion of human bone marrow-derived stromal progenitor cells (mesenchymal progenitor cells): implications for therapeutic use. *Bone marrow transplantation*, 16(4), pp.557–64.

Lee, J.H. et al., 2013. The synergistic immunoregulatory effects of culture-expanded mesenchymal stromal cells and CD4(+)25(+)Foxp3+ regulatory T cells on skin allograft rejection. *PloS one*, 8(8), p.e70968.

Lee, R.H. et al., 2009. Intravenous hMSCs improve myocardial infarction in mice because cells embolized in lung are activated to secrete the anti-inflammatory protein TSG-6. *Cell stem cell*, 5(1), pp.54–63.

Lee, S.T. et al., 2002. Treatment of high-risk acute myelogenous leukaemia by myeloablative chemoradiotherapy followed by co-infusion of T cell-depleted haematopoietic stem cells and culture-expanded marrow mesenchymal stem cells from a related donor with one fully mismatched hu. *British Journal of Haematology*, 118(4), pp.1128–1131.

Lepelletier, Y. et al., 2010. Galectin-1 and semaphorin-3A are two soluble factors conferring T-cell immunosuppression to bone marrow mesenchymal stem cell. *Stem cells and development*, 19(7), pp.1075–9.

Leung, D. et al., 1989. Vascular endothelial growth factor is a secreted angiogenic mitogen. *Science*, 246(4935), pp.1306–1309.

Levine, J.E. et al., 2008. Etanercept plus methylprednisolone as initial therapy for acute graft-versus-host disease. *Blood*, 111(4), pp.2470–5.

Li, H. et al., 2012. Profound depletion of host conventional dendritic cells, plasmacytoid dendritic cells, and B cells does not prevent graft-versus-host disease induction. *Journal of immunology (Baltimore, Md. : 1950)*, 188(8), pp.3804–11.

Li, J.-F. et al., 2014. The potential of human umbilical cord-derived mesenchymal stem cells as a novel cellular therapy for multiple sclerosis. *Cell transplantation*.

Li, Y., Li, H. & Weigert, M., 2002. Autoreactive B cells in the marginal zone that express dual receptors. *The Journal of experimental medicine*, 195(2), pp.181–8.

Li, Z.Y. et al., 2014. Effects of bone marrow mesenchymal stem cells on hematopoietic recovery and acute graft-versus-host disease in murine allogeneic umbilical cord blood transplantation model. *Cell biochemistry and biophysics*, 70(1), pp.115–22.

Liang, J. et al., 2010. Allogenic mesenchymal stem cells transplantation in refractory systemic lupus erythematosus: a pilot clinical study. *Annals of the rheumatic diseases*, 69(8), pp.1423–9.

Liang, Z. et al., 2007. CXCR4/CXCL12 axis promotes VEGF-mediated tumor angiogenesis through Akt signaling pathway. *Biochemical and biophysical research communications*, 359(3), pp.716–22.

Lieber, M.R. et al., 1988. The defect in murine severe combined immune deficiency: joining of signal sequences but not coding segments in V(D)J recombination. *Cell*, 55(1), pp.7–16.

Lin, C.-S., Lin, G. & Lue, T.F., 2012. Allogeneic and xenogeneic transplantation of adipose-derived stem cells in immunocompetent recipients without immunosuppressants. *Stem cells and development*, 21(15), pp.2770–8.

Van Lint, M.T. et al., 1998. Early treatment of acute graft-versus-host disease with high- or low-dose 6-methylprednisolone: a multicenter randomized trial from the Italian Group for Bone Marrow Transplantation. *Blood*, 92(7), pp.2288–93.

Van Lint, M.T. et al., 2006. Treatment of acute graft-versus-host disease with prednisolone: significant survival advantage for day +5 responders and no advantage for nonresponders receiving anti-thymocyte globulin. *Blood*, 107(10), pp.4177–81.

Liu, Y. et al., 2014. IL-35 mitigates murine acute graft-versus-host disease with retention of graft-versus-leukemia effects. *Leukemia*.

Liu, Y. et al., 2010. Therapeutic potential of human umbilical cord mesenchymal stem cells in the treatment of rheumatoid arthritis. *Arthritis research & therapy*, 12(6), p.R210.

Llufriu, S. et al., 2014. Randomized Placebo-Controlled Phase II Trial of Autologous Mesenchymal Stem Cells in Multiple Sclerosis. *PloS one*, 9(12), p.e113936.

Loder, F. et al., 1999. B cell development in the spleen takes place in discrete steps and is determined by the quality of B cell receptor-derived signals. *The Journal of experimental medicine*, 190(1), pp.75–89.

De Luca, A. et al., 2011. Role of the EGFR ligand/receptor system in the secretion of angiogenic factors in mesenchymal stem cells. *Journal of cellular physiology*, 226(8), pp.2131–8.

Maccario, R. et al., 2005. Interaction of human mesenchymal stem cells with cells involved in alloantigen-specific immune response favors the differentiation of CD4+ T-cell subsets expressing a regulatory/suppressive phenotype. *Haematologica*, 90(4), pp.516–25.

MacLennan, I.C.M., 1995. Autoimmunity: Deletion of autoreactive B cells. *Current Biology*, 5(2), pp.103–106.

MacMillan, M.L. et al., 2002. Early antithymocyte globulin therapy improves survival in patients with steroid-resistant acute graft-versus-host disease. *Biology of blood and marrow transplantation : journal of the American Society for Blood and Marrow Transplantation*, 8(1), pp.40–6.

Madec, A.M. et al., 2009. Mesenchymal stem cells protect NOD mice from diabetes by inducing regulatory T cells. *Diabetologia*, 52(7), pp.1391–9.

Maeda, Y. et al., 2005. Both perforin and Fas ligand are required for the regulation of alloreactive CD8+ T cells during acute graft-versus-host disease. *Blood*, 105(5), pp.2023–7.

Magenau, J.M. et al., 2010. Frequency of CD4(+)CD25(hi)FOXP3(+) regulatory T cells has diagnostic and prognostic value as a biomarker for acute graft-versus-host-disease. *Biology of blood and marrow transplantation : journal of the American Society for Blood and Marrow Transplantation*, 16(7), pp.907–14.

Malisan, F. et al., 1996. Interleukin-10 induces immunoglobulin G isotype switch recombination in human CD40-activated naive B lymphocytes. *The Journal of experimental medicine*, 183(3), pp.937–47.

Maloisel, F. et al., 2003. Long-term outcome with pentostatin treatment in hairy cell leukemia patients. A French retrospective study of 238 patients. *Leukemia*, 17(1), pp.45–51.

Manning, D.D. & Jutila, J.W., 1972. Immunosuppression in mice injected with heterologous anti-immunoglobulin antisera. *Journal of immunology (Baltimore, Md. : 1950)*, 108(1), pp.282–5.

Markey, K.A., MacDonald, K.P.A. & Hill, G.R., 2014. The biology of graft-versus-host disease: experimental systems instructing clinical practice. *Blood*, 124(3), pp.354–62.

Martin, P.J. et al., 1990. A retrospective analysis of therapy for acute graft-versus-host disease: initial treatment. *Blood*, 76(8), pp.1464–72.

Martin, P.J. et al., 2010. Prochymal Improves Response Rates In Patients With Steroid-Refractory Acute Graft Versus Host Disease (SR-GVHD) Involving The Liver And Gut: Results Of A Randomized, Placebo-Controlled, Multicenter Phase III Trial In GVHD. *Biology of Blood and Marrow Transplantation*, 16(2), pp.S169–S170.

Matthyssens, G., Hozumi, N. & Tonegawa, S., Somatic generation of antibody diversity. *Annales d'immunologie*, 127(3-4), pp.439–48.

McCormick, L.L. et al., 1999. Anti-TGF-beta treatment prevents skin and lung fibrosis in murine sclerodermatous graft-versus-host disease: a model for human scleroderma. *Journal of immunology (Baltimore, Md. : 1950)*, 163(10), pp.5693–9.

McManus, D.P. & Dalton, J.P., 2006. Vaccines against the zoonotic trematodes Schistosoma japonicum, Fasciola hepatica and Fasciola gigantica. *Parasitology*, 133 Suppl, pp.S43–61.

Meisel, R. et al., 2004. Human bone marrow stromal cells inhibit allogeneic T-cell responses by indoleamine 2,3-dioxygenase-mediated tryptophan degradation. *Blood*, 103(12), pp.4619–21.

Menard, C. et al., 2013. Clinical-grade mesenchymal stromal cells produced under various good manufacturing practice processes differ in their immunomodulatory properties: standardization of immune quality controls. *Stem cells and development*, 22(12), pp.1789–801.

Méndez-Ferrer, S. et al., 2010. Mesenchymal and haematopoietic stem cells form a unique bone marrow niche. *Nature*, 466(7308), pp.829–34.

Messina, C. et al., 2008. Prevention and treatment of acute GvHD. *Bone marrow transplantation*, 41 Suppl 2(S2), pp.S65–70.

Mestas, J. & Hughes, C.C.W., 2004. Of mice and not men: differences between mouse and human immunology. *Journal of immunology (Baltimore, Md. : 1950)*, 172(5), pp.2731–8.

Mond, J.J., Lees, A. & Snapper, C.M., 1995. T cell-independent antigens type 2. *Annual review of immunology*, 13, pp.655–92.

Montoya, C.J. et al., 2007. Characterization of human invariant natural killer T subsets in health and disease using a novel invariant natural killer T cell-clonotypic monoclonal antibody, 6B11. *Immunology*, 122(1), pp.1–14.

Moretta, L. et al., 2002. Human natural killer cells: their origin, receptors and function. *European journal of immunology*, 32(5), pp.1205–11.

Morris, S.C. et al., 1990. Allotype-specific immunoregulation of autoantibody production by host B cells in chronic graft-versus host disease. *Journal of immunology (Baltimore, Md. : 1950)*, 144(3), pp.916–22.

Mosier, D.E. et al., 1988. Transfer of a functional human immune system to mice with severe combined immunodeficiency. *Nature*, 335(6187), pp.256–9.

Mudrabettu, C. et al., 2014. Safety and Efficacy of Autologous Mesenchymal Stromal Cells Transplantation in patients undergoing Living Donor Kidney Transplantation: A Pilot Study. *Nephrology (Carlton, Vic.)*.

Müller, I. et al., 2008. Application of multipotent mesenchymal stromal cells in pediatric patients following allogeneic stem cell transplantation. *Blood cells, molecules & diseases*, 40(1), pp.25–32.

Murphy, J.M. et al., 2002. Reduced chondrogenic and adipogenic activity of mesenchymal stem cells from patients with advanced osteoarthritis. *Arthritis and rheumatism*, 46(3), pp.704–13.

Najar, M. et al., 2009. Mesenchymal stromal cells promote or suppress the proliferation of T lymphocytes from cord blood and peripheral blood: the importance of low cell ratio and role of interleukin-6. *Cytotherapy*, 11(5), pp.570–83.

Nakao, N. et al., 2010. Adipose tissue-derived mesenchymal stem cells facilitate hematopoiesis in vitro and in vivo: advantages over bone marrow-derived mesenchymal stem cells. *The American journal of pathology*, 177(2), pp.547–54.

Nemazee, D. & Buerki, K., 1989. Clonal deletion of autoreactive B lymphocytes in bone marrow chimeras. *Proceedings of the National Academy of Sciences of the United States of America*, 86(20), pp.8039–43.

Németh, K. et al., 2009. Bone marrow stromal cells attenuate sepsis via prostaglandin E(2)-dependent reprogramming of host macrophages to increase their interleukin-10 production. *Nature medicine*, 15(1), pp.42–9.

Nemoto, Y. et al., 2013. Bone marrow-mesenchymal stem cells are a major source of interleukin-7 and sustain colitis by forming the niche for colitogenic CD4 memory T cells. *Gut*, 62(8), pp.1142–52.

Di Nicola, M., 2002. Human bone marrow stromal cells suppress T-lymphocyte proliferation induced by cellular or nonspecific mitogenic stimuli. *Blood*, 99(10), pp.3838–3843.

Nie, Y. et al., 2010. Defective phenotype of mesenchymal stem cells in patients with systemic lupus erythematosus. *Lupus*, 19(7), pp.850–9.

Nie, Y. et al., 2004. The role of CXCR4 in maintaining peripheral B cell compartments and humoral immunity. *The Journal of experimental medicine*, 200(9), pp.1145–56.

Noone, C. et al., 2013. IFN-γ stimulated human umbilical-tissue-derived cells potently suppress NK activation and resist NK-mediated cytotoxicity in vitro. *Stem cells and development*, 22(22), pp.3003–14.

Nuñez, C. et al., 1996. B cells are generated throughout life in humans. *Journal of immunology (Baltimore, Md. : 1950)*, 156(2), pp.866–72.

Nwabo Kamdje, A.H. et al., 2011. Notch-3 and Notch-4 signaling rescue from apoptosis human B-ALL cells in contact with human bone marrow-derived mesenchymal stromal cells. *Blood*, 118(2), pp.380–9.

O'Shea, D. et al., 2010. Natural killer cells in obesity: impaired function and increased susceptibility to the effects of cigarette smoke. *PloS one*, 5(1), p.e8660.

Oh, J.Y. et al., 2010. Anti-inflammatory protein TSG-6 reduces inflammatory damage to the cornea following chemical and mechanical injury. *Proceedings of the National Academy of Sciences of the United States of America*, 107(39), pp.16875–80.

Paczesny, S. et al., 2009. A biomarker panel for acute graft-versus-host disease. *Blood*, 113(2), pp.273–8.

Pal, R. et al., 2010. Functional recovery after transplantation of bone marrow-derived human mesenchymal stromal cells in a rat model of spinal cord injury. *Cytotherapy*, 12(6), pp.792–806.

Pan, L. et al., 1999. Granulocyte colony-stimulating factor-mobilized allogeneic stem cell transplantation maintains graft-versus-leukemia effects through a perforin-dependent pathway while preventing graft-versus-host disease. *Blood*, 93(12), pp.4071–8.

Del Papa, B. et al., 2013. Notch1 modulates mesenchymal stem cells mediated regulatory T-cell induction. *European journal of immunology*, 43(1), pp.182–7.

Papadopoulou, A. et al., 2012. Mesenchymal stem cells are conditionally therapeutic in preclinical models of rheumatoid arthritis. *Annals of the rheumatic diseases*, 71(10), pp.1733–40.

Parker, D.C., 1993. T cell-dependent B cell activation. *Annual review of immunology*, 11, pp.331–60.

Patel, P. et al., 2014. Combination of Linear Accelerator-Based Intensity-Modulated Total Marrow Irradiation and Myeloablative Fludarabine/Busulfan: A Phase I Study. *Biology of blood and marrow transplantation : journal of the American Society for Blood and Marrow Transplantation*.

Patel, S.A. et al., 2010. Mesenchymal stem cells protect breast cancer cells through regulatory T cells: role of mesenchymal stem cell-derived TGF-beta. *Journal of immunology (Baltimore, Md. : 1950)*, 184(10), pp.5885–94.

Pearson, T., Greiner, D.L. & Shultz, L.D., 2008. Creation of "humanized" mice to study human immunity. *Current protocols in immunology / edited by John E. Coligan ... [et al.]*, Chapter 15, p.Unit 15.21.

Peccatori, J. & Ciceri, F., 2010. Allogeneic stem cell transplantation for acute myeloid leukemia. *Haematologica*, 95(6), pp.857–9.

Pelanda, R. et al., 1997. Receptor Editing in a Transgenic Mouse Model: Site, Efficiency, and Role in B Cell Tolerance and Antibody Diversification. *Immunity*, 7(6), pp.765–775.

Pelanda, R. & Torres, R.M., 2012. Central B-cell tolerance: where selection begins. *Cold Spring Harbor perspectives in biology*, 4(4), p.a007146.

Peng, Y. et al., 2014. Mesenchymal stromal cells infusions improve refractory chronic graft versus host disease through an increase of CD5+ regulatory B cells producing interleukin 10. *Leukemia*.

Pérez-Simón, J.A. et al., 2005. Influence of the intensity of the conditioning regimen on the characteristics of acute and chronic graft-versus-host disease after allogeneic transplantation. *British journal of haematology*, 130(3), pp.394–403.

Pidala, J. et al., 2009. Infliximab for managing steroid-refractory acute graft-versus-host disease. *Biology of blood and marrow transplantation : journal of the American Society for Blood and Marrow Transplantation*, 15(9), pp.1116–21.

Pieper, K., Grimbacher, B. & Eibel, H., 2013. B-cell biology and development. *The Journal of allergy and clinical immunology*, 131(4), pp.959–71.

Pittenger, M.F. et al., 1999. Multilineage potential of adult human mesenchymal stem cells. *Science (New York, N.Y.)*, 284(5411), pp.143–7.

Plumas, J. et al., 2005. Mesenchymal stem cells induce apoptosis of activated T cells. *Leukemia*, 19(9), pp.1597–604.

Polchert, D. et al., 2008. IFN-gamma activation of mesenchymal stem cells for treatment and prevention of graft versus host disease. *European journal of immunology*, 38(6), pp.1745–55.

Prockop, D.J. & Oh, J.Y., 2012. Mesenchymal stem/stromal cells (MSCs): role as guardians of inflammation. *Molecular therapy : the journal of the American Society of Gene Therapy*, 20(1), pp.14–20.

Radic, M.Z. et al., 1993. B lymphocytes may escape tolerance by revising their antigen receptors. *The Journal of experimental medicine*, 177(4), pp.1165–73.

Radtke, F., Wilson, A. & MacDonald, H.R., 2004. Notch signaling in T- and B-cell development. *Current opinion in immunology*, 16(2), pp.174–9.

Rafei, M. et al., 2009. Allogeneic mesenchymal stem cells for treatment of experimental autoimmune encephalomyelitis. *Molecular therapy : the journal of the American Society of Gene Therapy*, 17(10), pp.1799–803.

Raida, L. et al., 2014. Comparison of reduced conditionings combining fludarabine with melphalan or 3-day busulfan in patients allografted for myeloid neoplasms. *International journal of hematology*.

Rasmusson, I. et al., 2007. Mesenchymal stem cells stimulate antibody secretion in human B cells. *Scandinavian journal of immunology*, 65(4), pp.336–43.

Ratanatharathorn, V. et al., 2000. Anti-CD20 chimeric monoclonal antibody treatment of refractory immune-mediated thrombocytopenia in a patient with chronic graft-versus-host disease. *Annals of internal medicine*, 133(4), pp.275–9.

Ratanatharathorn, V. et al., 2001. Chronic graft-versus-host disease: clinical manifestation and therapy. *Bone marrow transplantation*, 28(2), pp.121–9.

Reddy, P. et al., 2009. GVHD: a continuing barrier to the safety of allogeneic transplantation. *Biology of blood and marrow transplantation : journal of the American Society for Blood and Marrow Transplantation*, 15(1 Suppl), pp.162–8.

Reddy, P. & Ferrara, J.L.M., 2003. Immunobiology of acute graft-versus-host disease. *Blood reviews*, 17(4), pp.187–94.

Ren, G. et al., 2010. Inflammatory cytokine-induced intercellular adhesion molecule-1 and vascular cell adhesion molecule-1 in mesenchymal stem cells are critical for immunosuppression. *Journal of immunology (Baltimore, Md. : 1950)*, 184(5), pp.2321–8.

Ren, G. et al., 2008. Mesenchymal stem cell-mediated immunosuppression occurs via concerted action of chemokines and nitric oxide. *Cell stem cell*, 2(2), pp.141–50.

Ren, G. et al., 2009. Species variation in the mechanisms of mesenchymal stem cell-mediated immunosuppression. *Stem cells (Dayton, Ohio)*, 27(8), pp.1954–62.

Rezanka, L.J., Kenny, J.J. & Longo, D.L., 2005. 2 BCR or NOT 2 BCR - receptor dilution: a unique mechanism for preventing the development of holes in the protective B cell repertoire. *Immunobiology*, 210(10), pp.769–74.

Ringdén, O. et al., 2006. Mesenchymal stem cells for treatment of therapy-resistant graft-versus-host disease. *Transplantation*, 81(10), pp.1390–7.

Rolink, A.G. & Gleichmann, E., 1983. Allosuppressor- and allohelper-T cells in acute and chronic graft-vs.-host (GVH) disease. III. Different Lyt subsets of donor T cells induce different pathological syndromes. *The Journal of experimental medicine*, 158(2), pp.546–58.

Roncarolo, M.G. et al., 2006. Interleukin-10-secreting type 1 regulatory T cells in rodents and humans. *Immunological reviews*, 212, pp.28–50.

Rosado, M.M. et al., 2014. Inhibition of B-Cell Proliferation and Antibody Production by Mesenchymal Stromal Cells Is Mediated by T Cells. *Stem cells and development*.

Rubio, M.-T. et al., 2012. Early posttransplantation donor-derived invariant natural killer T-cell recovery predicts the occurrence of acute graft-versus-host disease and overall survival. *Blood*, 120(10), pp.2144–54.

Ryan, J.M. et al., 2007. Interferon-gamma does not break, but promotes the immunosuppressive capacity of adult human mesenchymal stem cells. *Clinical and experimental immunology*, 149(2), pp.353–63.

Ryan, J.M. et al., 2005. Mesenchymal stem cells avoid allogeneic rejection. *Journal of inflammation (London, England)*, 2, p.8.

Safinia, N. et al., 2013. Promoting transplantation tolerance; adoptive regulatory T cell therapy. *Clinical and experimental immunology*, 172(2), pp.158–68.

Sakaguchi, S. et al., 1995. Immunologic self-tolerance maintained by activated T cells expressing IL-2 receptor alpha-chains (CD25). Breakdown of a single mechanism of self-tolerance causes various autoimmune diseases. *Journal of immunology (Baltimore, Md. : 1950)*, 155(3), pp.1151–64.

Sallusto, F. et al., 1999. Two subsets of memory T lymphocytes with distinct homing potentials and effector functions. *Nature*, 401(6754), pp.708–12.

Sallusto, F., Geginat, J. & Lanzavecchia, a, 2004. Central memory and effector memory T cell subsets: function, generation, and maintenance. *Annu Rev Immunol*, 22, pp.745–763.

Samuels, J. et al., 2005. Impaired early B cell tolerance in patients with rheumatoid arthritis. *The Journal of experimental medicine*, 201(10), pp.1659–67.

Sattler, C. et al., 2011. Inhibition of T-cell proliferation by murine multipotent mesenchymal stromal cells is mediated by CD39 expression and adenosine generation. *Cell transplantation*, 20(8), pp.1221–30.

Schatz, D.G. & Ji, Y., 2011. Recombination centres and the orchestration of V(D)J recombination. *Nature reviews. Immunology*, 11(4), pp.251–63.

Schmaltz, C. et al., 2003. Donor T cell-derived TNF is required for graft-versus-host disease and graft-versus-tumor activity after bone marrow transplantation. *Blood*, 101(6), pp.2440–5.

Schneidawind, D. et al., 2014. CD4+ invariant natural killer T cells protect from murine GVHD lethality through expansion of donor CD4+CD25+FoxP3+ regulatory T cells. *Blood*, pp.blood–2014–05–576017.

Schneider, P. et al., 1999. BAFF, a novel ligand of the tumor necrosis factor family, stimulates B cell growth. *The Journal of experimental medicine*, 189(11), pp.1747–56.

Schrepfer, S. et al., 2007. Stem cell transplantation: the lung barrier. *Transplantation proceedings*, 39(2), pp.573–6.

Schroeder, M.A. & DiPersio, J.F., 2011. Mouse models of graft-versus-host disease: advances and limitations. *Disease models & mechanisms*, 4(3), pp.318–33.

Schwarz, A. et al., 2010. Biopsy-diagnosed renal disease in patients after transplantation of other organs and tissues. *American journal of transplantation : official journal of the American Society of Transplantation and the American Society of Transplant Surgeons*, 10(9), pp.2017–25.

Seddiki, N. et al., 2006. Expression of interleukin (IL)-2 and IL-7 receptors discriminates between human regulatory and activated T cells. *The Journal of experimental medicine*, 203(7), pp.1693–700.

Selmani, Z. et al., 2008. Human leukocyte antigen-G5 secretion by human mesenchymal stem cells is required to suppress T lymphocyte and natural killer function and to induce CD4+CD25highFOXP3+ regulatory T cells. *Stem cells (Dayton, Ohio)*, 26(1), pp.212–22.

Serreze, D. V, Gaedeke, J.W. & Leiter, E.H., 1993. Hematopoietic stem-cell defects underlying abnormal macrophage development and maturation in NOD/Lt mice: defective regulation of cytokine receptors and protein kinase C. *Proceedings of the National Academy of Sciences of the United States of America*, 90(20), pp.9625–9.

Shinkai, Y. et al., 1992. RAG-2-deficient mice lack mature lymphocytes owing to inability to initiate V(D)J rearrangement. *Cell*, 68(5), pp.855–67.

Shlomchik, W.D., 2007. Graft-versus-host disease. *Nature reviews. Immunology*, 7(5), pp.340–52.

Shultz, L.D. et al., 2012. Humanized mice for immune system investigation: progress, promise and challenges. *Nature reviews. Immunology*, 12(11), pp.786–98.

Shultz, L.D. et al., 1995. Multiple defects in innate and adaptive immunologic function in NOD/LtSz-scid mice. *Journal of immunology (Baltimore, Md. : 1950)*, 154(1), pp.180–91.

Shultz, L.D. et al., 2000. NOD/LtSz-Rag1null mice: an immunodeficient and radioresistant model for engraftment of human hematolymphoid cells, HIV infection, and adoptive transfer of NOD mouse diabetogenic T cells. *Journal of immunology (Baltimore, Md. : 1950)*, 164(5), pp.2496–507.

Siddappa, R. et al., 2007. Donor variation and loss of multipotency during in vitro expansion of human mesenchymal stem cells for bone tissue engineering. *Journal of orthopaedic research : official publication of the Orthopaedic Research Society*, 25(8), pp.1029–41.

Siegel, G. et al., 2013. Phenotype, donor age and gender affect function of human bone marrow-derived mesenchymal stromal cells. *BMC medicine*, 11(1), p.146.

Sims, G.P. et al., 2005. Identification and characterization of circulating human transitional B cells. *Blood*, 105(11), pp.4390–8.

Skert, C. et al., 2006. Sclerodermatous chronic graft-versus-host disease after allogeneic hematopoietic stem cell transplantation: incidence, predictors and outcome. *Haematologica*, 91(2), pp.258–61.

Snapper, C.M. et al., 1992. Induction of IgG3 secretion by interferon gamma: a model for T cell-independent class switching in response to T cell-independent type 2 antigens. *The Journal of experimental medicine*, 175(5), pp.1367–71.

Snell, G.D., 1948. Methods for the study of histocompatibility genes. *Journal of Genetics*, 49(2), pp.87–108.

SNELL, G.D. & HIGGINS, G.F., 1951. Alleles at the histocompatibility-2 locus in the mouse as determined by tumor transplantation. *Genetics*, 36(3), pp.306–10.

Sotiropoulou, P.A. et al., 2006. Interactions between human mesenchymal stem cells and natural killer cells. *Stem cells (Dayton, Ohio)*, 24(1), pp.74–85.

Spaggiari, G.M. et al., 2008. Mesenchymal stem cells inhibit natural killer-cell proliferation, cytotoxicity, and cytokine production: role of indoleamine 2,3-dioxygenase and prostaglandin E2. *Blood*, 111(3), pp.1327–33.

Spaggiari, G.M. et al., 2009. MSCs inhibit monocyte-derived DC maturation and function by selectively interfering with the generation of immature DCs: central role of MSC-derived prostaglandin E2. *Blood*, 113(26), pp.6576–83.

Spyridopoulos, I. et al., 1997. Vascular endothelial growth factor inhibits endothelial cell apoptosis induced by tumor necrosis factor-alpha: balance between growth and death signals. *Journal of molecular and cellular cardiology*, 29(5), pp.1321–30.

Stern, L.J. et al., 1994. Crystal structure of the human class II MHC protein HLA-DR1 complexed with an influenza virus peptide. *Nature*, 368(6468), pp.215–21.

Studier, F.W., 1973. Analysis of bacteriophage T7 early RNAs and proteins on slab gels. *Journal of molecular biology*, 79(2), pp.237–48.

Sudres, M. et al., 2006. Bone marrow mesenchymal stem cells suppress lymphocyte proliferation in vitro but fail to prevent graft-versus-host disease in mice. *Journal of immunology (Baltimore, Md. : 1950)*, 176(12), pp.7761–7.

Sugamura, K. et al., 1996. The interleukin-2 receptor gamma chain: its role in the multiple cytokine receptor complexes and T cell development in XSCID. *Annual review of immunology*, 14, pp.179–205.

Sun, L. et al., 2009. Mesenchymal stem cell transplantation reverses multiorgan dysfunction in systemic lupus erythematosus mice and humans. *Stem cells (Dayton, Ohio)*, 27(6), pp.1421–32.

Sun, L. et al., 2010. Umbilical cord mesenchymal stem cell transplantation in severe and refractory systemic lupus erythematosus. *Arthritis and rheumatism*, 62(8), pp.2467–75.

Sun, L.Y. et al., 2007. Abnormality of bone marrow-derived mesenchymal stem cells in patients with systemic lupus erythematosus. *Lupus*, 16(2), pp.121–8.

Tabera, S. et al., 2008. The effect of mesenchymal stem cells on the viability, proliferation and differentiation of B-lymphocytes. *Haematologica*, 93(9), pp.1301–9.

Tangye, S.G. et al., 2013. The good, the bad and the ugly - TFH cells in human health and disease. *Nature reviews. Immunology*, 13(6), pp.412–26.

Tarlinton, D. et al., 2003. Architectural defects in the spleens of Nkx2-3-deficient mice are intrinsic and associated with defects in both B cell maturation and T cell-dependent immune responses. *Journal of immunology (Baltimore, Md. : 1950)*, 170(8), pp.4002–10.

Taylor, P.A., Lees, C.J. & Blazar, B.R., 2002. The infusion of ex vivo activated and expanded CD4(+)CD25(+) immune regulatory cells inhibits graft-versus-host disease lethality. *Blood*, 99(10), pp.3493–9.

Thomas, M. et al., 2007. Notch activity synergizes with B-cell-receptor and CD40 signaling to enhance B-cell activation. *Blood*, 109(8), pp.3342–50.

Tiegs, S.L., Russell, D.M. & Nemazee, D., 1993. Receptor editing in self-reactive bone marrow B cells. *The Journal of experimental medicine*, 177(4), pp.1009–20.

Tobin, L.M. et al., 2013. Human mesenchymal stem cells suppress donor CD4(+) T cell proliferation and reduce pathology in a humanized mouse model of acute graft-versus-host disease. *Clinical and experimental immunology*, 172(2), pp.333–48.

Tokoyoda, K. et al., 2009. Professional memory CD4+ T lymphocytes preferentially reside and rest in the bone marrow. *Immunity*, 30(5), pp.721–30.

Tolar, J., Villeneuve, P. & Keating, A., 2011. Mesenchymal stromal cells for graft-versus-host disease. *Human gene therapy*, 22(3), pp.257–62.

Toma, C. et al., 2009. Fate of culture-expanded mesenchymal stem cells in the microvasculature: in vivo observations of cell kinetics. *Circulation research*, 104(3), pp.398–402.

Tonegawa, S. et al., 1974. Evidence for somatic generation of antibody diversity. *Proceedings of the National Academy of Sciences of the United States of America*, 71(10), pp.4027–31.

Traggiai, E. et al., 2008. Bone marrow-derived mesenchymal stem cells induce both polyclonal expansion and differentiation of B cells isolated from healthy donors and systemic lupus erythematosus patients. *Stem cells (Dayton, Ohio)*, 26(2), pp.562–9.

Trenado, A. et al., 2003. Recipient-type specific CD4+CD25+ regulatory T cells favor immune reconstitution and control graft-versus-host disease while maintaining graft-versus-leukemia. *The Journal of clinical investigation*, 112(11), pp.1688–96.

Trzonkowski, P. et al., 2009. First-in-man clinical results of the treatment of patients with graft versus host disease with human ex vivo expanded CD4+CD25+CD127- T regulatory cells. *Clinical immunology (Orlando, Fla.)*, 133(1), pp.22–6.

Tse, W.T. et al., 2003. Suppression of allogeneic T-cell proliferation by human marrow stromal cells: implications in transplantation. *Transplantation*, 75(3), pp.389–97.

Tsirigotis, P. et al., 2012. Extracorporeal photopheresis in the treatment of chronic graft-versus-host disease. The Hellenic experience: a study by the Hellenic association of hematology. *Transfusion and apheresis science : official journal of the World Apheresis Association : official journal of the European Society for Haemapheresis*, 46(2), pp.173–80.

Tuscano, J.M., Harris, G.S. & Tedder, T.F., 2003. B lymphocytes contribute to autoimmune disease pathogenesis: current trends and clinical implications. *Autoimmunity reviews*, 2(2), pp.101–8.

Tussiwand, R. et al., 2009. Tolerance checkpoints in B-cell development: Johnny B good. *European journal of immunology*, 39(9), pp.2317–24.

Uccelli, A., Moretta, L. & Pistoia, V., 2006. Immunoregulatory function of mesenchymal stem cells. *European journal of immunology*, 36(10), pp.2566–73.

Via, C.S. et al., 1996. Differential effect of CTLA4Ig on murine graft-versus-host disease (GVHD) development: CTLA4Ig prevents both acute and chronic GVHD development but reverses only chronic GVHD. *Journal of immunology (Baltimore, Md. : 1950)*, 157(9), pp.4258–67.

Vinuesa, C.G., Sanz, I. & Cook, M.C., 2009. Dysregulation of germinal centres in autoimmune disease. *Nature reviews. Immunology*, 9(12), pp.845–57.

Vos, Q. et al., 2000. B-cell activation by T-cell-independent type 2 antigens as an integral part of the humoral immune response to pathogenic microorganisms. *Immunological reviews*, 176, pp.154–70.

Vossen, J.M. et al., 2014. Complete suppression of the gut microbiome prevents acute graft-versus-host disease following allogeneic bone marrow transplantation. *PloS one*, 9(9), p.e105706.

Vukman, K. V et al., 2013. The effects of Fasciola hepatica tegumental antigens on mast cell function. *International journal for parasitology*, 43(7), pp.531–9.

Wang, D. et al., 2014. Umbilical cord mesenchymal stem cell transplantation in active and refractory systemic lupus erythematosus: a multicenter clinical study. *Arthritis research & therapy*, 16(2), p.R79.

Wang, H. et al., 2011. Adipogenic differentiation alters the immunoregulatory property of mesenchymal stem cells through BAFF secretion. *Hematology (Amsterdam, Netherlands)*, 16(5), pp.313–23.

Wang, L. et al., 2013. Human umbilical cord mesenchymal stem cell therapy for patients with active rheumatoid arthritis: safety and efficacy. *Stem cells and development*, 22(24), pp.3192–202.

Wang, Q. et al., 2008. Murine bone marrow mesenchymal stem cells cause mature dendritic cells to promote T-cell tolerance. *Scandinavian journal of immunology*, 68(6), pp.607–15.

Wang, R.-X. et al., 2014. Interleukin-35 induces regulatory B cells that suppress autoimmune disease. *Nature medicine*, 20(6), pp.633–41.

Wardemann, H. et al., 2003. Predominant autoantibody production by early human B cell precursors. *Science (New York, N.Y.)*, 301(5638), pp.1374–7.

Weng, J.Y. et al., 2010. Mesenchymal stem cell as salvage treatment for refractory chronic GVHD. *Bone marrow transplantation*, 45(12), pp.1732–40.

Weninger, W. et al., 2001. Migratory properties of naive, effector, and memory CD8(+) T cells. *The Journal of experimental medicine*, 194(7), pp.953–66.

Wood, K.J. & Sakaguchi, S., 2003. Regulatory T cells in transplantation tolerance. *Nature reviews. Immunology*, 3(3), pp.199–210.

Yamout, B. et al., 2010. Bone marrow mesenchymal stem cell transplantation in patients with multiple sclerosis: a pilot study. *Journal of neuroimmunology*, 227(1-2), pp.185–9.

Yang, S.-H. et al., 2009. Soluble mediators from mesenchymal stem cells suppress T cell proliferation by inducing IL-10. *Experimental & molecular medicine*, 41(5), pp.315–24.

Youd, M. et al., 2010. Allogeneic mesenchymal stem cells do not protect NZBxNZW F1 mice from developing lupus disease. *Clinical and experimental immunology*, 161(1), pp.176–86.

Yu, X. et al., 2008. Neutralizing antibodies derived from the B cells of 1918 influenza pandemic survivors. *Nature*, 455(7212), pp.532–6.

Yurasov, S. et al., 2005. Defective B cell tolerance checkpoints in systemic lupus erythematosus. *The Journal of experimental medicine*, 201(5), pp.703–11.

Zangi, L. et al., 2009. Direct imaging of immune rejection and memory induction by allogeneic mesenchymal stromal cells. *Stem cells (Dayton, Ohio)*, 27(11), pp.2865–74.

Zaph, C. et al., 2004. Central memory T cells mediate long-term immunity to Leishmania major in the absence of persistent parasites. *Nature medicine*, 10(10), pp.1104–10.

Zappia, E. et al., 2005. Mesenchymal stem cells ameliorate experimental autoimmune encephalomyelitis inducing T-cell anergy. *Blood*, 106(5), pp.1755–61.

Van Zelm, M.C. et al., 2007. Replication history of B lymphocytes reveals homeostatic proliferation and extensive antigen-induced B cell expansion. *The Journal of experimental medicine*, 204(3), pp.645–55.

Zhang, C. et al., 2006. Donor CD4+ T and B cells in transplants induce chronic graft-versus-host disease with autoimmune manifestations. *Blood*, 107(7), pp.2993–3001.

Zhang, J. et al., 1988. B cell memory to thymus-independent antigens type 1 and type 2: the role of lipopolysaccharide in B memory induction. *European journal of immunology*, 18(9), pp.1417–24.

Zhang, P. et al., 2012. Allospecific CD4(+) effector memory T cells do not induce graft-versus-host disease in mice. *Biology of blood and marrow transplantation : journal of the American Society for Blood and Marrow Transplantation*, 18(10), pp.1488–99.

Zheng, H. et al., 2009. Central memory CD8+ T cells induce graft-versus-host disease and mediate graft-versus-leukemia. *Journal of immunology (Baltimore, Md. : 1950)*, 182(10), pp.5938–48.

Zheng, Z.H. et al., 2008. Allogeneic mesenchymal stem cell and mesenchymal stem cell-differentiated chondrocyte suppress the responses of type II collagen-reactive T cells in rheumatoid arthritis. *Rheumatology (Oxford, England)*, 47(1), pp.22–30.

Zhou, H. et al., 2000. Akt regulates cell survival and apoptosis at a postmitochondrial level. *The Journal of cell biology*, 151(3), pp.483–94.

Zhou, H. et al., 2010. Efficacy of bone marrow-derived mesenchymal stem cells in the treatment of sclerodermatous chronic graft-versus-host disease: clinical report. *Biology of blood and marrow transplantation : journal of the American Society for Blood and Marrow Transplantation*, 16(3), pp.403–12.

Zhou, K. et al., 2008. Transplantation of human bone marrow mesenchymal stem cell ameliorates the autoimmune pathogenesis in MRL/lpr mice. *Cellular & molecular immunology*, 5(6), pp.417–24.

Zhu, N. et al., 2002. CD40 signaling in B cells regulates the expression of the Pim-1 kinase via the NF-kappa B pathway. *Journal of immunology (Baltimore, Md. : 1950)*, 168(2), pp.744–54.

Zinöcker, S. & Vaage, J.T., 2012. Rat mesenchymal stromal cells inhibit T cell proliferation but not cytokine production through inducible nitric oxide synthase. *Frontiers in immunology*, 3, p.62.

Zuo, D. et al., 2013. Study on the interactions between transplanted bone marrow-derived mesenchymal stem cells and regulatory T cells for the treatment of experimental colitis. *International journal of molecular medicine*, 32(6), pp.1337–44.